LANDSLIDE HAZARD, VULNERABILITY AND RISK ASSESSMENT OF AIZAWL MUNICIPAL AREA, MIZORAM, INDIA USING GEOSPATIAL TECHNIQUES

A THESIS SUBMITTED IN PARTIAL FULFILMENT OF THE REQUIREMENTS FOR THE DEGREE OF DOCTOR OF PHILOSOPHY

Z. D. LALTANPUIA

ORCID iD: 0000-0003-2522-0483

MZU Registration: 1807373

Ph. D. Registration: MZU/Ph.D/1277 of 03.08.2018

DEPARTMENT OF GEOLOGY

SCHOOL OF EARTH SCIENCES & NATURAL RESOURCES MANAGEMENT

MIZORAM UNIVERSITY

NOVEMBER, 2025

LANDSLIDE HAZARD, VULNERABILITY AND RISK ASSESSMENT OF AIZAWL MUNICIPAL AREA, MIZORAM, INDIA USING GEOSPATIAL TECHNIQUES

By

Z. D. LALTANPUIA

Research Scholar

Department of Geology, Mizoram University, Aizawl, Mizoram

Prof. K. SRINIVASA RAO

Supervisor

Department of Geology, Mizoram University, Aizawl, Mizoram

Dr TAPAS R. MARTHA

Co-Supervisor

Geosciences Group, National Remote Sensing Centre (NRSC)

Indian Space Research Organisation (ISRO), Hyderabad, Telengana

Submitted

In partial fulfilment of the requirement of the Degree of

Doctor of Philosophy in Geology of Mizoram University, Aizawl

DEDICATION

This thesis is dedicated

In loving and eternal memory of my mother,

THANGMAWII (1947 – 2010)

Her life was a testament to selfless love and unwavering sacrifice for her children and her family. Her quiet strength and tireless efforts paved the way for opportunities she never had herself, and this achievement is built upon the foundation of her boundless dedication. Though she is not here to share this moment, her spirit and her legacy of love are woven into every page.

And to my dear father,

Z.D. ZOTLUANGA

With all my love and deepest gratitude. His steadfast support, wisdom, and encouragement have been my guide throughout this long journey. Despite his present frailty and ill health, his faith and strength remain deeply motivating and have sustained me throughout this academic journey.

I dedicate this humble work as an expression of my gratitude and reverence to them, and as a tribute to the values they both instilled in me.

DEPARTMENT OF GEOLOGY
MIZORAM UNIVERSITY
(A Central University established by an Act of Parliament)
भौमिकी विभाग, मिज़ोरम विश्वविद्यालय
Mizoram : Aizawl - 796 004
मिज़ोरम : आइज़ोल – ७९६ ००४

Prof. K. Srinivasa Rao

www.mzu.edu.in
ksrao@mzu.edu.in
srkoduri4@rediffmail.com
7005609873

CERTIFICATE

I hereby certify that the thesis entitled ***"Landslide Hazard, Vulnerability and Risk Assessment of Aizawl Municipal Area, Mizoram, India, using Geospatial Techniques"*** is a record of bona fide research work carried out by **Mr. Z. D. Laltanpuia** (Ph.D. Regn. No. MZU/Ph.D/1277 of 03.08.2018), for the award of the degree of Doctor of Philosophy in Geology at Mizoram University, Aizawl. This work has been carried out under the joint supervision and guidance of **Prof. K. Srinivasa Rao** and **Dr Tapas R. Martha**.

I further certify that the candidate has fulfilled all the necessary requirements laid down in the Ph.D. regulations of the University. This thesis, either in whole or in part, has not been submitted to any other University or Institute for any research degree or diploma.

K. Srinivasa Rao

Date: 27th November, 2025

Place: Aizawl

(Prof. K. SRINIVASA RAO)

Supervisor

Professor
Department of Geology
Mizoram University

भारत सरकार
अन्तरिक्ष विभाग
राष्ट्रीय सुदूर संवेदन केन्द्र
बालानगर, हैदराबाद - 500 037, तेलंगाना, भारत
टेलिफोन : +040-23879572-76
+040-23879261-65
फैक्स : +040-23878648

Government of India
Department of Space (DOS)
National Remote Sensing Centre
Balanagar, Hyderabad - 500 037, Telangana, India
Telephone : +040-23879572-76
: +040-23879261-65
Fax : +040-23878648

CERTIFICATE

I hereby certify that the thesis entitled ***"Landslide Hazard, Vulnerability and Risk Assessment of Aizawl Municipal Area, Mizoram, India, using Geospatial Techniques"*** is a record of bonafide research work carried out by **Mr. Z. D. Laltanpuia** (Ph.D. Regn. No. MZU/Ph.D./1277 of 03.08.2018), for the award of the degree of Doctor of Philosophy in Geology at Mizoram University, Aizawl. This work has been carried out under the joint supervision and guidance of **Prof. K. Srinivasa Rao** and **Dr Tapas R. Martha**.

I further certify that the candidate has fulfilled all the necessary requirements laid down in the Ph.D. regulations of the University. This thesis, either in whole or in part, has not been submitted to any other University or Institute for any research degree or diploma.

Date: 20-11-2025
Place: Hyderabad

(Dr. Tapas R. Martha)
Co-Supervisor

डॉ. तापस रंजन मार्था / Dr. TAPAS RANJAN MARTHA
Scientist-SG & Head
Geohazards and Mineral Exploration Division
Remote Sensing Application Area (RSAA)
राष्ट्रीय सुदूर संवेदन केंद्र / National Remote Sensing Centre
Indian Space Research Organisation
Dept. of Space, Govt. of India
बालानगर, हैदराबाद-500 037 / Balanagar, Hyderabad-500 037

DECLARATION

MIZORAM UNIVERSITY

November, 2025

I, **Z. D. Laltanpuia**, hereby declare that the subject matter of this thesis is the record of work done by me, that the contents of this thesis did not form basis of the award of any previous degree to me or to the best of my knowledge to anybody else, and that the thesis has not been submitted by me for any research degree in any other University/Institute.

This is being submitted to the Mizoram University for the Degree of Doctor of Philosophy in Geology.

Date: 27th November, 2025

Place: Aizawl

(Z. D. LALTANPUIA)
Research Scholar

(Prof. K. SRINIVASA RAO)
Supervisor

Professor
Department of Geology
Mizoram University

(Dr TAPAS R. MARTHA)
Co-Supervisor

डॉ. तापस रंजन मार्था / Dr. TAPAS RANJAN MARTHA
[illegible] / Scientist-SG & Head
[illegible]
Geohazards and Mineral Exploration Division
सुदूर संवेदन अनुप्रयोग क्षेत्र [illegible]
Remote Sensing Application Area (RSAA),
राष्ट्रीय सुदूर संवेदन केंद्र / National Remote Sensing Centre
भारतीय अंतरिक्ष अनुसंधान संगठन / Indian Space Research Organisation
अंतरिक्ष विभाग, भारत सरकार / Dept. of Space, Govt. of India
बालानगर, हैदराबाद-500 037 / Balanagar, Hyderabad-500 037

(Dr J. MALSAWMA)
Head of the Department

Head
Department of Geology and
Centre for Petroleum Exploration (CPEX)
Mizoram University

CERTIFICATE ON PLAGIARISM CHECK

Name of Research Scholar	Z. D. LALTANPUIA	
Ph.D. Registration Number	MZU/Ph.D/1277 of 03.08.2018	
Title of Ph.D. thesis	Landslide Hazard, Vulnerability and Risk Assessment of Aizawl Municipal Area, Mizoram, India using Geospatial Techniques	
Name & Institutional Address of the Supervisor/Joint Supervisor	Prof. K. SRINIVASA RAO, Supervisor, Department of Geology, Mizoram University, Aizawl, Mizoram Dr TAPAS R. MARTHA, Co-Supervisor, Geosciences Group, National Remote Sensing Centre (NRSC), Indian Space Research Organisation (ISRO), Hyderabad, Telengana	
Name of the Department and School	Department of Geology, School of Earth Sciences and Natural Resources Management	
Date of Submission	27 November, 2025	
Date of Plagiarism check	19 November, 2025	
Name of the Software used	TURNITIN	
Percentage of similarity detected by the **TURNITIN** Software	Core Areas	**6%**
	Non-Core areas	**1%**
Percentage of similarity permissible under MZU regulations	Core Areas	A common knowledge or coincidental terms and/or up to fourteen (14) consecutive words, if option is available in the software
	Non-Core areas	Up to 10%

I hereby declare/certify that the Ph.D. Thesis submitted by me is complete in all respect, as per the guidelines of the Mizoram University (MZU) for this purpose. I also certify that the Thesis (soft copy and print version) has been checked for plagiarism using **TURNITIN** similarity check software. Copy of the Report generated by the **TURNITIN** software is also enclosed.

Date: 27th November, 2025
Place: Aizawl

(Z. D. LALTANPUIA)
Research Scholar

(Prof. K. SRINIVASA RAO)
Supervisor

(Dr TAPAS R. MARTHA)
Co-Supervisor

(Dr J. MALSAWMA)
Head of the Department

ZD Laltanpuia

Core.docx

Mizoram University

Document Details

Submission ID

trn:oid:::10015:121985946

Submission Date

Nov 19, 2025, 12:18 AM PST

Download Date

Nov 19, 2025, 12:20 AM PST

File Name

Core.docx

File Size

66.4 KB

45 Pages

14,146 Words

83,126 Characters

6% Overall Similarity

The combined total of all matches, including overlapping sources, for each database.

Filtered from the Report

- Bibliography
- Quoted Text
- Cited Text
- Small Matches (less than 14 words)

Match Groups

45 Not Cited or Quoted 6%
Matches with neither in-text citation nor quotation marks

0 Missing Quotations 0%
Matches that are still very similar to source material

0 Missing Citation 0%
Matches that have quotation marks, but no in-text citation

0 Cited and Quoted 0%
Matches with in-text citation present, but no quotation marks

Top Sources

0% Internet sources

4% Publications

6% Submitted works (Student Papers)

Integrity Flags

0 Integrity Flags for Review

No suspicious text manipulations found.

Our system's algorithms look deeply at a document for any inconsistencies that would set it apart from a normal submission. If we notice something strange, we flag it for you to review.

A Flag is not necessarily an indicator of a problem. However, we'd recommend you focus your attention there for further review.

Match Groups

- **45** Not Cited or Quoted 6%
  Matches with neither in-text citation nor quotation marks
- **0** Missing Quotations 0%
  Matches that are still very similar to source material
- **0** Missing Citation 0%
  Matches that have quotation marks, but no in-text citation
- **0** Cited and Quoted 0%
  Matches with in-text citation present, but no quotation marks

Top Sources

0% Internet sources
4% Publications
6% Submitted works (Student Papers)

Top Sources

The sources with the highest number of matches within the submission. Overlapping sources will not be displayed.

1	Submitted works	mzu on 2025-01-12	4%
2	Publication	Z. D. Laltanpuia, Tapas R. Martha, K. Srinivasa Rao. "Integrating Social and Physic...	2%
3	Publication	Javed Iqbal, Xinbin Tu, Ling Xu. "Landslide Hazards in Reservoir Areas: Case Study...	<1%
4	Submitted works	Nepal Open University on 2025-03-23	<1%
5	Publication	Yubraj Bikram Shahi, Sushma Kadel, Harish Dangi, Ganesh Adhikari, Diwakar KC, ...	<1%
6	Publication	Mojtaba Ghorbani Asiabar, Morteza Ghorbani Asiabar, Alireza Ghorbani Asiabar. "...	<1%
7	Submitted works	University of KwaZulu-Natal on 2023-11-29	<1%
8	Internet	c.coek.info	<1%

ZD Laltanpuia

Non-Core.docx

Mizoram University

Document Details

Submission ID

trn:oid:::10015:121985301

Submission Date

Nov 19, 2025, 12:13 AM PST

Download Date

Nov 19, 2025, 12:17 AM PST

File Name

Non-Core.docx

File Size

186.0 KB

107 Pages

35,968 Words

211,049 Characters

1% Overall Similarity

The combined total of all matches, including overlapping sources, for each database.

Filtered from the Report

- Bibliography
- Quoted Text
- Cited Text
- Small Matches (less than 14 words)

Match Groups

19 Not Cited or Quoted 1%
Matches with neither in-text citation nor quotation marks

0 Missing Quotations 0%
Matches that are still very similar to source material

0 Missing Citation 0%
Matches that have quotation marks, but no in-text citation

0 Cited and Quoted 0%
Matches with in-text citation present, but no quotation marks

Top Sources

0% Internet sources
1% Publications
1% Submitted works (Student Papers)

Integrity Flags

0 Integrity Flags for Review

No suspicious text manipulations found.

Our system's algorithms look deeply at a document for any inconsistencies that would set it apart from a normal submission. If we notice something strange, we flag it for you to review.

A Flag is not necessarily an indicator of a problem. However, we'd recommend you focus your attention there for further review.

Match Groups

- **19** Not Cited or Quoted 1%
  Matches with neither in-text citation nor quotation marks
- **0** Missing Quotations 0%
  Matches that are still very similar to source material
- **0** Missing Citation 0%
  Matches that have quotation marks, but no in-text citation
- **0** Cited and Quoted 0%
  Matches with in-text citation present, but no quotation marks

Top Sources

0% Internet sources
1% Publications
1% Submitted works (Student Papers)

Top Sources

The sources with the highest number of matches within the submission. Overlapping sources will not be displayed.

1	Submitted works	mzu on 2025-01-12	<1%
2	Internet	researchinventy.com	<1%
3	Internet	unece.org	<1%
4	Publication	Z. D. Laltanpuia, Tapas R. Martha, K. Srinivasa Rao. "Integrating Social and Physic...	<1%
5	Submitted works	Fatih University on 2016-07-01	<1%
6	Internet	www.hrvoice.org	<1%
7	Publication	Arip Syaripudin Nur, Yong Je Kim, Boo Hyun Nam, Kyungwon Park. "Sinkhole Susc...	<1%
8	Publication	John (Jack) F. Shroder, Jr., Lubica Cverckovà, Kimberlee L. Mulhern. "Slope-failure ...	<1%
9	Internet	coek.info	<1%
10	Submitted works	Yonsei University on 2015-07-16	<1%

11 Internet

journals.ametsoc.org <1%

12 Internet

www.ngi.no <1%

13 Publication

Peng Xia, Bowen Zeng, Jie Liu, Yiheng Pan. "Study on the Stability Evaluation Inde... <1%

PLAGIARISM VERIFICATION CERTIFICATE

This is to certify that the plagiarism check has been performed for Ph.D Thesis titled, *"Landslide Hazard, Vulnerability and Risk Assessment of Aizawl Municipal Area, Mizoram, India, using Geospatial Techniques"* submitted by **Mr Z. D. LALTANPUIA**, under the supervisions of **Prof. K. SRINIVASA RAO**, Department of Geology, School of Earth Sciences and Natural Resources Management, Mizoram University, and **Dr TAPAS R. MARTHA**, Geosciences Group, National Remote Sensing Centre (NRSC), ISRO, Hyderabad. The check performed by the Scholar is found correct/adheres to MZU regulations, and authentic software, **TURNITIN** has been used for the similarity check.

Date: 19th November, 2025

Place: Aizawl

(Prof. V. P. SATI)
Dean,
School of Earth Sciences &
Natural Resources Management,
Mizoram University, Aizawl.

Dean
School of Earth Sciences
& Natural Resources Management
Mizoram University
Aizawl - 796004
Mizoram, India

ACKNOWLEDGEMENTS

Embarking on this Ph.D journey as a part-time scholar, while at the same time managing professional and family responsibilities after crossing 40 years has been both a demanding and challenging experience. The path was sometimes difficult which was fraught with obstacles that tested my resolve. This achievement, therefore, would not have been possible without the collective support, guidance and encouragement received from several individuals and institutions, to whom I am deeply indebted.

First and foremost, I thank God for His immense grace and guidance throughout every stage of my research. I experienced His presence and love during the most difficult and uncertain times of this academic journey. This humble work is a testament and a witness to His faithfulness and bountiful blessings.

I extend my sincere gratitude to my Supervisor, Prof. K. Srinivasa Rao, for his valuable guidance, supervision, and continued encouragement throughout the course of my research. Beyond his academic supervision, I am particularly grateful for his invaluable assistance in handling all the administrative formalities and University requirements to ensure my research process proceeded smoothly.

I am deeply indebted to my Co-Supervisor, Dr Tapas R. Martha, Scientist SG, Head of the Geohazards & Mineral Exploration Division, Geosciences Group, National Remote Sensing Centre (NRSC), ISRO, Hyderabad. His scientific insight, critical and meticulous observations, suggestions, and emphasis on quality research have truly influenced the development of my research. His considerate, understanding and technical guidance, and commitment to scientific excellence have enhanced my understanding of quantitative analysis, data interpretation, and scientific writing which enabled me to produce the research that I once felt was beyond my capabilities. I am privileged to have worked under his mentorship which helped me better equipped in both academic and professional terms.

I acknowledge with sincere thanks the contributions of Ms Kirti Khanna (then at NRSC, now Technology Project Manager at Accenture Technology) for her assistance in the quantitative statistical analyses in the early stage of my research. Her contributions added significant value to my research work.

I am especially grateful to Dr Susana Pereira, from the Centre of Studies in Geography and Spatial Planning, Faculty of Arts and Humanities, University of Porto, Portugal. She graciously arranged an online meeting to discuss the vulnerability and risk components of my research. Her insightful suggestions and comments were exceptionally valuable which provided direction for the later stages of my work.

My sincere gratitude extends to the authorities at the Mizoram Remote Sensing Application Centre (MIRSAC), Directorate of Science & Technology, Govt. of Mizoram. I am deeply thankful to Dr R. K. Lallianthanga, then Member Secretary, for granting me the initial permission and institutional support to pursue this research. My gratitude also goes to Er H. Lalsawmliana, the present Member Secretary, for his continued encouragement and steadfast support. My heartfelt thanks are also due to Mrs Hmingthanpuii, Principal Scientist, MIRSAC, for her consistent support and kind words of encouragement which were always a source of motivation.

I am fortunate to be surrounded by a wonderful and supportive group of colleagues at MIRSAC. Their understanding, patience, and goodwill made a remarkable difference in my academic pursuit. Among them, I am especially grateful to Dr H. Lalhmachhuana, Dr Lalramdina, Mr C. Lalzawngliana, Mr C. Vanlalengkima, and Mr R. Lalfamkima, for their collegial support and motivation, practical help, and for fostering a positive working environment.

Many thanks go to Mr Lalthanpuia, Scientist B, State Climate Change Centre, Directorate of Science & Technology, Govt. of Mizoram, for his insightful suggestions and assistance in the later stages of my research.

I am thankful to the Directorate of Geology & Mining (DGM), Govt. of Mizoram, for sharing their landslide inventory data for my study area which formed an important input for generating the landslide susceptibility maps. I am particularly grateful to Mr H. Lalbiakkima, the then Joint Director of DGM, who personally handed over the data.

I am also indebted to the elected members of various Local Councils within the Aizawl Municipality for helping classify and cross-verify the building typologies within their respective areas. I am equally thankful to the various *Mizo Upa Pawl* (Senior Citizens Organization) Units within Aizawl for sharing their members' record which formed one of the vital inputs for social vulnerability assessment.

This long journey was also made more bearable by the steadfast encouragement of my close friends. I am deeply thankful to Dr Lalrokima Chenkual, Deputy Director (Training), Directorate of Disaster Management & Rehabilitation, Govt of Mizoram, and Dr F. Lalbiakmawia, Asst. Hydrogeologist, Public Health Engineering Department, Govt of Mizoram. As fellow professionals, they uniquely understood the pressures and challenges I faced during this academic pursuit. Their unwavering support, words of encouragement, and belief in my ability to complete this research provided a morale boost during challenging times.

The faculty and staff of the Department of Geology, Mizoram University were very helpful and supportive throughout the course of my research. I am particularly thankful to Dr Jimmy Lalnunmawia, Dr J. Malsawma, Dr Paul Lalnuntluanga, and Dr Lalchawimawii, for their institutional support and encouragement during the entire period of my research.

My deepest and most heartfelt gratitude is reserved for my family. To my father, Z.D. Zotluanga, who is now bed-ridden due to his declining health condition, I fondly dedicate this humble achievement. His resilience, strength, and blessings amidst ill health have been a constant source of inspiration and motivation. And, of course, to my dear wife, Ruth Ramngaihawmi, I owe more than words can express. Her constant support, understanding, patience and faith in me were truly motivating. She shouldered the immense responsibility of managing our household and our children, especially during those periods when my research and office duties demanded most of my attention. This accomplishment is as much hers as it is mine. I am equally thankful to our children, Lalpekmawia Zadeng, Lalruatmawii Zadeng, and Lalremmawia Zadeng, for their affection, patience, and love which have been a constant source of motivation and joy even during the most difficult times.

Lastly, I thank all those others whom I have not mentioned by name, who helped and supported me in reaching this far.

Date: 27th November, 2025 (Z.D. LALTANPUIA)

Place: Aizawl

CONTENTS

DEDICATION	i
SUPERVISORS' CERTIFICATE	ii
DECLARATION	iv
CERTIFICATE ON PLAGIARISM CHECK	v
PLAGIARISM REPORTS	vi
PLAGIARISM VERIFICATION CERTIFICATE	xiii
ACKNOWLEDGEMENTS	xiv
CONTENTS	xvii
LIST OF TABLES	xxi
LIST OF FIGURES	xxiii
LIST OF PHOTO PLATES	xxv
ABBREVIATIONS/ACRONYMS	xxvi
CHAPTER 1 - INTRODUCTION	
1.1 Background	1
1.2 Statement of the Problem	3
1.3 Research Gap and Motivation	6
1.4 Research Questions and Objectives	7
1.5 Assumptions	8
1.6 Research Hypotheses	9
1.7 Significance of the Study	9
1.8 Definitions of the Terms	10
1.10 Organization of the Thesis	12
CHAPTER 2 - REVIEW OF LITERATURE	
2.1 Definition of Landslide	14
2.2 Morphology of Landslide	16
2.3 Classification of Landslide	19
2.4 Landslide Movement Types	22
2.4.1 Falls	23
2.4.2 Topples	24
2.4.3 Slides	24
2.4.4 Lateral Spreads	24
2.4.5 Flows	25
2.4.6 Complex Landslides	26
2.5 Landslide Susceptibility Vs Landslide Hazard Mapping	27
2.6 Landslide Susceptibility Mapping	28
2.6.1 Basic Assumptions	29

2.6.2 Landslide Inventory Mapping 30
2.6.2.1 Types of Inventory Maps 30
2.6.2.2 Methods and Techniques 31
2.6.3 Landslide Causative Factors 34
2.6.4 Mapping Unit 37
2.6.5 Mapping Scale 40
2.6.6 Methods of Landslide Susceptibility Zonation 41
2.6.6.1 Qualitative Approach 41
2.6.6.2 Quantitative Approach 44
2.6.6.3 Other Approaches 50
2.6.7 Classification of Landslide Susceptibility Maps 54
2.6.8 Model Evaluation and Validation 55
2.6.8.1 Data Partitioning Strategies 56
2.6.8.2 Data Splitting Ratio in Random Partitioning 57
2.6.8.3 Techniques or Metrics used 58
2.7 Vulnerability 60
2.7.1 The Paradigm Shift in Understanding Vulnerability 62
2.7.2 Components of Vulnerability 64
2.7.3 Dimensions of Vulnerability 65
2.8 Social Vulnerability 67
2.8.1 Factors Influencing Social Vulnerability 68
2.8.2 Approaches for Social Vulnerability Measurements 70
2.9 Physical Vulnerability 74
2.9.1 Defining Physical Vulnerability: Diverse Perspectives 74
2.9.2 Factors Influencing Physical Vulnerability 77
2.9.3 Assessment Approaches/Models 78
2.10 Risk Assessment 82
2.10.1 Definitions and Concepts 82
2.10.2 Conceptual Frameworks 83
2.10.3 Risk Assessment Approaches 86
2.10.4 Challenges and Limitations 89
2.11 Previous Works on Landslide Assessment within Aizawl City 90
2.11.1 Site Specific Studies 90
2.11.2 Synoptic and Hazard/Susceptibility Zonation Studies 95
2.12 Summary 100

CHAPTER 3 - STUDY AREA
3.1 Location & Extent 101
3.2 Origin and History 101
3.3 Growth and Expansion 103
3.4 Administration 105

3.5 Demography and Socio-Economic Conditions 106
3.6 Transportation & Road Network 108
3.7 Climate 110
3.8 Temperature 110
3.9 Rainfall 111
3.10 Geology and Geomorphology 112
3.11 Soils 118
3.12 Drainage 118
3.13 Past Landslide incidents in Aizawl municipal area 120

CHAPTER 4 - LANDSLIDE SUSCEPTIBILITY ASSESSMENT
4.1 Data 128
4.2 Landslide Inventory Preparation 129
4.3 Generation of Predisposing Factors 130
4.3.1 Topographical Factors 131
4.3.2 Geological Factors 135
4.3.3 Hydrological Factors 135
4.3.4 Land Cover Factors 139
4.4 Landslide Susceptibility Models 141
4.4.1 Information Value (IV) Model 141
4.4.2 Frequency Ratio Model 142
4.4.3 Weight of Evidence Model 142
4.5 Validation of the Models 144
4.6 Summary 145

CHAPTER 5 - VULNERABILITY AND RISK ASSESSMENTS
5.1 Data 147
5.2 Social Vulnerability Assessment 148
5.2.1 Sensitivity 150
5.2.2 Lack of Resilience 151
5.2.3 Standardization and Social Vulnerability Index Calculation 153
5.3 Physical Vulnerability Assessment 154
5.3.1 Classification of Buildings and Roads 155
5.3.2 Assignment of Weights 157
5.3.3 GIS-based intersection and Vulnerability index calculation 158
5.4 Combination of Social and Physical Vulnerabilities 159
5.5 Risk Assessment 160
5.6 Summary 161

CHAPTER 6 - RESULTS AND DISCUSSION
6.1 Landslide Susceptibility Map Generation and Classification 162

6.2 Validation of Landslide Susceptibility Models 165
6.3 Spatial Correlation of Predisposing Factors and Landslide Occurrence 167
6.4 Social Vulnerability 172
6.5 Physical Vulnerability 176
6.6 Combined Vulnerability 180
6.7 Landslide Risk 182
6.8 Limitations of the Study 186

CHAPTER 7 - CONCLUSION AND RECOMMENDATIONS
7.1 Landslide Susceptibility 188
7.2 Social Vulnerability 189
7.3 Physical Vulnerability 190
7.4 Combined Vulnerability 191
7.5 Landslide Risk 191
7.6 Recommendations 192
7.6.1 For Landslide Risk Reduction and Management 193
7.6.2 For Future Research and Methodological Improvements 194

REFERENCES 197

Brief Bio-data of the Candidate
Particulars of the Candidate
Publications

LIST OF TABLES

Table 1.1	Global landslide statistics during 2000–2024 as per EM-DAT database	2
Table 1.2	Important landslides within Mizoram	5
Table 2.1	Definitions of landslide features referred to in Figure 2.1 & 2.2	18
Table 2.2	*Varnes (1978)* classification of landslides updated by *Cruden and Varnes (1996)*	22
Table 2.3	Classification of velocity of movement of landslides (*Cruden & Varnes, 1996; AGS, 2002*)	23
Table 2.4	Landslide Causative Factors	35
Table 2.5	Classification and characteristics of different mapping units (after *Zhao et al., 2021*)	39
Table 2.6	Landslide zoning mapping scales and their application (after *Fell et al., 2008*)	42
Table 2.7	The main metrics used in model evaluation (after *Huang et al., 2022*)	61
Table 2.8	Some key definitions of Vulnerability	63
Table 2.9	Definitions of Social Vulnerability (adapted from *Tapsell et al., 2010*)	68
Table 2.10	Factors that influence social vulnerability (adapted from *Cutter et al., 2003*)	71
Table 2.11	Definitions of Physical Vulnerability (adapted from *Fuchs et al., 2018*)	75
Table 2.12	Overview of existing models for physical building vulnerability assessment (modified from *Papathoma-Kohle et al., 2017; Singh et al., 2017a* and *Fuchs et al., 2019*)	80
Table 2.13	Summary of landslide risk assessment approaches	88
Table 3.1	Lithostratigraphic succession of the study area (after *Haokip et al., 2024*)	114
Table 3.2	List of Important Landslide Events within Aizawl	126
Table 4.1	Details of data used in the study	128
Table 5.1	Indicators for Sensitivity	149
Table 5.2	Indicators for Lack of Resilience	149
Table 5.3	Social Vulnerability Class	154
Table 5.4	Number of different building types and their weights	157

Table 5.5	Length of different road classes and their weights	157
Table 5.6	Physical Vulnerability Classes	159
Table 5.7	Combined Vulnerability Class	160
Table 6.1	Area occupied by different susceptibility zones	164
Table 6.2	Spatial association of factor classes with landslides in the IV, FR & WofE models	168
Table 6.3	Distribution of social vulnerability class across various local councils	173
Table 6.4	Distribution of building vulnerability class	177
Table 6.5	Distribution of road vulnerability class	178
Table 6.6	Distribution of combined vulnerability class	181
Table 6.7	Distribution of building risk class	183
Table 6.8	Distribution of road risk class	184

LIST OF FIGURES

Figure No.	Figure Caption	Page
Fig. 2.1	Block diagram of idealized rotational failure earth flow, modified after *Varnes (1978)*	17
Fig. 2.2	A diagrammatic illustration of Landslide features (after *IAEG, 1990; Cruden and Varnes, 1996)*	17
Fig. 2.3	Different types of Landslides (after *Highland & Bobrowsky*, *2008*)	26
Fig. 2.4	A diagrammatic illustration of the bivariate statistical method after *van Westen et al. (1997)*	45
Fig. 2.5	An overview of the multivariate statistical method after *van Westen et al. (1997)*	48
Fig. 2.6	General workflow of the physically based approaches after *Ye et al. (2025)*	50
Fig. 2.7	Deductive approach for social vulnerability assessment adapted from *Tate (2012)*	72
Fig. 2.8	Inductive approach for social vulnerability assessment adapted from *Tate (2012)*	72
Fig. 2.9	Framework for Landslide Risk Assessment and Management after *Fell et al. (2008)*	86
Fig. 3.1	Location map of the study area showing different municipal wards	102
Fig. 3.2	Map showing the 76 Local Councils within the Aizawl Municipal area	107
Fig. 3.3	Road network map of the Aizawl municipal area	109
Fig. 3.4	Trend of average annual maximum, mean and minimum temperature of Aizawl from 1986 to 2024	111
Fig. 3.5	Annual total rainfall of Aizawl (in mm) from 1986 to 2024	112
Fig. 3.6	Geological Map of Aizawl Municipal Area (Background image: ESRI)	115
Fig. 3.7	Soil Map of the study area (modified after *SRSC, 2006*)	119
Fig. 3.8	Drainage Map of the study area (Background image: ESRI)	121
Fig. 4.1	Landslide Inventory Map of the Study Area	130
Fig. 4.2	Slope Aspect Map of the Study Area	132
Fig. 4.3	Slope Gradient Map of the Study Area	132
Fig. 4.4	Elevation Map of the Study Area	133
Fig. 4.5	Plan Curvature Map of the Study Area	134

Fig. 4.6	Profile Curvature Map of the Study Area	134
Fig. 4.7	Lineament Density Map of the Study Area	136
Fig. 4.8	Drainage Density Map of the Study Area	137
Fig. 4.9	Stream Power Index Map of the Study Area	138
Fig. 4.10	Topographic Wetness Index Map of the Study Area	138
Fig. 4.11	LULC Map of the Study Area	139
Fig. 4.12	NDVI Map of the Study Area	140
Fig. 4.13	Flowchart of the Methodology for preparing Landslide Susceptibility Maps	145
Fig. 5.1	Building footprints and roads delineated from Google Image	148
Fig. 5.2	Indicators for Sensitivity. a) Children Population, b) Elders Population, c) Female Population, d) Illiterate Population, and e) Population Density	150
Fig. 5.3	Indicators for Lack of Resilience. a) Rented Accommodation, b) Without Electricity, c) Without Assets, d) Low Income, and e) Non-Workers	152
Fig. 5.4	Maps showing a) Sensitivity and b) Lack of Resilience	153
Fig. 5.5	Typical buildings of the study area. a) RCC building, b) Semi-RCC building, and c) AT building	155
Fig. 5.6	Different road types of the study area. a) Metalled Road, b) Bridge, and c) Unmetalled Road	156
Fig. 5.7	Vulnerability Matrix. Red colour indicates high, yellow colour represents moderate, and green colour indicates low classes	158
Fig. 5.8	Methodological flowchart of the Landslide Risk Assessment	161
Fig. 6.1	Landslide Susceptibility Map prepared using IV Method	163
Fig. 6.2	Landslide Susceptibility Map prepared using FR Method	163
Fig. 6.3	Landslide Susceptibility Map prepared using WofE Method	164
Fig. 6.4	Area occupied by different landslide susceptibility zones	165
Fig. 6.5	Distribution of landslides falling into different susceptibility zones. a) IV Method, b) FR Method, and c) WofE Method	166
Fig. 6.6	Curves showing a) Success rate of the landslide susceptibility models, b) Prediction rate of the landslide susceptibility models	166
Fig. 6.7	Social Vulnerability Map of the Study Area	173
Fig. 6.8	Contributions of the indicators to the Social Vulnerability	175
Fig. 6.9	Physical Vulnerability Map of the Study Area	176
Fig. 6.10	Combined Vulnerability Map of the Study Area	180
Fig. 6.11	Landslide Risk Map of the Study Area	183

LIST OF PHOTO PLATES

Photo Plate No.	Caption	Page
Photo Plate 3.1	Aizawl Bazaar in 1890	104
Photo Plate 3.2	Aizawl in the year 1954	105
Photo Plate 3.3	A panoramic view of Aizawl city in the present-day	105
Photo Plate 3.4	Massive Sandstone bed overlain by thinly-bedded Shale	113
Photo Plate 3.5	Thinly-bedded weathered Shale unit	113
Photo Plate 3.6	A highly-jointed Shale unit	116
Photo Plate 3.7	A narrow flatland along Chite valley surrounded by dissected hills	117
Photo Plate 3.8	The Laipuitlang landslide (11 May, 2013) was one of the deadliest incidents	122
Photo Plate 3.9	The landslide along Bawngkawn-Thuampui road corridor (26 July, 2019)	123
Photo Plate 3.10	The landslide at the BSUP complex, Durtlang (2 July, 2019)	124
Photo Plate 3.11	The landslide at Melthum (28 May, 2024)	125
Photo Plate 3.12	Recurrent landslide activity at Hunthar Veng	125

ABBREVIATIONS/ACRONYMS

ACC	Accuracy
AGS	Australian Geomechanics Society
AHP	Analytical Hierarchy Process
AI	Artificial Intelligence
ALARP	“As Low As Reasonably Practicable”
ALOS	Advanced Land Observing Satellite
AMC	Aizawl Municipal Corporation
ANN	Artificial Neural Networks
AT	Assam-Type (Building)
AUC	Area Under the Curve
BGS	British Geological Survey
BIS	Bureau of Indian Standards
BMTPC	Building Materials Technology Promotion Council
BSUP	Basic Services to Urban Poor
CNN	Convolutional Neural Network
COSMO	COnstellation of small Satellites for Mediterranean basin Observation
CoSMR	Continuous Slope Mass Rating
CRED	Centre for Research on the Epidemiology of Disasters
DEM	Digital Elevation Model
DInSAR	Differential Interferometric SAR
DL	Deep Learning
DLNN	Deep Learning Neural Networks
DM&R	Disaster Management & Rehabilitation
DRR	Disaster Risk Reduction
DT	Decision Tree
DTM	Digital Terrain Model
EM-DAT	Emergency Events Database
EPOCH	European Programme on Climate and Natural Hazards
FCC	False Colour Composite
FCN	Fully Convolutional Network
FN	False Negatives
FoS/FS	Factor of Safety
FP	False Positives
FPR	False Positive Rate
FR	Frequency Ratio

GBDT	Gradient Boosting Decision Trees
GB-InSAR	Ground-Based Interferometric SAR
GCI	Galvanized Corrugated Iron
GIS	Geographic Information System
GSI	Geological Survey of India
HRVA	Hazard Risk and Vulnerability Analyses
IAEG	International Association of Engineering Geology
IDNDR	International Decade for Natural Disaster Reduction
InSAR	Interferometric SAR
IPCC	Intergovernmental Panel on Climate Change
IRS	Indian Remote Sensing Satellites
ISSMGE	International Society of Soil Mechanics and Geotechnical Engineering
IUGS	International Union of Geological Sciences
IV	Information Value
JNNURM	Jawaharlal Nehru National Urban Renewal Mission
KNN	K-Nearest Neighbour
LAD	Local Area Development
LEM	Limit Equilibrium Method
LHEF	Landslide Hazard Evaluation Factor
LHI	Landslide Hazard Index
LHZ	Landslide Hazard Zonation
LiDAR	Light Detection and Ranging
LIME	Local Interpretable Model-agnostic Explanations
LISS	Linear Imaging Self-Scanning Sensor
LNRF	Landslide Nominal Risk Factor
LR	Logistic Regression
LRA	Landslide Risk Assessment
LSI	Landslide Susceptibility Index
LSTM	Long Short-Term Memory Networks
LSZ	Landslide Susceptibility Zonation
LULC	Land Use Land Cover
MAE	Mean Absolute Error
MCC	Matthews Correlation Co-efficient
MIRSAC	Mizoram Remote Sensing Application Centre
ML	Machine Learning
MoRTH	Ministry of Road Transport & Highways
MOVE	Methods for the Improvement of Vulnerability Assessment in Europe
MSE	Mean Squared Error

MTD	Mass-Transport Deposits
MTI	Multi-temporal Interferometry
MUP	Mizo Upa Pawl
NB	Naive Bayes
NDMA	National Disaster Management Authority
NDVI	Normalized Difference Vegetation Index
NH	National Highway
NPV	Negative Predictive Value
NRSC	National Remote Sensing Centre
OA	Overall Accuracy
OBIA	Object-Based Image Analysis
OFDA	Office of U.S. Foreign Disaster Assistance
OOA	Object-Oriented Analysis
PAN	Panchromatic
PBIA	Pixel-Based Image Analysis
PCA	Principal Component Analysis
PDP	Partial Dependence Plot
PPV	Positive (or Precision) Predictive Value
PRC	Prediction Rate Curve
PRS	Personal Residence Surcharge
PSI	Persistent Scatterer Interferometry
RCC	Reinforced Cement Concrete
RF	Random Forest
RFE	Recursive Feature Elimination
RHRS	Rockfall Hazard Rating System
RMR	Rock Mass Rating
RMSE	Root Mean Square Error
RNN	Recurrent Neural Networks
ROC	Receiver Operating Characteristic
RS	Remote Sensing
SAR	Synthetic Aperture Radar
SD&SM	Slope Development and Slope Modification
SDFC	Standardized Discriminant Function Coefficient
SHALSTAB	Shallow Landslide Stability
SHAP	SHapley Additive exPlanations
SHETRAN	Système Hydrologique Européen TRANsport
SINMAP	Stability Index Mapping
SMR	Slope Mass Rating
SoVI or SVI	Social Vulnerability Index

SPI	Stream Power Index
SQM	Semi-Quantitative Method
SRC	Success Rate Curve
SRSC	State Remote Sensing Application Centre
SSI	Structural Similarity Index
SVM	Support Vector Machine
TEHD	Total Estimated Hazard
TN	True Negatives
TOPSIS	Technique for Order Preference by Similarity to Ideal Solution
TP	True Positives
TPR	True Positive Rate
TRIGRS	Grid-based Regional Slope-stability
TSS	Total Skill Score
TWI	Topographical Wetness Index
UAV	Unmanned Aerial Vehicle
UNDRO	Office of the United Nations Disaster Relief Co-ordinator
UNDRR	United Nations Office for Disaster Risk Reduction
UNESCO	United Nations Educational, Scientific and Cultural Organization
UNISDR	United Nations International Strategy for Disaster Reduction
USDA	U.S. Department of Agriculture
USGS	U.S. Geological Survey
UTM	Universal Transverse Mercator
VC	Village Council
VHR	Very High Resolution
WGS	World Geodetic System
WP/WLI	Working Party on World Landslide Inventory
XAI	eXplainable Artificial Intelligence
XGB	XGBoost
YS-Slope	Yonsei Slope

CHAPTER 1

INTRODUCTION

1.1 Background

Landslides, being one of the most destructive natural hazards, cause significant damage to life and property around the world. They are considered as the third most significant type of natural disaster on a global scale (van Westen et al., 2011). During the 1990s, about 9% of worldwide occurrence of all natural disasters were attributed to landslides (Yilmaz, 2009; Mousavi et al., 2011). It has been estimated that every year, landslides claim the lives of roughly 1000 people and destroy property worth $4 billion[1] (Lee & Pradhan, 2007; Karsli et al., 2009). Between 2006 and 2016, a total of 4,862 catastrophic landslide events were recorded which resulted in more than 55,000 fatalities worldwide (Froude & Petley, 2018). In 2019, landslides account for 17% of the fatalities associated with natural hazards each year (Aristizábal & Sánchez, 2020; Sim et al., 2022). Due to the unplanned urbanization and fast pace of increase in population, the developing countries are even more vulnerable to landslide hazard (Petley, 2012a). The developing countries experienced more than 95% of all disasters and deaths associated with landslide and other types of mass movement (Hansen, 1984; Aleotti & Chowdhury, 1999). Landslides cost developing countries 0.5% of their gross national product each year (Mandal & Mondal, 2019). Many researchers conclude that the threats from landslides are much greater than are generally recognized in many countries, causing an annual loss of property greater than any other natural disaster, including earthquakes, storms and floods (Glade, 1998; Guzzetti et al., 1999). Landslide research has drawn worldwide attention owing to a growing awareness and concern on the socio-economic impact of landslides (Aleotti & Chowdhury 1999; Champati Ray & Lakhera, 2004). It is also partly due to its frequency of occurrence among other natural hazards. According to the International Disaster Database (EM-DAT) data, during 2000–2024, landslides caused 18,653 deaths and affecting over 8 million people worldwide (Table 1.1). In reality, however, the number of deaths, people affec-

[1] Unless otherwise specified, all Dollar ($) references used in the chapter are in US Dollars

ted and property damages will be much more, as data on a global scale may not include several unreported incidents. This often leads to underestimation of the impacts and number of landslide events in the report (Petley, 2012a; Kirschbaum et al., 2015; Froude & Petley, 2018).

Table 1.1
Global landslide statistics during 2000–2024 as per EM-DAT database (OFDA/CRED 2025)

Continents		No. of Events	Total Deaths	Injured	Homeless	Total Affected	Damage US (000'S)
Africa	Total	65	3,449	604	23,878	2,85,344	71,312
	Avg/event	-	53	9	367	4,390	1,097
Americas	Total	90	3,292	1,153	2,07,293	5,64,153	25,85,741
	Avg/event	-	37	13	2,303	6,268	28,730
Asia	Total	244	11,641	2,472	1,80,610	78,83,939	31,95,509
	Avg/event	-	48	10	740	32,311	13,096
Europe	Total	10	66	37	3	7,381	10,41,887
	Avg/event	-	7	4	0	738	1,04,189
Oceania	Total	12	205	32	10,000	19,044	60,000
	Avg/event	-	17	3	833	1,587	5,000
TOTAL		**421**	**18,653**	**4,298**	**4,21,784**	**87,59,861**	**69,54,449**

In addition to the loss of life, landslides also cause severe economic damage. The estimated global annual economic loss due to landslides is $20 billion, representing 17% of total global disaster losses from 1980-2013, which amount to $121 billion annually (Klose et al., 2016). Japan and Italy suffer the highest economic loss, with estimated annual losses of $4 billion and $2.6–5 billion, respectively. Other countries with significant financial losses include India ($1.3 billion), China ($0.5 billion), and Brazil ($0.35 billion) (Sim et al., 2022). In Colombia, landslides have resulted in economic damages exceeding $654 million from 1900 to 2018 (Aristizábal & Sánchez, 2020). Moreover, in the US alone, landslides cause approximately $2 billion economic losses and thousands of deaths each year (Hart, 2024). With the increasing occurrence of severe weather events linked to global climate change, the worldwide impacts of landslides are increasing further. This emphasizes the urgent need for improved risk assessment, mitigation strategies, and policy interventions.

India is a vast country with varied topographic as well as climatic conditions, and frequent occurrence of landslide disasters are no exception. In fact, India ranks the first in terms of fatal landslide occurrences in the world (Froude & Petley, 2018). About 12.6% of land area of the country (approximately 0.42 million km^2) is susceptible to landslide hazard (Kaur et al., 2017; Mani et al., 2024). In India, landslide activity is mostly observed in the Himalayan region, the Western Ghats and the Nilgiri ranges in the south (Martha et al., 2021). During the year 1998–2018, more than 75,000 landslide events were recorded across the country (NRSC, 2023). Among these, the Northwest Himalayan region accounts for 66.5% of the total events while the Northeast Himalayas account for 18.8%. It is no surprise that the Himalayan region contribute to almost 15% of the global rainfall-induced landslides (Dikshit et al., 2020a; Bhat, 2024). The National Disaster Management Authority (NDMA), in 2019, estimated that the annual losses due to landslides in India were approximately ₹150–200 crores (Das et al., 2023). In terms of fatalities, more than 300 lives were lost every year due to landslides in India as per the reports by the National Crime Records Bureau (2010–2019) (Roy et al., 2022). These figures are likely to increase in the present-day situations considering the climatic change scenarios and the fast pace of population growth in the hilly regions (Stanley et al., 2024).

1.2 Statement of the problem

Mizoram, located in the north-east India is the southern extension of the north-east Indian Himalayas and is considered to be one of the most landslide prone regions in the country. According to the Landslide Atlas of India (NRSC, 2023), Mizoram topped the list in recording the highest number of landslide incidences across the country during 1998–2022. Landslide is the most frequent natural hazards experienced by the state. A number of landslides have been reported each year from various locations, particularly during the monsoons. This causes a great deal of misery to public, and sometimes results in the loss of life and property. It also damages transportation lines and communication networks, apart from causing economic burden on the society. Neo-tectonism, young geology, high degree of slope and relief, heavy precipitation and unplanned land use practices are the factors which contribute to the high susceptibility of landslides in the region (Tiwari et al., 1996).

In the past years, several disastrous landslides have occurred within Mizoram. The year 1929 was known as *Minpui Kum* which literally means “Year of Mass Landslides” where it rained continuously for ten days, causing numerous landslides across the state. On 9 August, 1992, a stone quarry collapsed at Hlimen locality within Aizawl which claimed about 66 lives, and damaged 17 houses. Heavy cloudburst on 16 and 17 May, 1995 resulted in massive mass movements at Lawngtlai and Saiha districts, wherein 33 people lost their lives and affected 737 houses. As per the Disaster Management & Rehabilitation (DM&R) Department records, landslides resulted in 127 fatalities and injured 110 people between 2006 and 2023, besides affecting 8,758 houses within the entire state (DM&R, 2020; 2023). More recently, due to heavy rainfall which accompanied Cyclone Remal in May 2024, devastating landslides occurred at several places. This event claimed approximately 40 lives with several properties destroyed across the entire state. Some of the severe landslides occurred within Mizoram are presented in Table 1.2.

Aizawl city, the state capital has experienced several decades of rapid and uncontrolled urbanization, which resulted in unplanned development and haphazard construction along the steep and unstable slopes (Rodgers & Tobin, 2014). Construction of infrastructural developmental activities have often been carried out without considering the bearing capability of the land, which increase the vulnerability of both the population and physical structures to landslide hazards. The basic infrastructures including roads, drainages and sewerage systems have not kept pace with its rapid growth. Many of the buildings were constructed without strictly adhering to the building codes and engineering designs. Moreover, as urbanization continues, there is a proportional increase in population density which subsequently led to the increasing vulnerability of the local residents. The risks of landslides in Aizawl are further amplified by factors such as increasing population, unplanned urbanization, disparities in socio-economic conditions, constructions in high-hazard zones, and increasing climatic change. These issues collectively pose a significant threat to the city and its long-term development. In view of all these, it is important to develop and adopt a scientific approach to assess vulnerabilities and risks associated with landslides. This will be a valuable tool for administrators and decision-makers involved in disaster mitigation and risk reduction programmes.

Table 1.2 *Important landslides within Mizoram* (DM&R, 2020; 2023)

Date/Year	Location	Description	Casualty/Affected
1 – 10 June, 1929	Whole Mizoram	Known as "Minpui kum". Due to incessant rainfall, numerous landslides occurred in the entire state	Data not available
11 July, 1986	South Hlimen, Aizawl	Landslide/Rockslide	4 persons dead
1991	Sihpui & Ramthar Veng, Aizawl	Sinking/subsidence of hill slope	70 houses destroyed
9 August, 1992	South Hlimen, Aizawl	Stone quarry collapsed	66 persons dead; 17 houses destroyed
1992	Hunthar Veng, Aizawl	Recurrent slide/sinking occurred. This occurred again in 1993, 1995, 1996, 1997, 2001, 2003, 2005, 2006, 2007, 2008, 2010, 2011	NH-44A and 17 houses damaged
16– 17 May, 1995	Lawngtlai and Saiha Districts	Heavy coudburst results in massive landslides	33 persons dead; 6 others injured; 737 houses damaged
2004	Ngopa Village	Subsidence of land within the settlement	45 houses along with 55 families affected
2004-05	Armed Veng, Aizawl	Subsidence of land	More than 100 houses affected; 25 houses vacated
2005	Chanmari West, Aizawl	Subsidence/sinking of land	30 houses vacated
September, 2007	Mamit District	Several landslides throughout the district	NH-44A blocked for 13 days
2010	Mamit Town and Ngopa Village	Subsidence of land within the settlement	66 and 10 houses destroyed in Mamit town and Ngopa village, respectively
21 July, 2012	Keifang Stone Quarry	Rockfall at the quarry swept a bus down a ravine	19 persons killed and injured 16 others
8 August, 2012	Aizawl-Tuirial Road	Debris slide swept a local taxi down a cliff	3 persons killed and injured 3 others
11 August, 2012	Ramhlun Sports Complex and Ramhlun Vengthar, Aizawl	Reactivation of Subsidence/sinking of land from 2004	7 houses damaged; 56 families were evacuated
11 May, 2013	Laipuitlang, Aizawl	Landslide of translational character	17 persons killed and injured 9 persons; destroyed 12 houses
July, 2013	Ramhlun Sports Complex and Ramhlun Vengthar, Aizawl	Reactivation of Subsidence/sinking of land	15 houses destroyed and several families evacuated

Table 1.2 (continued)

Date/Year	Location	Description	Casualty/Affected
May - July, 2017	Aizawl, Lunglei and Lawngtlai Districts	Heavy rainfall caused flooding along the major rivers within the district, along with several landslides	13 persons dead; 1,144 pucca houses and 2,878 kutcha houses were damaged
4 June, 2018	Lunglawn, Lunglei	Debris slide	10 persons died; one house completely damaged
11 June, 2018	Kanaan Veng, Hnahthial Town	Landslide	Total damage of NH-06
12 June, 2018	Hunthar Veng, Aizawl	Recurrent slide/sinking occurred	29 families evacuated during 2015-2019
19 July, 2019	Aizawl to Champhai Road	Landslide	NH-06 totally damaged near Haidai stream
19 July, 2019	Mualkhang	Landslide	NH-306 completely blocked
25 July, 2019	Bawngkawn, Aizawl	Landslide	NH-06 completely blocked
July, 2019	College Veng, Lunglei	Subsidence/sinking of land	12 families were evacuated; 7 residential houses dismantled
2 July, 2019	Durtlang, Aizawl	Landslide of translational character	3 blocks of BSUP concrete building collapsed as a result of which 3 persons dead and injured 11 others; 138 families were evacuated

1.3 Research Gap and Motivation

Within the Aizawl municipal area, quite a number of hazard assessment studies have been undertaken in the form of hazard and/or susceptibility zonation, geotechnical and site-specific studies. However, studies on the different vulnerabilities and risks associated with landslides are very meagre and limited. The effects of landslides on the various indicators of vulnerability such as physical, socio-economic and demographics, and the subsequent risk analyses have not yet been thoroughly investigated and studied. The lack of comprehensive and detailed studies in this aspect highlights a significant lacuna in understanding and addressing the damages caused by landslides. Furthermore, translating research findings into actionable information for decision-makers still remains a challenge.

In order to address all these issues, the present study is taken up to assess the landslide susceptibility/hazard, to examine and evaluate the vulnerabilities, both physical and socio-economic aspects in order to have a clear picture on the exposure of people and infrastructures to landslide hazard. By integrating both hazard and vulnerabilities, landslide risk assessment in the Aizawl municipal area is carried out. Focusing on quantitative statistical models for susceptibility mapping, and quantifying the vulnerabilities, this research aims to provide a more comprehensive and accurate understanding of landslide risk. The findings of this research are expected to contribute to a more understanding of the spatial distribution of landslide hazard, vulnerabilities and risk, better-informed land-use planning decisions, and ultimately, enhanced resilience to landslide disasters.

1.4 Research Questions and Objectives

The aim of this research is to assess the different levels of landslide risk within the study area, derived from the analyses of landslide hazard/susceptibility and the physical and socio-economic vulnerabilities. Therefore, the present study aims to answer the following questions:

- What is the spatial distribution of landslide hazard/susceptibility within the study area?
- What are the most contributing factors for the susceptibility of landslides within the study area?
- What are the elements at risk?
- What is the level of physical vulnerability based on building and road network?
- What is the level of social vulnerability based on different socio-economic and demographic indicators?
- What are the most contributing factors of social vulnerability?
- What is the level of landslide risk within the Aizawl municipal area?
- What factor influences the risk of landslide?

With a view to answer the above questions, the present study has been carried out with the following objectives:

1) To map the landslide-prone areas within the study area

2) To assess physical and social aspects of vulnerability

3) To assess the degree of landslide risk within the study area

1.5 Assumptions

While carrying out the present research, the following assumptions were made:

- Landslide susceptibility conditions, particularly rainfall-triggered shallow landslides, are assumed consistent throughout the period of this study.
- Data obtained for the present study from various sources including official sources, fieldwork, and previous studies, along with the methodological frameworks adopted are reliable and adequate for the analyses.
- Geospatial and statistical models used are calibrated to represent realistic conditions.
- The socio-economic and demographic data (from the 2011 Census) provide a baseline for assessing social vulnerability, with the recognition and acceptance that remarkable demographic and socio-economic changes over the past decade may not be fully captured, which can influence the current vulnerability assessment.
- Structural resilience is assumed to be adequately represented by the materials used in the construction in spite of data constraints in other factors.
- Risk assessment results specifically for infrastructures within the study area are valid despite the absence of past landslide damage data for validation.
- The exclusion of landslide magnitude, temporal characteristics, and population-specific risk assessments due to data limitations is acceptable for the current study scope.

1.6 Research Hypotheses

The present research aims to test the following hypotheses:

- Landslide susceptibility varies with topographic factors (e.g., slope angle), land use/land cover, and lithological variations.
- Physical vulnerability remarkably differs based on the type of construction materials used.
- Socio-economic vulnerability is influenced by demographic factors such as gender, dependency ratios, literacy rates, housing conditions, and population density.
- Higher combined vulnerability correlates positively with higher levels of landslide risk within the study area.

1.7 Significance of the Study

Landslides represent a significant and persistent threat to human life, infrastructure, and economic stability, particularly in rapidly urbanizing hilly settlements such as Aizawl. This study holds great significance for several reasons. Firstly, it contributes directly to enhancing disaster management practices within Mizoram by providing spatial insights into the landslide susceptibility, hazard, vulnerabilities and associated risks. Such knowledge is specifically important for informed policy-making, strategic urban planning, and the implementation of targeted mitigation measures. Secondly, the comprehensive evaluation of both physical and socio-economic vulnerabilities in the present study offers some important perspectives that are often overlooked in conventional landslide studies, thereby promoting a broader understanding of disaster impacts on diverse community sectors. Thirdly, by utilizing geospatial and statistical techniques, this research serves as a methodological framework that can be replicated in similar geographic and socio-economic contexts across other landslide-prone areas. Consequently, the outcomes of this study are anticipated to substantially contribute to the knowledge on landslide risk reduction, disaster resilience, and sustainable urban development in Aizawl and similar contexts worldwide.

1.8 Definitions of the terms

In the context of landslide risk assessment, the terms hazard, vulnerability, and risk are often used in an interdisciplinary manner, comprising physical, environmental, and socio-economic dimensions. Owing to the complexity and overlapping interpretations of these terms across different scientific domains, it is essential to adopt clear and consistent definitions that align with widely accepted frameworks. This section provides the working definitions of these concepts as used throughout the present study.

Hazard: A hazard is a potentially damaging physical event, phenomenon, or human activity that may cause the loss of life or injury, property damage, social and economic disruption, or environmental degradation. In the context of geomorphological processes, natural hazards include phenomena such as landslides, earthquakes, cyclones, and floods. As per the United Nations Office for Disaster Risk Reduction (UNDRR, 2020), a hazard is defined as "a process, phenomenon or human activity that may cause loss of life, injury or other health impacts, property damage, social and economic disruption or environmental degradation."

Hazards can be natural (landslides, earthquakes), technological (industrial accidents), or anthropogenic (human-induced). Wisner et al. (2004) emphasized that the notion of hazard must also consider the social construction of risk, particularly how certain populations are more exposed due to systemic vulnerabilities.

Susceptibility: In the context of landslides, susceptibility refers to the likelihood or spatial probability of landslide occurrence in a given area based on the intrinsic characteristics of the terrain (Brabb, 1984), without considering the temporal frequency or potential consequences of such events. It represents the predisposition of a slope or terrain unit to fail under existing environmental and geological conditions.

According to Corominas et al. (2015 & 2023), susceptibility is formally defined as "a quantitative or qualitative assessment of the volume (or area) and spatial distribution of landslides that exist or potentially may occur in an area. Susceptibility may also include a description of the velocity and intensity of the existing or potential landslides". Landslide susceptibility assessment is the initial step toward comprehensive landslide hazard and risk assessment (Martha et al., 2013). It can also be an end product used for land-use planning and environmental impact assessment, especially in areas where data scarcity prevents a full hazard evaluation (Corominas et al., 2014).

Vulnerability: Vulnerability refers to the conditions determined by physical, social, economic, and environmental factors or processes which increase the susceptibility of an individual, a community, assets, or systems to the impacts of hazards. Vulnerability determines the degree to which a system or element is likely to experience harm due to exposure to a hazard.

The Intergovernmental Panel on Climate Change (IPCC, 2014) defines vulnerability as "the propensity or predisposition to be adversely affected. Vulnerability encompasses a variety of concepts and elements including sensitivity or susceptibility to harm and lack of capacity to cope and adapt."

In landslide risk assessment, vulnerability is often categorized into different dimensions, such as physical vulnerability (structural susceptibility of infrastructure), social vulnerability (demographic and socioeconomic attributes), economic vulnerability (livelihood dependence and resource loss), and environmental vulnerability (eco-system fragility and degradation).

Wisner et al. (2004) further highlighted that vulnerability is deeply rooted in socio-political structures and inequalities, which often dictate differential access to resources and decision-making power, thus shaping the uneven distribution of disaster impacts.

Risk: In the context of landslides, risk refers to the expected consequences resulting from the interaction between landslide hazards and the exposed elements at risk, considering their vulnerability. It quantifies the potential for losses such as fatalities, injuries, property damage, infrastructure disruption, and economic impacts arising from landslide occurrences within a specified area and timeframe.

Following Varnes (1984), landslide risk can be defined as "the expected number of lives lost, persons injured, damage to property, or disruption of economic activity due to a landslide hazard for a given area and period." This formulation emphasizes both the probability of a landslide event and the severity of its consequences on vulnerable elements exposed to the hazard.

The assessment of landslide risk requires integration of spatial data on landslide susceptibility or hazard, demographic and infrastructure exposure, and the degree of vulnerability of these elements. This risk-based approach enables prioritization of mitigation strategies and supports effective decision-making in land-use planning and disaster risk reduction.

In the context of landslides, risk assessment seeks to quantify the expected consequences such as fatalities, building damage, or economic losses due to landslide activities. Risk can be qualitative, semi-quantitative, or quantitative, depending on data availability and methodological approaches. van Westen et al. (2008) expanded upon these principles by developing spatially explicit methods to model risk through the integration of hazard zonation, vulnerability indices, and exposure layers.

1.9 Organization of the Thesis

This thesis is organized into seven chapters, each of which addresses specific components of the research related to landslide hazard, vulnerability and risk assessment in the Aizawl municipal area. A brief overview of each chapter is presented below:

Chapter 1 serves as the introduction to the research. It firstly presents the background of the study by discussing the global and national significance of landslides as a hazard. It outlines the problem statement, identifies the research gaps that motivate this study, and defines the research questions and objectives. The significance of the study along with definitions of important terms used in the thesis are also presented.

Chapter 2 provides a comprehensive review of the existing literature. It presents a detailed review of the fundamental concepts of landslides, including their definitions, types, and classifications. The chapter examines current trends and methodologies in landslide research, with a specific focus on susceptibility and hazard using geospatial technologies. The chapter further explores the concepts of social and physical vulnerabilities, and also the concepts and frameworks of landslide risk. A brief review of previous landslide studies conducted in the study area is also included.

Chapter 3 presents a detailed account of the study area. It covers the geographical location, historical development, administrative setup, and socio-economic profile of the area. It also describes the physical characteristics that influence landslide occurrences, such as climate, rainfall, geology, soil, and drainage systems, and recounts the significant historical landslide events within the study area.

Chapter 4 outlines the methodology for the quantitative assessment of landslide susceptibility. It presents the preparation of the landslide inventory and the selection and processing of twelve landslide conditioning factors. The chapter also provides a thorough explanation of the three bivariate statistical models employed, including the process for model validation.

Chapter 5 focuses on the methodology and analysis of landslide vulnerability and risk. It explains the approaches taken to evaluate both social and physical vulnerability. The chapter details how socio-economic data and physical infrastructure data were utilized to create vulnerability indices, which were then integrated with the landslide hazard map to generate a final landslide risk index for the study area.

Chapter 6 presents the results and discussion of the analyses conducted. It describes the landslide susceptibility maps generated from the three models and discusses their performance and validation in addition to the discussion on the spatial correlation of various factors and landslides. This chapter also presents the findings of the social, physical, and combined vulnerability assessments. The final landslide risk index is presented, and the spatial patterns of susceptibility, vulnerability, and risk across the study area are analyzed and discussed along with the implications of the results.

Chapter 7 summarizes the major findings and contributions of the study. It synthesizes the outcomes of the susceptibility, vulnerability, and risk assessments. The chapter concludes by providing recommendations for policy, planning, and future research directions based on the findings of the study.

CHAPTER 2

REVIEW OF LITERATURE

This chapter presents a comprehensive review of the fundamental concepts related to landslides, including their definitions and classifications along with important parameters which influence their occurrence and behavior. An examination of existing literatures on landslide research trends with emphasis on susceptibility and hazard assessments using geospatial technologies (Remote Sensing and GIS) is also presented. It also explores the concepts and methodologies utilized in vulnerability assessments, particularly on both the social and physical dimensions, and their integration into landslide risk assessment models. An overview of previous landslide studies conducted within the study area is also provided.

2.1 Definition of Landslide

The term *landslide* was used for the first time by James Dwight Dana in 1838 (Cruden, 2003; Hedding, 2020). Landslide was then initially understood only in broad terms, and systematic scientific study lagged behind the terminology. One of the first scientific investigations of landslides was conducted by Swiss geologist Albert Heim on the catastrophic Elm rockslide of 1881 (Wieczorek & Snyder, 2009). He and other early European geologists began to conduct scientific studies on landslides, from which a more systematic definition and classification of landslides have originated. One of the key pioneers was C. F. Stewart Sharpe who defined landslides as “the perceptible downward sliding or falling of a relatively dry mass of earth, rock, or a mixture of the two” (Sharpe, 1938). The definition given by Sharpe was a foundational attempt to describe slope failures and was influential in early geomorphologic and engineering studies.

As understanding of landform and slope processes began to broaden, researchers realized the need for broader definitions of landslides. Terzaghi (1950) defined a landslide as “a rapid displacement of a mass of rock, residual soil, or sediments adjoining a slope, in which the center of gravity of the moving mass advances in a downward and outward direction”. This definition broadened the scope beyond Sharpe’s definition by including any rapid downslope movement of slope-forming materials. The phrase "downward and outward movement" used by Terzaghi introduced a key concept that would reappear in later definitions.

These early definitions proposed, while seminal at the same time, had ambiguities particularly regarding the movement rate and water content. In 1958, an American geologist David Joseph Varnes introduced a more comprehensive definition and classification schemes. He defined landslide broadly as the "downward and outward movement of slope-forming materials composed of natural rock, soils, artificial fills, or combinations of these materials" (Varnes, 1958). This definition echoed the description given by Terzaghi, and became a cornerstone for subsequent landslide literature. Varnes (1978) presented an updated definition of landslide in similar broad terms as "constitut[ing] the group of slope movements wherein shear failure occurs along a specific surface or combination of surfaces". He replaced the term *landslide* with *slope movement* to include a variety of mass movement processes, rather than a specific type of sliding along a defined surface.

In 1984, Varnes revised the definition of landslide to encompass almost all slope movements: "the term landslide comprises almost all varieties of mass movements on slopes, including some, such as rockfalls, topples, and debris flows, that involve little or no sliding" (Varnes, 1984). This definition explicitly acknowledged that landslides are not limited to the literal sense of *land* and *sliding*. Other types of mass movements such as rockfalls and debris flows were now considered types of landslides, despite the lack of a discrete sliding surface. In the meantime, Chorley et al. (1984) proposed another widely accepted definition as, "the detachment and downslope transport of soil and rock materials under the influence of gravity. The sliding or flowing of these materials is due to their position and gravitational forces, but mass movement is accelerated by the presence of water, ice and/or air. This definition of mass movement permits consideration of the movement of earth materials at all scales and at all rates". This definition implies that gravity alone acts as the primary factor, and excludes the involvement of other transporting agents like wind, water flow, ice, or molten lava.

As landslide research expanded globally, with more researchers engaged in landslide studies, there was a concerted effort by the international scientific community to formalize landslide definitions and nomenclature. The International Geotechnical Society, in collaboration with UNESCO, formed Working Party on World Landslide Inventory (WP/WLI). The Working Party defined a landslide as "the movement of a mass of rock, earth or debris down a slope" in 1990. A year later, Cruden (1991) published the same definition which was intended for non-technical and informal use (Hedding, 2020). The definition proposed by the WP/WLI was adopted and suggested for informal use in the International Decade for Natural Disaster Reduction (1990-2000). This definition was recommended for widespread adoption, and indeed, it was soon embraced in both research and official glossaries, and became one of the most (if not the most) cited definitions in landslide literatures. Cruden and Varnes (1996) also reaffirmed the definition proposed by the Working Party and Cruden (1991).

Despite these refinements, however, some scholars argued that the term *landslide* has remained somewhat ambiguous, as it is used synonymously with various mass movement processes. Shanmugam and Wang (2015) argued that the term *landslide* has been used inconsistently for which it lacks conceptual clarity. They stated that it was erroneous to describe and include those processes such as debris flows or topples with no true sliding motion as landslides. They suggested to reserve the term for phenomena where sliding can be empirically verifiable. They further recommended the use of the broader term, *mass-transport deposits* (MTD) when such confirmation is lacking.

Thus, it can be recognized that the broad range of landslide occurrences and their intricate interactions with the surrounding environment make them challenging to adopt a single, universally accepted definition for landslides. It can also be observed that contemporary definitions of *landslide* are the product of over a century of refinement. Ultimately, owing to the effort of WP/WLI (1990) and Cruden (1991), a near-consensus definition emerged that remains in use today.

2.2 Morphology of Landslide

Before going further, it is important to first introduce a common terminology for describing and defining the various features, geometry, and dimensions associated with landslides. A clear understanding of these terms is essential for studying the landslide hazard assessment. Figure 2.1 presents a block diagram of an idealized rotational failure earth flow, as originally proposed by Varnes (1978) where each characteristic feature is labelled and defined. This diagram served as a foundational reference for identifying and categorizing landslide components. Figure 2.2 shows another diagram proposed by the International Association of Engineering Geology (IAEG) Commission on Landslides (IAEG, 1990), and Cruden and Varnes (1996), which further elaborated and defined landslide features. The description of the terminology in these diagrams is subsequently presented in Table 2.1.

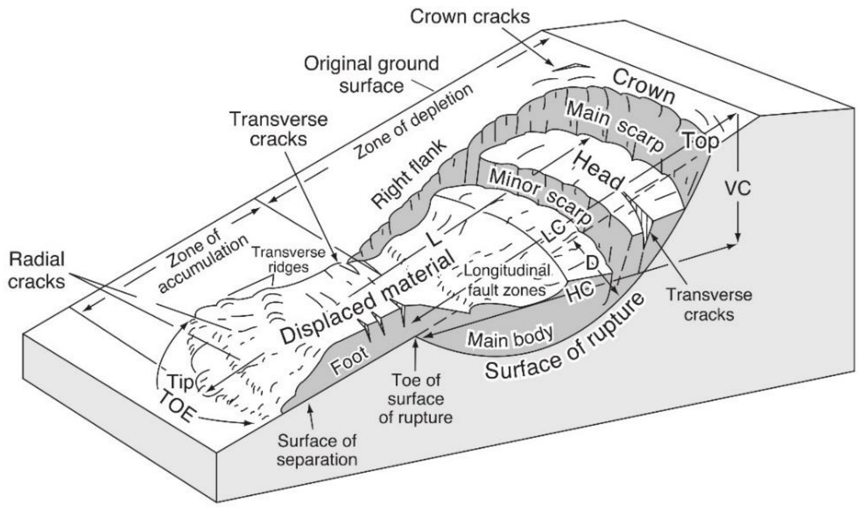

Fig. 2.1 *Block diagram of idealized rotational failure earth flow, modified after* Varnes (1978)

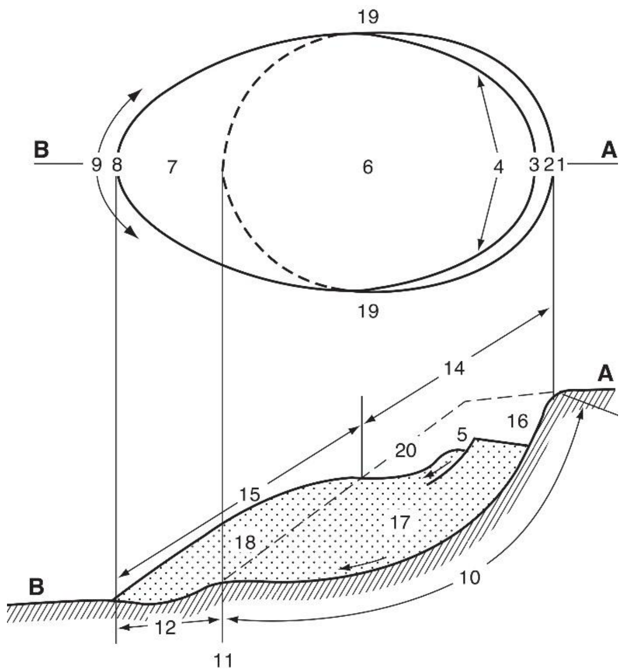

Fig. 2.2 *A diagrammatic illustration of Landslide features after* IAEG (1990) *and* Cruden and Varnes (1996)

Table 2.1 *Definitions of landslide features referred to in Figure 2.1 & 2.2*

Sl. No.	Name	Definition
1	Crown	Practically undisplaced material adjacent to highest parts of main scarp
2	Main scarp	Steep surface on undisturbed ground at upper edge of landslide caused by movement of displaced material (13, stippled area) away from undisturbed ground – that is, it is visible part of surface of rupture (10)
3	Top	Highest point of contact between displaced material (13) and main scarp (2)
4	Head	Upper parts of landslide along contact between displaced material and main scarp (2)
5	Minor scarp	Steep surface on displaced material of landslide produced by differential movements within displaced material
6	Main body	Part of displaced material of landslide that overlies surface of rupture between main scarp (2) and toe of surface of rupture (11)
7	Foot	Portion of landslide that has moved beyond toe of surface of rupture (11) and overlies original ground surface
8	Tip	Point on toe (9) farthest from top (3) of landslide
9	Toe	Lower, usually curved, margin of displaced material of a landslide, most distant from main scarp (2)
10	Surface of rupture	Surface that forms (or that has formed) lower boundary of displaced material (13) below original ground surface (20)
11	Toe of surface of rupture	Intersection (usually buried) between lower part of surface of rupture (10) of a landslide and original ground surface (20)
12	Surface of separation	Part of original ground surface (20) now overlain by foot (7) of landslide
13	Displaced material	Material displaced from its original position on slope by movements in landslide; forms both depleted mass (17) and accumulation (18): stippled on Figure 2.2
14	Zone of depletion	Area of landslide within which displaced material (13) lies below original ground surface (20)
15	Zone of accumulation	Area of landslide within which displaced material (13) lies above original ground surface (20)
16	Depletion	Volume bounded by main scarp (2), depleted mass (17) and original ground surface (20)
17	Depleted mass	Volume of displaced material (13) that overlies surface of rupture (10) but underlies original ground surface (20)
18	Accumulation	Volume of displaced material (13) that lies above original ground surface (20)
19	Flank	Undisplaced material adjacent to sides of surface of rupture (right and left is as viewed from crown)
20	Original	Surface of slope that existed before landslide took place ground surface

2.3 Classification of Landslide

Classification of landslides provides a systematic way to describe and compare slope failures, which is important for scientific analysis and hazard assessment. Over a century, several classification frameworks have been proposed by geologists, geomorphologists and engineers using different criteria and factors which were refined and modified through ages. The modern nomenclature systems were built on the pioneering work of early classifications.

The first classification of landslides was attempted by Dana in 1863, where his categorization of landslides laid the foundation for the subsequent development of modern landslide classification systems (Sharpe, 1938; Cruden, 2003). He differentiated mass movements into three types based on their characteristics, which were eventually identified as debris flows, earth spreads, and rock slides. Baltzer (1875) and Heim (1882) both investigated the widespread mass movements observed in the European Alps. Their classifications were based on the type of movement and the materials involved. Baltzer identified them as fall, slide, and flow, whereas Heim classified them as "soil slip, earth slide, earth fall, rock slip, rock fall, compound slide, and unclassified and special case" (Li & Mo, 2019).

Early in the 20th century, Howe (1909) introduced additional categories such as creep and slump, apart from several other categories of slides. Stiny (1910) provided one of the first detailed and inclusive classification systems by categorizing mass movements based on the types of movements and materials, and the driving forces where gravity acts either directly or is assisted by water, ice, or snow (Müller, 1979). Later, Heim (1932) presented a revised classification scheme that included up to 20 different types of landslips having involvement with water in the process. Ladd (1935) based his classification on the lithology of the shear plane and mechanics of failure as primary factors, while type of movement and water content were considered as secondary factors. Savarenskii (1937) came up with another classification scheme which was based on the type of material and shape of the slip surface.

Sharpe (1938) undertook extensive literature reviews on previous classification systems to aggregate them into a unified and comprehensive scheme. He used the type of movement and type of material as primary factors, with velocity and the amount and phase of water (or ice) as secondary factors. His classification scheme not only synthesized earlier ideas but also set the stage for subsequent classifications (Shroder et al., 2005). Utilizing morphological attributes or the geometry of failure as primary criteria for the first time, Skempton (1953) devised another classification scheme, specifically considering the depth-to-length ratio of landslides. His approach of classification showed the importance of landslide geometry and mechanics.

Varnes (1958) developed a matrix classification system which was built on Sharpe (1938) framework. His scheme categorized landslides into three principal types of movement, namely, falls, slides, and flows, and two primary types of material (rock and engineering soils). He also differentiated between rotational and planar slides apart from incorporating the involvement of water and deformation of the materials in the process. However, it faced certain limitations, such as the ambiguity in categorizing rapid flows of rock fragments and placing lateral spreads under the category of slides (Shroder et al., 2005). Varnes (1978) updated his original classification where the nomenclature was revised from *landslide* to *slope failure*, to include a wider range of phenomena. Additionally, the updated classification included debris and earth under the engineering soils, and also incorporated topples as a distinct type, and categorized lateral spreads separately even though they might fit within the complex category. He also reassigned rock fragment flows to the complex category, and introduced rock flow or deep creep to include the newly recognized sackung (sagging) type of movement. The simplicity, clarity and relevance of this updated classification led to its widespread adoption, and it set the stage for later refinements. Towards the end of the 20th century, the International Geotechnical Society's UNESCO Working Party on World Landslide Inventory (WP/WLI) under the International Association of Engineering Geologists (IAEG) adopted the landslide classification framework proposed by Varnes (1978) to standardize landslide nomenclature. The WP/WLI then formulated a series of methods to report, to prepare summary, to describe, and to quantify the rate of landslides based on this classification (WP/WLI, 1990; 1991; 1993 & 1995).

In the 20th century, several peripheral classification systems emerged to make minor modifications. For instance, Hutchinson (1968) expanded the concept of landslides by incorporating various categories of creep and subsidence. Zaruba and Mencl (1969) based their classification on geological features and age of landslide events. Carson and Kirkby (1972) highlighted distinctions among flows, slides, and heaves. Nemčok et al. (1972) introduced a classification specifically suited for engineering geological mapping based on the geomechanical characteristics and velocity of movement. While Erskine (1973) emphasized the degree of landslide activity, Blong (1973) and Crozier (1973) both based their classifications on the morphological attributes. Coates (1977), on the other hand, focused his classification on the type of material and the nature of the movement.

The modifications and refinements for the widely adopted and influential classification system proposed by Varnes (1978) were attempted by various workers during the late 20th century. For instance, Hutchinson (1988) contributed by introducing new concepts, such as sagging-failure classification and rebound movements which was linked to natural erosion or anthropogeny. Brunsden (1984) substituted the term *earthflow*, to a much less precise term *mud slide*. In Europe, the EPOCH classification system, published in 1993, gained popularity as it was considered "simple and suitable for European conditions" (Dikau et al., 1996). Another notable revision was done by Cruden and Varnes (1996) without much change, and preserved the original framework (Table 2.2). However, instead of treating the *complex* category as a separate type, they suggested using it as a descriptive term for landslides that involve multiple movements. They also incorporated a standardized landslide velocity scale (from extremely slow to extremely rapid) to the classification to describe movement speed in a consistent way (Table 2.3).

Hungr et al. (2014) proposed a comprehensive update to the Varnes (1978) classification system to align with modern geotechnical and geological terminology. They updated the material definitions to better distinguish between grain-size distributions and origins. They also introduced a more precise terminology for certain movements and included landslide types that had been studied in recent decades. This updated scheme featured formal definitions for 32 distinct landslide types which comprised a wide range of landslide phenomena. One pronounced modification was the exclusion of *complex landslides* from separate category to allow room for creating multiple type names for landslides involving more than one type of movement.

Table 2.2 Varnes (1978) *classification of landslides updated by* Cruden and Varnes (1996)

<table>
<tr><td colspan="3" rowspan="3">Mechanism of movement</td><td colspan="3">Type of material</td></tr>
<tr><td rowspan="2">Bedrock</td><td colspan="2">Engineering soil</td></tr>
<tr><td>Predominantly fine</td><td>Predominantly coarse</td></tr>
<tr><td colspan="3">Falls</td><td>Rockfall</td><td>Earthfall</td><td>Debris fall</td></tr>
<tr><td colspan="3">Topples</td><td>Rock topple</td><td>Earth topple</td><td>Debris topple</td></tr>
<tr><td rowspan="3">Slides</td><td colspan="2">Rotational</td><td>Rock slump</td><td>Earth slump</td><td>Debris slump</td></tr>
<tr><td rowspan="2">Translational</td><td>Few units</td><td>Rock block slide</td><td>Earth block slide</td><td>Debris block slide</td></tr>
<tr><td>Many units</td><td>Rockslide</td><td>Earthslide</td><td>Debris slide</td></tr>
<tr><td colspan="3">Lateral spreads</td><td>Rock spread</td><td>Earth spread</td><td>Debris spread</td></tr>
<tr><td colspan="3" rowspan="3">Flows</td><td>Rockflow</td><td>Earthflow</td><td>Debris flow</td></tr>
<tr><td>Rock avalanche</td><td></td><td>Debris avalanche</td></tr>
<tr><td>(Deep creep)</td><td>(Soil creep)</td><td></td></tr>
<tr><td colspan="3">Complex and compound</td><td colspan="3">Combination in time and/or space of two or more principal types of movement</td></tr>
</table>

Among the various frameworks proposed so far, the classification proposed by Varnes (1978), refined by Cruden and Varnes (1996), and which was later updated by Hungr et al. (2014) remained the most widely accepted in contemporary landslide studies and hazard assessments. This approach is now routinely used by the WP/ WLI and national organizations such as the U.S. Geological Survey (USGS) and the British Geological Survey (BGS). Its widespread acceptance indicated its practicality in both field investigations and engineering applications.

2.4 Landslide Movement Types

As stated earlier, the Varnes (1978) classification of landslides was widely used and adopted by the WP/WLI and other organizations. According to this scheme of classification, landslides are classified based on the type of movement into five principal categories, viz., falls, topples, slides (with rotational and translational sub-types), lateral spreads, and flows. Each category is defined by the kinematics of the failure (how the material moves) rather than the material type alone. Complex movements that involve more than one failure mechanism are also recognized as complex or compound landslides.

Table 2.3
Classification of velocity of movement of landslides (Cruden & Varnes, 1996; AGS, 2002)

Velocity Class	Description	Velocity (mm/s)	Typical Velocity	Probable destructive significance
7	Extremely Rapid			Disaster of major violence, buildings destroyed by impact of displaced material, many deaths, escape unlikely
		5×10^{3}	5 m/s	
6	Very Rapid			Some lives lost; velocity too great to permit all persons to escape
		5×10^{1}	3 m/min	
5	Rapid			Escape evacuation possible; structures, possessions and equipment destroyed
		5×10^{-1}	1.8 m/hr	
4	Moderate			Some temporary and insensitive structures can be temporarily maintained
		5×10^{-3}	13 m/month	
3	Slow			Remedial construction can be undertaken during movement; insensitive structures can be maintained with frequent maintenance work if total movement is not large during a particular acceleration phase
		5×10^{-5}	1.6 m/year	
2	Very slow			Some permanent structures undamaged by movement
		5×10^{-7}	16 mm/year	
1	Extremely slow			Imperceptible without instruments, construction possible with precautions

2.4.1 Falls

Falls are abrupt, vertical or near-vertical movements in which masses of rock or soil detach from a steep slope or cliff and move mainly by free-fall, bouncing, and rolling (Varnes, 1958; 1978). In a rockfall, blocks or boulders break loose along fractures, joints, or bedding planes and plunge through the air which strike the slope face on the way down (Fig. 2.3a). Falls are characterized by very rapid to extremely rapid type of movements, and the velocity depends on the steepness of the slope.

2.4.2 Topples

Topples involve the forward rotation and overturning of a mass of rock or soil out of the slope, pivoting about a point or axis near or below the base of the moving mass (Varnes, 1958; 1978). In a topple, a block of rock or column of soil tilts forward and may eventually collapse, which often leads to a fall or slide of the same material once it rotates past a critical angle (Fig. 2.3b). The speed of movement in topples can be slow or rapid.

2.4.3 Slides

Slides are characterized by a distinct zone of weakness separating the moving material from the stable ground underneath. Slides are subdivided into two main kinematic types based on the geometry of the failure surface:

i) Rotational Slides: A rotational slide is also called a slump, and it occurs along a curved, concave-up rupture surface, which resulted in a backward-rotating movement of the slide mass (Fig. 2.3c). Rotational slides create a steep head scarp at the upslope end and an uplifted toe where the displaced material piles up. These slides involve relatively soft, homogeneous materials that can sustain a spoon-shaped failure surface.

ii) Translational Slides: A translational slide occurs when a landslide mass moves outwards and downwards along a roughly planar surface with little to no rotation of the blocks (Fig. 2.3d). The failure plane is a pre-existing structural surface in the ground. The distinct feature of translational slides is the planar nature of the failure, and unlike rotational slides, there is no spoon-shaped surface.

2.4.4 Lateral Spreads

Lateral spreads are a type of landslide characterized by horizontal extension and fracturing on gentle or nearly flat slopes due to the sudden loss of strength in an underlying layer (Fig. 2.3e). In a lateral spread, the solid upper crust of ground breaks up and spreads apart, riding horizontally over a softer or liquefied substrate. The movement can be subtle or more catastrophic if the material completely loses strength. Lateral spreads are most commonly triggered by earthquake shaking.

2.4.5 Flows

Flows are landslides in which the moving material behaves as a viscous or fluid-like mass, with internal deformation distributed throughout the moving debris. There are four common sub-types of flows:

i) Debris Flow: This is a fast-moving slurry of mixed coarse debris constituting of rock, soil, vegetation and water (Fig. 2.3f). Debris flows occur when intense rainfall or rapid snowmelt generates torrents of water that mobilize loose slope materials into a flowing mass (Highland & Bobrowsky, 2008). Debris flows can be rapid to extremely rapid, and can travel at velocities of several miles or kilometers per hour.

ii) Debris Avalanche: These are extremely large and rapid debris flow which occur on steep open slopes rather than channels (Fig. 2.3g). Debris avalanches involve a shallow, highly fluid cascade of soil and debris that can fan out over large areas at the slope foot (Highland & Bobrowsky, 2008). Snow or ice sometimes take part in the movement process along with water which results in what is known as *lahars*.

iii) Earthflow: This is a plastic, slow-to-rapid flow of fine-grained soil or weathered rock that occurs on moderate slopes (Highland & Bobrowsky, 2008). Earthflows have a characteristic *hour-glass* shape which is usually narrow source area at the top, feeding into a widening, elongated flow track and spreading out at the toe (Fig. 2.3h). They are relatively slower, and usually pose more long-term disruption than sudden violent impact.

***iv) Creep*:** Creep is the informal name for a slow earthflow with steady downward creep of soil or rock under gravity (Highland, 2004). The movement is slow to extremely slow which is in the order of millimeters to centimeters per year (Fig. 2.3i). Owing to the slowness of movement, it is difficult to detect. Creep is identified from the bending of tree trunks, leaning poles or retaining walls, tilted grave-stones, and soil ripples (Highland, 2004).

2.4.6 Complex Landslides

A complex landslide is sometimes called a composite landslide, and involves two or more types of movement in the same event or landslide mass (Highland, 2004). In other words, the failure does not fit neatly into one category but is a combination or sequence of different movement mechanisms. Complex landslides occur when an initial slope failure of one type triggers or transitions into another type.

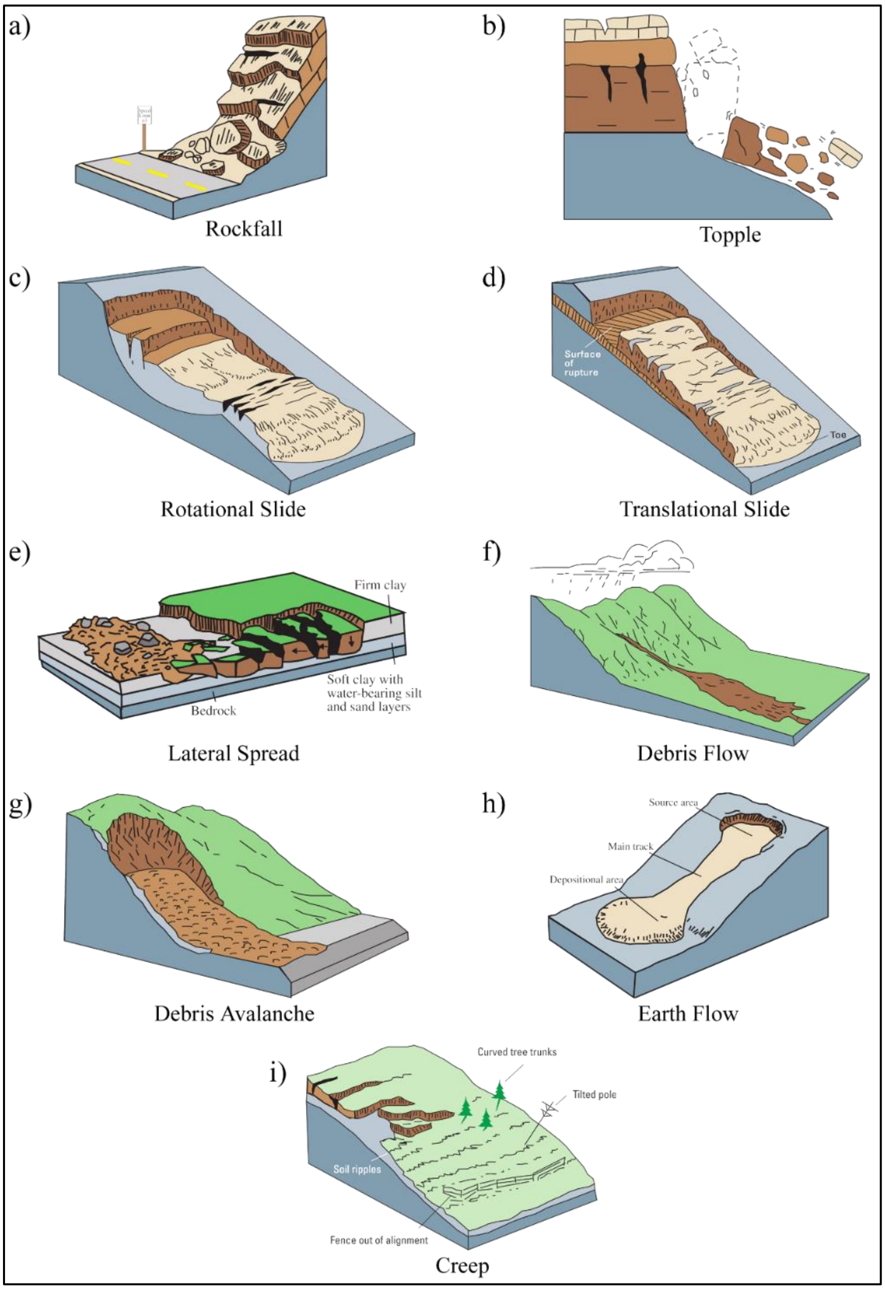

Fig. 2.3 *Different types of Landslides.* ***a)*** *Fall,* ***b)*** *Topple,* ***c)*** *Rotational Slide,* ***d)*** *Translational Slide,* ***e)*** *Lateral Spread,* ***f)*** *Debris Flow,* ***g)*** *Debris Avalanche,* ***h)*** *Earth Flow, and* ***i)*** *Creep* (*after* Highland & Bobrowsky, 2008)

2.5 Landslide Susceptibility Vs Landslide Hazard Mapping

In landslide literature, there often exists confusion between the terms *landslide susceptibility* and *landslide hazard* (Chacón et al., 2006; Corominas et al., 2023), with the two terms frequently used interchangeably or synonymously. Indeed, analyses of 367 research articles from 1972 to 2021 revealed that approximately 15% of publications mistakenly used *susceptibility* and *hazard* terms as synonyms (Tyagi et al., 2022). In the true sense, however, the two terms express different concepts (Fell et al., 2008; Reichenbach et al., 2018). Landslide susceptibility refers to the probability that a landslide may occur in an area based on the terrain conditions (Brabb, 1984; Soeters & van Westen, 1996). It reflects the extent to which a terrain is prone to slope instability, and estimates *where* landslides are likely to take place. As such, susceptibility analysis does not account for the temporal aspect of failure, i.e., *when* or *how* often landslides might occur, nor does it incorporate the magnitude, i.e., the potential size or destructiveness of such events (Guzzetti, 2005). Landslide susceptibility is therefore, the spatial probability or propensity of slope failures under certain geo-environmental conditions.

In contrast, landslide hazard is defined as the probability of a landslide of a given magnitude occurring within a given period and in a given location (Varnes, 1984). Unlike susceptibility, hazard assessments address *when* or *how* frequently a landslide may occur, and *how large* it is expected to be (Guzzetti et al., 2006a). Because hazard incorporates both spatial and temporal components, it is more challenging to determine than susceptibility, which represents only the spatial component. In general, the main difference between the two concepts lies in that landslide susceptibility involves assessments of past landslide occurrences, while landslide hazard implies the prediction of future landslide events (Guzzetti, 2005).

Despite advancements in remote sensing and statistical modelling, landslide hazard assessment continues to face certain challenges due to the limited availability and quality of landslide data (van Westen et al., 2008). In many instances, historical records often miss small, non-catastrophic, or events located in remote areas (Hervás & Bobrowsky, 2009; Steger et al., 2021). Even when these are recorded, they often lack precise spatial and temporal details, particularly in areas with frequent and numerous landslide events (Blais-Stevens & Septer, 2008), which are essential for understanding landslide frequency and magnitude. Furthermore, quantitative data such as landslide volume, runout distance, or triggering thresholds are often missing, which make it difficult to apply detailed mechanistic or probabilistic models (Peres & Cancelliere, 2014; Sun et al., 2021). As a result, researchers are often compelled to rely on susceptibility assessments as a substitute, even though these do not fully represent hazard potential (Froude & Petley, 2018; Caleca et al., 2022).

To overcome some of these limitations, researchers have utilized multi-temporal aerial photographs and satellite imageries to compile landslide inventories over various time periods (Guzzetti et al., 2012). However, the efficacy of this approach is often constrained by issues such as image resolution, data acquisition frequency, and subjective interpretation (Fernández et al., 2021). Consequently, in many data-scarce environments, landslide hazard assessments are either highly generalized or substituted by susceptibility maps (Singh et al., 2021; Riaz et al., 2023), which affects the accuracy of subsequent risk assessments and mitigation planning (Caleca et al., 2022).

2.6 Landslide Susceptibility Mapping

Landslide susceptibility mapping is defined as an assessment, either quantitative or qualitative, of the classification, size (volume or area), and spatial distribution of landslides that already exist or could potentially occur in an area (Fell et al., 2008). A central aim of landslide susceptibility mapping is to predict *where* landslides are likely to occur (Reichenbach et al., 2018). A landslide susceptibility map divides the terrain into zones that show different likelihoods for the occurrence of specific types of landslides, and its assessment may also include descriptions of the velocity and intensity of potential or existing landsliding (Ercanoglu & Sonmez, 2018). Landslide susceptibility mapping is recognized as an important step in landslide hazard and risk assessment and management (Ercanoglu & Sonmez, 2018; Lee, 2019). At the same time, it may also function as a standalone output that serves as a valuable tool for improving landuse planning, avoiding development in threatened areas, reducing potential damage and loss of life, and informing environmental impact assessments (Cascini, 2008; Fell et al., 2008; Corominas et al., 2014). Therefore, landslide susceptibility mapping is of immense importance for producing dependable hazard and risk maps (Ercanoglu & Sonmez, 2018).

2.6.1 Basic Assumptions

There exist wide differences in opinion among the researchers on the methodology or the scope of landslide susceptibility zonation (LSZ) mapping (Brabb, 1984; Guzzetti et al., 1999). Quite a number of approaches have been developed for LSZ mapping, each with its own set of strengths and limitations. Despite these lack of consensus on the methods and scope of LSZ, all the proposed approaches are based on certain fundamental assumptions which are universally accepted (Varnes, 1984; Carrara et al., 1991; Hutchinson, 1992; Turner & Schuster, 1996; Guzzetti et al., 1999). These are:

i) Landslides leave identifiable features, many of which can be detected, classified, and mapped either directly in the field or through stereoscopic interpretation of aerial photographs, satellite imageries, and others (Rib & Liang, 1978; Varnes, 1978; Hansen, 1984; Hutchinson, 1988; Dikau et al., 1996; Turner & Schuster, 1996). If a landslide does not produce observable or measurable changes, it cannot be identified or mapped, either in the field or with remotely sensed images.

ii) Landslides do not happen by chance (Guzzetti et al., 2002; Turcotte et al., 2002). Instead, they result from the interaction of various physical processes, and are dictated by mechanical laws that can be evaluated through empirical, statistical, or deterministic models. The predictive models of landslide occurrence can be developed by identifying and mapping the instability factors which influence both the initiation and propagation of landslides (Crozier, 1986; Hutchinson, 1988; Dietrich et al., 1995).

iii) The conditions which rendered slope failures in the past and present are considered likely to induce similar instabilities in the future (Varnes, 1984; Carrara et al., 1991; Hutchinson, 1992; Aleotti & Chowdhury, 1999; Guzzetti et al., 1999). This implies that understanding of the past and present landslide events is important for forecasting future occurrences. This assumption, which is based on the principle of uniformitarianism, indicates that slope failures are the outcome of ongoing and consistent processes operating over time.

iv) The spatio-temporal occurrence of landslides can be assessed through heuristic investigations, determined from the analysis of environmental variables, or simulated using physically-based models. Based on such analyses, an area can be classified into different susceptibility (or hazard) zones, each representing varying levels of probability (Carrara et al., 1995; Soeters & van Westen, 1996; Aleotti & Chowdhury, 1999; Guzzetti et al., 1999).

In an ideal practice, any method used for landslide mapping and evaluation should incorporate all these assumptions, failure to which the applicability of the method will be limited regardless of the scope or the goal of the evaluation (Guzzetti et al., 1999). However, it is extremely difficult to apply all these principles in reality due to lack of historical data, uneven distribution of landslides, and the subjectivity in the method employed (Aleotti & Chowdhury, 1999).

2.6.2 Landslide Inventory Mapping

A landslide inventory map is a type of map that presents records of landslide phenomena (Mihalić Arbanas et al., 2023). It is a spatial distribution of landslides which is represented as polygons or points (Wieczorek, 1984). It is considered the fundamental initial step in any landslide study (Dai et al., 2002; Fell et al., 2008; Guzzetti et al., 2012), and serves as a basis to understand their spatial and temporal occurrences (Martha et al., 2010a). It contains the location, run-out distance, volume, classification, date of occurrence, and other characteristics of landslides happening in an area (Wieczorek, 1984; Guzzetti et al., 2000; Fell et al., 2008).

2.6.2.1 Types of Inventory Maps

Based on the type of mapping, there are two main types of inventory maps: archive and geomorphological maps (Guzzetti et al., 2000; Malamud et al., 2004). The archive inventories are compiled based on information from literature or other archive sources without involved procedures of landslide detection and mapping (Brabb, 1995; Glade, 1998; Salvati et al., 2009). These are generally small scale and synoptic inventory maps (Guzzetti et al., 2012). Geomorphological inventories, on the other hand, contain landslide data derived through the interpretation of remote sensing data, such as aerial photographs, Very High Resolution (VHR) satellite images, Digital Terrain Models (DTMs), and limited ground surveys or field checks (Mihalić Arbanas et al., 2023). They can be either medium- or large-scale inventory maps (Reichenbach et al., 2005;

Martha & Kerle, 2010; Ghosh et al., 2011). The geomorphological inventories can be further classified into the following types (Guzzetti et al., 2012):

i) Historical Inventories: This type of inventory maps represents the cumulative effects of several landslide events over long periods, which can be in terms of tens, hundreds, or thousands of years (Brabb & Pampeyan, 1972; Galli et al., 2008). The age of the landslide in historical inventory cannot be estimated, and is represented as recent, old or very old, or sometimes undifferentiated (Guzzetti et al., 2012).

ii) Event Inventories: These represent landslides caused by a single triggering event, such as rainfall, earthquake, or snowmelt events (Harp & Jibson, 1996; Martha & Kerle, 2012; Xian et al., 2022). The date or period of the triggering event is usually considered as the date of occurrence of landslides. They are useful for documenting the full extent of events, and in determining the landslide size and area (Guzzetti et al., 2002; Malamud et al., 2004).

iii) Seasonal Inventories: These are the "landslides triggered by single or multiple events during a specific season or a few seasons" (Fiorucci et al., 2011). Seasonal landslide inventory can be generated using several sets of aerial or satellite images taken at different time periods or dates (Guzzetti et al., 2004; Galli et al., 2008; Martha et al., 2021).

iv) Multi-temporal Inventories: These types of inventories represent landslides triggered by multiple events over longer or extended periods, such as years to decades (Guzzetti et al., 2005; Martha et al., 2021). These are also prepared based on various sets of satellite or aerial images captured at different dates. A complete multi-temporal inventory can sometimes be achieved by combining the interpretation of historical records with participatory mapping (van Westen et al., 2012).

2.6.2.2 Methods and Techniques

The various methods and techniques for preparing landslide inventory maps have evolved over time, ranging from traditional field-based approaches to more advanced remote sensing techniques. This is basically due to the advancement of both geospatial technologies and computational techniques, as well as methodological innovations. These techniques are briefly discussed below:

1) Conventional Methods: These are traditional techniques that have been used for a long time, and often rely heavily on visual interpretation and fieldwork (Guzzetti et al., 2012). This type of mapping techniques includes:

i) Geomorphological Field Mapping: This involves direct observation and mapping of landslide features in the field (Cardinali et al., 2002). Fieldwork can be used to identify individual or small groups of landslides and collect data to improve the interpretation of images (Catani et al., 2025). While providing high detail, field mappings are costly, time-consuming, and inefficient for large areas (Guzzetti et al., 2012; Li, 2025). Nowadays, field mappings are mainly undertaken to support and integrate remote sensing techniques (Scaioni et al., 2014).

ii) Visual interpretation of aerial photographs: This has historically been a major source for landslide inventory map preparation (Rib & Liang, 1978; Martha et al., 2010a; Catani et al., 2025), which uses stereoscopic interpretation of aerial photography (Carrara et al., 1995; Turner & Schuster, 1996). It allows identification of land use, geologic and geomorphic features related to landslides (Mollard & Janes, 1984). However, this is an empirical and uncertain method that requires expertise and training apart from well-defined set of rules for interpretation (Antonini et al., 2002; Catani et al., 2025).

2) New and Emerging Methods: Over the past few decades, there has been a significant shift towards employing recent and new methods, largely driven by the need for rapid mapping over large areas, increased data availability, and technological advancements in remote sensing and artificial intelligence (AI) (Petley, 2012b; Novellino et al., 2024; Lissak, 2025). These new methods are discussed below:

i) Remote Sensing-based Techniques: These are based on satellite, airborne, and terrestrial remote sensing technologies (Casagli et al., 2017) which facilitate quick and easy landslide inventory mapping by reducing the time and resources needed for systematic updates and compilation (Guzzetti et al., 2012). VHR optical satellite imagery (Murillo-García et al., 2015; Martha et al., 2016a) and its derivatives like panchromatic (Martha et al., 2012; Lacroix et al., 2013), pan sharpen (Zhang, 2008; Huang et al., 2019), false colour composites (FCCs) (Abdallah et al., 2007; Domakinis et al., 2008) and ratioing of the bands (Chen et al., 2024) are effectively used for landslide detection and mapping. Synthetic Aperture Radar (SAR) images are less sensitive to weather conditions like clouds, rain, and fog (Xu et al., 2023), and are considered an effective option for landslide mapping and detection (Mondini et al., 2021). Interferometric SAR (InSAR) and its advanced forms such as Differential Interferometric SAR (Din-SAR), Multi-temporal Interferometry (MTI), Persistent Scatterer Interferometry (PSI), and Ground-Based Interferometric SAR (GB-InSAR) techniques are employed for monitoring slope movement and measuring ground deformation (Metternicht et al., 2005; Wasowski & Bovenga, 2014). Both air-borne and terrestrial Light Detection and Ranging (LiDAR) data provide extra high resolution, and are increasingly utilized for detection and mapping of small and shallow landslides hidden by vegetation and cloud cover (McKean & Roering, 2004; van Den Eeckhaut et al., 2007). In addition, the VHR Digital Elevation Models (DEMs) and shaded relief derived from LiDAR and optical satellite imageries are also employed for analyzing surface morphology and for estimation of landslide volumes (Kasai et al., 2009; Martha et al., 2010b; 2016b). Landslide mapping using Unmanned Aerial Vehicle (UAV) is a relatively new technique which is increasingly graining grounds, and provide a very detailed information on landslide features (Casagli et al., 2017; Ilinca & Şandric, 2025).

ii) Data Processing and Analysis Techniques: This represents the techniques used for processing and analyzing the remote sensing data and its derived features to identify and map the landslides. One of the most commonly used techniques include the change detection method where satellite images acquired before and after an event are compared to detect changes indicative of landslides (Martha et al., 2016a; Coluzzi et al., 2025). Another frequently used technique involves semi-automatic method for pixel- and object-based satellite image analyses (Keyport et al., 2018; Lissak, 2025). In Pixel-Based Image Analysis (PBIA), the changes in color or luminosity pixel by pixel between pre- and post-event images are analyzed (Meena et al., 2022; Bhuyan et al., 2023; Casagli et al., 2023). The Object-Based Image Analysis (OBIA) or Object-Oriented Analysis (OOA) takes into account the spatial context of pixels by grouping them into meaningful objects or segments on the basis of their spatial and spectral characteristics (Lissak, 2025). This technique has been effectively utilized for landslide detection and mapping by various researchers (Martha et al., 2010a; 2011; 2012; Amatya et al., 2021; Ghorbanzadeh et al., 2022a).

iii) Artificial Intelligence (AI)-based Techniques: AI-based methods such as Machine Learning (ML) and Deep Learning (DL) are increasingly employed to enhance and improve the accuracy of landslide detection and mapping (Bhuyan et al., 2023; Akosah et al., 2024; Sandric et al., 2024). These methods offer opportunities to simplify, improve, and quicken landslide mapping, and to identify features such as inactive old landslides (Létal et al., 2025). AI models are mainly used for classifying or segmenting image pixels into probable landslide instances (Catani et al., 2025) by using either pixel- or object-based segmentation techniques (Karantanellis et al., 2021; Meena et al., 2022). For both the techniques, ML methods such as Support Vector Machine (SVM) (van Den Eeckhaut et al., 2012) and Random Forest (RF) (Tavakkoli Piralilou et al., 2019) have been employed to identify and detect landslides. The Fully Convolutional Networks (FCNs) of the DL algorithms, and its variants such as the ResU-Net was successfully used for landslide detection in conjunction with OBIA technique (Ghorbanzadeh et al., 2022b). Another DL algorithm called Convolutional Neural Networks (CNN) was also found to be effective for landslide inventory mapping (Ghorbanzadeh et al., 2019; Ji et al., 2020).

2.6.3 Landslide Causative Factors

The occurrence of landslides is influenced by a wide variety of factors that include geological, hydrological, meteorological, morphological and anthropogenic domains. These factors were broadly divided into two categories (Crozier, 1986; Dikau et al., 1996; Kanungo et al., 2009): i) the internal or preparatory factors, and ii) the external or triggering factors. The internal factors represent the most conducive set of conditions under which mass movements are likely to occur, particularly when acted upon by an external triggering agent such as prolonged rainfall or seismic activity. The internal causative factors, which comprise the inherent geomorphological characteristics of the terrain, undergo temporal changes in both their material properties and geometry. The two major categories of landslide causative factors are shown in Table 2.4.

Table 2.4 Landslide Causative Factors

Sl. No.	Category	Factors
1	Internal or Preparatory Factors	Lithology
		Geological Structure (Faults, Lineaments, Joints, etc)
		Geomorphology (Slope, Aspect, Curvatures, etc)
		Vegetation
		Hydrogeology
2	External or Triggering Factors	Seismicity
		Climate (Precipitation, Snowmelt)
		Anthropogeny
		Undercutting by River/Waves

A brief description of these causative factors is presented in the following paragraph.

i) Lithology: Lithology influences the strength, porosity, and permeability of rock and soil materials. Weak lithological units are more susceptible to slope failure due to their poor mechanical properties and high rates of weathering (Sajinkumar et al., 2011; Regmi et al., 2013). Highly fractured or sheared rocks also provide less resistance to deformation and fail more easily under gravitational stress. In areas of interbedded lithologies, the juxtaposition of strong and weak layers often forms planes of weakness that facilitate mass movement (Liu et al., 2023).

ii) Geological Structure: Structural discontinuities such as faults, fractures, lineaments, joints, and bedding planes influence slope stability by acting as planes of weakness or by transmitting subsurface water, thereby promoting instability (Stead & Wolter, 2015). Fault zones often consist of crushed and altered rock material that exhibits low shear strength (Lockner & Beeler, 2002; Ben-Zion & Sammis, 2003). Moreover, the orientation of structural features relative to slope aspect also plays a critical role. Bedding planes parallel to the slope gradient are particularly conducive to planar failures (Pipatpongsa et al., 2022; Singh et al., 2017a).

iii) Geomorphology: Geomorphic variables of the terrain influence both the internal and external stability of slopes. Slope gradient is one of the most direct influencing factors of landslide susceptibility (Dai et al., 2001). Steeper slopes are subjected to greater gravitational forces which sometimes reduce slope stability. Aspect governs microclimatic conditions such as solar radiation, evapotranspiration, and soil moisture retention, which indirectly affect vegetation growth and soil development (McGuire et al., 2016; Li et al., 2024). The curvature of the terrain controls water accumulation and the spatial distribution of stresses (Krebs et al., 2015).

iv) Vegetation: Vegetation plays an important role in slope stability. Root systems contribute to slope stability by increasing soil cohesion, intercepting rainfall, reducing surface runoff, and mitigate the mechanical impact of raindrops (Greenway, 1987; Reubens et al., 2007). However, removal of vegetation by deforestation, forest fires, or disease outbreaks can reduce slope resistance by exposing soils to erosion and saturation, which further lead to increased landslide activities (Glade, 2003). Shallow-rooted species may be ineffective in stabilizing deep-seated failures (Singh, 2010).

v) Hydrogeology: Hydrogeological conditions, including the presence of perched water tables, aquifers, or zones of high infiltration, affect slope stability by increasing pore water pressure (Bogaard & Greco, 2016; Tang et al., 2020). Increased pore water pressure reduces the effective normal stress acting on potential failure planes, which further lowers shear strength and ultimately induces slope failure (Iverson, 2000). Infiltration of water into highly permeable materials or along structural discontinuities exacerbates this effect. Seasonal saturation cycles, particularly during heavy monsoon or snowmelt periods, often coincide with high landslide incidence (Osawa et al., 2018; Fan et al., 2025).

vi) Earthquakes: Seismic shaking generates dynamic stresses that can induce failure in marginally stable slopes. Earthquakes often reduce soil cohesion, increase pore pressure in saturated materials, and cause liquefaction in loose, granular soils which activate rapid slope failures (Keefer, 1984; Jibson, 1996). Landslides triggered by earthquakes are common in seismically active regions such as the Himalayas (Parkash, 2013), where ground motion frequently exceeds slope stability thresholds. Moreover, seismic events can also reactivate older, dormant landslide scars (van Den Eeckhaut et al., 2009a).

vii) Climate: Climatic variables, particularly rainfall and snowmelt, serve as the primary external triggers of landslides worldwide. Intense or prolonged rainfall increases soil moisture and pore pressure, and reduces shear strength which eventually results in slope failure (Zhang et al., 2011). In areas experiencing snowfall, rapid snowmelt can saturate soils and lead to shallow landslides (Chiarelli et al., 2023). In addition, freeze–thaw cycles in high-altitude areas cause expansion and contraction of soil and rock materials, further weakening slope materials over time (Liu et al., 2024a).

viii) Anthropogeny: Human interventions in the natural environment are among the leading contributors to slope instability (Alexander, 1992). Activities such as road construction, excavation, deforestation, unplanned urbanization, and mining disturb the natural equilibrium of slopes (Jaboyedoff et al., 2018; Maki Mateso et al., 2023). These activities often involve deforestation, changes of slope geometry, and obstruction or redirection of drainages. All these contribute to an increase in landslide frequency and magnitude.

ix) Undercutting by Rivers and Waves: Erosional processes at the base of slopes, caused by river incision or wave action remove base support and steepen the slope toe. This undercutting leads to over-steepened profiles and retrogressive failure, particularly in river valleys and coastal cliffs (Martinsen, 1994; Gutiérrez et al., 2023). This mechanism is especially prominent during high-flow events, storm surges, or sea-level changes that intensify erosion.

These causative factors form the basis for landslide susceptibility mapping (Ercanoglu & Sonmez, 2018). There are no strict guidelines or standardized rules in the selection of the type and number of causative factors in the landslide susceptibility mapping (Chawla et al., 2018; Pandey et al., 2019). It depends on the local terrain conditions, availability of data, and based on the empirical field observations (Das et al., 2023).

2.6.4 Mapping Unit

For any LSZ mapping, preliminary selection of suitable mapping unit is required (Guzzetti et al., 1999). A terrain mapping (or modelling) unit, by definition, refers to a distinct portion of the land surface characterized by a unique combination of ground conditions, which are distinguishable from those of neighbouring units through clearly identifiable boundaries (Hansen, 1984; Carrara et al., 1995; van Westen et al., 1997). The mapping/modelling unit represents both the internal homogeneity and external (between units) heterogeneity of the terrain (Alvioli et al., 2016). The mapping units can be classified into five types, as follows (Guzzetti et al., 1999):

i) Grid-cells or pixels, which are commonly used in raster-based GIS frameworks, divide the study area into uniform square units of pre-defined dimensions. Each cell functions as an analytical unit and is assigned values corresponding to the selected landslide conditioning factors, such as morphological, geological, or land-use attributes. Grid-cells units are widely adopted in landslide susceptibility studies due to their ease of implementation and scalability across various levels of analysis (Reichenbach et al., 2018).

ii) Slope units, also sometimes referred to as slope facets, refers to a geomorphologically consistent terrain unit characterized by relatively uniform slope aspect and gradient, divided by natural topographic features such as ridgelines, spurs, gullies, and stream channels (Carrara et al., 1991; Anbalagan, 1992). These are generated either from high-resolution Digital Terrain Models (DTMs) through GIS software, or manually delineated from topographic maps.

iii) Unique-condition units are derived by categorizing each landslide causative factor into few significant classes within individual thematic layer or map. By overlaying these layers sequentially, spatial zones with consistent combinations of factor classes, referred to as *unique conditions* are generated (Bonham-Carter, 1994; van Westen et al., 1997; Chung & Fabbri, 1999). The spatial configuration and number of these units depend on the classification scheme applied to the input variables.

iv) Terrain units are based on the principle of observed interrelations between various natural geological and geomorphological processes and forms which resulted in the creation of distinct natural boundaries. Traditionally, these units are utilized by geomorphologists, and they form the foundation of the land-system classification method, which is widely employed in various land resource studies (Verstappen, 1983; Hansen et al., 1995).

v) Topographic units are sub-divisions of slope units defined by the perpendicular intersections of contours and flow boundaries. The local morphometric characteristics and the total drainage area contributed by all upslope elements are calculated for each topographic unit.

Literature reviews show that grid-cells unit is the most commonly employed mapping unit followed by slope unit (Reichenbach et al., 2018; Huang et al., 2022; Lima et al., 2022; Das et al., 2023). It has been found that slope units are widely recognized as the more accurate and geomorphologically appropriate mapping unit for LSZ mapping (Erener & Düzgün, 2012; Ba et al., 2018). The selection of a suitable mapping unit for landslide susceptibility assessment is influenced by several factors, such as the type of landslide phenomena being investigated, the scale of the study, and the availability of both technical and financial resources. Additional considerations include the quality, resolution, and scale of the thematic data required, as well as the accessibility of appropriate tools for information management and spatial analysis. Each method of dividing the terrain has certain advantages and limitations, which can be either enhanced or reduced depending on the susceptibility evaluation technique employed (Carrara et al., 1995; Guzzetti et al., 1999). The characteristics of the different mapping units are given in Table 2.5.

Table 2.5
Classification and characteristics of different mapping units (*after* Zhao et al., 2021)

Unit Type	**Primary Ideas**	**Advantages**	**Limitations**
Grid unit	Divide the territory into regular squares with same size	Small sampling limit and easy gridding	The natural slope is separated, and the connection with geological and geomorphic information is lacking
Terrain unit	According to geomorphological and geological boundary	The relationship between landslide and land surface is easy to analysis	Needs a lot of topography geology information, and it is subjective
Unique condition unit	Overlay all the landslide factor layers, delete the smallest polygon, and get the element	Covering different factor attributes for statistical analysis	Regional environment differences are not considered, and it is subjective
Slope unit	Divide the territory into independent slopes by ridge line and valley line	Has definite geological significance	Poor automation
Topographic unit	Dividing by the intersections of contours and flow tube boundaries	Suitable for predicting shallow landslide under the control of surface saturation and topography	Not closely related to deep or complex landslides

2.6.5 Mapping Scale

The selection of appropriate mapping scale is one of the most important factors to be considered in landslide susceptibility, hazard and risk assessments. It influences the methods used, data requirements, and the ultimate purpose and applicability of the resulting maps (Soeters & van Westen, 1996; Kanungo et al., 2009; Corominas et al., 2014). Mapping scale refers to the "ratio between distance on the map and the corresponding distance on the ground" and this has been used "to define a map's level of detail, its content, and its positional accuracy" (Goodchild, 2011). The mapping scale in landslide studies determines the level of detail and spatial resolution at which landslide inventory, susceptibility, hazard and risk areas are identified and delineated (Fell et al., 2008; Meena & Nachappa, 2019).

In the literature, there are different categories of mapping scales, each associated with specific spatial extents, purposes, and methodological considerations. These can be classified into the following types (Soeters & van Westen, 1996; Cascini, 2008; Fell et al., 2008):

i) Small (or National) Scale (<1:100,000 or <1:250,000 or <1:1 million): These generally cover an area larger than 10,000 km^2, and are mainly used for landslide inventory mapping and zoning of landslide susceptibility for the purposes of information to the general public and policy makers (Cascini, 2008; Fell et al., 2008; Corominas et al., 2014). The level of details is low, as the assessment is undertaken mainly based on generally applicable rules (Soeters & van Westen, 1996). Hence, they are not recommended for statutory zoning purposes (Fell et al., 2008).

ii) Medium Scale (1:100,000 to 1:25,000 or 1:25,000 to 1:200,000): These mapping scales are appropriate for areas ranging from 1,000 to 10,000 km^2, and are mainly used for landslide inventory and susceptibility zoning for regional development or very large-scale engineering projects (Cascini, 2008; Fell et al., 2008). However, maps at this scale may not provide data required for design purposes, and are used for landslide inventory and landslide susceptibility mapping for regional development (Soeters & van Westen, 1996).

iii) Large Scale (1:25,000 to 1:5,000 or 1:5,000 to 1:15,000): This type of mapping scale covers relatively small areas, which generally ranges from 10 to 1,000 km^2, and is suitable for local level mapping of landslide inventory, susceptibility, hazard and risk assessments (Cascini, 2008; Fell et al., 2008). It can also be applied during site investigations conducted prior to the design phase of engineering projects (Soeters & van Westen, 1996; Corominas et al., 2014). Deterministic or process-based techniques are often applied at this scale (Cascini, 2008; Shano et al., 2022).

iv) Detailed or Site-Specific Scale (>1:5000 or >1:1000): This scale focuses on areas ranging from “several hectares to tens of square kilometres”, and is appropriate for “intermediate and advanced hazard zoning levels for local and site-specific areas,” as well as “for the design phase of large engineering structures, roads, and railways” (Cascini, 2008; Fell et al., 2008). This is the only scale suitable for statutory purposes in site investigation before the design phase (Soeters & van Westen, 1996; Corominas et al., 2014), and involves intensive, site-specific analyses of individual slopes or landslide bodies (Wang et al., 2013a; Ercanoglu & Sonmez, 2018).

A summary of these mapping scales and their applicability are presented in Table 2.6.

2.6.6 Methods of Landslide Susceptibility Zonation

In literature, landslide susceptibility zonation methods are broadly categorized into qualitative (direct) and quantitative (indirect) approaches (Kanungo et al., 2009; Corominas et al., 2014; Reichenbach et al., 2018). Qualitative approaches are subjective, ascertain susceptibility heuristically, and portray susceptibility levels using descriptive (qualitative) terms (Guzzetti et al., 1999; Reichenbach et al. 2018). The quantitative methods, on the other hand, are based on statistical techniques that incorporate understanding of past landslides and the predisposing factors to predict the areas susceptible to landslides (van Westen et al., 2006; Lee et al., 2020).

2.6.6.1 Qualitative Approach

The qualitative methods are also sometimes referred to as heuristic or knowledge-driven approach which relies on expert judgment regarding the influence of various cau-

Table 2.6 Landslide zoning mapping scales and their application (after Fell et al., 2008)

Scale description	Indicative range of scales	Examples of zoning application	Typical area of zoning
Small	<1:100,000	Landslide inventory and susceptibility to inform policy makers and the general public	>10,000 km^2
Medium	1:100,000 to 1:25,000	Landslide inventory and susceptibility zoning for regional development; or very large scale engineering projects Preliminary level hazard mapping for local areas	1,000–10,000 km^2
Large	1:25,000 to 1:5,000	Landslide inventory, susceptibility and hazard zoning for local areas Intermediate to advanced level hazard zoning for regional development Preliminary to intermediate level risk zoning for local areas and the advanced stages of planning for large engineering structures, roads and railways	10–1,000 km^2
Detailed	>5,000	Intermediate and advanced level hazard and risk zoning for local and site-specific areas and for the design phase of large engineering structures, roads and railways	Several hectares to tens of square kilometres

sative factors contributing to landslide occurrence. Data inputs are generally obtained through field investigations, interpretation of aerial photographs, and the integration of remote sensing data. This approach consists of techniques such as distribution analysis, direct geomorphological evaluation, and map overlay or combination methods.

1) Distribution Analysis: The distribution analysis method, also known as landslide inventory mapping, is among the more straightforward techniques for landslide susceptibility assessment (Soeters & van Westen, 1996). It involves documenting the spatial distribution of landslides within a given area using satellite imagery, aerial photographs, field observations, and existing historical records (Wieczorek, 1984; Espizua & Bengochea, 2002). The resulting inventory is generally represented on a map using polygons or point features, and may also be utilized to generate landslide density maps (Wright et al., 1974). Although this method does not establish a correlation between landslide occurrences and their predisposing factors, it provides a quantitative depiction of landslide distribution and serves as a back-bone for other assessment techniques (Dai & Lee, 2002; Galli et al., 2008). However, its major limitations lie in its inability to indicate the susceptibility level for future landslides and its lack of temporal information regarding landslide events (Soeters & van Westen, 1996).

2) Geomorphological Analysis: In this approach, experienced geomorphologists delineate landslide-prone areas by interpreting field observations (Kienholz et al., 1984; Pachauri & Pant, 1992; Reichenbach et al., 2005). Direct knowledge about the terrain and professional experience with a comprehensive understanding of the various causative factors are required in this approach. The terrain is subdivided by the experts into zones of relative stability or instability directly in the field based on the geomorphological/geological setting and the observed phenomena (Corominas et al., 2014). Direct geomorphological mapping allows for the detailed observation of terrain features, which can lead to more accurate landslide susceptibility maps. Also, it captures the complexity of geomorphological features that might be generalized or overlooked in indirect methods (van Westen et al., 2003). At the same time, however, the process is inherently subjective, and the results depend on the experience of the expert which may vary widely between individuals (Shano et al., 2020). Moreover, it is difficult to quantify accuracy or reproduce results, since it lacks a formal validation against landslide inventories (Pardeshi et al., 2013).

3) Map Combination Method: This is also called index-based method which was once widely used for LSZ mapping owing to its simplicity and accuracy. This approach relies on a priori knowledge, and its reliability largely depends on the understanding of the investigator on the various geomorphological processes influencing slope stability. In this approach, the instability factors are categorized, assigned ranks, and weighted based on their assumed or expected importance in inducing slope failures (Hansen et al., 1995; Lallianthanga & Laltanpuia, 2014). Accordingly, heuristic and subjective decision rules are formulated based on this information to identify unstable zones and delineate landslide susceptibility areas (Anbalagan, 1992; Sarkar et al., 1995). Eventhough this approach is simple and straightforward, the assignment of ranks and weights to the instability factors and their respective sub-classes remains largely subjective, which is informally termed as *blind weighting* (Gee, 1992). Furthermore, LSZ maps produced through this approach exhibit region-specific biases, which are difficult to eliminate due to its dependence on expert judgment (Kanungo et al., 2009).

While qualitative methods offer advantages such as simplicity, cost-effectiveness, and applicability in data-scarce regions, they are limited by their subjectivity, lack of reproducibility, and difficulty in validation (Guzzetti et al., 1999). Despite these limitations, qualitative approaches continue to be widely used, particularly in preliminary assessments and in areas where detailed quantitative data are not available (Pardeshi et al., 2013; Sujatha & Sudharsan, 2024).

2.6.6.2 Quantitative Approach

In quantitative method, the relationship between slope instability and controlling factors are numerically quantified (Aleotti & Chowdhury, 1999) by producing numerical estimates such as probabilities of landslide occurrence or factors of safety (Guzzetti et al., 1999). These methods are generally considered more objective than the qualitative approaches because they rely on data-driven analysis and mathematical or statistical techniques rather than solely on expert judgment, and generate reproducible results. The quantitative approach of LSZ mapping is mainly represented by the Statistical and Deterministic methods.

1) Statistical Methods: This method is based on the analysis of the functional relationships between the past and existing spatial distribution of landslides and their instability factor using GIS tools (Chacón et al., 2006; van Westen et al., 2008). The statistical methods were used for landslide analysis and mapping since mid-1970's, and represent one of the early methods employed for LSZ mapping. Neuland (1976) was considered the first to employ this approach for his slope failure prediction study in Germany. A few years later, Carrara (1983) used the statistical method to predict landslides in southern Italy based on the geological and geomorphological attributes. Following these pioneering works, a number of landslide susceptibility studies were undertaken by several researchers across diverse geographical regions using various statistical methods (Reichenbach et al. 2018). The various statistical methods used for LSZ mapping are broadly categorized into bivariate and multivariate models.

i) Bivariate statistical models: This model examines two variables to assess or determine the correlation between independent and dependent variables (Bertani et al., 2018; Krysik, 2018). In this approach, each causative factor map and the landslide distribution (landslide inventory map) are combined together, and the weighting values for each parameter class are calculated based on landslide densities (Soeters & van Westen, 1996; van Westen et al., 1997; Corominas et al., 2014). A diagrammatic overview of the general concepts of bivariate methods is given in Figure 2.4.

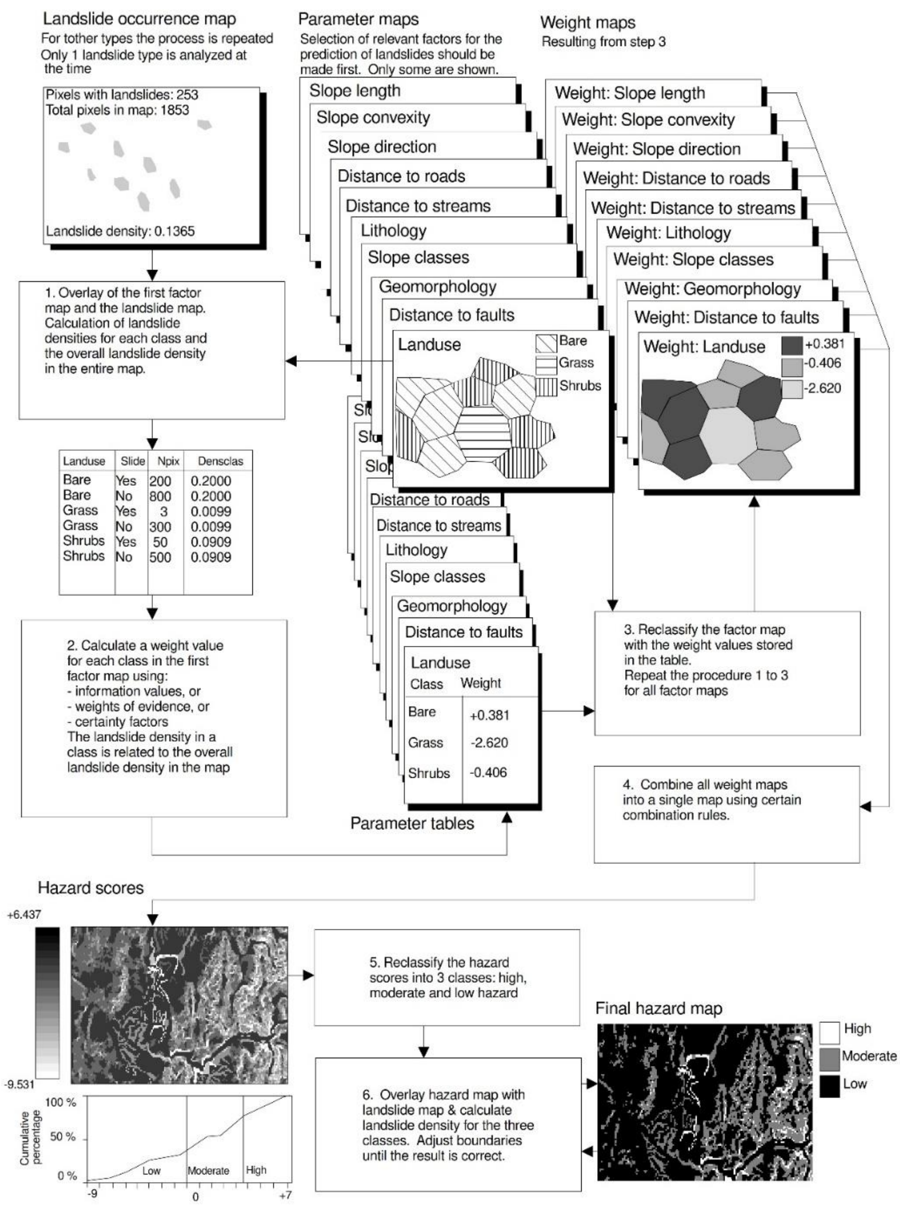

Fig. 2.4 *A diagrammatic illustration of the bivariate statistical method after* van Westen et al. (1997)

There are different types of bivariate models which are briefly described below:

a) Frequency Ratio (FR): This method calculates the ratio of the landslide occurrence probability to non-occurrence for a given factor class (Lee & Talib, 2005; Pradhan, 2010). In practice, FR is computed as the percentage of landslide area in a class divided by the percentage of total area occupied by that class (Kumar & Anbalagan, 2015; Wang & Li, 2017). An FR value >1 indicates that landslides are more likely than average in that class, while FR value <1 means less likely or lower susceptibility to landslides (Wu et al., 2016; Li et al., 2017). These ratios serve as weights and ratings for the factors and their respective classes, which are then subsequently combined to generate the LSZ map (Chimidi et al., 2017; Liu et al., 2022).

b) Information Value (IV): This method is also sometimes called the *statistical index* (Rautela & Lakhera, 2000; Zhang et al., 2016a), *landslide index* (Rawat & Joshi, 2012; Posner & Georgakakos, 2015), or *relative effect* (Pradhan & Kim, 2014; Ramesh & Anbazhagan, 2015) methods. The IV method was initially introduced by Yin and Yan (1988) to predict the spatial probability of slope instability. The method involves assigning weight to each class by computing the natural logarithm of the ratio between the conditional probability of landslide occurrence within a specific class of a thematic factor and the overall landslide probability (Jade & Sarkar, 1993; Lin & Tung, 2004; Sarkar et al., 2013). Positive IV values indicate a greater likelihood of landslide occurrence, while negative values suggest a lower likelihood (Saha et al., 2005; Khouz et al., 2022).

c) Weights-of-Evidence (WofE): This is based on Bayes' theorem and conditional probability which was originally developed for mineral potential mapping (Bonham-Carter, 1994; Agterberg et al., 1993), and later applied to landslides (Neuhäuser & Terhorst, 2007; Martha et al., 2013; Laltanpuia et al., 2024). The method operates as a log-linear form of the Bayesian probability model to derive weights for each factor class based on presence or absence of landslides (Goetz et al., 2015; Cao et al., 2021). For each class, WofE computes a positive weight (for landslide presence) and a negative weight (for absence) using prior (unconditional) and posterior (conditional) probabilities. The difference (weight contrast) indicates the net effect of that class on landslide occurrence (Sterlacchini et al., 2011; Neuhäuser et al., 2012). When a class of a factor is strongly associated with landslides, it will have high positive and low negative weights. The weights for all evidence layers can then be summed to produce a landslide susceptibility score (Ilia & Tsangaratos, 2016; Vakhshoori & Zare, 2016).

These are the most frequently used bivariate statistical models for LSZ mapping. Apart from these, there are other models within this category which are also employed in landslide studies. These include Evidential Belief Function (Althuwaynee et al., 2012; Nohani et al., 2019), Index of Entropy (Pourghasemi et al., 2012a; Devkota et al., 2013), Shannon Entropy (Shadman Roodposhti et al., 2016; Addis, 2023), Landslide Nominal Risk Factor (LNRF) method (Gupta & Joshi, 1990; Saha et al., 2005) Yule's Co-efficient (Ram et al., 2020; Khan et al., 2024), and Matrix-Assessment Approach (Cross, 1998; De Graff et al., 2012).

ii) Multivariate Statistical Models: This model considers the relative contribution of multiple causative factors simultaneously to the total landslide susceptibility within a defined area (Ayalew & Yamagishi, 2005; Kanungo et al., 2009). In this method, the percentage of landslide occurrences associated with each mapping unit is evaluated, and the corresponding data layer representing the presence or absence of landslides is generated through statistical modelling (van Westen et al., 1997; Kavzoglu et al., 2015; Baeza & Corominas, 2001). The generalized working principle of the multivariate methods is shown in Figure 2.5.

The common techniques of multivariate statistical methods include logistic regression and discriminant analysis.

a) Logistic Regression (LR): This method employs a dichotomous dependent variable which represents landslide and non-landslide conditions, to model the probability of landslide occurrence based on a set of explanatory variables (Gorsevski et al., 2006; Lee & Pradhan, 2007). LR finds the best-fitting equation that relates a binary dependent variable (presence or absence of landslide) to a set of independent variables (Ohlmacher & Davis, 2003; Ayalew & Yamagishi, 2005). The result constitutes a set of coefficients for the variables, which can be exponentiated to odds ratios through the logit function indicating each factor influence (Sujatha & Sridhar, 2021; Erener et al., 2016). When a factor is significant for landslide occurrence, the odds are positive, whereas

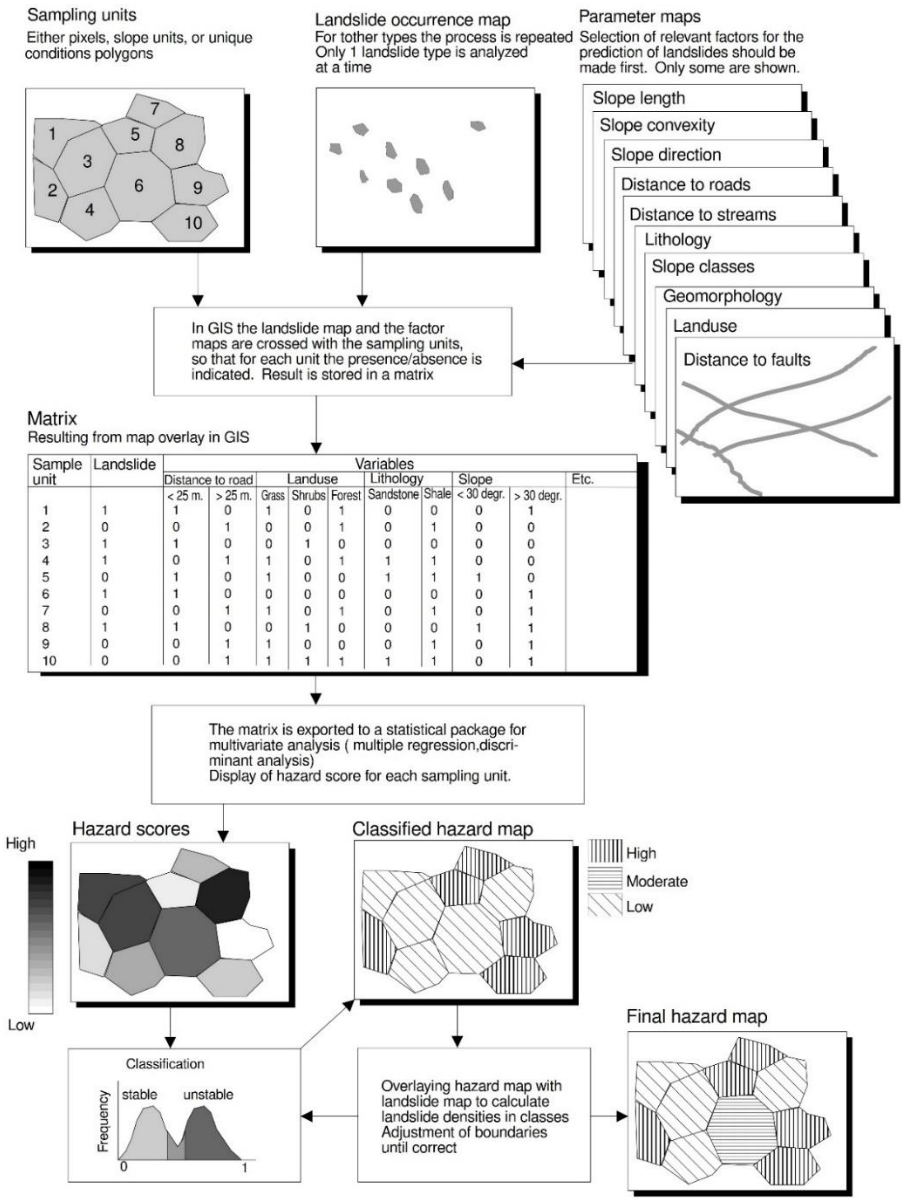

***Fig. 2.5** An overview of the multivariate statistical method after* van Westen et al. (1997)

for less influential factors, the odds are negative. The logistic link function is then applied to fit the data to an S-shaped logistic curve for the estimation of landslide probability values ranging from 0 (no probability) to 1 (certain occurrence) (Pradhan & Lee, 2010; Bui et al., 2011; Mousavi et al., 2011). Literature reviews show that LR is the most widely used method for LSZ mapping (Brenning, 2005; Pourghasemi et al., 2018; Reichenbach et al., 2018; Lee, 2019; Huang et al., 2022; Lima et al., 2022).

b) Discriminant Analysis: For landslide susceptibility assessment, this method evaluates the maximum difference between landslide and non-landslide groups for each landslide causative factor (independent variable), and assigns corresponding weights to these factors (Lee et al., 2008; Rossi et al., 2010). Slope units are then classified based on the presence or absence of landslide classes. Standardized Discriminant Function Coefficient (SDFC) is computed to express the relative importance of each variable in terms of discriminant function as a predictor of potential landslide event (Carrara et al., 1991; Guzzetti et al., 2006b; Galli et al., 2008). Variables showing high SDFC are considered strongly associated with absence or presence of landslide (van Den Eeckhaut et al., 2009b). Discriminant analysis is an effective method for LSZ due to its objectivity, efficiency, and ability to handle multiple variables (Santacana et al., 2003; Youssef & Pourghasemi, 2021).

2) Deterministic Methods: These are also known as physically-based or geotechnical models which rely on physical laws and mathematical relationships to analyze slope stability (Montgomery & Dietrich, 1994; Terlien et al., 1998). The deterministic method is particularly employed for investigating rainfall-induced shallow landslides using Geographic Information Systems (GIS) (van Westen & Terlien, 1996; Terlien, 1998). It aims to assess the potential for slope failure based on the relationship between the driving and resisting forces, and computes a stability indicator, called Factor of Safety (FoS) for each slope or terrain unit (Gökceoglu & Aksoy, 1996; Bednarik et al., 2024). An FoS value less than 1.0 indicates potential instability or failure, while a value greater than 1.0 is considered stable. The method combines a hydrological model to analyze pore-water pressure with an infinite slope-stability model to calculate the FoS (Wu & Siddle, 1995; Iverson, 2000). These methods include Shallow Landsliding Stability (SHALSTAB) (Montgomery & Dietrich, 1994; Meisina & Scarabelli, 2007), Stability Index Mapping (SINMAP) (Pack et al., 1998; Terhorst & Kreja, 2009), Transient Rainfall Infiltration and Grid-based Regional Slope-stability (TRIGRS) (Baum et al., 2008; Godt et al., 2008), Système Hydrologique Européen Transport (SHETRAN) (Burton & Bathurst, 1998; Zhao et al., 2019), and Yonsei Slope (YS-Slope) (Kim et al., 2014; Jeong et al., 2019) models. The deterministic methods provide reliable and accurate slope stability assessment when relevant geotechnical data are available (Rossi et al., 2013; Alvioli & Baum, 2016). A schematic workflow of the physically-based models is shown in Figure 2.6.

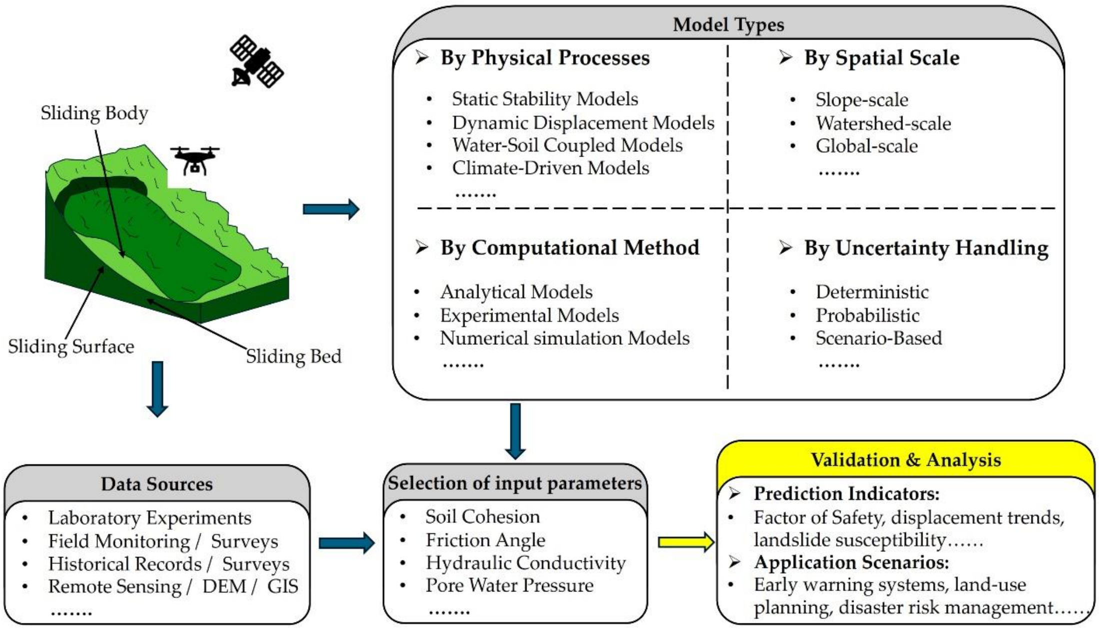

Fig. 2.6 *General workflow of the physically based approaches after* Ye et al. (2025)

2.6.6.3 Other Approaches

Apart from these methods, semi-quantitative method (SQM) and machine learning (ML) approaches are other categories which have been increasingly employed for LSZ mapping. These two methods have not been recognized or treated them as separate categories by several researchers (Soeters & van Westen, 1996; van Westen et al., 1997; Aleotti & Chowdhury, 1999; Guzzetti et al., 1999; Dai et al., 2002; Huabin et al., 2005; Kanungo et al., 2009; Corominas et al., 2014; Reichenbach et al., 2018). This may be due to the conceptual grouping of all data-driven methods under *statistical/quantitative* category (for ML), and all expert-driven methods under *qualitative/heuristic* category (for SQM). It may also be due to the inheritance of early classification frameworks which defined broad methods before the advent of SQM and ML. Many modern reviews, however, have included them either under the data-driven/quantitative or as separate category (Pardeshi et al., 2013; Shano et al., 2020; Lima et al., 2022; Tyagi et al., 2022; Das et al., 2023; Li & Duan, 2024; Segoni et al., 2024; Caleca et al., 2025).

1. Semi-Quantitative Methods (SQM): The SQM are described as a hybrid of both qualitative and quantitative methods (Tyagi et al., 2022), or as those methods which employ a mix of techniques from both the qualitative and quantitative approaches (Sujatha & Sudarshan, 2024). Similar to qualitative methods, they may involve subjective judgments (Mandal et al., 2018; Roy et al., 2019). However, they calibrate the subjective operation, sometimes in terms of statistical evaluation (Ghosh et al., 2011; Pal et al., 2019) or by multi-criteria evaluation (Barredo et al., 2000). These methods are used to make decisions in the determination of ratings and weights of factors and their classes by using criteria like expert knowledge or past landslide data or a combination of both (Tyagi et al., 2022). Prominent model used for LSZ mapping under this approach is the Analytical Hierarchy Process (AHP) (Das et al., 2022; Liu et al., 2024b). Other SQM include Fuzzy logic (Kanungo et al., 2006; Vakhshoori & Zare, 2016), Weighted Overlay (Kaur et al., 2023; Arshid et al., 2024), Weighted Linear Combination (Ayalew et al., 2004; Li et al., 2023a), and Ordered Weighted Average (Ahmed, 2015; Gigović et al., 2019).

2. Probabilistic Methods: The probabilistic method is generally classified under quantitative approaches for LSZ mapping (Aleotti & Chowdhury, 1999; Kanungo et al., 2009; Nath et al., 2020; Tyagi et al., 2022), and is mostly categorized under the statistical methods. The main concept of this method is to evaluate the degree of relationship between the spatial distribution of landslides and their causative factors within a probabilistic framework (Kanungo et al., 2009; Lari et al., 2014). This is then converted into a numerical value by probability distribution function (Pardeshi et al., 2013; Shano et al., 2022). This probability can refer to the spatial probability of landslide, and in some cases, the temporal probability of occurrence and size/volume probability (Guzzetti et al., 2005; Lari et al., 2014). Representative models of the probabilistic method of LSZ include Conditional Probability (Chung & Fabbri, 1999; Pourghasemi et al., 2012a), Certainty Factor (Ma et al., 2023; Ding et al., 2025), Favourability Function (Remondo et al., 2003a; Li & Lan, 2023). Apart from this, a Bayesian probability model such as WofE is also sometimes included under this method.

3. Machine Learning (ML)-based Methods: These methods are classified under the quantitative/data-driven approaches of LSZ mapping (Das et al., 2023; Caleca et al., 2025). ML methods were used for LSZ from the early 2000s (Alvioli et al., 2024; Teke & Kavzoglu, 2024a), and emerged as a powerful, data-driven approach for LSZ mapping and other related studies (Reichenbach et al., 2018; Pugliese Viloria et al., 2024). ML-based techniques have gained popularity due to their ability to handle complex datasets, identify hidden patterns, and enhance prediction accuracy (Merghadi et al., 2020; Al-Najjar et al., 2024). ML-based methods for LSZ are classified into conventional, deep learning, hybrid and ensemble models (Ado et al., 2022; Ganesh et al., 2023).

i) Conventional ML models: These are standalone ML models that have been widely used for LSZ and are known for showing good prediction accuracy. They are employed as benchmarks for evaluating newer or more complex models (Ado et al., 2022; Kavzoglu et al., 2019). There are several conventional ML models used for landslide studies. Among them, Artificial Neural Networks (ANN) (Lee et al., 2003; Ermini et al., 2005; Yilmaz, 2009), Support Vector Machines (SVM) (Marjanović et al., 2011; Bui et al., 2012a), Random Forest (RF) (Catani et al., 2013; Akinci et al., 2020), Naive Bayes (NB) (Bui et al., 2012a; Pham et al., 2017), Decision Tree (DT) (Pradhan, 2013; Dou et al., 2019), k-nearest neighbour (KNN) (Abraham et al., 2021; Agrawal & Dixit, 2023) are some of the popular conventional ML models used in LSZ studies.

ii) Deep Learning (DL) models: A major development in recent years is the introduction of Deep Learning (DL) models for LSZ studies. DL is a subset of ML, which refers to neural networks with many layers that can automatically learn feature representations (Saha et al., 2021; Aslam et al., 2023). Deep Learning Neural Networks (DLNN) offer satisfactory alternatives as they often outperform various conventional ML techniques in predicting landslide susceptibility zones (Bui et al., 2020; Van Dao et al., 2020). However, DLNN models generally demand high computational resources, and require a large number of inventory datasets to avoid overfitting (Xia et al., 2019; Kudaibergenov et al., 2025). Popular DL models include Convolutional Neural Networks (CNN) (Ruggieri et al., 2021; Cardellicchio et al., 2023), Long Short-Term Memory Networks (LSTM) (Wang et al., 2021; Zuo et al., 2025), and Recurrent Neural Networks (RNN) (Wang et al., 2020; Habumugisha et al., 2022).

iii) Ensemble models: These methods combine multiple individual ML models, which are referred to as base (or weak) learners by aggregating the predictions through techniques like voting or averaging (Liu et al., 2023). This approach aims to enhance predictive accuracy and robustness, reduce variance, and mitigate overfitting by leveraging the collective intelligence of multiple models (Ado et al., 2022; Kudaibergenov et al., 2025). The common ensemble techniques include Bagging, Boosting, Stacking, Blending, Simple/Weighted Averaging, Rotation Forest (RotFor), Random Forest (RF), XGBoost, and Gradient Boosting Decision Trees (GBDT).

iv) Hybrid Models: These models combine either multiple ML and DL models or statistical models with ML models through optimization or feature selection techniques to enhance the capabilities and strengths of each model, and to effectively increase the performance and accuracy of the overall model (Yuan et al., 2022; Lu et al., 2024). These hybrid algorithms were used to filter out the redundant, and select only the relevant conditioning factors to enhance the quality of datasets (Kavzoglu et al., 2015; Ado et al., 2022). Models such as CNN, Geodetectors and Recursive Feature Elimination (RFE) are commonly employed for this purpose.

These ML-based models have no doubt achieved high predictive and accurate performance in generating LSZ maps. However, they are often considered "black boxes" because their internal workings are difficult to understand which make it challenging for practitioners to understand the rationale behind specific predictions (Dahal & Lombardo, 2023; Pradhan et al., 2023; Teke & Kavzoglu, 2024b). Researchers have incorporated a technique called eXplainable Artificial Intelligence (XAI) to suitably enhance transparency and interpretability of complex ML-based models (Pradhan et al., 2023; Al-Najjar et al., 2024). Prominent XAI models include SHapley Additive exPlanations (SHAP) (Zhou et al., 2022; Wang et al., 2024), Local Interpretable Model-agnostic Explanations (LIME) (Qiu et al., 2024; Teke & Kavzoglu, 2024b), and Partial Dependence Plot (PDP) (Phinzi & Szabó, 2024; Sun et al., 2024).

It can be observed, from the foregoing discussions that LSZ mapping approaches have gone through progressive evolution from a simple heuristic, knowledge-driven approach to a more advanced data- and technology-driven method. This is mainly due to the increasing availability of higher quality data, technological advancements in RS & GIS, and computational intelligence. A wide range of LSZ mapping methods, therefore, exists which results in variation of the classification and nomenclature of LSZ mapping method itself. This is due to the fact that the classification of the methods is somewhat subjective and influenced by the specific aspects or criteria emphasized by the researchers or reviewers (Aleotti & Chowdhury, 1999; Lee et al., 2017; Pourghasemi et al., 2018). At the same time, it is important to note that these different methods have their own advantages and limitations. Therefore, selection of appropriate approach is of paramount importance before undertaking any LSZ mapping. The choice depends on many factors including the scale and scope of the study, data availability, practical knowledge and experience of the practitioner, and others (Corominas et al., 2014; Vakhshoori & Zare, 2016).

2.6.7 Classification of Landslide Susceptibility Maps

The classification of LSI into distinct susceptibility classes or zones involves defining specific threshold values to demarcate the boundaries between different levels of susceptibility which is further calibrated with the landslide inventory (Ermini et al., 2005; Catani et al., 2013). There are various methods for defining these thresholds, and the choice depends on the specific distribution of the LSI values and the particular purpose of the map (Das et al., 2023). The Jenk's Natural Break method is the widely used approach which statistically determines class breaks by grouping similar values and maximizing differences between groups, specifically by finding adjacent pairs with relatively large differences in data value (Irigaray et al., 2007). This approach aims to minimize variability within classes while maximizing variability between them (Segoni et al., 2024). It is considered suitable for every type of data distribution but can be difficult to compare or replicate, and is sensitive to outliers (Das et al., 2023). The Quantile (or Percentile) classification, also referred to as ranking equal-number classes, sorts all pixels or mapping units based on their calculated LSI values in descending order, and divides them into a predefined number of classes so that each resulting class contains an equal number of pixels (Chung & Fabbri, 1999; 2003; Steger et al., 2020). Although it ensures an equal count of pixels per class, pixels with different susceptibility values might be grouped into the same class if they fall within the quantile range (Adnan et al., 2025).

The Geometric interval classification defines the breaks between the different classes based on a geometric progression of the data range. It systematically refines class boundaries and reveals minimal variations within the lowest range of data values, and is suitable for data that is not evenly distributed (Das et al., 2023). This method of classification is one of the most widely employed method for discretizing the continuous values of the LSI into distinct susceptibility classes. The Equal interval classification divides the entire range of LSI values into a predefined number of intervals of equal size. While the range of each interval is identical, the number of units or pixels falling into each class can vary significantly (Chung & Fabbri, 2003). This approach may emphasize one class over others (Ayalew & Yamagishi, 2005), and could complicate comparisons if the underlying pixel values have different meanings (Chung & Fabbri, 2003). Classification approaches based on the Success Rate Curve are also employed to classify the LSI values into different susceptibility classes to reduce subjectivity and arbitrariness (Martha et al., 2013; Sangeeta et al., 2020; Laltanpuia et al., 2024). The classification depends on the relationship between the cumulative percentage of landslide occurrences and the percentage of the study area in different susceptibility classes.

The choice of classification method is important as it can influence the spatial representation of susceptibility and the distribution of risk zones on the final map (Abdelkader & Csámer, 2025). Different methods can result in varied distributions of susceptibility values across the landscape. The appropriate method selection depends on several factors, including the nature of the susceptibility index values, the specific objectives of the mapping, the study scale, data availability, and the expertise of the evaluator. While the transformation from continuous values to discrete classes is a common practice to enhance usability, it is a process that requires careful consideration (Segoni et al., 2024).

2.6.8 Model Evaluation and Validation

Evaluation or validation of the models is an important step in LSZ to assess the reliability, accuracy, and the practical applicability of the resulting maps and the models (Chung & Fabbri, 2003; Frattini et al., 2010; Segoni et al., 2024). It is also essential to supply the reliability and scientific rigor to a study (Lima et al., 2022). Without validation, susceptibility maps are considered untested hypotheses, and their practical use for decision-making and land-use planning is limited (Chung & Fabbri, 2003; Remondo et al., 2003b; Abdelkader & Csámer, 2025). Validation helps to check the reliability of the maps and validate the results, gauging the model performance and determining whether the LSZ maps correctly distinguish between potentially landslide-free and landslide-prone areas (Corominas et al., 2014; Das et al., 2023). A thorough quality assessment through validation is necessary for increasing the reliability, transparency, and acceptance of landslide analyses among stakeholders and decision-makers (Fleuchaus et al., 2021). Evaluation or validation can also highlight issues that enable the improvement of future susceptibility maps, guiding data collection, field practices, and the selection of optimal functions and variables, and is, thus considered an integral part of the landslide susceptibility modeling workflow (Alvioli et al., 2024).

2.6.8.1 Data Partitioning Strategies

The first step in validation of the models constitutes the partitioning or sub-setting of the available landslide inventory into training and testing datasets (Corominas et al., 2014; Reichenbach et al., 2018; Huang et al., 2022; Alvioli et al., 2024), which is mostly used in machine learning and statistical models (Joseph, 2022). This data splitting is, however, not applicable for qualitative and semi-quantitative methods (Segoni et al., 2024). While a training dataset is used to build or calibrate the model, a testing dataset (or validation dataset in some contexts) is used to assess the model performance, particularly its predictive capability, using data not utilized for training (Fell et al., 2008; Fleuchaus et al., 2021). This data segregation is intended to provide an unbiased evaluation and help avoid overfitting (Segoni et al., 2024). There are basically three partitioning strategies commonly used for model validation process which include random, spatial and temporal partitioning (Chung & Fabbri, 2003; Remondo et al., 2003b). In random partitioning, the landslide inventory is randomly divided into training and testing subsets based on a predefined proportion (Huang et al., 2022). Literature reviews revealed that random partitioning is the most frequently adopted sampling strategy for model validation (Reichenbach et al., 2018; Huang et al., 2022; Lima et al., 2022), and showed better prediction results than the spatial or temporal partitions (Remondo et al., 2003b; Zêzere et al., 2004; Pereira et al., 2012).

The spatial partitioning divides the study area or its landslides geographically into different regions (Hong et al., 2018; Khanna et al., 2021). This means that data from one region is used for training, and data from another region is used for testing or validation (Chung & Fabbri, 2003; 2005). However, this approach can pose problem if thematic variables differ significantly between the training and validation areas, which make it difficult or impossible to apply the derived classification function (Guzzetti et al., 2006b). The temporal partitioning strategy involves dividing the landslide inventory based on the time of occurrence (Zêzere et al., 2004; Khanna et al., 2021; Dahal et al., 2024). Usually, older landslides are used for training, while more recent landslides are utilized for testing or validation (Reichenbach et al., 2018). This method is considered the most adequate for assessing the model ability to predict future events (Remondo et al., 2003b; Deng et al., 2017), but it requires a multi-temporal inventory over a sufficiently long period, which is often difficult to obtain (Irigaray et al., 1999; Zêzere et al., 2017; Yordanov & Brovelli, 2021).

Apart from these partitioning strategies, another method called repeated multiple partitioning (or cross-validation) is also employed (Brenning, 2012; Steger et al., 2020). This involves repeatedly splitting the data into training and testing sets and averaging the results (Lima et al., 2022), which can reduce the randomness associated with a single random split and provide a more robust evaluation (Petschko et al., 2014; Goetz et al., 2015), especially with limited data (Huang et al., 2022).

2.6.8.2 Data Splitting Ratio in Random Partitioning

While it is a common practice, there is no single standard or universally accepted guideline for the specific data splitting ratio to be used in the random partitioning strategy (Ercanoglu & Sonmez, 2018; Segoni et al., 2024; Abdelkader & Csámer, 2025). The choice of the splitting ratio can vary between different studies, and depends on factors like the characteristics of the study area, the availability of landslide data, the type of model employed, and the resolution of the spatial data (Huang et al., 2022). In the literatures, quite a number of splitting ratios were used which include 90:10 (Shirzadi et al., 2019), 80:20 (Mondini et al., 2023), 75:25 (Sharma & Mahajan, 2018), 70:30 (Yu et al., 2023), 60:40 (Yang, 2017) and 50:50 (Oh & Lee, 2017).

Despite the lack of a formal standard, the 70:30 ratio (70% for training and 30% for testing or validation) is the most widely used and preferred splitting ratio among many researchers in landslide susceptibility studies using random partitioning (Huang et al., 2022; Ebrahim et al., 2024; Segoni et al., 2024). Several studies have specifically investigated different splitting ratios and found the 70:30 ratio to be effective or the most efficient for their models and datasets (Mancini et al., 2010; Catani et al., 2013; Yordanov & Brovelli, 2021). Meanwhile, Selamat et al. (2023) concluded that the 80:20 ratio achieved the best accuracy with an Artificial Neural Network (ANN) model, followed by 70:30 ratio. Conversely, Jaafari et al. (2019) and Sahin et al. (2020) both found out that the 90:10 ratio has the lowest performance in terms of predictive accuracy. Among the three ratios (70:30, 60:40, 50:50) considered by Vakhshoori and Zare (2018), none of them have differential impact on the validity of the models employed. Thus, it is evident that different ratios can lead to varying results, and there is no clear consensus on which particular splitting ratio consistently yields the best outcomes (Huang et al., 2022).

2.6.8.3 Techniques or Metrics used

To quantify both model fit and predictive performance, a variety of statistical metrics and evaluation techniques are employed in landslide susceptibility modeling (Guzzetti et al., 2006b; Frattini et al., 2010; Rossi et al., 2010). In earlier studies, model accuracy was often evaluated through simple visual comparison of actual landslides with susceptibility classifications (Brabb, 1984; Gökceoglu & Aksoy, 1996), or sometimes in terms of basic statistics like efficiency or accuracy (Carrara, 1983). However, these simple statistics were later found to pose some problems as they often required defining a cut-off value for classification (Frattini et al., 2010). Landslide density within different susceptibility classes was another common metric employed (Montgomery & Dietrich, 1994; Ercanoglu & Gokceoglu, 2002; Crosta & Frattini, 2003), which is sometimes referred to as *degree of fit* (Irigaray et al., 1999; Baeza & Corominas, 2001; Fernández et al., 2003) or *b/a ratio* (Lee & Min, 2001; Lee et al., 2003). These methods were usually based on comparing the susceptibility map with the same movements used to create it (Irigaray et al., 1996), which could determine if the map explained past landslides but not necessarily predict future ones (Irigaray et al., 1999). Some early validation techniques involved comparing the resulting map to observed data (Corominas et al., 2014).

Over time, particularly after the year 2000, the field witnessed a remarkable increase in the diversity and complexity of evaluation techniques and metrics (Reichenbach et al., 2018). Quantitative validation approaches began to replace qualitative procedures for more objective evaluation (Frattini et al., 2010). A prominent development was the introduction of cutoff-independent performance criteria. The Receiver Operating Characteristic (ROC) curve and its associated Area Under the Curve (AUC or AUROC) were widely adopted, and became the most frequently used validation techniques (Pourghasemi et al., 2012b; Lima et al., 2022; Segoni et al., 2024; Abdelkader et al., 2025). The ROC curve plots the probability of correctly identified landslides (True Positive Rate or Sensitivity) against the probability of falsely identified landslides (False Positive Rate or 1-Specificity) as a cut-off probability varies (Gorsevski et al., 2006). The AUC value is used to evaluate the compatibility and predictability of a model, with a higher AUC indicating better predictive accuracy. The AUC varies from 0.5 (random chance) to 1, where 1 signifies perfect predictive capacity of the model (Swets, 1988; Brown & Davis 2006). Another commonly applied technique is the Success Rate Curve (SRC) and Prediction Rate Curve (PRC) metrics. The success rate curve compares the prediction image with the training data used for modelling (Chung & Fabbri, 2003), and help in determining how well the resulting susceptibility maps classify existing landslides (Bui et al., 2012b). The prediction rate curve compares model results with an independent validation dataset, and explain how well the model predicts results based on data not used in building the model (Chung & Fabbri, 1993). A curve further from the random diagonal indicates better performance in both the cases (Remondo et al., 2003b). Interpretation of the area under the success/prediction-rate curves is done using similar rules applied for the ROC AUC (Deng et al., 2017; Zêzere et al., 2017).

The confusion matrix, or contingency table forms a basis for many evaluation metrics (Stehman, 1997). The confusion matrix involves four components, viz., True Positives (TP), False Positives (FP), True Negatives (TN), and False Negatives (FN), which represent correctly and incorrectly classified landslides (Abdelkader & Csámer, 2025). Several performance metrics are calculated from these values including Accuracy (ACC), Positive (or Precision) Predictive Value (PPV), Negative Predictive Value (NPV), Recall (Sensitivity), Specificity, Fallout, Total Skill Score (TSS), and F1 Score. The overall accuracy (OA) is a combination of metrics like Accuracy, F1 Score and AUC where the greater OA value signifies the better results (Ng et al., 2021; Ebrahim et al., 2024). Other metric derived from the confusion matrix is the Cohen's kappa Coefficient (or index) (Cohen, 1960; Hoehler, 2000). This index measures the agreement between predicted and actual landslide classifications which accounts for the possibility of agreement by chance (Guzzetti et al., 2006b). Metrics derived from the confusion matrix often require defining a susceptibility cut-off value, which can introduce limitations (Frattini et al., 2010). The Root Mean Square Error (RMSE) and Mean Squared Error (MSE) are other metrics used to quantify the difference between predicted values and actual values, often used in regression analyses (Nguyen et al., 2019), where lower values indicate better performance (Zhou et al., 2018). The Mean Absolute Error (MAE) is similar to MSE and RMSE, but it measures the average magnitude of errors in predictions (Collini et al., 2022). The common techniques and metrics used in model evaluation is shown in Table 2.7.

Apart from these, there are several other evaluation techniques including R-Index, Structural Similarity Index (SSI), Brier score, Cost curves, Matthews Correlation Coefficient (MCC), etc. The number and variety of performance metrics and techniques have continued to increase as more researches continue. Reichenbach et al. (2018) identified at least 92 unique metrics for model fit and 60 unique metrics for prediction performance up to the year 2016, while Huang et al. (2022) recognized a greater number of unique metrics. Despite the significant increase in the number and sophistication of evaluation techniques, there is still no universal consensus on which method or metric is the best or superior than others for all situations (Reichenbach et al., 2018; Ebrahim et al., 2024; Segoni et al., 2024). Different metrics provide different insights, and it is widely recommended to use a comprehensive set of multiple metrics for evaluation (Reichenbach et al., 2018; Huang et al., 2022). Researchers are actively working to design new and more reliable evaluation methods to enhance the credibility and usefulness of landslide susceptibility maps.

2.7 Vulnerability

The word "vulnerability" originates from the Latin verb *vulnerare*, meaning "to wound," or the noun *vulnus*, meaning "wound" (Alexander, 2005; Fekete & Montz, 2018; Andharia, 2022). Originally, the term expressed the idea of being "capable of being physically wounded", and since the late 1600s, it has been used to denote "defencelessness against non-physical attacks" (Andharia, 2022). The term itself holds a commonplace meaning of 'being prone to' or 'susceptible to damage or injury' (Blaikie et al., 1994). Generally, it refers to the potential for loss or other adverse impacts

Table 2.7 *The main metrics used in model evaluation* (*after* Huang et al., 2022)

Metrics	Formulas	Descriptions
AUC	$AUC = \frac{\sum TP + \sum TN}{P + N}$	The area under the ROC curve is defined as the AUC value. A higher value of AUC denotes better model performance
Accuracy	$\text{Accuracy} = \frac{TP + TN}{TP + FP + TN + FN}$	Accuracy is the proportion of land-slide and non-landslide pixels that are classified correctly
Sensitivity	$\text{Sensitivity} = \frac{TP}{TP + FN}$	Sensitivity (or recall or true positive rate) means the proportion of land-slide pixels that are correctly classi-fied
Specificity	$Specificity = \frac{TN}{FP + TN}$	Specificity (or true negative rate) in-dicates the ability of the test to cor-rectly distinguish non-landslide pix-els
Precision	$Precision = \frac{TP}{TP + FP}$	Precision (or positive predictive rate) represents the proportion of actual landslide pixels to those classified as landslides by the model
Kappa index	$kappa = \frac{Accuracy - Accuracy_{exp}}{1 - Accuracy_{exp}}$ $Accuracy_{exp} = \frac{(TP+FN)(TP+FP)+(FP+TN)(TN+FN)}{(TP+TN+FP+FN)^2}$	Measure the agreement between true classes and the classifications
Negative predictive rate	$\text{Negative predictive rate} = \frac{TN}{TN + FN}$	The probability that predictive non-landslide pixels have actual non-land-slide occurrences
False positive rate	$\text{False positive rate} = \frac{FP}{FP + TN}$	The rate of non-landslide instances falsely classified as landslide pixels
F-measure	$F = \frac{2 * Sensitivity * Precision}{Sensitivity + Precision}$	The harmonic mean of precision and recall
Root mean square error	$\text{Root mean square error} = \sqrt{\frac{1}{n}\sum_{i=1}^{n}(X_i - \bar{X}_i)^2}$	Show the error measure between the predicted and actual values
Mean square error	$\text{Mean square error} = \frac{1}{n}\sum_{i=1}^{n}(X_i - \bar{X}_i)^2$	Show the error measure between the predicted and actual values
Mean absolute error	$\text{Mean absolute error} = \frac{1}{n}\sum_{i=1}^{n}\lvert X_i - \bar{X}_i\rvert$	An error-based measure to check the performance of the models

TP true positive, *TN* true negative, *FN* false negative, *FP* false positive. *P* and *N* represent the total number of landslides and non-landslides, respectively. *n* is the total number of samples. X_i and $\bar{X}_i$ are the predicted and actual values of outputs, respectively

(Alexander, 2005; Cutter, 1996). Within the context of natural hazards and disaster risk research, its meaning is multifaceted, dynamic, and subject to intense debate and varying interpretations across different academic domains and stakeholders (Birkmann, 2006a; Tapsell et al., 2010; Fuchs et al., 2011; Fekete & Montz, 2018).

Due to its multi-dimensional and interdisciplinary nature, there exists a wide variety of definitions of vulnerability (Papathoma-Köhle et al., 2017). One of the best-known and generally accepted definitions is given by the United Nations/International Strategy for Disaster Reduction (UNISDR) which defines vulnerability as "the conditions determined by physical, social, economic and environmental factors or processes, which increase the susceptibility of a community to the impact of hazards" (UNISDR, 2004). Meanwhile, Blaikie et al. (1994) introduced a prominent definition from the social science perspective which states that "the characteristics of a person or group and their situation that influence their capacity to anticipate, cope with, resist and recover from the impact of a natural hazard". From the climate change science perspective, the Intergovernmental Panel on Climate Change (IPCC) defines vulnerability as "the propensity or predisposition to be adversely affected. Vulnerability encompasses a variety of concepts and elements including sensitivity or susceptibility to harm and lack of capacity to cope and adapt" (IPCC, 2014). Apart from these, there are several other definitions proposed by various scholars, some of which are presented in Table. 2.8. It should be noted that while specific definitions are widely used within particular disciplines or by certain international bodies, the broader academic and practical landscape reveals that a single, universally accepted definition of vulnerability remains elusive. The complexity of the concept, its various dimensions, and differing research objectives contribute to this ongoing debate and the proliferation of definitions.

2.7.1 The Paradigm Shift in Understanding Vulnerability

The early perception and conception of vulnerability in the context of natural hazards and risk originated from a predominantly hazard-centric and technocratic viewpoint (Birkmann et al., 2017). Initially, disasters were often viewed as inevitable "acts of God" (Steinberg, 2000; Weichselgartner, 2001) or "acts of nature," (Stallings, 2006; de León, 2007) with mitigation efforts predominantly concentrating on the physical

Table 2.8 *Some key definitions of Vulnerability*

Author(s)	Definition of vulnerability
Gabor & Griffith (1980)	Vulnerability is the threat (to hazardous materials) to which people are exposed (including chemical agents and the ecological situation of the communities and their level of emergency preparedness).
Timmerman (1981)	Vulnerability is the degree to which a system acts adversely to the occurrence of a hazardous event. The degree and quality of the adverse reaction are conditioned by a system's resilience (a measure of the system's capacity to absorb and recover from the event).
Susman et al. (1984)	The degree to which different classes in society are differentially at risk, both in terms of the probability of occurrence of an extreme event and the degree to which the community absorbs the effects of extreme physical events and helps different classes to recover.
Dow (1992)	Vulnerability is the differential capacity of groups and individuals to deal with hazards, based on their positions within physical and social worlds.
Cutter (1993)	Vulnerability is the likelihood that an individual or group will be exposed to and adversely affected by a hazard. It is the interaction of the hazards of place (risk and mitigation) with the social profile of communities.
Bohle et al. (1994)	Vulnerability is best defined as an aggregate measure of human welfare that integrates environmental, social, economic and political exposure to a range of potential harmful perturbations.
Buckle et al. (2000)	The degree of loss to a given element at risk or set of such elements resulting from the occurrence of a natural phenomenon of a given magnitude and expressed on a scale from 0 (no damage) to 1 (total loss) or in per cent of the new replacement value in the case of damage to property.
Alexander (2002)	The susceptibility of people and infrastructure to loss due to a given level of hazard, a given probability of a hazard occurring at a given time, in a given place, in a given manner and with a given magnitude.
Turner et al. (2003)	Vulnerability is the degree to which a system, subsystem, or system component is likely to experience harm due to exposure to hazard, either a perturbation or stress/stressor.
Adger (2006)	Susceptibility to damage due to exposure to stresses associated with environmental and social change, and lack of adaptive capacity.
Thywissen (2006)	Vulnerability is the intrinsic and dynamic feature of an element at risk (community, region, state, infrastructure, environment etc.) that determines the expected damage/ harm resulting from a given hazardous event and is often even affected by the harmful event itself.
Hufschmidt (2011)	Vulnerability is understood as a concept describing the differences in the degree of damage incurred from natural hazards that are manifested for an individual person, for a whole community, a city, or an entire region.

impacts of extreme natural events. This *hazard-centric technocratic* approach, prevalent until the late 1970s, addressed merely physical vulnerabilities or direct side effects of disasters through technical solutions (Joseph, 2013). However, a significant paradigm shift occurred in the late 1970s and early 1980s, when social scientists began to challenge this purely technocratic approach, arguing that increasing disaster losses were not solely attributable to natural occurrences but were largely influenced by prevailing societal conditions and human actions (O'Keefe et al., 1976; Cardona, 2004; Schneiderbauer et al., 2017). It was during these periods (late 1970s to early 1980s) that the concept of vulnerability was introduced "as a response to the hazard-centric perception of disasters" (Birkmann et al., 2017). The establishment of the 1990-1999 UN International Decade for Natural Disaster Reduction (IDNDR) further propelled this shift, which highlighted the critical role of vulnerability in disaster risk reduction (Wisner & Luce, 1993; Blaikie et al., 1994; Fuchs & Thaler, 2018). This period has witnessed vulnerability emerging as a "pre-existing condition" or a "state that exists within a system before it encounters a hazard," rather than solely as a measure of damage after an event (Fuchs et al., 2011; Ciurean et al., 2013; Sterlacchini et al., 2014). Thus, vulnerability is broadly viewed from the perspective of natural science or engineering, and from the perspective of social science domains.

2.7.2 Components of Vulnerability

Within the various conceptual frameworks, vulnerability is often disaggregated into several core components, though their precise delineation can vary widely. These components are briefly described below:

Exposure: This describes the extent to which a unit (e.g., people, property, systems, or natural assets) falls within the geographical or temporal range of a hazard event (Rufat, 2024), and refers to fixed physical attributes or human systems like livelihoods and economies that are spatially bound (Birkmann et al., 2014). While some frameworks consider exposure as a part of vulnerability (Turner et al., 2003; Birkmann, 2006b), others integrate it as a component of vulnerability or a hybrid between vulnerability and the natural hazard (Cardona & Barbat, 2000).

Susceptibility (or Sensitivity/Fragility): This component describes the predisposition of elements at risk (be they social or ecological) to suffer harm (Birkmann et al., 2014; Rufat, 2024). Susceptibility points to deficiencies that determine the likelihood of experiencing severe harm and loss due to adverse events. The term *susceptibility* is preferred over *sensitivity* in natural hazards and climate change contexts, as *sensitivity* can imply movement in both positive and negative directions, and is also used in ecology with a different meaning (Birkmann, 2013).

Coping Capacity: This denotes the ability of a person, group, or system to use its own resources "to anticipate, cope with, resist, and recover from the impact of a natural hazard" or "to face and manage emergencies, disasters, or adverse conditions" (Blaikie et al., 1994; Pelling, 2013). Coping mechanisms frequently build on past experiences and are usually hazard-related and short-term oriented, and focuses on the immediate reaction during a crisis (Birkmann, 2011; Welle et al., 2013).

Adaptive Capacity: This refers to the "ability to deal with, recover from, or reduce the future impact of pressures", which aim to modify and change the situation to improve a society's ability to live with environmental and socio-economic changes over time (Birkmann et al., 2013; Kok & Jäger, 2013). A low adaptive capacity is associated with increased vulnerability, whereas a high adaptive capacity promotes resilience (Lanlan et al., 2024).

2.7.4 Dimensions of Vulnerability

Vulnerability is recognized as a multidimensional phenomenon, encompassing various thematic aspects that interact to shape its overall manifestation. These dimensions include the following:

Physical Vulnerability: This dimension encompasses the predisposition of physical assets, such as built-up areas, infrastructure, and open spaces, to suffer damage (Birkmann et al., 2017; Fuchs et al., 2018). This includes the susceptibility of structures and infrastructure to damage (Fuchs & Thaler, 2018), which is usually influenced by construction materials, building standards, and maintenance (Fuchs, 2009; Tierney, 2022).

Social Vulnerability: This dimension delves into "aspects of justice, social differentiation, and societal organisation, as well as individual strength" (Adger, 2006; Few, 2007; Birkmann, 2013). It encompasses factors such as poverty, powerlessness, social marginalization, demographic characteristics (e.g., age groups, gender), education, migration, social networks, health and well-being, and risk perception (Cutter et al., 2003; Dwyer et al., 2004).

Economic Vulnerability: This dimension relates to the propensity for loss of economic value from damage to physical assets and/or disruption of productive capacity (Birkmann et al., 2014; 2017). It includes impacts on savings, property, and other physical assets, and is related to the wealth of a society, economic patterns, and the ability to earn income (Blaikie et al., 1994; Tapsell et al., 2010).

Institutional Vulnerability: This refers to the "potential for damage to governance systems, organisational forms, and functions of organisations that govern societies through formal or informal rule systems" (Ciurean et al., 2013; Birkmann et al., 2017). It considers weaknesses embedded in institutions, public policy, and administration that reduce the capacity of a society to withstand, resist, cope, or recover from natural hazards (Fuchs & Thaler, 2018).

Environmental Vulnerability: This dimension pertains to the potential for damage to all ecological and biophysical systems and their different functions (Birkmann et al., 2017), including specific ecosystem functions and environmental services (Renaud et al., 2013). Environmental degradation can increase human vulnerability, particularly for populations dependent on ecosystem services and resources (Guo et al., 2010; Adla et al., 2022).

Cultural Vulnerability: This dimension characterises the potential for damage to intangible values, such as meanings attributed to artefacts, customs, habitual practices, and natural or urban landscapes, including indigenous beliefs (Tapsell et al., 2010; Birkmann et al., 2017). These cultural factors can influence the preparedness and willingness of a population to engage in risk-reduction efforts, as well as their capacity to learn from past events (Schneiderbauer & Ehrlich, 2004; Schneiderbauer et al., 2017). From the foregoing discussion, it can be observed that the concept of vulnerability has undergone a profound evolution, moving from its etymological origins to becoming a central and intricate pillar in disaster risk science. The journey from a hazard-centric, technocratic viewpoint to a more holistic understanding reveals an important paradigm shift (Birkmann, 2017) that disasters are no longer seen as purely natural events, but as outcomes of the complex interactions between a hazard and the pre-existing conditions of a society (O'Keefe et al., 1976; Cardona, 2004). The lack of a single, universally accepted definition is not a weakness, but rather a testament to the multifaceted and dynamic nature of the concept, which fosters interdisciplinary collaboration (Adger, 2006; Fekete et al., 2014).

2.8 Social Vulnerability

Social vulnerability is a foundational concept in understanding how natural hazards translate into disasters, and emphasizes that the impacts of such events are not solely determined by physical forces but are deeply shaped by social, economic, and political factors (Blaikie et al., 1994; Cutter & Finch, 2008; Birkmann et al., 2013; Cutter, 2024). At its core, social vulnerability refers to "the characteristics of a person or group and their situation that influence their capacity to anticipate, cope with, resist, and recover from the impact of a natural hazard", and quantifies the degree to which the life, livelihood, property, and other assets of an individual or a community are put at risk by an extreme natural event or process (Blaikie et al., 1994). The United Nations International Strategy for Disaster Reduction defines it as "the characteristics and circumstances of a community, system or resource that make it susceptible to the harmful effects of a hazard" (UNISDR 2009), and recognizes that it is fundamentally linked to social and spatial inequality processes and outcomes (Cutter et al., 2003; Cutter, 2024). The very definition of social vulnerability can vary depending on the research perspective (Frigerio & De Amicis, 2016), for instance, focusing on intangible losses (Ciurean et al., 2013), the underlying socioeconomic factors (Cutter et al., 2003), or integrating susceptibility with coping and adaptive capacities (Nguyen et al., 2017). As such, there is no single, universally accepted definition, and several scholars use this term with different meanings (Tapsell et al., 2010). Some definitions of social vulnerability are presented in Table 2.9.

***Table 2.9** Definitions of Social Vulnerability* (*adapted from* Tapsell et al., 2010)

Social Vulnerability Definition	Reference Source
A term used to define the susceptibility of social groups to potential losses from hazard events or society's resistance and resilience to hazard.	Blaikie et al. (1994); Hewitt (1997)
The characteristics of a person or group and their situation that influence their capacity to anticipate, cope with, resist and recovery from the impact of a natural hazard … It involves a combination of factors that determine the degree to which someone's life, livelihood, property and other assets are put at risk by a discrete and identifiable event … in nature and in society.	Wisner et al. (2004)
Social vulnerability derives from the activities and circumstances of everyday life or its transformations.	Hewitt (1997)
The condition of a given area with respect to hazard, exposure, preparedness, prevention, and response characteristics to cope with specific natural hazards. It is a measure of the capability of this set of elements to withstand events of a certain physical character.	Weichselgartner (2001)
The product of social inequalities 'it is defined as the susceptibility of social groups to the impacts of hazards, as well as their resiliency or ability to adequately recover from them … susceptibility is not only a function of demographic characteristics … but also more complex constructs such as health care provision, social capital and access to lifelines.	Cutter and Emrich (2006)
Emanates from social factors that place people in highly exposed areas, affect the sensitivity of people to that exposure, and influence their capacity to respond.	Yarnal (2007)

2.8.1 Factors Influencing Social Vulnerability

The factors contributing to social vulnerability are diverse and interconnected, and varies across different geographical and societal contexts (Tapsell et al., 2010). These factors can be broadly categorized into several key dimensions:

1. Socioeconomic Status: These are the primary drivers, with lack of wealth and poverty being consistently identified as major contributors to increased vulnerability (Adger, 1999; Cutter et al., 2003). Individuals and communities with limited financial resources often lack the reserves or safety nets to absorb shocks, diversify income sources, or access vital resources for recovery (Cutter et al., 2003; Bergstrand et al., 2015;

Nor Diana et al., 2021). Related to this are factors like employment status, occupation, and income diversity, which influence a household economic stability and resilience (Cutter et al., 2003; Cutter & Morath, 2013).

2. Demographic Characteristics: These are another notable factor which play an important role. Age (e.g., children, elderly, or dependent adults) is an important indicator, since these groups may have reduced mobility, fewer resources, or require specialized assistance during and after a disaster (Adger, 2003; Dwyer et al., 2004; Tate et al., 2010). Gender can also indicate increased vulnerability due to potential lack of information, wealth, or societal biases (Schmidtlein et al., 2011; Tate, 2012). Minority populations and those facing disability are more vulnerable due to social marginalization, discrimination, or specific needs not adequately met by mainstream systems (Adger & Kelly, 2001; Cutter et al., 2003). Other demographic factors include family structure, population growth, and population density (Eidsvig et al., 2014; Frigerio & De Amicis, 2016).

3. Access to resources: This is a broad factor encompassing tangible and intangible assets. It includes not only financial resources but also access to information, knowledge, and technology (Cutter et al., 2003; Nor Diana et al., 2021). Communities with limited access to quality education or high illiteracy rates tend to be more vulnerable, as education can influence preparedness and recovery capabilities (Tapsell et al., 2010; Aksha et al., 2019).

4. Built Environment and Infrastructure: The quality and age of housing, as well as the type and density of infrastructure and lifelines, are important drivers of social vulnerability (Eidsvig et al., 2014; Zhou et al., 2014). Poor infrastructure, lack of basic services, and unplanned urban development contribute to higher vulnerability (Tasnuva et al., 2021; Goto et al., 2022). High population density can also exacerbate vulnerability, which suggests more people would be affected and face greater difficulty in evacuation or rescue (de Loyola Hummell et al., 2016; Xiao et al., 2022).

5. Institutional and Governance Factors: The effectiveness of institutional arrangements for preparedness, planning, warning, and services determines collective vulnerability (Adger, 1999; Burton et al., 2018). Lack of access to resources and political power/representation renders populations more vulnerable (McLaughlin et al., 2002;

Bergstrand et al., 2015). Social capital, which comprises social networks and connections, plays a critical role in increasing individual and group resilience and accessing information and assistance (de Oliveira Mendes, 2009; Nor Diana et al., 2021). Institutional failure and lack of social security can increase vulnerability (Frerks et al., 2011).

It is important to note that social vulnerability is a dynamic concept, constantly evolving and varying widely across different geographical contexts (Schmidtlein et al., 2008; Kuhlicke et al., 2011), the scales of analysis (O'Brien et al., 2004; Boruff et al., 2005), and over time (Cutter & Finch, 2008; Santos et al., 2022). The relevance and weighting of different factors can change depending on the specific hazard type, the stage of the disaster cycle, and local socio-cultural particularities (Tapsell et al., 2010; Drakes & Tate, 2022). This complexity makes it challenging to define a single, universal set of indicators or a one-size-fits-all approach to assessment which necessitates context-specific investigations (Tapsell et al., 2010; Lee, 2014). The factors which influence social vulnerability are shown in Table 2.10.

2.8.2 Approaches for Social Vulnerability Measurements

Various approaches have been developed to measure social vulnerability, reflecting its complex, multidimensional nature and the varying disciplinary perspectives of researchers. These approaches can broadly be categorized into quantitative, qualitative, and mixed-methods. These are briefly described below:

1. Quantitative Approaches: Quantitative methods aim to measure and quantify social vulnerability through the development of indices, called social vulnerability indices (SVIs) which aggregate multiple social indicators into a single measure (Cutter et al., 2003; von Szombathely et al., 2023). These indices aim to quantify vulnerability, and make it possible to compare different places or groups and identify dominant drivers (Tierney, 2006; Cutter & Finch, 2008). Two primary methods for constructing SVIs are deductive and inductive approaches (Yoon, 2012). Both techniques aim to quantify social vulnerability using indicators and indices, but they differ in how variables are selected and aggregated.

Table 2.10 *Factors that influence social vulnerability* (*adapted from* Cutter et al., 2003)

Factor	Examples
Lack of access to resources	*Information* (e.g. of hazards, protective action decision options, etc); *knowledge* (i.e., this translates to more informed and prepared citizens and includes understanding of warning sources (environmental, informal and formal) and mitigation, preparedness and response actions); and *technology* (e.g. warning communication devices such as radios, cell phones, televisions)
Limited access to decision making	Political power and representation
Lack of social capital	Social networks and connections
Beliefs and customs	That neglect or ignore hazards or mitigation of hazards and their effects. Ethno-cultural differences, for example, Perception of hazards as 'Acts of God'
Building stock and age	Number, density and type of buildings and whether or not their age predates significant building design codes and enforcement
Frail and physically limited individuals	Those who are unable to take protective actions or require outside assistance to do so (e.g. very young or old, sick, disabled)
Weakness in infrastructure and lifelines	Type and density of infrastructure and lifelines
Population shifts	Population shifts which result in more people living in at risk areas
Increased mobility	More people live in new surroundings and are unfamiliar with the risks in their new areas, and how to respond to them

i) Deductive Approach: This is a top-down methodology that constructs a social vulnerability index by selecting a limited number of variables based on a priori theory and existing literature or research (Kapuka & Hlásny, 2020). This method emphasizes theoretical frameworks to identify the most important dimensions of social vulnerability before data analysis begins (Tate, 2012). Variables fewer than ten are generally used which are then standardized using z scores or linear scaling, and aggregated into one index (Wu et al., 2002; Chakraborty et al., 2005). This approach is relatively simpler and more direct in its procedure, and is useful when the research goal requires a specific, targeted set of variables (Yoon, 2012). The working principle of the deductive method is shown in Figure 2.7.

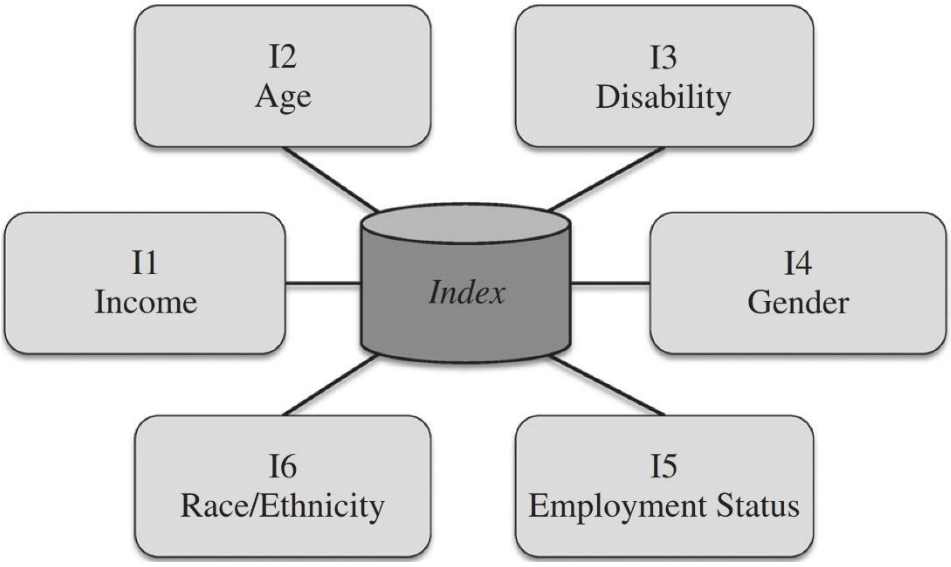

Fig. 2.7 *Deductive approach for social vulnerability assessment adapted from* Tate (2012)

ii) Inductive Approach: This is a data-driven, bottom-up methodology that begins with a larger and more extensive set of variables (mostly from census data) and reducing them into a smaller set of uncorrelated factors using statistical techniques like Principal Component Analysis (PCA) (Spielman et al., 2020; Santos et al., 2022). The identified factors are then interpreted, and often summed or multiplied, to construct the final index (Chen et al., 2013). The inductive approach forms the foundation of most of the vulnerability indices employed in the contemporary social vulnerability studies (Finch et al., 2010; Schmidtlein et al., 2011). The Social Vulnerability Index (SoVI®) by Cutter et al. (2003) is the most recognized example of an inductive approach. This technique can effectively handle a large number of variables and identify underlying patterns that might not be obvious with a deductive approach (Cutter, 2024). The inductive approach for social vulnerability assessment is shown in Figure 2.8.

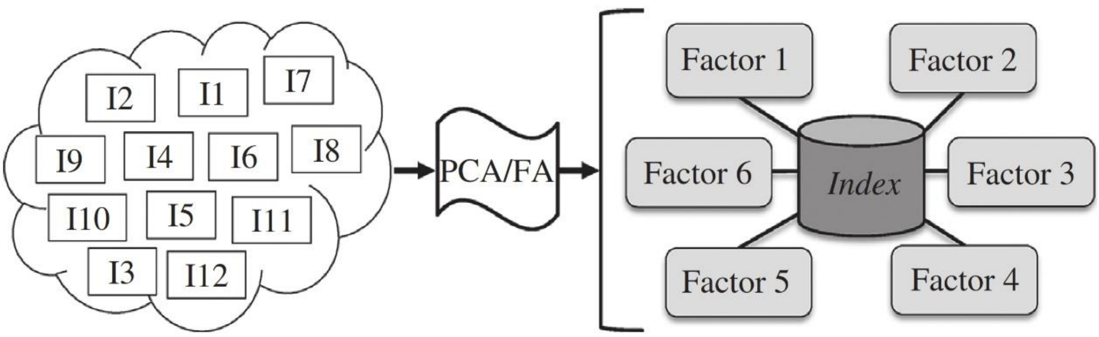

Fig. 2.8 *Inductive approach for social vulnerability assessment adapted from* Tate (2012)

Both deductive and inductive approaches have their own strengths and weaknesses, and are valuable for quantitative social vulnerability assessment. While deductive methods are theory-driven and selective, inductive approaches are data-driven and aim for comprehensive statistical representation (Yoon, 2012). Both are influenced by data availability and quality (King, 2001), which can vary widely by local, region and country (Cutter et al., 2003; Boruff et al., 2005; Santos et al., 2022).

2. Qualitative Approaches: The qualitative methods focus on an in-depth and context-specific understanding of social vulnerability, particularly at the community or household level (Ahmed & Kelman, 2018; Török, 2018). These approaches aim to uncover the processes and relationships that contribute to vulnerability by emphasizing the perspectives of affected populations (Wisner et al., 2004; Kuhlicke et al., 2011; Burton et al., 2018). The methods include structured interviews, focus groups, participatory assessments, and the incorporation of indigenous knowledge and cultural perceptions (Ahmed, 2021; Kalaycıoğlu et al., 2023). They are essential for capturing *immaterial* aspects such as local knowledge, cultural norms, social networks, and trust in institutions, which are difficult to quantify (Kuhlicke, 2010; Scolobig et al., 2008).

3. Mixed or Hybrid Approaches: Mixed or hybrid approaches to social vulnerability measurement involve the integration and combination of both quantitative and qualitative data and methodologies to provide a more comprehensive and insightful understanding of vulnerability (Nguyen et al., 2017; Ahmed & Kelman, 2018). This integration allows for triangulation of standard and non-standard methods, where quantitative indicators can be tested and evaluated in specific contexts using qualitative insights (Kuhlicke et al., 2011). By combining the statistical robustness of quantitative data with the nuanced insights from qualitative research, a more holistic understanding of the interaction between social structures and environmental risks can be achieved (Pengapenga & Mzuza, 2023). The hybrid methods help to mitigate the inherent weaknesses present both in the quantitative and qualitative approaches (Ahmed & Kelman, 2018).

Regardless of the approach, several important considerations influence social vulnerability assessment. The scale of analysis is an essential factor, as vulnerability can be spatially and socially differentiated (Cutter, 1996), and the choice of scale impacts data availability and interpretation (Rygel et al., 2006; Tate, 2013). The temporal dynamics is another important factor since social vulnerability is influenced by ongoing societal trends, policy changes, and other factors that vary over time and space (Tapsell et al., 2010). Ultimately, the purpose of the assessment, whether for policy-making, resource allocation, or risk reduction, should guide the selection of appropriate methodologies and indicators (Eakin & Luers, 2006; Tapsell et al., 2010). It should be noted that there is no single, universally accepted methodology for measuring social vulnerability (Yoon, 2012; Ciurean et al., 2013; Fekete & Montz, 2018).

2.9 Physical Vulnerability

In the context of landslide hazard, physical vulnerability assessment is a fundamental and challenging aspect of understanding and quantifying the risks posed by a landslide hazard to the built environment and human lives (Papathoma-Köhle, 2016; Chen et al., 2020). This assessment is considered indispensable for evaluating risk and predicting the consequences of hazard events (Fuchs, 2009). The main purpose is to estimate the potential for damage to physical assets, particularly buildings and infrastructure, and to translate hazard levels into an estimated level of risk, which is essential for mitigation planning and emergency management (Papathoma-Köhle et al., 2012). Assessment of physical vulnerability is vital for several reasons as it enables the formulation of reliable forecasts regarding the hazard impacts (Fuchs et al., 2018), and guides in land use planning and civil protection initiatives (Leal et al., 2021). It also helps prioritize which buildings require immediate intervention, and also indicates suitable locations for safer construction (Chen et al., 2020). Besides, it supports cost-benefit analyses (Holub & Fuchs, 2008; Bera et al., 2020) and thorough risk assessments for future scenarios (Mazzorana et al., 2012).

2.9.1 Defining Physical Vulnerability: Diverse Perspectives

The concepts and definitions of physical vulnerability vary across existing literatures (Brooks, 2003; Akbas et al., 2009), which results in a lack of universal consensus (Füssel, 2007). Table 2.11 shows some of the definitions proposed by different scholars.

Table 2.11 *Definitions of Physical Vulnerability* (*adapted from* Fuchs et al., 2018)

Authors	Definition
Brooks (2003)	"The term 'biophysical' [vulnerability] … suggests both a physical component associated with the nature of the hazard and its first-order physical impacts, and a biological or social component associated with the properties of the affected system that act to amplify or reduce the damage resulting from these first-order impacts."
Akbas et al. (2009)	"the degree of loss to a given element at risk, particularly to built structures, resulting from the occurrence of a hazard of a given magnitude."
Birkmann et al. (2015)	"potential for damage to physical assets including built-up areas, infrastructure and open spaces."
Cardona et al. (2004)	"the degree of exposure and fragility of the exposed elements to the action of the phenomena."
Cutter et al. (2000)	"Social and bio-physical vulnerability are broader in scope and refer to social groups and landscapes that have the potential for loss from environmental hazards events."
UNDRO (1984)	"degree of loss to a given element, or set of elements, within the area affected by a hazard. It is expressed on a scale of 0 (no loss) to 1 (total loss)."
Fell (1994) and Varnes (1984)	"Thus, vulnerability – often referred to as 'technical' or 'physical' vulnerability – is defined as the expected degree of loss for an element at risk as a consequence of a certain event."
Fuchs (2009)	Vulnerability "is defined as the expected degree of loss for an element at risk, occurring due to the impact of a defined hazardous event. These events are themselves conditioned by a certain intensity, frequency and duration, all of which affect vulnerability."

Physical vulnerability is generally understood and approached from two main perspectives. The first perspective focuses on the *ex-post* outcome or "degree of loss," which defines physical vulnerability as "the degree of loss to a given element, or set of elements, within the area affected by a hazard. It is expressed on a scale of 0 (no loss) to 1 (total loss)" (UNDRO, 1984). This approach is referred to as the technical or engineering perspective and focuses on the consequences of a hazardous event (Ciurean et al., 2013; Sterlacchini et al., 2014). It aims to quantify the expected level of damage by establishing a relationship between the hazard intensity (e.g., debris height, velocity, impact pressure for landslides; inundation depth for floods) and the resulting degree of loss (Quan Luna et al., 2011; Tarbotton et al., 2015; Papathoma-Köhle et al., 2017). The various methods commonly employed under this perspective include vulnerability (or damage) curves and vulnerability matrices (Papathoma-Köhle et al., 2017). This perspective requires substantial empirical data from past events to develop reliable relationships, which can be a significant challenge for less frequent hazards (Tarbotton et al., 2015; Fuchs et al., 2018).

The second perspective views physical vulnerability as an *ex-ante* "pre-existing conditions" or susceptibility of elements at risk. According to this, physical vulnerability is understood as the "characteristics and circumstances of a community, system, or asset that makes it susceptible to the damaging effects of a hazard" (UNISDR, 2009). This approach gives less emphasis to the process magnitude or intensity directly in its initial definition (Fuchs et al., 2011), and instead, focuses on the intrinsic properties and resistance capacity of the element at risk to withstand an impact (Fuchs, 2009; Totschnig et al., 2011; Silva & Pereira, 2014). It seeks to identify the underlying factors, or vulnerability indicators, that contribute to the susceptibility of a structure to damage (Birkmann, 2006a; Kappes et al., 2012; Bera et al., 2020). These indicators include a wide range of building characteristics such as construction material, number of floors, age, structural typology, state of maintenance, etc. While primarily qualitative or semi-quantitative, modern approaches under this perspective seek to integrate hazard intensity and building susceptibility into a physical vulnerability index to provide a more comprehensive assessment (Li et al., 2010; Singh et al., 2018).

Across these perspectives, physical vulnerability is consistently seen as a function of both the hazard intensity and the resistance or intrinsic characteristics of the exposed element (Fell, 1994; Fell & Hartford, 1997). Although historically used in isolation or even seen as conflicting, a more holistic understanding of physical vulnerability increasingly emphasizes the complementary nature of these two perspectives (Papathoma-Köhle, 2016; Papathoma-Köhle et al., 2017). The *degree of loss* approach provides concrete, quantitative results of *what* the damage is, while the *pre-existing condition* approach helps to understand the *drivers* of that vulnerability and *why* certain elements are more susceptible, both of which support targeted mitigation and preparedness strategies (Papathoma-Köhle, 2016). Both approaches involve uncertainties, whether due to limited knowledge (epistemic) or natural variability (aleatory), and their quantification remains a significant challenge for improving the reliability of vulnerability assessments (Ciurean et al., 2013; Papathoma-Köhle et al., 2017; Khan et al., 2022).

2.9.2 Factors Influencing Physical Vulnerability

Factors which influence the physical vulnerability can be broadly categorized into two main groups. The first one is called the extrinsic factors or the hazard characteristics which refers to the magnitude and intensity of the event. This is usually measured by parameters such as the landslide area or volume (Lee & Jones, 2014; Li et al., 2010), velocity (Uzielli et al., 2015a; Guillard-Gonçalves et al., 2016), the depth of affected material or deposition height, and impact pressure (Quan Luna et al., 2011; Totschnig & Fuchs, 2013). The type of landslide movement (e.g., rapid debris flow or slow-moving landslide) also dictates the potential impact on the structures (Cardoso et al., 2023; Wang & Mao, 2025). The proximity of the element to the landslide or hazard zone plays an important role in determining the degree of exposure and potential damage (Singh et al., 2019; Mirdda et al., 2022). The temporal and spatial variability of the hazard also influences vulnerability (Papathoma-Köhle et al., 2011; 2015).

The other one called the intrinsic factor relates to the inherent capacity of the building to resist and withstand an impact or its susceptibility to damage (Agliata et al., 2021). These are often evaluated using a set of indicators which include construction materials and techniques (e.g., brick masonry, concrete, reinforced concrete), state of maintenance, number of floors, structural typology, foundation depth, orientation, building age, and the presence of protection measures or early warning systems (Fell & Hartford, 1997; Fuchs et al., 2007; Li et al., 2010; Singh et al., 2018; Shi et al., 2024). The surrounding environment and the location of the building relative to the hazard are also important factors considered (Papathoma-Köhle et al., 2007; Singh et al., 2019). Some studies also incorporate geomorphic conditions as part of resistance indicators, particularly in mountainous regions (Bera et al., 2020).

The physical vulnerability of buildings is, therefore, determined by the complex interaction of these hazard-specific and building-specific characteristics. The weighting of these various indicators, especially in areas with limited historical damage data, often relies on expert judgment (Sterlacchini et al., 2014; Cardoso et al., 2023). This introduces subjective elements and contributes to inherent uncertainties in physical vulnerability assessments (Uzielli et al., 2015b; Guillard-Gonçalves et al., 2016).

2.9.3 Assessment Approaches/Models

Till now, there is no single, universally accepted methodology for assessing physical vulnerability, as the methods vary depending on the specific study, hazard type, and available data (Glade & Crozier, 2005; Papathoma-Köhle, 2016; Luo et al., 2023). These approaches can be broadly classified into two main categories: qualitative methods which include experience-based and indicator-based models; and quantitative methods which comprise data-driven and mechanism-based models (Luo et al., 2023). These are briefly described below:

1. Experience-Based Models (Qualitative): These models assess physical vulnerability based on expert experience or opinion and historical data (Fell & Hartford, 1997; Michael-Leiba et al., 2002; Silva & Pereira, 2014), and present the results as a single vulnerability value or qualitative description (Luo et al., 2023). They frequently use vulnerability matrices or tables where the level of damage is described qualitatively (e.g., slight, moderate, significant, partial, complete) and assign a numerical vulnerability value ranging from 0 to 1 (Leone et al., 1996; Papathoma-Köhle et al., 2017). The models are relatively simple and do not require *ex-ante* (before the event) data or highly detailed information, and are generally easy to use in practice (Fuchs et al., 2019; Luo et al., 2023). They can also be adapted for multiple hazard types and elements at risk, such as people and roads (Cardinali et al., 2002; Bell & Glade, 2004).

2. Indicator-Based Models (Qualitative/Semi-Quantitative): These models use a set of vulnerability indicators which are characteristics of the exposed asset and its surroundings, to assess vulnerability (Papathoma-Köhle et al., 2007; Kappes et al., 2012). The process involves selecting relevant indicators, identifying their importance and assigning weights, and then aggregating them into a vulnerability index (Papathoma-Köhle et al., 2011; Khan et al., 2022). "The weight of each attribute was assessed using a semi-quantitative standardization method to determine the physical vulnerability." (Bera et al., 2020). Indicator-based approaches are flexible and user-friendly, adaptable to different hazards and specific user needs (Kappes et al., 2012; Cardoso et al., 2023). They allow for assessing vulnerability at an individual building level and can show relative variations among houses (Bera et al., 2020).

3. Data-Driven Models (Quantitative): These models constitute the most popular approach which are developed through statistical analysis of post-disaster data by linking landslide intensity and building damage (Luo et al., 2023; Li et al., 2025). However, they do not explicitly involve building resistance in the model. Most data-driven models are expressed as vulnerability curves (or functions) or fragility curves. Vulnerability curves (or functions) relate hazard intensity (on the x-axis) and the expected degree of loss (on the y-axis) which are expressed as a damage ratio (Totschnig et al., 2011; Tarbotton et al., 2015). The curves are either developed from empirical data (Fuchs et al., 2007; Akbas et al., 2009), numerical modeling (Quan Luna et al., 2011; Rheinberger et al., 2013), or from laboratory experiments (Gems et al., 2016; Zhang et al., 2016b). The fragility curves, on the other hand, express the conditional probability of reaching or exceeding a certain damage state (e.g., slight, moderate, extensive, complete damage) for a given hazard intensity (Douglas, 2007; Haugen & Kaynia, 2008). The data-driven models provide quantitative, measurable results that can be translated into monetary costs, which is useful for cost-benefit analyses of structural protection measures (Mazzorana et al., 2009; Papathoma-Köhle et al., 2017).

4. Mechanism-Based Models (Quantitative): These are also called analytical methods (Ciurean et al., 2013; Sterlacchini et al., 2014) or numerical models (Wang et al., 2025), and are considered the most promising type of quantitative vulnerability models (Luo et al., 2023). These models focus on the behaviour of buildings and structures based on engineering criteria, and employ physical modeling tests or computer simulation techniques (Baiges & Codina, 2010; Parisi & Sabella, 2017). This is achieved by defining a performance function to generate fragility curves (Del Zoppo et al., 2022; Luo et al., 2022). These curves express the probability of a structure reaching or exceeding a specific damage state given a certain level of hazard intensity (Fotopoulou & Pitilakis, 2017). Mechanism-based models provide a “better understanding of the relationship between the intensity of the hazardous phenomenon and the expected degree of damage” (Cardoso et al., 2023). They are also useful for investigating structural behaviour, proposing vulnerability reduction measures, and evaluating their efficiency.

A general overview of the various approaches for assessing physical vulnerability is presented in Table 2.12 (Luo et al., 2023):

Table 2.12 Overview of existing models for physical building vulnerability assessment (*modified from* Papathoma-Kohle et al., 2017; Singh et al., 2017a; Fuchs et al., 2019).

Type	Model	Expression form	Advantages	Limitations
Qualitative models	Experience-based models	Use vulnerability matrices/ tables (qualitative expression or an empirical value)	1. Easy to establish, no need for hazard/damage data or detailed information	1. Results may not be translated into monetary loss 2. Specific hazard intensities are objective or even not considered
	Indicator-based models	Use vulnerability functions that contain relevant indicator scores with their weightings	1. Characteristics of the element at risk are taken into consideration 2. Results may be the basis for the adoption of local adaptation measures and simple vulnerability reduction actions 3. Usually designed to be applied at local level 4. Adopted to other areas with similar building characteristics 5. Flexible to establish or modified	1. Hazard intensity is not considered 2. Relative vulnerability index 3. The requirement of detailed information is high, depending on the indicators considered. 4. Not expressed in monetary damage 5. Subjective assessment
Quantitative models	Data-driven models	Use vulnerability or fragility curves that established by regression analysis	1. The method is quantitative and may "translate" an event into monetary cost 2. Common in the case of hazards that affect larger areas and a considerable number of buildings 3. Reliability of the curve is high due to a rather high amount of available data	1. Important characteristics of the natural process (e.g. duration, direction etc.) as well as the element at risk (number of floors, construction material) are ignored 2. Highly-demanding in ex-post information. A large number of affected buildings are required. 3. Vulnerability curves cannot be transferred to areas with different housing types 4. Lack of reliable empirical data regarding building loss 5. Information on the intensity of the process on a detailed scale (intensity per building) is necessary, which is challenging to be recorded and expressed

Table 2.12 (continued)

Type	Model	Expression form	Advantages	Limitations
Quantitative models	Mechanism-based models	Use fragility curves that express the probability of reaching or exceeding certain damage state given a level of hazard intensity	1. Specialized hazard characteristics and the induced failure mechanisms of elements at risks are considered 2. Uncertainties on characteristics of both elements at risk and hazards are quantified 3. Adopted to other areas with similar building characteristics 4. Demanding in hazard/damage data is low	1. Requires a clear understanding of hazard-element at risks interaction mechanisms 2. Always developed using numerical tools, which may have great computational burden

2.10 Risk Assessment

Landslide Risk Assessment (LRA) is an important and evolving field in natural hazard management. It offers a structured approach to understanding and mitigating the devastating impacts of slope instability on human lives, property, and the environment (Dai et al., 2002; Caleca et al., 2025). Historically, risk management in landslide and slope engineering was often informal, and relied on the engineering judgment of experienced professionals (AGS, 2000). However, the concept of landslide risk assessment has undergone a significant transformation, sometimes referred to as the *risk revolution*, which was driven by increased recognition of the inherent uncertainties in natural phenomena and a growing need for formalized decision-making processes (Lee & Jones, 2014; Lei et al., 2023). Important landslide events at the time, such as the 1997 *Thredbo landslide* in Australia (Bilboe, 1998; Mostyn & Sullivan, 2002), spurred the development of comprehensive guidelines, including those by the Australian Geomechanics Society (AGS) in 2000 and 2007 (Lee & Jones, 2014). International bodies like the International Union of Geological Sciences (IUGS) Working Group on Landslides (IUGS, 1997) and the International Society of Soil Mechanics and Geotechnical Engineering (ISSMGE) (Nadim, 2005) have also played a pivotal role in standardizing terminology and frameworks to enhance communication and consistency across various disciplines.

2.10.1 Definitions and Concepts

In general, risk is defined as "a measure of the probability and severity of an adverse effect to health, property, or the environment" (IUGS, 1997; AGS, 2000; ISSMGE, 2004; Fell et al., 2008). While it was estimated as the product of probability and consequences, a more general interpretation of risk involves a non-product comparison of these two factors (IUGS, 1997; AGS, 2000). In the context of landslides, several definitions have been proposed by various workers. One of the most popular definitions is given by Varnes (1984) which states that "the expected number of lives lost, persons injured, damage to properties and disruption of economic activities due to landslides for a given area and a reference period". At the same time, Lee and Jones (2014) also defined landslide risk as "the potential for adverse consequences, loss, harm or detriment as a result of landsliding, as viewed from a human perspective, within a stated period and area". According to Corominas et al. (2015), risk is a "measure of the probability and severity of an adverse effect to life, health, property, or the environment", which can also be expressed as "probability of an adverse event times the consequences if the event occurs". It is also conceptualized as the "the potential for adverse consequences or loss for the population and human property due to the occurrence of a landslide" (Kanungo et al., 2008).

LRA itself is described as "the structured gathering of the information available about risks and the forming of judgements about them" (DoE, 1995). It serves as a broader framework for considering the threat and costs associated with landsliding and for determining the most effective ways to manage both landslides and the risks they pose (Lee & Jones, 2014). Its primary function is to furnish factual information that links scientific understanding with decision-making, and provide a solid foundation for better-informed decisions for managing landslide risk. LRA also determines the likelihood of losses from landslides by analyzing the hazard and evaluating the vulnerability of exposed elements (Dai et al., 2002; UNISDR, 2009; Martha et al., 2013).

2.10.2 Conceptual Frameworks

The fundamental components of landslide risk are widely conceptualized as the combination of hazard, vulnerability, and elements at risk. This relationship is usually expressed mathematically as (Varnes, 1984):

$$\text{Risk} = \text{Hazard} \times \text{Vulnerability} \times \text{Elements at Risk}$$

A comprehensive conceptual framework for landslide risk assessment and management comprises three fundamental components: Risk Analysis, Risk Estimation, Risk Evaluation, and Risk Management (AGS, 2000; Bell & Glade, 2004; Crozier & Glade, 2005). These components collectively address critical questions: 'What might happen?', 'How likely is it?', 'What damage or injury may result?', 'How important is it?', and 'What can be done about it?' (AGS, 2000).

i) Risk Analysis: This is the initial phase which includes defining the scope to ensure the analysis addresses relevant issues and to qualify its limits (Fell et al., 2005). It involves defining the primary area of interest, the types of losses to be addressed, the extent of investigations, the analytical approach, and the basis for assessing acceptable risks (AGS, 2000; Fell et al., 2005). The risk analysis includes the following components:

a) Hazard Assessment: This component focuses on the development of hazard models and the estimation of the nature, size (magnitude), and frequency characteristics of hazardous landslide events (Guzzetti et al., 2005; Martha et al., 2013; Lee & Jones, 2014). Hazard identification and characterization requires a deep understanding of slope processes, their relationship to geomorphology, geology, hydrogeology, failure mechanics, climate, and vegetation to determine the spatial probability (Fell et al., 2005). It also involves identifying possible landslide types, locations, sizes, mechanisms, velocities, and travel distances (IUGS, 1997). The frequency analysis (temporal probability) is another component which estimates the likelihood of a landslide occurring within a specified period (Einstein, 1988; AGS, 2000). The methods include analysis of historical records (Cruden, 1997), statistical models (Bui et al., 2013), physically-based models (Fell et al., 1991), and expert judgment (Koirala & Watkins, 1988). Another component in the hazard assessment is the magnitude and intensity of a landslide. This describes the size and potential damaging power of a landslide (Caleca et al., 2025), with intensity usually related to velocity, volume, and impact pressure (Hungr, 1997; Cardinali et al., 2002; Luo et al., 2019).

b) Elements at Risk and Exposure: Elements at risk refer to people, property, infrastructure, and environmental assets that could be affected by a landslide. Exposure quantifies these elements within the potential impact zone (Pereira et al., 2020; Acosta-Quesada & Quesada-Román, 2025). It is important to determine the number, characteristics, and spatial/temporal variability of the elements at risk (IUGS, 1997; Bell & Glade, 2004).

c) Vulnerability Analysis: This assesses the degree of loss or probability of loss to elements at risk due to interaction with the landslide (Fell, 1994; IUGS, 1997; Corominas et al., 2014). Vulnerability assessment is complex, involving social, political, and physical elements, and can be expressed as a damage function or a single estimated value, ranging from 0 (no loss) to 1 (total destruction) (IUGS, 1997; Galli & Guzzetti, 2007).

d) Consequence Analysis: This component characterizes the potential outcomes of a landslide hazard, and comprises both direct losses (property damage, fatalities, injuries) and indirect losses (disruption of economic activities, environmental impact, corporate image) (Cascini et al., 2005; Fell et al., 2005; Puissant et al., 2014). The ability to assess economic and ecological losses is often emphasized in the analyses (Turner, 2018; Wang et al., 2019a).

ii) Risk Estimation: This stage combines the outputs of hazard and consequence analyses to derive a measure of risk (Ko Ko et al., 1999; Cascini et al., 2005). It can be quantitative, based on numerical values for probability, vulnerability, and consequences, yielding a numerical risk value (Fell & Hartford, 1997; Pereira et al., 2017), or qualitative, using numerical rating scales or descriptive (e.g., low, moderate, high) for describing the intensity of potential consequences (Abella & van Westen, 2007; Wang et al., 2013b). Quantitative risk estimation is preferred for its rigor and systematic assessment, which improves communication in technical and political decision-making (Uzielli et al., 2015b).

iii) Risk Evaluation: This is a critical step where the assessed risks are compared against predetermined acceptance and tolerability criteria (Wise et al., 2004; Sterlacchini et al., 2007; Sim et al., 2022). Acceptable risk is a level which is considered broadly acceptable, and where no further action is required unless low-cost, practical measures are available (Amarasinghe et al., 2024). Tolerable risk is a level that society might accept to secure certain benefits, but requires ongoing review and reduction where feasible, usually guided by the "As Low As Reasonably Practicable" (ALARP) principle (AGS, 2002; Fell et al., 2005; Lee & Jones, 2014; Sim et al., 2022). The establishment of such criteria often depends on the legal framework and regulatory controls of a country (Leroi et al., 2005).

iv) Risk Management: This is the final stage which provides the methodology for controlling risk, and involves implementing strategies to reduce or manage the identified risks (AGS, 2000). The options include accepting the risk, avoiding the risk, reducing the likelihood of a landslide, reducing the consequences, or transferring the risk (Crozier & Glade, 2005; Amarasinghe et al., 2024). Monitoring and review are essential to track changes in risk levels, assess the effectiveness of implemented measures, and identify new risks, thus necessitating periodic updates or re-assessments (Lee & Jones, 2014). The overall framework of landslide risk assessment and management is shown in Figure 2.9.

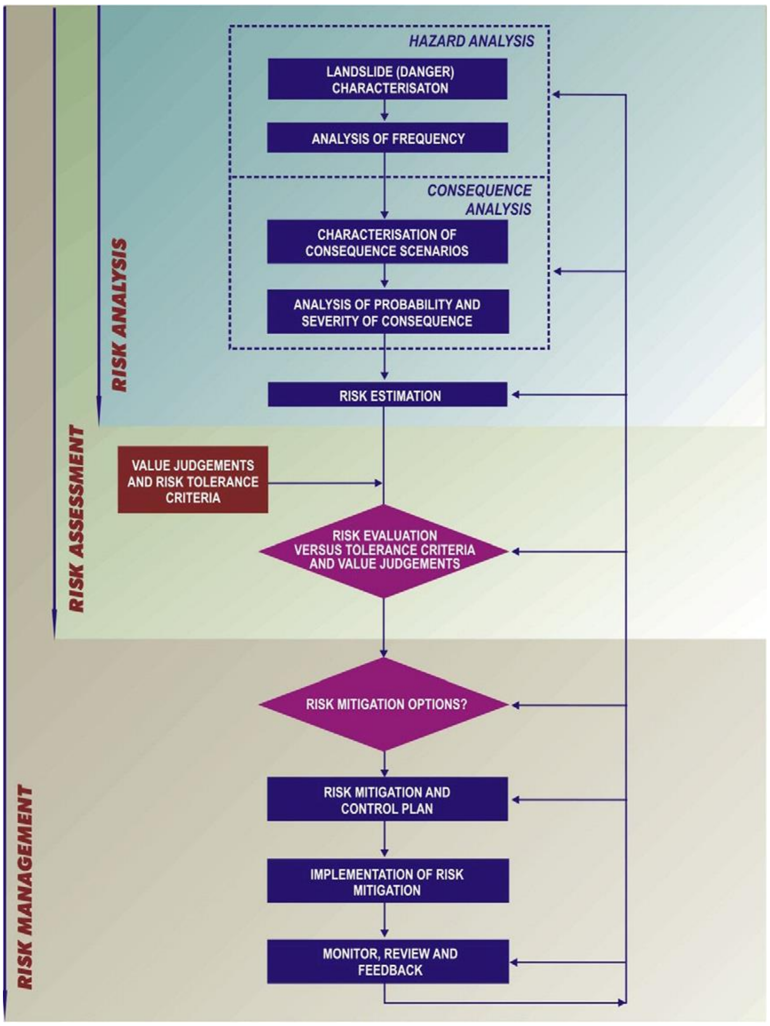

Fig. 2.9 *Framework for Landslide Risk Assessment and Management after* Fell et al. (2008)

2.10.3 Risk Assessment Approaches

The methodologies employed in LRA are broadly categorized into qualitative, semi-quantitative, and quantitative approaches, each suited for different contexts, data availabilities and scales, (AGS 2000; Chowdhury & Flentje 2003; Sarkar, 2018). Some classifications further refine these into *soft* approaches, which address regional or conceptual risk, and *hard* approaches, which focus on the mechanics and numerical simulations of individual landslides (Lei et al., 2023).

i) Qualitative Approaches: Qualitative LRA methods involve the systematic acquisition of knowledge regarding hazards, elements at risk, and their vulnerabilities, which are expressed through descriptive terms or ranked values rather than numerical attributes (IUGS, 1997). These approaches heavily rely on expert judgment, direct geomorphological mapping, and the qualitative combination of thematic maps (Leroi, 1996; Cardinali et al., 2002; Michael-Leiba et al., 2003). They are particularly advantageous for large study areas where detailed quantitative data are limited or unavailable, or for initial screening processes (AGS, 2000). In qualitative assessment, risk is usually categorized into descriptive terms such as very *high, high, medium, low,* and *very low* (Chowdhury & Flentje 2003; van Westen et al., 2006; Corominas et al., 2014). While straightforward and adaptable to data-scarce environments (Dikshit et al., 2020b), qualitative assessments can be subjective and lack reproducibility, as they depend on the individual experience and interpretation of the geomorphologist or expert (Chowdhury & Flentje 2003; Lee & Jones, 2014; Hungr, 2016; Caleca et al., 2025).

ii) Semi-Quantitative Approaches: Semi-quantitative LRA methods represent an intermediate step between purely qualitative and fully quantitative evaluations, and combines elements from both (Abdulwahid & Pradhan, 2017; Biçer & Ercanoglu, 2020). These approaches involve assigning numerical weights or scores to various factors that influence landslide occurrence and impact, frequently within a hierarchical system of risk classes (Abella & van Westen, 2007; Kanungo et al., 2008). They are especially useful when the level of risk does not necessitate extensive quantitative analysis, numerical data are limited, or as an initial screening tool to identify high-risk areas (AGS, 2000; Althuwaynee & Pradhan, 2017). These methods commonly employ risk ranking matrices (Anbalagan & Singh, 1996; Cardinali et al., 2002), multi-criteria decision-making techniques such as the Analytic Hierarchy Process (AHP) (Perera et al., 2020; Sangeeta & Maheshwari, 2022), fuzzy set theory and danger pixel approach (Kanungo et al., 2008; Shano et al., 2022; Riaz et al., 2023).

iii) Quantitative Approaches: Quantitative LRA methods represent the most rigorous and comprehensive approach, involving the numerical quantification of all risk components to calculate a specific risk value (van Westen, 2004; Caleca et al., 2022). This approach aims to provide objective and reproducible results, enabling comparative analysis with risks from other hazards, facilitating cost-benefit evaluations, and supporting informed decision-making and resource prioritization in risk management (Michael-Leiba et al., 2003; Corominas et al., 2014; Lee & Jones, 2014). At its core, quantitative risk is expressed as a function of hazard, vulnerability, and the elements at risk (van Westen, 2004; Crozier & Glade, 2005; Lee & Jones, 2014). A comprehensive quantitative landslide risk assessment involves assessments of the hazard based on the spatial, magnitude and temporal characteristics with runout analysis, vulnerability of the elements at risk and the exposure of these elements (Fell et al., 2005 & 2008; Corominas et al., 2014). A brief summary of the various methods of landslide risk assessment is given in Table 2.13.

Table 2.13 *Summary of landslide risk assessment approaches*

Approach	Description	Advantages	Limitations
Qualitative	Relies on expert judgement, existing knowledge, and qualitative data (e.g., landslide inventories, literature, expert opinions) to classify areas into relative risk classes.	Relatively simple and quick to implement, useful for initial assessments.	Subjective, lacks numerical precision, heavily dependent on expert experience.
Semi-Quantitative	Combines elements of both qualitative and quantitative methods, using weighting and rating schemes for various hazard and vulnerability factors to derive a risk score or index.	More objective than purely qualitative methods, can handle some uncertainties.	Requires careful parameter selection and weighting, may still contain some subjectivity.
Quantitative	Aims to quantify risk by calculating the expected losses based on the spatial, temporal, and magnitude probability of land-slides, the vulnerability of elements at risk, and the exposure of these elements within the hazard area.	Provides a more objective and detailed assessment, suitable for comparing sites and resource prioritization.	Requires extensive and high-quality data, complex calculations, data limitations can introduce uncertainty.

These diverse approaches to landslide risk assessment are influenced by several factors. Firstly, the scale of analysis, ranging from site-specific investigations to regional or broad-scale studies, dictates the appropriate methodology (Corominas et al., 2014; Lee & Jones, 2014; Caleca et al., 2025). The specific objectives of the assessment define the necessary degree of quantification, which allow for either qualitative, semi-quantitative, or quantitative evaluations AGS, 2000; Dai et al., 2002). Moreover, the availability and quality of empirical data, including historical landslide inventories, runout distances, and vulnerability of the elements, impose significant constraints on the chosen approach (Corominas et al., 2014; Crawford et al., 2022). Finally, the inherent nature and type of landslide phenomenon, along with the specific consequences (e.g., property damage, human injury, or loss of life) under consideration, are important in guiding methodological selection (AGS, 2000; Fell et al., 2005; Caleca et al., 2025).

2.10.4 Challenges and Limitations

A primary challenge in LRA arises from data limitations and inherent uncertainties (AGS, 2000; Lee & Jones, 2014). Historical landslide inventories, which form the basis for assessing probability and recurrence, are frequently incomplete, and lack important details such as precise dates, types, volumes, and runout distances (Dai et al., 2002; van Westen et al., 2006; Althuwaynee & Pradhan, 2017; Li et al., 2023b). This scarcity of complete and reliable data hinders the development of robust predictive models and the validation of assessment findings (Ghosh et al., 2011; Crawford et al., 2022). Moreover, the lack of standardized data collection protocols further complicates comparative analysis and the generalization of findings across different areas (van Westen, 2004; van Den Eeckhaut & Hervás, 2012; Caleca et al., 2025). The absence of comprehensive socio-economic data (Althuwaynee & Pradhan, 2017; Nor Diana et al., 2021) and detailed damage records (Ghosh et al., 2011; Riaz et al., 2023) further exacerbates the difficulty, particularly in developing countries where such information is often under-reported or unavailable. This data scarcity makes it arduous to quantify elements at risk and their vulnerability accurately (van Westen et al., 2006; Li et al., 2023b; Caleca et al., 2024).

Apart from these, inherent uncertainties pervade every stage of the risk assessment process, arising from incomplete knowledge regarding future event probabilities and their potential consequences (Sterlacchini et al., 2007; Lee, 2016; Crawford et al., 2022). Many landslide risk studies, especially at regional scales, continue to use susceptibility as a proxy for hazard due to data constraints, leading to static rather than dynamic risk indicators (Guillard-Gonçalves & Zêzere, 2018; Arrogante-Funes et al., 2021; Singh et al., 2021; Caleca et al., 2022). The complexities of modeling runout distance and intensity for diverse landslide types also remain a significant hurdle (Fell et al., 2005; van Westen et al., 2006; Hungr, 2016; Singh et al., 2021; Lei et al., 2023). Further, a lack of a single, standardized methodology for vulnerability and risk assessment further contributes to inconsistencies in practice (Uzielli et al., 2015b; Singh et al., 2021; Ram & Gupta, 2022). The ability to generalize AI models in landslide detection is also limited by the spatial variability of soil and geological conditions across different regions (He et al., 2024). Lastly, while quantitative risk assessment is feasible for individual slopes or linear features, generating the comprehensive quantitative risk zonation maps for broader areas, especially at medium scales, remains a considerable challenge (van Westen et al., 2006).

2.11 Previous Works on Landslide Assessment within Aizawl City

Several studies on landslide hazard within Aizawl city have been taken up by various workers. These assessments range from site-specific to large-scale and synoptic, employing diverse methods and data. The causes, factors and remedial measures provided by these studies offer insights to understand the complex geodynamics of the area, where rapid urbanization and infrastructural development on unstable slopes have exacerbated susceptibility to mass movements. Most of these studies have confirmed that the inherent nature of the terrain, climate change and anthropogeny are the major factors contributing to slope instability in Aizawl. Such assessments are important for land-use planning and risk mitigation strategies, particularly in regions experiencing increased landslide activity due to both natural processes and human interventions.

2.11.1 Site Specific Studies

One of the first documented systematic landslide studies within Aizawl was undertaken by Prasad (1983). He investigated large-scale mass movements occurred at Electric Sihpui Veng, Armed Veng, Sarawn, and Vaivakawn areas which involved field investigations and plotting geological details on 1:5000 scale plans. He identified water charging of overburden slope material and toe erosion by local streams such as Theihai lui were the main causes of the mass movements. He also recommended implementing catch water drains, construction of strong retaining walls, and avoiding heavy buildings on slide-prone slopes. Choubey (1992) had carried out an in-depth study of the Vaivakawn landslide. He performed geotechnical evaluation by testing the samples from the slide materials in the laboratory, and suggested mitigation measures for the slide. Srivastava et al. (1993) investigated widespread landslides in Sarawn Veng, Sihpui block, Chanmari, Hunthar, Tuikual, Zemabawk, and Zuangtui power substation following heavy rains in June 1993. Their detailed field investigations on 1:2000 topomaps revealed that most slides were caused by saturation of soft, weak overburden material (siltstone and sandstone fragments in silty/clayey soil) and deepening of stream beds. They emphasized effective drainage and thorough ground evaluation for urban planning.

The devastating South Hlimen landslide of August 9, 1992, which killed 66 people and destroyed 17 houses, was extensively studied. Swamy (1992) conducted geotechnical studies, employing aerial photo-interpreted geological maps and sections. The indiscriminate stone quarrying from six quarries aligned near the road was attributed to the primary cause of the failure. He suggested protecting the debris slope with deep-rooting plantations and appropriate drainage networks. Kumar et al. (1997) also examined South Hlimen landslide area, and concluded that the instability was primarily due to the blocky nature of the sandstones, formed by the intersection of bedding planes and vertical joint planes. They also recommended a more mechanized and systematic quarrying approach from top to bottom, instead of haphazard excavation from the foothill, to protect the hill slopes and surrounding environment. In the same year, Tiwari and Kumar (1997) also critically examined the possible causes of the slope failure in South Hlimen, apart from suggesting mitigation measures. The same landslide incident was also studied by Beingachhi and Deka (2013), and Beingachhi and Vanlalhmangaihsangi (2017). They concluded that the primary cause was human activity, specifically haphazard stone quarrying that involved continuous removal of toe material, combined with rainwater saturation weakening joint planes. They further suggested systematic quarrying methods (top-to-bottom benching) and appropriate drainage.

A geotechnical appraisal of the landslide at Bawngkawn-Thuampui road section was undertaken by Tiwari et al. (1996). Based on the on-site examination, they evaluated the causes of the instability and provided measures for mitigation. Laldinpuia et al. (2011) and Laldinpuia (2019) undertook geotechnical, geological investigation and monitoring of a landslide at Ramhlun Vengthar/Sports Complex, where multiple landslides occurred in 1982, 1997, and 2007. They performed soil and rock analyses (specific gravity, particle size, shear strength), apart from Atterberg's limits, California bearing ratio, optimum moisture content and maximum dry density. They found that steep slopes, high moisture content, and toe erosion by Bangla lui as the main factors which cause slope instability. Draining seepage water to Bangla lui, and constructing a large, proper drainage system for Bangla lui were the recommended measures suggested. The same area was investigated by Vasudevan and Ramanathan (2016) who identified that high rainfall, erosion by the Bangla lui, and improper drainage system as the primary causes of the failure. Huang et al. (2016) employed Multi-temporal Interferometric Synthetic Aperture Radar (MT-InSAR), using data from ALOS (2007-2010) and COSMO-SkyMed (2012-2015) satellites to monitor surface deformation at Ramhlun Vengthar and Ramthar Veng landslide areas. They found out that the mean creep rate in these areas was 25 mm/year, which was significantly higher during wet seasons (50 mm/year) compared to dry seasons (19 mm/year). Schaeffer et al. (2014) also investigated two landslides located at the southern and eastern parts of Aizawl. A Shallow Slope Stability Analysis (SHALSTAB) model was used for mapping the different zones of relative hazard, while a Newmark Deformation Analysis was performed to assess landslide-inducing displacement. The findings revealed that 44% of the study area in Aizawl is unconditionally unstable, and nearly 50% of the area would experience landslide-inducing displacement from a magnitude 7 seismic event.

The Laipuitlang landslide of May 11, 2013, which caused 17 fatalities and destroyed 15 houses, was studied by Laldinpuia et al. (2013 & 2014), Verma (2014a), Chenkual (2015), Vasudevan and Ramanathan (2016), and Pant and Tabrez (2024). Investigations involved field observations, historical data, interviewing locals, Schmidt hammer tests, and remote sensing and GIS tools. These studies linked the disaster to soft, porous rock bedding (sandstone/siltstone), steep slopes, heavy rainfall, anthropogenic activities (quarrying, unsafe cutting), and overweight constructions. The recommendations included detailed geotechnical studies, enforcement of building regulations, prompt demolition of dangerous structures, enhanced community disaster preparedness, and construction of proper drainage within the affected area. In addition, Singh et al. (2016 & 2017b) also examined the same landslide event occurred at Laipuitlang by carrying out field investigation, laboratory experiments (strength, durability), and numerical simulation (Distinct Element Method) to model hydro-mechanical loading. Their findings include directional strength variation, block detachment accelerated by orthogonal joints, slaking from weathering, and a dominant planar, surficial failure mechanism driven by water pressure.

Verma (2014b) undertook a case study analysis to determine the causes of the Ngaizel landslide that occurred on May 23, 2011. The study focused on the geological, hydrological conditions and the role of bedding and joint intersections. The study concluded that the Ngaizel landslide was a rock slide resulting from the combined effects of excessive rainfall, adverse geological factors (lithology and dipping beds), and structural discontinuities leading to wedge failure. Lalhlimpuia et al. (2019) also carried out detailed investigation to determine the rock mass quality and identifying hazard-prone areas along the Ngaizel road cutting slope. They applied Rock Mass Rating (RMR) method to assess the geomechanical condition of the rock mass, and Rockfall Hazard Rating System (RHRS) which considers factors such as slope height, precipitation, block size, road width, and traffic conditions. They found that the Ngaizel road cutting section comprises very poor rock mass, with very low shear strength, and a very high possibility of rockfall in the area. In another study, Sardana et al. (2019a) evaluated the rock slope stability along Kulikawn to Saikhamakawn road section via Ngaizel area. They performed kinematic analysis to identify potential failure modes based on discontinuity orientations. They also used Geological Strength Index (GSI), Slope Mass Rating (SMR), and Continuous Slope Mass Rating (CoSMR) to evaluate slope stability. The main findings revealed that five out of nine locations exhibited potential for wedge, flexural topple, or direct topple failures, while four locations showed no potential for failure. They concluded that most rock slopes in this region are unstable and prone to failure.

Dinpuia (2019) analyzed the Rangvamual landslide along the Aizawl Airport Road which occurred in September 2014. Through geotechnical and Limit Equilibrium Method (LEM) analyses, he classified the landslide as a ‘debris slide and earth slide’ of translational type, which was triggered by unscientific slope cutting and incessant rainfalls. The study revealed Factor of Safety (FS) values below unity (0.52), which indicates more than 90% probability of slope failure. He found that weak cohesion, low angle of friction, and loose soils contributed to the instability, and further recommended the area unsuitable for large constructions. Verma et al. (2021) also examined the same landslide at Rangvamual area, and carried out field investigations with GIS database analysis, using Satellite Data (IRS P6/LISS4) from which various thematic layers were generated. LEM analysis was also carried out to determine the safety factor based on the Mohr-Coulomb criterion. From the GIS analysis, they categorized the Rangvamual landslide as a "Very High Hazard Zone". The LEM analysis yielded Factor of Safety values below the acceptable limit of >1.2 for a safe slope. Verma and Blick (2018) conducted estimation of landslide hazard in the Thakthing Veng road section using the BIS 14496 (Part 2):1998 methodology. The study included the assessment of various Landslide Hazard Evaluation Factors (LHEF), including several geo-environmental factors. They classified the area as "Very High Hazard Zone" with TEHD value equivalent to 8.30. They further recommended structural reinforcements at the site, including meshing and retaining walls, as preventive measures. Sardana et al. (2019b) evaluated thirteen road cut slopes along NH-44A where the study covered part of the Aizawl city area. They utilized RMR, GSI, kinematic analysis, original SMR, Chinese SMR (CSMR), and CoSMR in the study. The findings revealed that wedge failure was the most prominent failure mode observed, especially in the Lengpui and Phunchawng areas, while Aizawl Zoo area exhibited both planar and wedge failure modes. While basic RMR generally suggested fair rockmass quality for most slopes, the CoSMR consistently yielded lower scores. They also found that lower RMR values often correlated with higher kinematic failure potential.

Several other case studies were also undertaken by various researchers. Verma (2019) examined the College Veng road section landslide, which occurred after intense rainfall in September 2017. He carried out field-based observational study, focusing on geological mapping, lithological analysis, and identification of causative factors using stereographic and rose diagram plotting. He found that the saturated shale layer facilitated translational sliding, and advocated for improved slope management, surface drainage, and community relocation from high-risk zones. A detailed geotechnical assessment was conducted at the Saron Veng landslide by Lallawmsanga et al. (2022), including field mapping, Schmidt hammer tests, grain size analysis, Atterberg limits, direct shear tests, and water quality analysis. Limit Equilibrium Method (LEM) using Slide 6.0 software was employed to evaluate slope stability. The study revealed that water seepage acted as a key lubricant for the debris slide, with a low safety factor ranging from 0.372 to 0.391. Vinoth et al. (2022) carried out a detailed investigation of landslide at Hunthar Veng. The study employed borehole drilling, sub-soil profiling, and back-analysis techniques using Geo5 software to determine the mechanical properties of the debris and underlying weathered rock. They found that the absence of bedrock, presence of loose debris, and poor drainage infrastructure contributed to slope instability. The study concluded that systematic stabilization measures, combined with drainage rehabilitation, were essential to mitigate future risk. Mazumder et al. (2025) investigated the rainfall-induced landslide that occurred in 2019 at the BSUP housing complex in Durtlang. They conducted laboratory physico-mechanical test and a petrographic study along with rainfall and soil moisture analysis, kinematic analysis, and 2D distinct element numerical simulation. The study revealed that water weakened the shale properties, with Uniaxial Compressive Strength, Brazilian Tensile Strength, and Point Load Index considerably decreased in wet conditions. Numerical simulations confirmed slope instability in wet conditions, as the Factor of Safety (FoS) dropped from 1.20 (dry) to 0.89 (wet). They concluded that all these findings, combined with heavy rainfall and increased soil moisture, triggered the planar landslide at the site.

2.11.2 Synoptic and Hazard/Susceptibility Zonation Studies

While a number of landslide studies within Aizawl city concentrated on individual landslide or site-specific studies, a relatively fewer number of synoptic studies covering entire Aizawl city were also conducted. Jaggi (1986) performed a geo-environmental appraisal of Aizawl Township, covering the core area and surroundings. The study examined urban growth, steep slopes, and high drainage density which contributed to environmental degradation and landslide problems. He observed that the erosion along nalas and high-water pressures induced slumping in the overburden material. He recommended to construct catch water drains to manage water, retaining structures to counter sliding tendencies, and avoiding heavy structures. Sawaiyan and Moirangcha (2007) conducted urban geological studies and landslide hazard zonation mapping of Aizawl and surrounding areas on 1:50,000 scale. The study involved surface geological mapping and compilation of existing geological, structural, seismo-tectonic, geomorphological, land use/cover, and drainage data. They identified Aizawl as mainly within high to very high hazard zones due to immature topography, fragile rocks, high rainfall, and frequent earth tremors. Chatterjee (2009) investigated engineering geological aspects and high landslide incidence in Aizawl. He prepared detailed landslide incidence maps through field surveys and various geological and environmental maps. His findings revealed that unstable slope conditions are severely exacerbated by its seismotectonic status, rapid and poorly controlled building construction with inadequate drainage, and extensive infrastructure development. He concluded that owing to its location in seismic zone V and ongoing neotectonic activity, earthquake-induced landslides cannot be ruled out in Aizawl.

Rodgers and Tobin (2014) also investigated Aizawl, and highlighted its high vulnerability to earthquakes and landslides due to inherently unstable geology and rapid, poorly controlled urban expansion. Their findings showed hillside concrete buildings and critical infrastructure are particularly vulnerable, and suggested recommendations for regulating slope cutting, improving drainage, enforcing building codes, and avoiding development in high-hazard zones to build resilience. Rakshit et al. (2017) examined the role of litho-units and precipitation in inducing landslide disasters through morpho-tectonic and sedimentological studies in the southern part of Aizawl. The study integrated morphotectonic analysis, geo-tectonic characterization, analysis of litho-units, and precipitation time series analysis. They found that "greater surface slope and similar bed attitude enhance the risk of slope failure", and concluded that the southern part of Aizawl area is tectonically active and lithologically vulnerable to landslide disasters.

Landslide assessment in the form of hazard/susceptibility zonation studies were also carried out. Lallianthanga and Laltanpuia (2008) employed Remote Sensing and GIS technologies for conducting Landslide Hazard Zonation (LHZ) mapping of entire Aizawl city on 1:25,000 scale. They were probably the first to undertake landslide hazard zonation studies using this technology within Aizawl. They utilized IRS 1D LISS III and PAN data for generating various thematic factors including geology, geomorphology, slope, land use/land cover, etc. By analyzing these various factors under GIS environment, entire Aizawl city was classified into five landslide hazard zones, ranging from very high to very low classes. In addition, the Mizoram Remote Sensing Application Centre (MIRSAC, 2011) also carried out micro level landslide hazard zonation mapping on 1:5,000 scale for Aizawl city using the same technique. The study employed Quickbird and IRS Cartosat-1 satellite imageries to generate various thematic factors. The landslide hazard map was classified into five different hazard classes. Moirangcha et al. (2014) conducted a holistic assessment of seismic and landslide hazards covering the Aizawl Master Plan area. For landslide hazard assessment, they used a modified BIS guidelines of GSI (2005), which is a heuristic/empirical (knowledge-driven) approach. This involved considering ten geo-environmental parameters, and assigning Landslide Hazard Evaluation Factor (LHEF) ratings to derive Total Estimated Hazard (TEHD) values, which categorized the area into three hazard classes.

A geospatial technique of landslide hazard zonation along State highway corridor from Aizawl city to Aibawk was attempted by Laldintluanga et al. (2016). They used Quickbird, IRS LISS III, Cartosat-1 data to generate five thematic layers. A qualitative knowledge-based technique was employed, where different weights and ranks were subjectively assigned to the different factors to finally produce the hazard map under GIS environment. Their study revealed that developmental activities along the road has profound impacts on the stability of slopes as landslide occurrences were mostly concentrated along newly constructed or widened roads. The same type of landslide zonation study along Aizawl city to Lengpui Airport Road corridor was taken up by Rao and Verma (2017). The study utilized Survey of India maps and IRS-P6 LISS IV (Mx) satellite data to derive various geo-environmental factors. Following Bureau of Indian Standards (BIS) 1998 guidelines, landslide zonation map with five hazard classes was generated. Their study showed that road corridors located near Aizawl city from Hunthar Veng to Rangvamual and Phunchawng sections were particularly prone to landslides. Barman et al. (2019) conducted delineation of landslide prone zones in the north western part of Aizawl city using remote sensing and GIS techniques. They used IRS LISS-III and Cartosat DEM data for generating various causative factors. An Index Overlay Analysis was employed in the GIS environment to compute a Landslide Hazard Index (LHI) by summing the weighted values of all factor classes. A landslide hazard map showing three classes was finally generated.

A very interesting study, perhaps the first of its kind in the form of published landslide risk study for Aizawl city, was attempted by Rohmingthangi et al. (2022). Their study focused on assessing and quantifying landslide risk dynamics and social vulnerability in Aizawl city. They employed computational intelligence methods, AHP-TOPSIS and fuzzy spatial overlay operations. They utilized satellite imagery, DEM, rainfall, and soil data to prepare thematic layers for influential factors, and found that rainfall was the most significant factor influencing landslides. The study concluded that the highest landslide risk zones are concentrated in the central and eastern parts of Aizawl, which are characterized by high population and household density. Prior to this study, the Mizoram Remote Sensing Application Centre (MIRSAC, 2019) carried out Hazard Risk and Vulnerability Analyses (HRVA) for Aizawl city and other seven district headquarters of Mizoram. The scope of the study focused on assessing the physical and social vulnerabilities, and the risks posed by three major hazards, viz., landslides, earthquakes, and wind/cyclonic events. However, this study was undertaken for government official uses only, and was therefore, remained unpublished. Laltanpuia et al. (2024) examined the landslide susceptibility of entire Aizawl municipal area using three bivariate statistical models. Google Earth image, Cartosat-1 DEM and Sentinel-2 data were utilized to derive twelve landslide conditioning (predisposing) parameters, with a total number of 381 landslide inventory data. Information Value, Frequency Ratio, and Weight of Evidence models were employed to generate landslide susceptibility maps, each having three different classes. Their study revealed that the Aizawl municipal area has experienced an increase in landslide susceptibility/hazard after comparing the results with the previous GSI landslide hazard map. This increase was attributed to climatic change and anthropogenic activities. Laltanpuia et al. (2025) attempted the assessment of landslide risk within Aizawl municipal area by combining social and physical vulnerabilities with a landslide susceptibility map. The study utilized Census 2011 data for social vulnerability, and a matrix-based approach for physical vulnerability of buildings and roads based on construction materials and exposure. Findings revealed that female population was the primary social vulnerability factor, while Reinforced Cement Concrete (RCC) buildings and metalled roads proved more resilient than Assam-Type (AT) buildings and unmetalled roads. The study concluded that landslide risk is influenced by the vulnerability of exposed elements, and not solely by hazard intensity.

There were certain event-based landslide studies within Aizawl city following Cyclone Remal in 2024. Haokip et al. (2024) conducted preliminary assessments of landslides induced by heavy rainfall that accompanied cyclone Remal in three districts including Aizawl. Within the Aizawl Municipal Corporation (AMC) area, 65 landslides were recorded, particularly in the western, southern, and southwestern parts of the city. The most affected area was Melthum which experienced 19 casualties, mainly due to a landslide caused by illegal construction with extensive slope cutting where the slope and bedrock dipped in the same direction. Hlimen area experienced two major landslides resulting in six deaths, attributed to high runoff and debris accumulation from cut slopes. They have identified intense rainfall as the primary trigger, but highlighted anthropogenic factors as major contributors. Sangi et al. (2025) also carried out a preliminary investigation into the cyclone-induced landslides in Aizawl, to assess social impacts and analyze failure mechanisms to guide future disaster preparedness. Geotechnical investigations were specifically carried out at nine rock slide sites, involving kinematic analysis, Uniaxial Compressive Strength, RMR and CoSMR, and slake durability tests. The geotechnical analyses indicated that most probable slope failures were of planar and wedge types, with rock masses classified as poor to fair and ranged from partially stable to completely unstable. They concluded that lack of expert consultation on slope modifications, weak rock mass characteristics, steep slopes coupled with inadequate infrastructure planning, and improper drainages were the main contributing factors for the catastrophic events.

From the foregoing discussions, it can be seen that a multitude of landslide studies in Aizawl were undertaken by various researchers. These studies mainly involved site-specific geological and geotechnical investigations of major landslide events, such as those at Hlimen, Ramhlun, Laipuitlang, Rangvamual, Hunthar Veng and Saron Veng. Additionally, landslide hazard/susceptibility zonation mapping, at both macro and micro-levels have been conducted for the city and along the road corridors utilizing remote sensing and GIS techniques. Majority of these studies highlighted that fragile geology, steep terrain, heavy rainfall, and anthropogenic activities like unplanned construction as the primary cause of slope instability (Chenkual, 2015; Laltanpuia et al., 2024; Pant & Tabrez, 2024; Sangi et al., 2025). Despite these efforts, however, significant challenges persist, in the form of data scarcity. A major challenge is the lack of comprehensive spatio-temporal landslide inventory data and detailed landslide characteristics such as magnitude, temporal probability, and types of movement. This absence considerably hinders quantitative risk assessments and the validation of results (Laltanpuia et al., 2025).

In future, it is important to regularly update landslide susceptibility maps prepared so far, to account for dynamic changes induced by rainfall patterns and human activities (Laltanpuia et al., 2024). Furthermore, there is a clear recommendation to frame and strictly enforce stringent building regulations based on micro-zonation and to designate "no development zones" in highly vulnerable areas (Chenkual, 2015; Sangi et al., 2025). Raising community awareness and building local technical capacity are also vital steps to build disaster-resilient society in the landslide-prone area of Aizawl city (Rodgers & Tobin, 2014; Chenkual, 2015).

2.12 Summary

This chapter comprehensively reviewed the fundamental concepts pertaining to landslides, including their evolving definitions, detailed morphology, and various classification systems, notably emphasizing the pervasive influence and subsequent refinements of the Varnes (1978) scheme. Methodologies for landslide susceptibility mapping were thoroughly examined, including inventory preparation, identification of causative factors, mapping units and scales, and the application of qualitative, quantitative, semi-quantitative, and machine learning zonation techniques. Critical aspects of model evaluation and validation, along with data partitioning and performance metrics were also addressed.

The discussion further delved into the multifaceted concept of vulnerability, tracing its paradigm shift from a hazard-centric view to a holistic understanding that integrates physical and social aspects, supported by various assessment models. The chapter also synthesized landslide risk assessment, and outlined its definitions and core components. It further discussed the qualitative, semi-quantitative, and quantitative approaches for estimation, evaluation, and management of landslide risk. Finally, a comprehensive literature review on the previous landslide studies within Aizawl city were presented, which ranged from site-specific geological and geotechnical investigations to synoptic studies in the form of susceptibility/hazard zonation mapping. It has been observed from these studies that several challenges persist, particularly concerning data scarcity for detailed spatio-temporal inventories and quantitative risk evaluations. These studies revealed that the inherent geological fragility, heavy rainfall, and anthropogenic activities as major causes of slope instability.

CHAPTER 3

STUDY AREA

The study area, which comprises the Aizawl Municipal Corporation area of Aizawl city, the capital of Mizoram and the administrative centre of Aizawl District, is located in the north-central part of the state. It is connected by National Highway 306 with Silchar, the district headquarters of Cachar, Assam at a distance of 180 km. It is also linked with Dharmanagar, the district headquarters of North Tripura by National Highway 108, and with Lamka, the district headquarters of Churachandpur of Manipur state by National Highway 02 (MoRTH, 2011). Lengpui Airport, located about 30 km from Aizawl city is linked with regular air services to and from Delhi, Kolkata, Guwahati and Shillong. The recent extension of a new railway line from Bairabi to Sairang, which is about 20 km from Aizawl, facilitated regular train services from Sairang to Delhi, Kolkata and Guwahati which further provided additional accessibility options.

3.1 Location & Extent

The study area is located between latitudes 23°39'23.366"N to 23°48'45.174"N and longitudes 92°39'17.978"E to 92°46'50.157"E, and it falls within the Survey of India topographical maps Nos. 84A/09, 84A/10, 84A/13 and 84A/14. The Aizawl Municipal Corporation area, which extends from Selesih in the north to Hlimen in the south, Zokhawsang and Beraw lui in the east to Phunchawng and Tanhril in the west, is approximately 120 km^2 in dimensions. Figure 3.1 shows the location of the study area.

3.2 Origin and History

The beginning and origin of Aizawl as a settlement date back to the early 1800s. As recorded by Zawla (1989), the nomadic *Lusei* chieftain, *Lalsavunga* by name, moved out from Hlimen village towards the north along with his 300 household-strength subjects in search of a better location for settlement in the hope of better livelihoods. They came to a favourable spot where they chose to establish a village. Thereafter, the village gradually grew in number in terms of population and households with in-

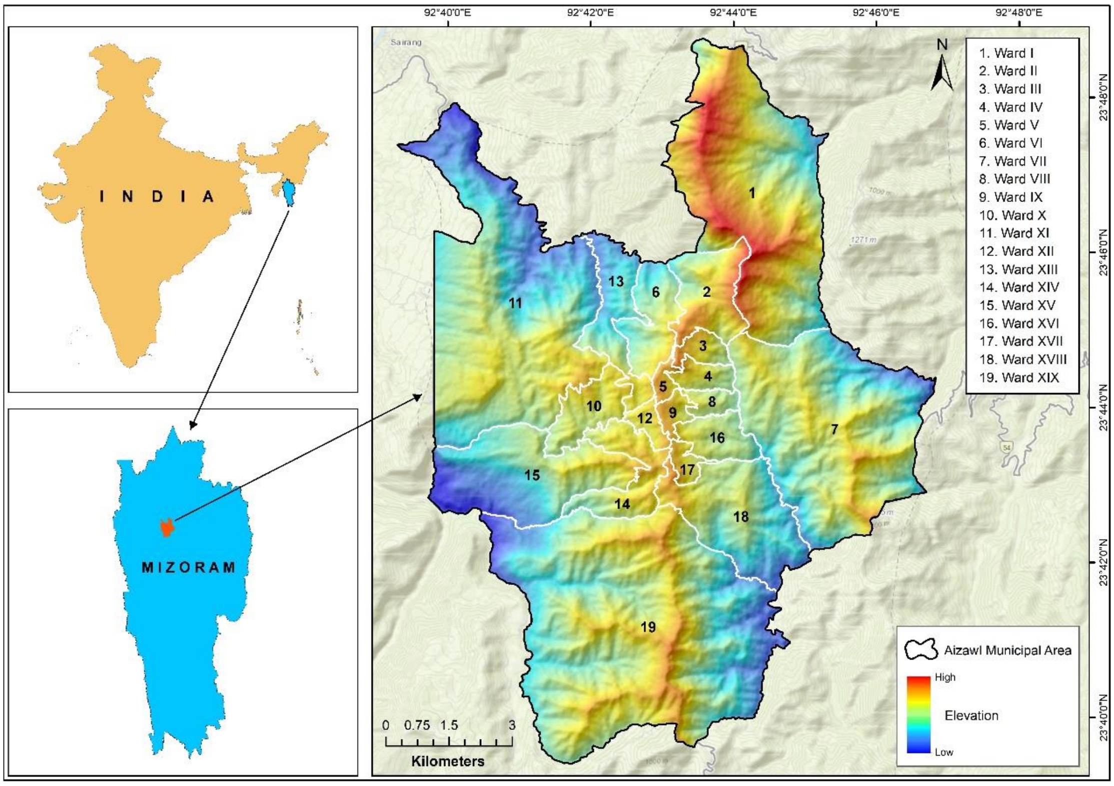

Fig. 3.1 *Location map of the study area showing different municipal wards*

creasing migration from the neighbouring villages. This village was considered the present-day Aizawl city. As per Zawla's record (1989), the establishment of Aizawl village by *Lalsavunga* took place in the year 1818, while Thanhlira (1983) maintained that *Lalsavunga* occupied the village from 1810 till 1821, thus recording Aizawl eight years older.

After *Lalsavunga* left Aizawl village and headed towards the east, many of his subjects chose to stay on. Thereafter, Aizawl continued to be a settlement till the arrival of the British-India army (East India Company) called *Lushai Expedition* in 1871. The colonial East India Company subsequently occupied the present location of Aizawl and then set up as a military station which was named as Fort Aijal in 1890. The establishment of Fort Aijal on 25 February, 1890 was considered the official establishment of Aizawl.

It is interesting to note that Aizawl got its name from a kind of indigenous plants from the *Zingiberaceae* family called *Aidu* (*Amomum dealbatum* Roxb.) and *Aichal* (*Alpinia bracteata* Roxb.), and the place where they grew (Saitluanga, 2017a). When *Lalsa-*

vunga moved out from Hlimen to establish a new village, they came across a plain area where these two plants grew in abundance. It was here that they established Aizawl village. So, Aizawl is a combination of 'Ai' meaning *Aidu* or *Aichal,* and 'zawl' which means 'flatland'. It means a small patch of flatland where *Aidu* or *Aichal* grows in abundance. The location from which Aizawl gets its name is currently being occupied by *Raj Bhavan* and its surrounding areas (Saitluanga, 2017a).

3.3 Growth and Expansion

The British-India army developed the Tlawng river as a waterway and constructed bullock-cart road connecting Sairang and Aizawl to facilitate the transportation of military supplies. This easy and convenient method of movement facilitated the migration of people from neighbouring areas into Aizawl (Lalchhuanawma & Khiangte, 2018). According to the Census of India, the population of Aizawl rose significantly from 325 to 2,890 during 1901–1911. However, the British-India army who already occupied Aizawl as a military fortified camp did not welcome the native people to settle near the military camp. In order to check the continual increasing migration into Aizawl and the subsequent encroachment of the cantonment area by the civilians, the authorities introduced restrictions on the number of houses allowed in each locality. In addition, a so-called tax, known as *Personal Residence Surcharge* (PRS) was also imposed to regulate the migration and to limit and discourage settlements in and around Aizawl (McCall, 1980). Sure enough, these regulatory and residential restriction measures had profound impacts on the native people. As a result, the population of Aizawl was only slightly more than 3,000 in the 1931 census (Saitluanga, 2017a).

With the end of the British rule in India, and the subsequent India's independence in 1947, the strict migration control policy was lifted. Naturally, this has resulted in remarkable rise in migration into Aizawl from different parts of the state. The decadal growth rate suddenly increased to 105.40% during 1951-1961 from 45.39% during 1941-1951. Urbanization in Aizawl was further driven by the socio-political instability caused by the 20-year insurgency during 1966 to 1986. During this period, people from different parts of the state, particularly the northern region moved into Aizawl seeking safety from violence, better economic prospects, and also opportunities to rebuild their livelihoods.

The transition of Mizoram from a District Council to Union Territory status in 1972 brought about an increase in government job opportunities, with parallel increase in other employment sectors (Saitluanga & Pachuau, 2015). This has attracted several aspirants from different parts of the state, many of whom chose to settle permanently in Aizawl. During the period from 1971 to 1981, Aizawl witnessed a spectacular growth in population, with the decadal growth rate reaching as high as 134.70%. Another factor which contributed to the rapid urbanization of Aizawl was the inclusion of several outlying settlements into Aizawl city limits. Consequently, the number of localities within Aizawl increased from only 26 in 1981 to 76 in 2011. Thus, Aizawl was transformed from a city characterized by distinct neighbourhoods into a densely populated urban area (Lallianpuii, 2017). Ultimately, on 30 December, 1999, Aizawl was officially recognized as a city (vide No. A-11013/5/91-LAD (Pt)-A). The historical images of Aizawl are shown in the Photo Plates 3.1 and 3.2, with the present-day image in 3.3.

Photo Plate 3.1 *Aizawl Bazaar in 1890*

At certain instances, Aizawl city has, of course experienced a period of stagnation in its process of urbanization. However, being the administrative capital and the cultural capital for Mizos living in the state, it offers better employment prospects, as well as better amenities and infrastructural services than any other parts of the state (Saitluanga, 2018; Kamath, 2020). As such, it attracts people from diverse backgrounds seeking improved and better livelihoods. Migration to Aizawl city is still taking place from various parts of the state. At present, more than a quarter of the entire population of the state lives in Aizawl city.

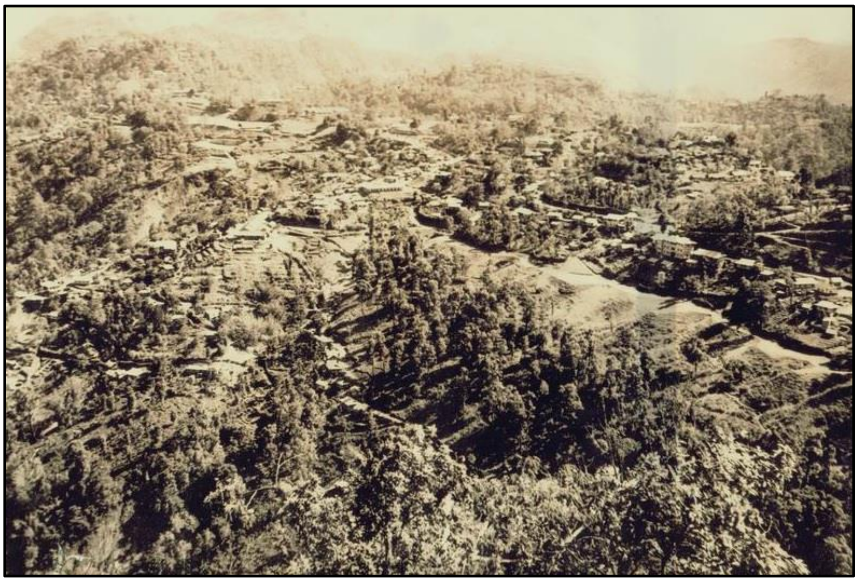

Photo Plate 3.2 *Aizawl in the year 1954*

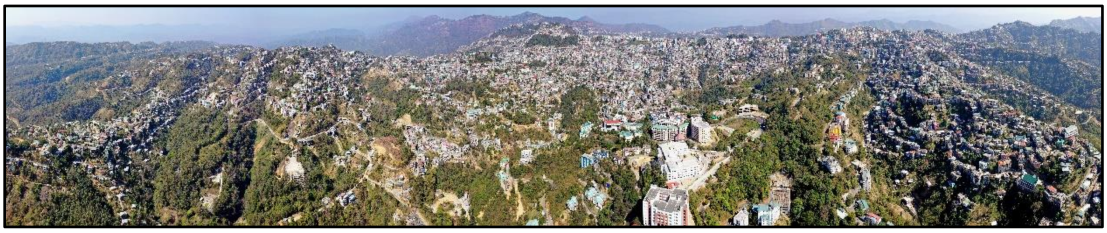

Photo Plate 3.3 *A panoramic view of Aizawl city in the present-day*

3.4 Administration

Until 2008, Aizawl remained as an agglomeration of several villages within an urban area. A traditional local governing body called the Village Council (VC) had been managing the administration of the area since 1954. Each locality was designated as village councils whose elected representatives handled the local administration based on Mizo customs and traditions. The state government designated the Local Area Development (LAD) Department to oversee the administration of the VCs and to ensure effective functioning by empowering them and providing professional and financial supports. However, as urbanization continued, there existed complexities and confusions with regard to the functions and responsibilities of the VCs, which ultimately created an administrative gap between the state government and the local bodies (Lalchhuanawma & Khiangte, 2018).

Recognizing the limitations of the traditional VC system in addressing rapid urbanization and modern developmental needs, the Aizawl Municipal Council was formed as a constitutional-based urban local body in 2008, under the Mizoram Municipalities Act, 2007. The formation of the municipal council was in line with the reform agenda of the Jawaharlal Nehru National Urban Renewal Mission (JNNURM) as well as the 74th Constitutional Amendment Act, 1992. The first election was held on 3 November, 2010. As the city's population grew, the Municipal Council was later elevated to the status of Aizawl Municipal Corporation (AMC) on 15 October, 2015. Thus, the AMC was constituted for the civic administration within the Aizawl municipality.

A three-tier urban administration structure was established for the AMC which includes a Municipal Body made up of elected corporators, a Ward Committee led by the respective corporators, and Local Councils composed of elected representatives from each locality. There are 19 municipal wards (Fig. 3.1), with each ward further sub-divided into several local councils. As per Census 2011, there were 76 local councils within the AMC which has increased to 83 as of today. The local councils are the smallest administrative unit. The map of the different local councils is shown in Figure 3.2.

3.5 Demography and Socio-Economic Conditions

As stated earlier, the exodus of people from rural to urban area, particularly in Aizawl due to social and political unrest which resulted in insurgency during 1966-1986, and the subsequent peaceful resolution of the conflicts is a significant factor for the increase of population in Aizawl (Rodgers & Tobin, 2014; Saitluanga, 2017a). Being the administrative capital and major commercial center of the state, Aizawl city offers better opportunities for livelihood. As such, it has witnessed a rapid pace of urbanization and infrastructural developmental activities over the last four decades. According to the 2011 Census of India, Aizawl city has a population of 293,416, out of which 144,913 are male and 148,503 are female, and has a gender or sex ratio of 1025 (females for every 1000 males). The female dominated the male population by approximately 2.5%. The population of Aizawl city comprises 26.74% of the entire population of the state. As per the 2011 Census data, the population density within the municipality is roughly 2,500 persons per sq. km. The literacy rate within the city is approximately 98.4% which is one of the highest in India.

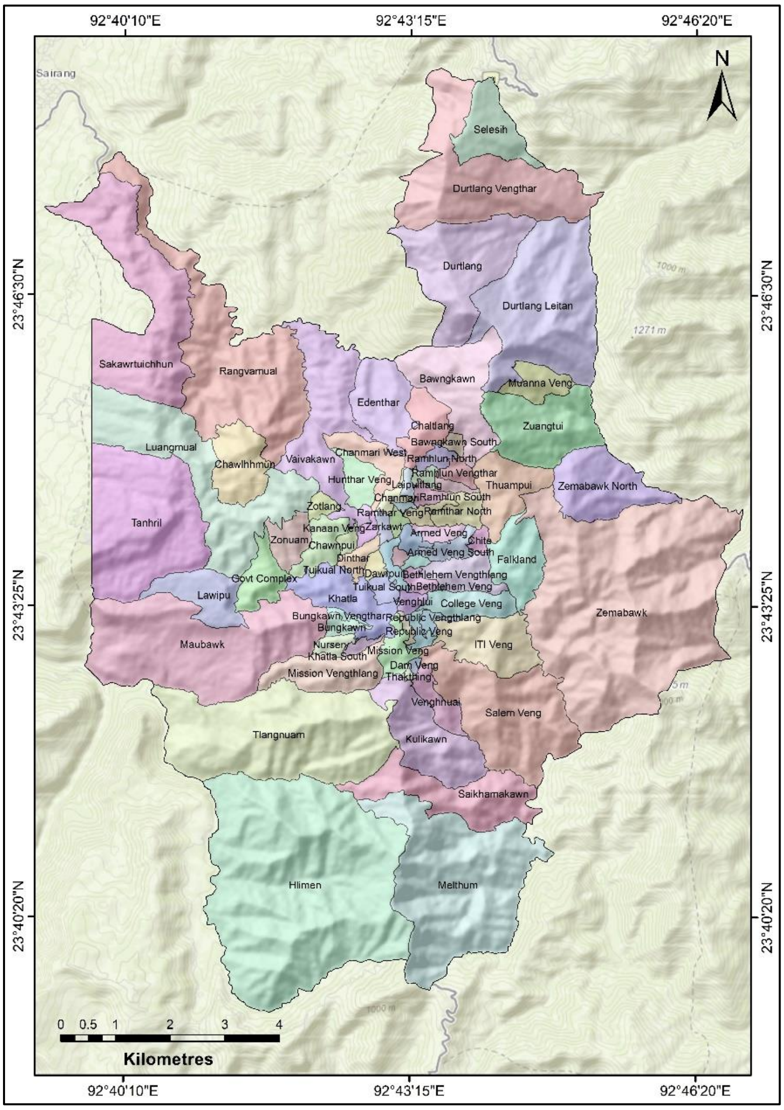

Figure 3.2 *Map showing the 76 Local Councils within the Aizawl Municipal area*

Ethnically, Aizawl city is largely dominated by the indigenous *Mizo* tribe which comprises about 91.95% of the total population (Saitluanga, 2014). Apart from the Mizos, there are smaller populations of Bengalis and Nepali Gorkhas who settled permanently. The remaining population is unevenly distributed among other ethnic groups who temporarily settled from the neighbouring states and countries. The economy of Aizawl city is predominantly driven by government service since it is the capital of the state as well as the district headquarters. Unlike many other big cities across the country, no major manufacturing centres or industries are located in Aizawl which can provide other employments for the sustenance of livelihood. A considerable portion of the population are engaged in commercial and entrepreneurial activities, livestock rearing, and animal husbandry as their primary occupations. In addition, there are individuals who earn their daily livelihoods as manual labourers, porters, barbers, etc. Approximately, a quarter of the population are also involved in farming and cultivation. One of the major challenges among the youths is unemployment opportunities in the state, particularly in the rural areas. As such, many unemployed youths from various parts of the state are compelled to migrate to Aizawl in search of work, which in turn resulted in heightened competition for limited job opportunities.

3.6 Transportation & Road Network

Aizawl city is characterized by a network of roads of various lengths and breadths. The roads range from metalled to unmetalled, including *kutcha* roads and footpaths. The National Highway No. 06 enters the Aizawl municipal area from Selesih in the north, and passes through Durtlang, Bawngkawn, Thuampui and Zemabawk till it runs out of the city near *Beraw Lui* in the east. This road connects the remaining districts of the state. The National Highway No. 108 starts from Bawngkawn and stretches along the western part of the city. This road is locally named *Airport Road* as it is the only main and nearest route to reach Lengpui airport from the city. There is another road which runs out of the city towards the southern part of the city which is informally named *World Bank Road*. This road serves as the main connectivity route for the remaining southern parts of the state.

The physiography of Aizawl city has a significant impact on its transportation network. As it is located along the slope of a ridge, many of the roads are winding and narrow, which limits expansion and overall capacity. The most prominent road within the city stretches along the crest of the main ridge in a north-south direction. It extends from Kulikawn to Bawngkawn from south to north direction for approximately 8 kms, and connects the most important social, political and economic institutions in the area. This road forms the main arterial road and accommodates majority of the vehicular traffic including major public transports such as city buses and local taxis within the city. The remainder of the network consists of feeder roads that branch off from this central corridor to serve the peripheral residential and commercial areas. Most of the roads within the heart of the city are catering heavy vehicular traffic far exceeding their capacity. Also, the capacities of roads along various sections were considerably reduced owing to limited space and encroachments. As a result, frequent traffic jams, congestion, delays, and overall chaos often ensued in the city.

Residential areas have been expanding along existing or new transportation lines, as well as unoccupied lands near existing communities that were previously unpopulated owing to the steep slope of the terrains. With inadequate transportation networks and accessibility issues, the proximity factor has become a significant element in deciding where to live (Saitluanga, 2017a). The road network map of the Aizawl municipal area is shown in Figure 3.3.

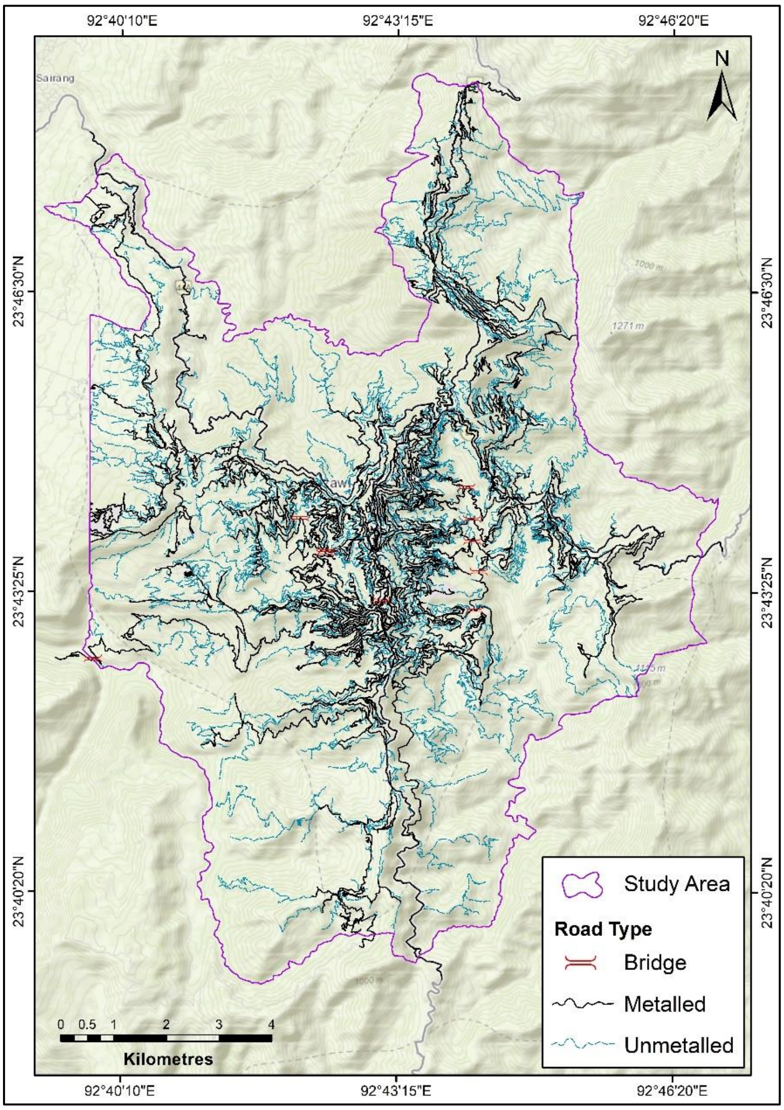

Figure 3.3 *Road network map of the Aizawl municipal area*

3.7 Climate

The climatic condition of Mizoram, as a whole is influenced by its geographic location, atmospheric pressure regime, physiographic features and proximity to the Bay of Bengal. Tropical air masses with moist and warm winds from the Bay of Bengal, and local mountains and valley breezes also influence the climate of the region to a considerable extent. In addition, major topographic features surrounding the state, such as the Arakan Yoma Hill ranges, the Chin Hill ranges in the southeast, and the Chittagong Hill Tracts in the west also play important role in modulating the climatic conditions of the region.

Although located in tropical region, Aizawl city is having pleasant and moderate climate owing to its high altitude and presence of fairly thick vegetation. Based on the Köppen-Geiger climate classification, the climate of Aizawl city is classified as *Cwa* type (Saitluanga, 2017a). Throughout the year, it is neither too hot nor too cold. The Indian southwest monsoon has a direct influence on the region. As a result, the area receives sufficient rainfall, resulting in a humid tropical climate with a short winter and a relatively long summer marked by heavy rainfall.

3.8 Temperature

The temperature profile of Aizawl city has been analyzed based on a fairly long-term data obtained from the State Meteorological Centre, Directorate of Science & Technology, Govt. of Mizoram. The dataset encompasses a continuous 39-year period, from 1986 to 2024, which provides a temporal framework for assessing variations of temperature trends in the area. During this period, the highest temperature recorded was 38.40ºC in 2013, and the lowest temperature recorded was 2.70ºC in 1993. These variations provide insight into the temperature variability experienced in Aizawl, and are indicative of broader climatic patterns that may be influenced by both local and regional climatic changes. The long-term temperature data can serve as an important input for further analysis of climate dynamics and their potential socio-environmental impacts in the area.

The respective averages of the annual maximum, mean and minimum temperatures during this period were also calculated (Fig. 3.4). It was observed that over a span of 39 years, the average maximum temperature has shown an increasing trend at a rate of 0.01°C per year, while the average minimum temperature has decreased at the same rate of 0.01°C per year. Consequently, the average mean temperature has also exhibited a downward trend, which decreases at a rate of 0.001°C per year.

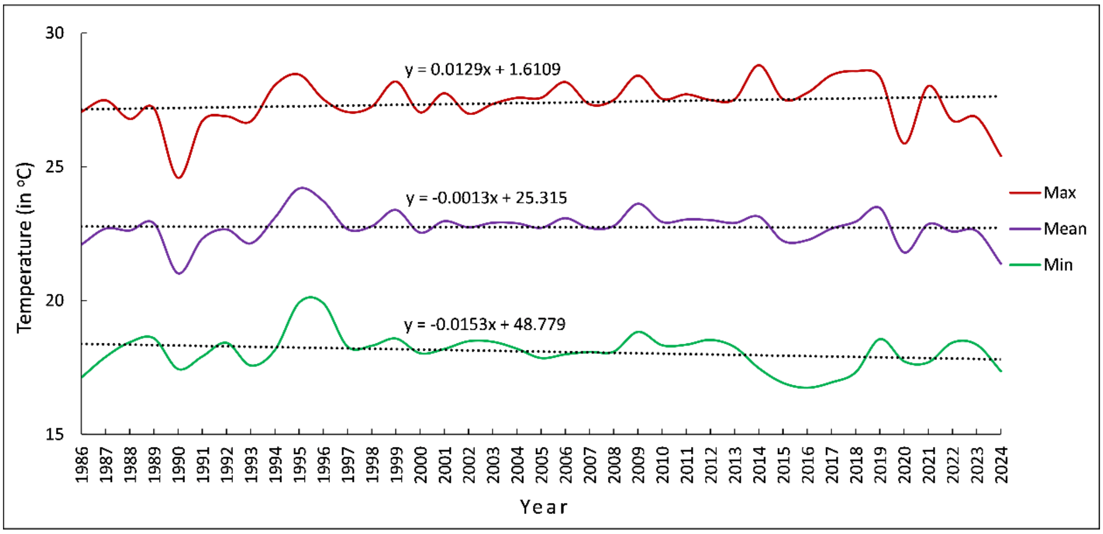

Figure 3.4 *Trend of average annual maximum, mean and minimum temperature of Aizawl (in °C) from 1986 to 2024.*

3.9 Rainfall

The state of Mizoram, as a whole, is directly influenced by the Indian southwest monsoon. Besides, tropical storms arising from the Bay of Bengal, which often cause thunderstorms and tropical disturbances also play an important role in influencing the rainfall in the region. As a result, Aizawl also receives sufficient rainfall during the period of monsoon season. Rainfall data for Aizawl city, spanning over a period of 39 years (1986–2024), was obtained from the State Climate Change Cell under the Directorate of Science and Technology, Government of Mizoram. Analysis of the rainfall data indicates that heavy rainfall usually begins in the latter part of May, and ends in the early part of October. Figure 3.5 shows the annual total rainfall during the year 1986 to 2024.

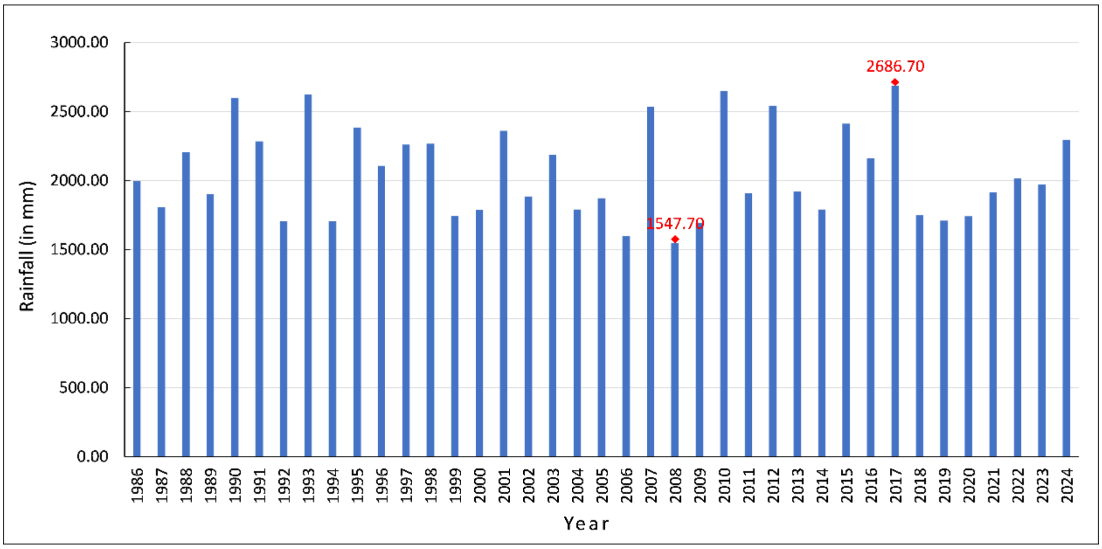

Figure 3.5 *Annual total rainfall of Aizawl (in mm) from 1986 to 2024*

A declining trend in annual rainfall has been observed, with an average decrease of 2.05 mm per year. This declining trend may be attributed to erratic nature and change in the climatic pattern over the years. During the 39-year period, the highest annual rainfall was recorded in 2017 with 2686.70 mm, while the lowest was in 2008 with an amount of 1547.70 mm. The average amount of annual rainfall received every year during this period was calculated to be 2059.68 mm.

3.10 Geology and Geomorphology

Geologically, Aizawl city is characterized by a repetitive succession of Neogene sediments of the Bhuban Formations of the Surma Group. Two rock formations, namely, Middle and Upper Bhuban Formations of Bhuban Sub-group have been identified (Muthu, 2005). The Middle Bhuban Formation is conformably overlain by the Upper Bhuban Formation with gradational and transitional contact. The Middle Bhuban Formation is predominantly argillaceous in nature, with shale as the major rock type. The other rock types in this formation include siltstones, mudstones, claystones and sandstones in relatively smaller quantities. The overall thickness of this formation within the study area is approximately 1600 m. In contrast, the Upper Bhuban Formation is mostly arenaceous constituting sandstone as the major rock type (Singh et al., 2016). Other rock types representing the Upper Bhuban Formation include siltstones, shales, claystones and mudstones in different proportions. This formation attains a maximum thickness of roughly 1400 m in the area. The rocks of the Middle Bhuban Formation are mostly exposed at the core of the Aizawl anticline while the rocks of the Upper Bhuban Formation form the limbs of the anticline. The typical rock types exposed in the study area are shown in Photo Plates 3.4 and 3.5.

Photo Plate 3.4 *Massive Sandstone bed overlain by thinly-bedded Shale*

Photo Plate 3.5 *Thinly-bedded weathered Shale unit*

Apart from these two rock units, Quaternary deposits in the form of unconsolidated boulders, pebbles, gravel, silt and sand unit were also present in the study area. These were formed as a result of the dynamic erosional processes such as rill erosion and sheet wash which were operative along the slopes (Haokip et al., 2024). These materials generally range in size from large boulders to silt and fine sand, and were mostly deposited along the major stream and river channels. The generalized lithostratigraphic succession of the area is shown in Table 3.1.

***Table 3.1** Lithostratigraphic succession of the study area* (*after* Haokip et al., 2024)

Age	Group	Formation	Unit	Generalized Lithology
Holocene		Recent	Colluvium/ Alluvium	Unconsolidated boulders, gravel, pebbles, sand, silt and clay
~~ Conformable Contact ~~~~~~~~~~~~~~~~~~~~~~~~~~~~				
Miocene	Surma	Bhuban	Upper Bhuban	Predominantly arenaceous; massive sandstone, at places thinly to thickly bedded sandstone is associated with sub-ordinate siltstone and shale, friable sandstone present at places.
			~~ Gradational and Transitional Contact ~~~~~~~~	
			Middle Bhuban	Predominantly argillaceous; thinly to thickly bedded shale, at places splintery shale with subordinate siltstone and sandstone. Finely laminated as well as thinly to thickly bedded siltstone present. Sandstone is thinly to thickly bedded, massive at places.
~~ Lower Bhuban Not Exposed ~~~~~~~~~~~~~~~~~~~~~~~~~~				

Based on the rock types exposed, six litho-units were tentatively established for the study area. These are classified as sandstone unit, shale-sandstone unit, shale-siltstone unit, shale unit, siltstone-shale unit, and gravel-sand-silt unit (Fig. 3.6). It is important to note that the correlation and demarcation of the two geological formations are rather difficult due to their similar lithological characteristics, and absence of index fossils and marker horizons. The sandstones within the study area are generally thickly bedded, hard and compact, and are medium to very fine grain in size. They exhibit light brown to bluish-ash grey colour. The shales, on the other hand, are thinly bedded, and usually splintery in nature. They generally range from light brown to dark grey in colour, with the darker colour attributed to the presence of carbonaceous materials.

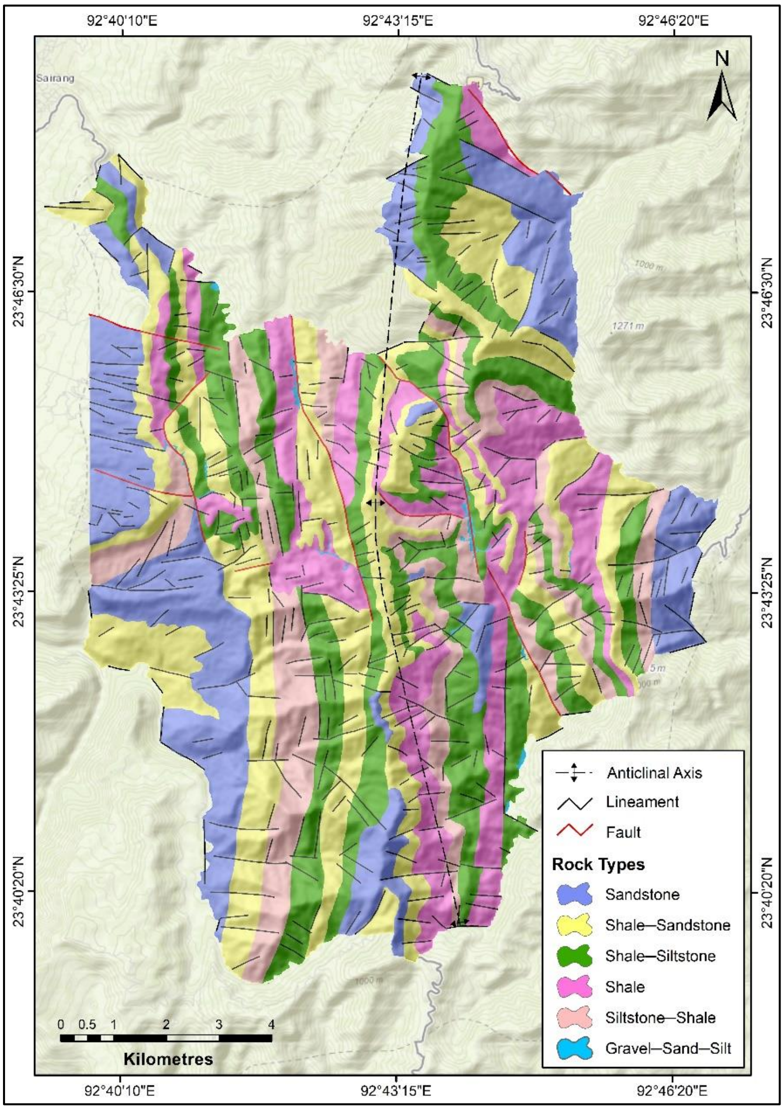

Figure 3.6 *Geological Map of Aizawl Municipal Area* (Background image: ESRI)

Structurally, Aizawl city forms two limbs of a doubly plunging asymmetrical Aizawl anticline trending in approximately N-S direction. The western limb is comparatively gentler than the eastern limb. The rocks of the area dip either towards east or west, and the dip amount varies from 20^o to 50^o with local variations within the vicinity of faults and other tectonically disturbed areas. While the rock beds in the northern part of the city dip towards east, those in the southern portion dip towards west (Kumar & Verma, 2010). The whole area is characterized by several second-order drag folds which are local in nature, and are mainly found in the incompetent shale layers. It was observed that three sets of joint planes generally traversed the rocks exposed within the study area (Photo Plate 3.6). The area exhibits both active tectonic and erosional process features which are evidenced by tilted river basins, and lineaments showing structural and lithological controls (Rakshit & Bezbaruah, 2016). The eastern limb of the anticline is offset by numerous transverse faults with the NW─SE trend (Tiwari & Kumar, 1996). Three prominent faults, namely—*Chite Lui* Fault, *Theihai Lui* Fault and *Selesih-Sihphir* Fault have been identified within the eastern limb of the Aizawl anticline. The western limb of the anticline is also offset by transverse faults of varying magnitude and length. The most prominent fault identified is the *Vaivakawn* Fault which extends from Khatla in the south up to *Vaivakawn Lui* near Hunthar Veng. *Thingrahbi Lui* Fault is another important fault noticed in the area which is a transverse fault oriented in E─W direction, extending along *Thingrahbi Lui* from Sakawrtuichhun ridge in the west to *Melnga Lui* in the east cutting across the Aizawl─Sairang road.

Photo Plate 3.6 *A highly-jointed Shale unit*

The sediments within the study area are characterized by various primary sedimentary structures which include ripple marks, cross lamination of sinusoidal type, ripple load convolutions and trough convolutions, and bedding structures of various kinds. In addition to these, slump structures, convolute laminations, and load casts also constitute prominent sedimentary structures. These structures suggested that the sediments were deposited under shallow marine to deltaic environment (Tiwari & Kumar, 1996).

Geomorphologically, Aizawl city is characterized by a series of undulating hills of varying elevations and dimensions. Some of these hills are very highly dissected with steep slope, sharp ridges along with cliffs and escarpments which reflect the dynamic erosional processes. In contrast, some areas are characterized by relatively gentler, low dissected and subdued hills which are indicative of immature topography. A prominent ridgeline extends across nearly the entire city in a north-south direction, along with several spurs mainly oriented in the east-west directions. The spurs on the eastern flank of the main ridge tend to be longer and exhibit gentler slopes compared to the relatively shorter and steeper spurs on the western side. A number of streams and *nalas* criss-crossing and traversing through these spurs, dividing them into multiple facets. Very few flatlands are found to occupy limited areas mostly along the streams and between the spurs. These are found mainly along *Chite Lui*, *Rangvamual Lui, Vaivakawn Lui* and *Tuikual Lui* with limited areal extent (Photo Plate 3.7). In the area between Luangmual and Maubawk, the prominent east-west joint and development of angulated drainage patterns has restricted north-south extension of individual ridge giving rise to isolated hillocks (Sawaiyan & Moirangcha, 2007). The overall geomorphology of the area is characterized by hills of structural origin with intervening narrow valley fills.

Photo Plate 3.7 *A narrow flatland along Chite valley surrounded by dissected hills*

3.11 Soils

The soils in Aizawl generally exhibit acidic properties which is basically due to high amount of rainfall in the area. They are rich in organic carbon and contain high proportion of available nitrogen but have low content in phosphorus and potassium. The area is characterized by a warm, humid sub-tropical climate, and is directly under the influence of heavy rainfall. Thus, based on precipitation and humidity levels, the soil moisture regime is categorized as *Udic*. It was observed that the mean seasonal temperature variation between summer and winter is approximately 7°C, which surpassed the 5°C threshold required for classification. Consequently, these soils meet the criteria for the *hyperthermic* temperature class, and qualify its use as a family modifier in soil taxonomy.

The soils of Aizawl city have been classified following the Soil Taxonomy system (USDA, 1994) on the basis of their morphological and physico-chemical properties (SRSC, 2006). At the order level, the predominant soil types within the Aizawl municipal area include *Entisols, Inceptisols* and *Ultisols*. A total of 14 distinct soil series were identified within the area based on their physico-chemical properties. The soils within the study area were found to have been formed under humid sub-tropical conditions with an average annual rainfall of 2100 mm. The *pedons* exhibit mixed mineralogical compositions and fall under the hyperthermic temperature class. Morphologically, the soils of Aizawl city are moderately deep to very deep, and range in colour from dark yellowish-brown to brown. Texturally, they vary from sandy clay loam to clay, displaying weak to moderately developed sub-angular blocky structures. They are naturally acidic, and their pH values varies between 4.5 and 6.5. The soil map of the study area is shown in Figure 3.7.

3.12 Drainage

Being located on a hill crest, Aizawl is traversed by several small streams and rivulets of varying lengths. On the basis of the topographic features, the drainages of the area can be broadly grouped into two systems—the Eastern and the Western Drainage Systems.

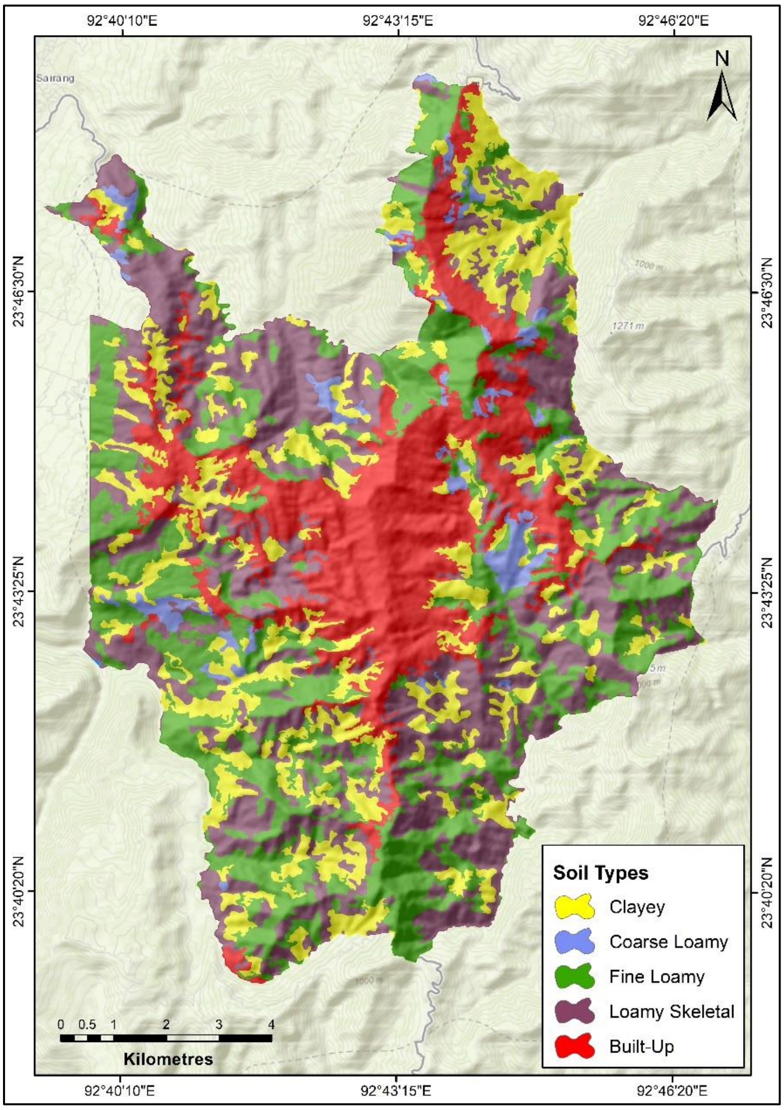

Fig. 3.7 *Soil Map of the study area* (*modified after* SRSC, 2006)

The eastern portions of the study area are mostly drained by *Muthi Lui, Tuipawl Lui* and *Chite Lui,* all of which flow eastwards and join the Tuirial river in the east. The south-eastern parts of the study area are drained by *Tuikhawhthla Lui* which originated from *Hlimen Tlang*. It flows towards the north and drains *Melli Lui* and *Melnga Lui*. Other important streams from this area include *Sihpui Lui, Mauhak Lui, Mualpui Lui* and *Kahthelh Lui*. All these streams enter into *Chite Lui* which is then ultimately draining into the Tuirial river. *Chite Lui* is considered to be the most prominent stream in the eastern section since almost two-third of all the drainages in the eastern portion are drained into it. Important incoming streams of *Chite Lui* include *Theihai Lui* and *Chanmari Lui*, both of which originate from the heart of the city, *Ramthar Lui, Mirawng Lui, Bangla Lui, Tlak Lui, Umpupuk Lui, Hmawngkai Lui, Lawibual Lui, Khawhnuai*

Lui, and *Melkaw Lui.* Most of the streams which flow into Chite Lui originate from the city, and drain the area through several second and third order tributaries (Sawaiyan & Moirangcha, 2007).

All the streams and streamlets of the western part of the study area drain themselves into the Tlawng river. Most of the streams of the southwestern part of the study area are drained by *Ser Lui* which originates from *Hlimen Tlang* in the southern border of the study area. It flows in the western direction before it makes a U-turn near *Chukvel Tlang* from where it flows in the northern direction. *Ser Lui* drains a number of streams including *Kanhlum Lui*, *Ramri Lui*, *Tuikhur Lui*, *Vai Lui*, *Sakhisih Lui* and *Zawngkawt Lui* before finally it drains into the Tlawng river.

On the central-western side of the study area, *Tuikual Lui* is the major stream that drains several streams and rivulets of the surrounding areas. *Hnimtheilo Lui, Quarry Lui, Sakei Lui, Rawngrut Lui, Mauhak Kawr* and *Kawnzau Lui* are the prominent streams drained by *Tuikual Lui* which ultimately empties itself into the Tlawng river. Majority of the streams around Vaivakawn, Hunthar, Rangvamual, Phunchawng, etc are drained by *Kurung Lui* which flows into the Tlawng river within Sairang village council. The streams of the area around Chaltlang, Bawngkawn, Chanmari, Edenthar are drained by *Leitan Lui* which joins *Kurung Lui*. Most of the streams of the westernmost portion within and around Tanhril and Sakawrtuichhun are drained by *Setlak Lui* which in turn enters into the Tlawng river.

The overall drainage pattern of the whole study area exhibits a dendritic to sub-dendritic pattern except for the south-western portion which exhibits parallel to sub-parallel drainage pattern. The drainage map of the study area is shown in Figure 3.8.

3.13 Past Landslide incidents in Aizawl municipal area

Majority of the Aizawl municipal area and its surroundings are highly susceptible to landslides. The area has witnessed a number of mass movements of varying magnitude and severity within the past few decades. The primary causes of slope instability are due to the inherent nature of the terrain, immature geology, heavy monsoon rainfall, and unregulated land-use practices. The frequency and intensity of the landslide activi-

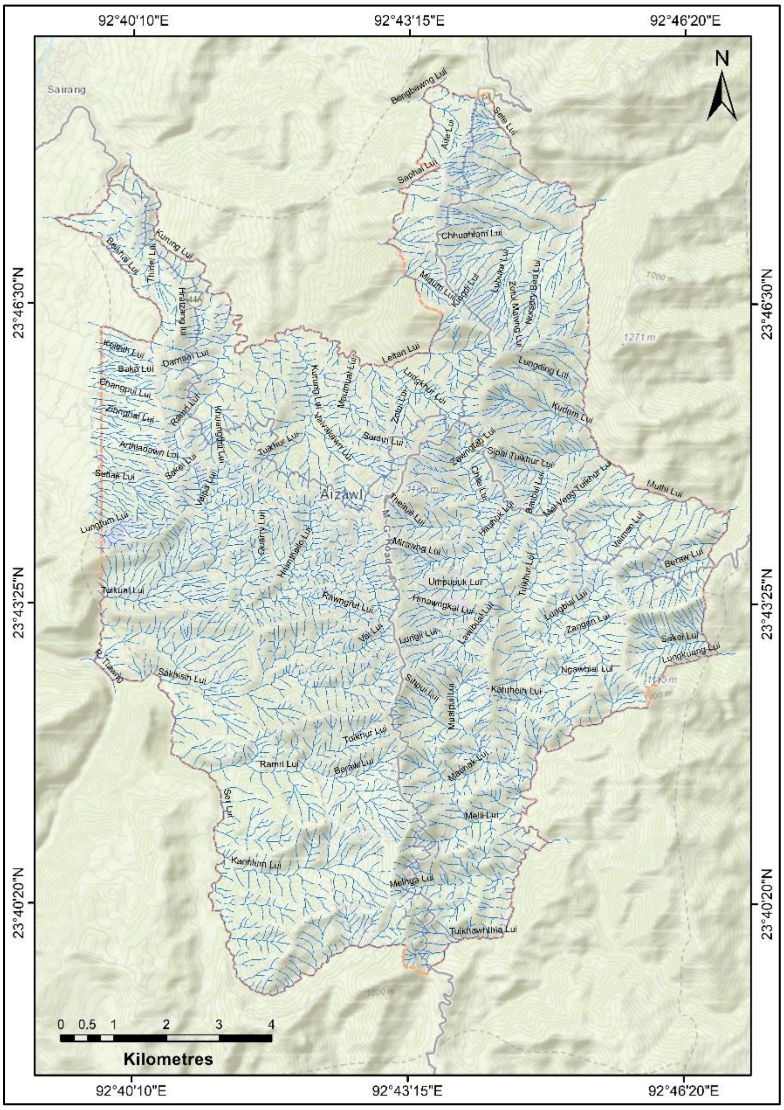

Fig. 3.8 Drainage Map of the study area (Background image: ESRI)

ties are further exacerbated by unplanned construction activities and deforestation that disturb the natural stability of slopes. These landslides have severe repercussions on public safety, property, and the environment which often leads to loss of life, disruption of communication, and massive financial losses.

One of the earliest documented landslide events within Aizawl occurred at Vaivakawn, Sihpui, Sarawn Veng and Armed Veng areas during the monsoon of 1983 in which approximately 200 houses were affected (Prasad, 1983). Fortunately, there were no human casualties due to the timely evacuation. The Sihpui area (now in Ramthar Veng) in particular, was characterized by large scale subsidence of the slope covering around 0.061 sq. km. (Srivastava et al., 1993). This place has experienced recurrent subsidence events in 1991, 1993 and the following years resulting in the damage of several houses within the vicinity.

The most devastating landslide occurrence ever recorded within Aizawl took place on 9 August, 1992 at a quarry site of South Hlimen locality, involving complete collapse of a stone quarry. It was reported that due to this disastrous incident, 66 people lost their lives apart from 17 houses destroyed (Swamy, 1992; Tiwari & Kumar, 1997). Prior to this catastrophic event, another rockslide happened on 11 July, 1986 in the same place, causing 4 fatalities (DM&R, 2020; 2023). This was followed by another equally destructive landslide event occurred at Laipuitlang on 11 May, 2013 (Photo Plate 3.8) resulting in 17 fatalities, 8 injuries, and the destruction of 15 houses (Laldinpuia et al., 2014; Chenkual, 2015).

Photo Plate 3.8 *The Laipuitlang landslide (11 May, 2013) was one of the deadliest incidents*

The Bawngkawn-Thuampui road corridor emerged as a recurring hotspot, with landslide events recorded in 1994, 2015, and 2019 which repeatedly blocked transportation routes, damaged houses, and displaced residents. For instance, the 17 September 1994 landslide disrupted traffic and impacted 20 households (Tiwari & Kumar, 1996), while the 27 August 2015 event destroyed 2 houses, and the 26 July 2019 event forced 14 families to evacuate (Photo Plate 3.9). On 20 August, 2003, a 3-storey reinforced concrete building collapsed at Mission Vengthlang which resulted in 3 fatalities. Other important events include the landslide event at Saikhamakawn in 2008, which caused 2 deaths, 4 injuries and destruction of 2 houses, and the Chhinga Veng landslide on 6 October, 2009, which claimed 3 lives and left 10 injured. The landslide at Zonuam in 2016 also resulted in 3 fatalities and the destruction of 1 house. Another tragic incident took place in Durtlang on 2 July, 2019 (Photo Plate 3.10), where the Basic Services to the Urban Poor residential blocks crumbled due to the impact of huge masses of debris, which results in the death of 3 persons and 11 injuries (Mazumder et al., 2025).

Recent years have also witnessed catastrophic landslide incidents. The heavy rainfall which accompanied the Cyclone Remal on 28 May, 2024 caused devastating landslides at several places within Aizawl municipal area. Among these, the landslides at

Photo Plate 3.9 *The landslide along Bawngkawn-Thuampui road corridor (26 July, 2019)*

Photo Plate 3.10 *The landslide at the BSUP complex, Durtlang (2 July, 2019)*

Melthum (Photo Plate 3.11) and Salem Veng claimed 19 and 3 lives, respectively, with several damages to property and infrastructure (Haokip et al., 2024; Sangi et al., 2025). Another tragic event occurred on 2 July, 2024 at Zuangtui which resulted in 3 fatalities along with 3 houses destroyed. Other recent landslide events include the landslides at Thuampui on 11 June, 2021 where a 2-storey building collapsed resulting in 4 fatalities. The 6 October 2020 event in Zemabawk Kananthar destroyed 2 houses and vehicles, and the 9 June, 2023 incident at Vaivakawn-Zohnuai blocked the National Highway and damaged 5 houses.

There have been reported incidents of continual reactivation of slope instabilities in some parts of the city. The most prominent of such activity was observed in Hunthar Veng (Photo Plate 3.12), covering an area of approximately 1,26,886 m^2 and affecting more than 100 houses (Vinoth et al., 2022). Subsequent subsidence and mass movement started in 1992, and continued to occur at irregular intervals until 2020 when the state government implemented slope stabilization measures, which have since prevented further activity. A vast area of Zuangtui – Muanna Veng was also affected by similar

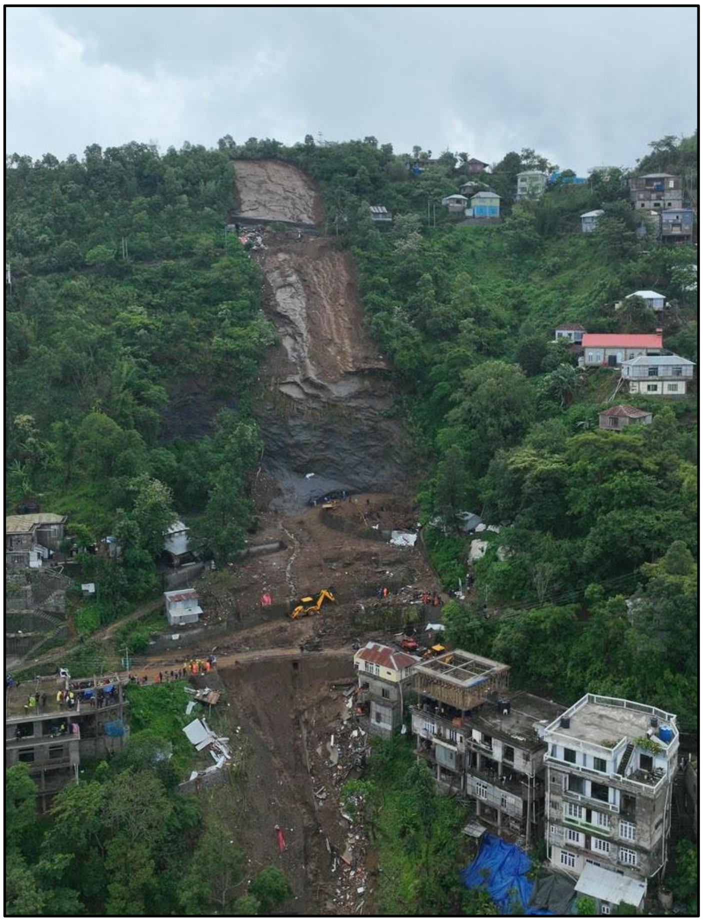

Photo Plate 3.11 *The landslide at Melthum (28 May, 2024)*

Photo Plate 3.12 *Recurrent landslide activity at Hunthar Veng* subsidence. In addition, the instability activity in Ramhlun Sports Complex was first observed as creep movement in 1994. It then continued as rock falls-debris slides in 2004, 2007 and 2012 till 2013 (Vasudevan & Ramanathan, 2016). Apart from these, occurrences of minor subsidence of land are also recorded at Dinthar Veng, Republic Veng and Zemabawk areas.

These landslide events represent the most prominent occurrences in the study area. However, there are several other significant incidents which caused substantial damage and disrupted the daily lives of the residents. The list of some of the important landslide events within the study area are shown in Table 3.2.

Table 3.2 *List of Important Landslide Events within Aizawl*

Date/Year	Location	Casualty/Damages
1983 - 2007	Ramthar Sihpui	Several houses destroyed and affected
1983 - 2005	Armed Veng	Several houses destroyed and affected
11 July, 1986	S. Hlimen	4 deaths
1987 - 2021	Zuangtui Muanna Veng	Several houses destroyed and affected
9 August, 1992	S. Hlimen	66 deaths; 17 houses destroyed
1992 to 2020	Hunthar Veng	Road damaged; several houses destroyed
17 September, 1994	Bawngkawn-Thuampui road	Road blocked; 20 houses affected
1994 to 2013	Ramhlun Sports Complex	Several houses destroyed and affected
19 May, 2001	Ngaizel	1 death; 1 house and 1 vehicle destroyed
5 May, 2002	Ramhlun Venglai	1 death; 1 house destroyed
20 August, 2003	Mission VT	3 deaths, 3-storey RC building collapsed
6 March, 2008	Saikhamakawn	2 deaths; 4 injuries; 2 houses destroyed
6 October, 2009	Chhinga Veng	3 deaths, 10 injuries
13 September, 2010	Tuikual S	1 death
18 September, 2010	Rangvamual	1 death; 1 house destroyed
11 August, 2012	Chanmari	1 death; 4 injuries
11 May, 2013	Laipuitlang	17 deaths; 8 injuries; 15 houses destroyed
14 July, 2014	Zemabawk Falkland Veng	1 death; 5 injuries; 1 house destroyed
27 August, 2015	Bawngkawn-Thuampui road	Road blocked; 2 houses destroyed
15 September, 2015	Zemabawk	3 houses destroyed; Road blocked

Table 3.3 (continued)

Date/Year	Location	Casualty/Damages
21 May, 2016	Zonuam	3 deaths; 1 house destroyed
13 June, 2017	Sarawn Veng	1 house destroyed; 6 houses affected
2 July, 2019	Durtlang	3 deaths; 11 injuries; 3 blocks of RC buildings destroyed
26 July, 2019	Bawngkawn-Thuampui road	Road blocked; 14 families evacuated
6 October, 2020	Zemabawk Kananthar	2 houses destroyed; 2 vehicles destroyed
11 June, 2021	Thuampui	4 deaths; 2-storey house destroyed
9 June, 2023	Vaivakawn-Zohnuai	5 houses destroyed; Road blocked
28 May, 2024	Melthum	14 deaths; 3 houses destroyed
28 May, 2024	Salem Veng	3 deaths; 1 house destroyed
2 July, 2024	Zuangtui	3 deaths; 3 houses destroyed

CHAPTER 4

LANDSLIDE SUSCEPTIBILITY ASSESSMENT

This chapter presents a quantitative assessment of landslide susceptibility within the Aizawl Municipal Area, using three bivariate statistical models, namely, Information Value (IV), Frequency Ratio (FR), and Weight of Evidence (WofE) models. Based on a comprehensive inventory of landslides and twelve conditioning factors, this chapter provides the methodology for generating susceptibility maps and validation of their accuracy. The content of this chapter has been published in the peer-reviewed journal, *Himalayan Geology*, Vol. 45(1), 2024, pp. 39-57.

4.1 Data

The present study utilized geospatial techniques for data collection, preparation and analysis. Satellite imagery from Cartosat-1, having spatial resolution of 2.5 m, Sentinel-2 data with 10 m resolution, and Google Earth® image with a resolution of 50 cm along with a 10 m resolution CartoDEM were used to generate various thematic factor maps. Apart from these, ancillary data such as historical landslide, and data collected from field surveys were also utilized for deriving various factor maps. All these thematic data were projected to WGS84 UTM Zone 46 N for analyses. The details of data used are shown in Table 4.1.

Table 4.1 *Details of data used in the study*

Data Type	Particulars	Scale/Resolution	Data derivative
Satellite Data	Google Earth®	0.5 m	LULC, Landslide Inventory, Lithology
	Sentinel-2	10 m	NDVI
	Cartosat-1	2.5 m	Drainage, Lineament
DEM	Cartosat-1 (Stereoscopic)	10x10 m grid	Slope, Aspect, Elevation, Curvatures, SPI, TWI
Ancillary Data	Historical Landslide	-	Landslide Inventory

4.2 Landslide Inventory Preparation

The landslide inventory for the study area was compiled from three different sources. The first source comprised historical records of landslide occurrences dating back to 1957 which were documented and maintained by the Directorate of Geology & Mining, Govt. of Mizoram. These archival records, however, were not generated through a systematic inventory mapping procedure, and therefore lacked important attributes, including information on the type of failure, exact date of occurrence and, more importantly, precise geographic coordinates. Thus, they were carefully scrutinized, cross-referenced and filtered before integrating some of them into the final inventory database. The second source constitutes online interpretation of multi-temporal Google Earth® images available online. Majority of the landslide inventory datasets were mapped through this source. However, one notable limitation of this approach was the absence of information regarding the date of occurrence for the landslides mapped. The third source consisted of detailed field surveys conducted within the study area. This served both as a primary data source for more recent landslide events and as a means to validate and update information obtained from archival records and remote sensing interpretation. The field surveys also facilitated the capture of photographic evidence and contextual observations on site-specific geomorphic and anthropogenic factors contributing to slope instability.

A total of 381 landslide inventory datasets were generated, all of which were represented by polygons (Fig. 4.1). It should be noted that all the landslides mapped were rainfall-induced shallow landslides, and were generally of small areal extent, with sizes ranging from approximately 100 m^2 to 120,000 m^2. Due to their small size, identifying the scarp from the remaining parts of the landslide body was rather difficult, especially from the satellite images (Khanna et al., 2021). Therefore, all the landslides were mapped as single polygons. The resulting inventory, therefore, comprises landslides involving different materials and various types of movement. For the purpose of model development and validation, the total landslide inventory was randomly partitioned into two distinct datasets. The 267 landslides (70% of the total) were allocated for model calibration or training, while the remaining 114 landslides (30%) were reserved for model validation.

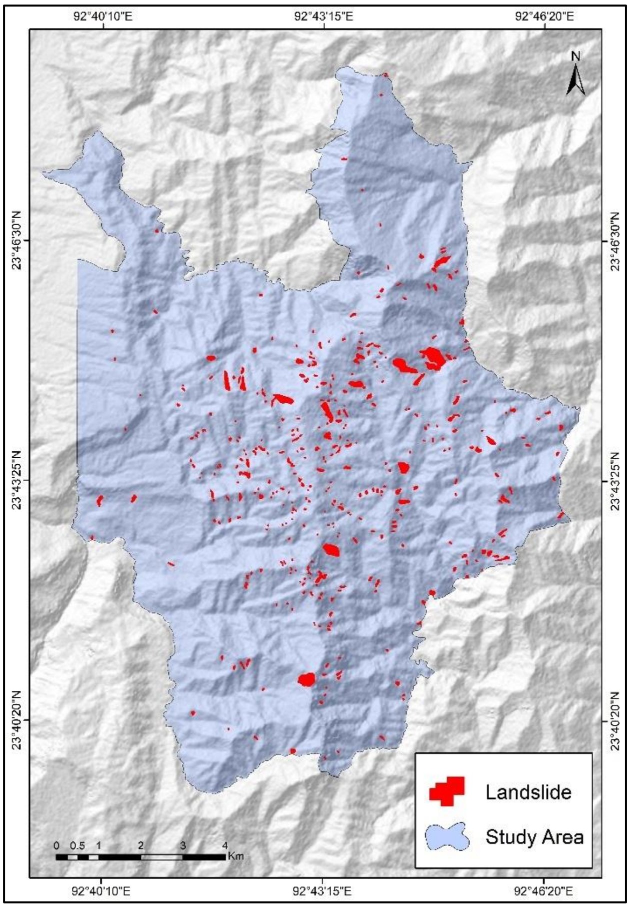

***Fig. 4.1** Landslide Inventory Map of the Study Area*

4.3 Generation of Predisposing Factors

There are no standardized set of rules or guidelines for selecting predisposing factors in landslide susceptibility mapping (Ayalew & Yamagishi, 2005). Based on data availability, characteristics of the study area and insights from the previous studies conducted in the area, 12 landslide conditioning factors were selected. These selected factors include elevation, slope aspect, lineament density, drainage density, Normalized Difference Vegetation Index (NDVI), lithology, land use/land cover (LULC), plan curvature, profile curvature, slope angle, Stream Power Index (SPI), and Topographical Wetness Index (TWI).

Satellite data were extensively utilized for preparing these thematic factors. A Cartosat-1 DEM was used for generating topographical parameters such as slope degree, slope aspect, plan and profile curvatures, elevation, SPI, and TWI. Cartosat-1 data was used for delineating drainage networks and lineaments, from which their respective density maps were subsequently prepared, while NDVI was generated from Sentinel-2 data. Extensive field work was conducted for preparing the lithological map of the study area. In addition, Google Earth® image was also utilized in the preparation of the land use/land cover map and for updating the lithology map in conjunction with field verification. All the vector layers were converted into raster format to 10m x 10m grid size for analyses. These predisposing factors were broadly categorized into topographical, geological, hydrological, and land cover types.

4.3.1 Topographical Factors

Topographical factors greatly influence the stability of hill slopes by directly affecting the distribution of shear stress, the accumulation and movement of water, and the overall morphology of the terrain. These include the slope aspect, slope angle, elevation, and terrain curvatures.

i) Slope Aspect: This refers to the directional orientation of a slope which indirectly influences slope instability by controlling microclimatic conditions, such as exposure to solar radiation, wind, and rainfall distribution. This in turn, impact soil moisture and vegetation cover. In the present study, the slope aspect was categorized into nine distinct classes, viz., "flat, north, northeast, east, southeast, south, southwest, west, and northwest". The slope aspect map of the study area is shown in Figure 4.2.

ii) Slope Angle/Gradient: The steepness of a slope is a fundamental determinant of its stability, with steeper slopes generally exhibiting higher susceptibility to landslides due to increased shear stress within the slope material. The slope angles in the study area ranged from 0° to over 45° and were classified into five categories (Fig. 4.3). Higher slope classes (35–45° and >45°) occupied smaller areas, whereas the 15–25° class covered the maximum area which is approximately 38.3% of the total study area.

iii) Elevation: While elevation does not have direct influence on landslide occurrences, it is an important conditioning factor which is often correlated with other parameters such as rainfall, soil types, vegetation types, and tectonic activity. The elevation within study area ranged from 130 m to more than 1000 m, and was divided into five elevation classes (Fig. 4.4). While the lowest elevation class (<300 m) covers only less than 1%, the 500–800 m elevation range extends over approximately 40% of the total study area.

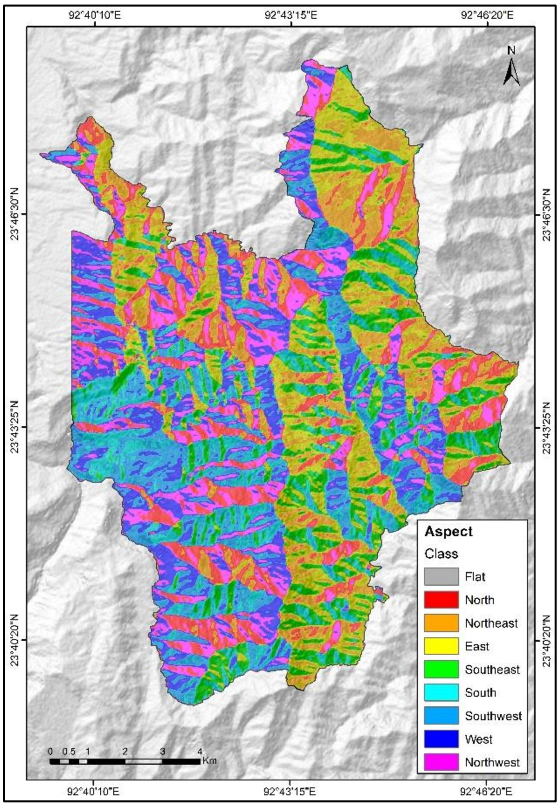

Fig. 4.2 *Slope Aspect Map of the Study Area*

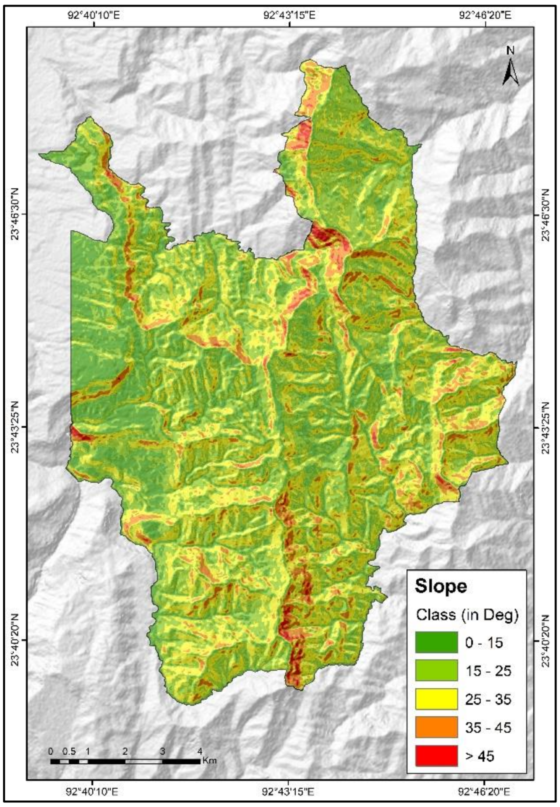

Fig. 4.3 *Slope Gradient Map of the Study Area*

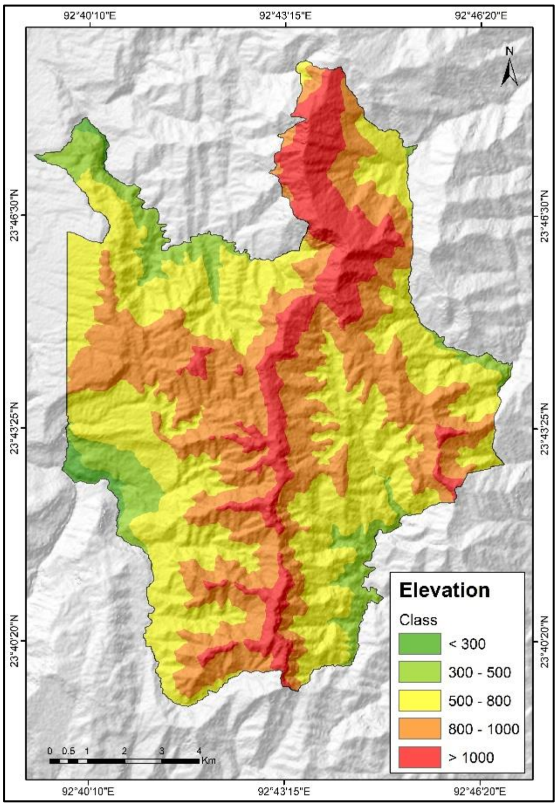

***Fig. 4.4** Elevation Map of the Study Area*

iv) Plan Curvature: This is “the curvature of a contour line formed by the intersection of a horizontal plane with the ground surface”. It influences the convergence or divergence of water flow on the surface and, therefore influences the stability conditions of the slope. Values of plan curvature are categorized as positive for convex contours and negative for concave contours, while a value of zero indicates a flat surface. The plan curvature of the study area was divided into five classes, as shown in the Figure 4.5.

v) Profile Curvature: This is the curvature measured in the vertical plane, parallel to the direction of the steepest slope or flow line. It quantifies the rate of change of slope along the flow path, and directly influences the acceleration or deceleration of water flow and downslope sediment movement, thereby affecting erosion and deposition processes. In the present study, the profile curvature was classified into five classes, as depicted in the Figure 4.6.

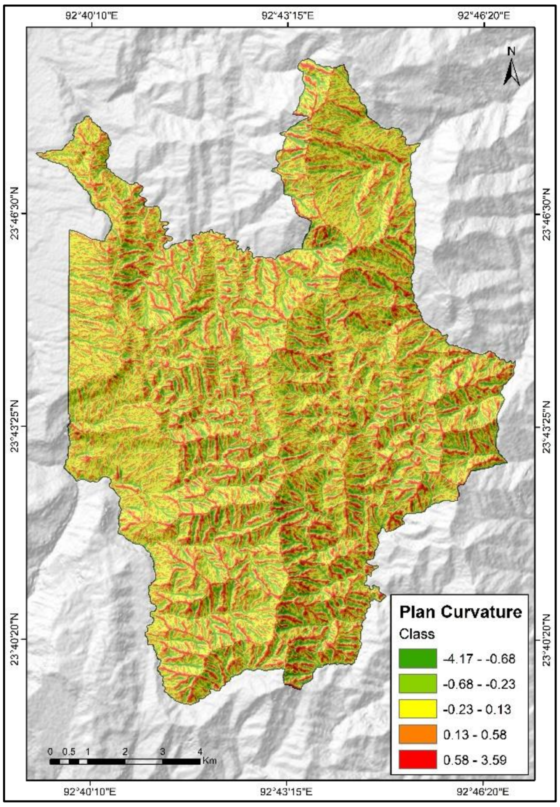

Fig. 4.5 *Plan Curvature Map of the Study Area*

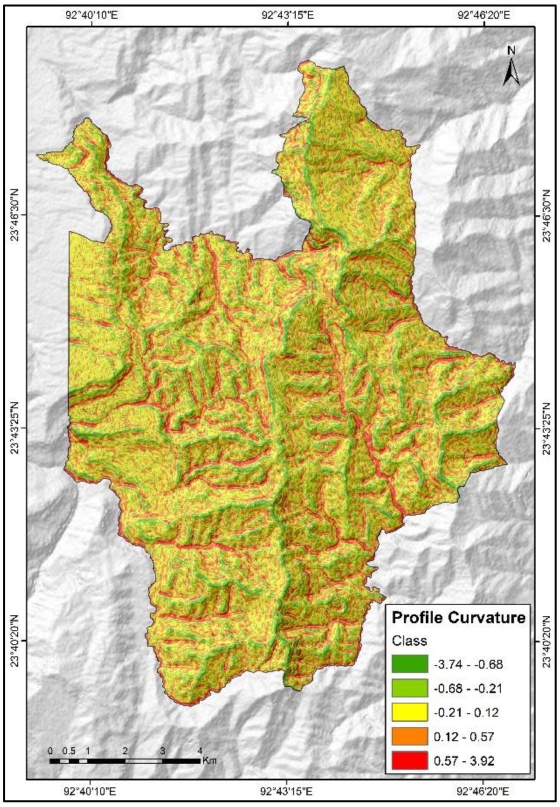

Fig. 4.6 *Profile Curvature Map of the Study Area*

4.3.2 Geological Factors

Geological factors are important in influencing landslide occurrences, as they represent the inherent attributes of the ground that predispose slopes to instability. Within this category, lithology and lineament density were the factors considered in the present study.

i) Lithology: Lithology profoundly influences landslide occurrences by determining the inherent strength, permeability, and resistance to weathering of rock and soil units. Stronger and less-weathered rocks are relatively more resistant to the driving forces, and are therefore, less susceptible to slope failure and vice versa. The rock types within the study area are composed of soft sedimentary rocks represented by sandstone, shale, siltstone and their intercalations. These were categorized into six lithological units (Please refer Figure 3.6).

ii) Lineament Density: Lineaments are linear geological features that are aligned in a rectilinear or curvilinear relationship, and represent zones of weakness and tectonic activity, faults, shear zones, and sharp lithological contacts within rock masses. Areas in close proximity to lineaments are generally more prone to mass wasting due to enhanced water percolation and potential for planar or wedge failures. Lineaments up to a minimum length of 152 m were mapped within the study area, and their density map was prepared and divided into five classes (Fig. 4.7).

4.3.3 Hydrological Factors

Hydrological factors constitute an important category influencing landslide occurrences by altering the mechanical properties of slope materials and initiating erosional processes. The hydrological factors considered in the present study include drainage density, SPI, and TWI.

i) Drainage Density: This is defined as "the ratio of the total length of streams and rivers in a drainage basin to the total area of the drainage basin". It serves as an important indicator of slope evolution, mass wasting, and related erosional processes within an area. Higher drainage density can indicate lower infiltration rates and faster surface flow, and contributes to accelerated surface erosion and mass wasting. In the

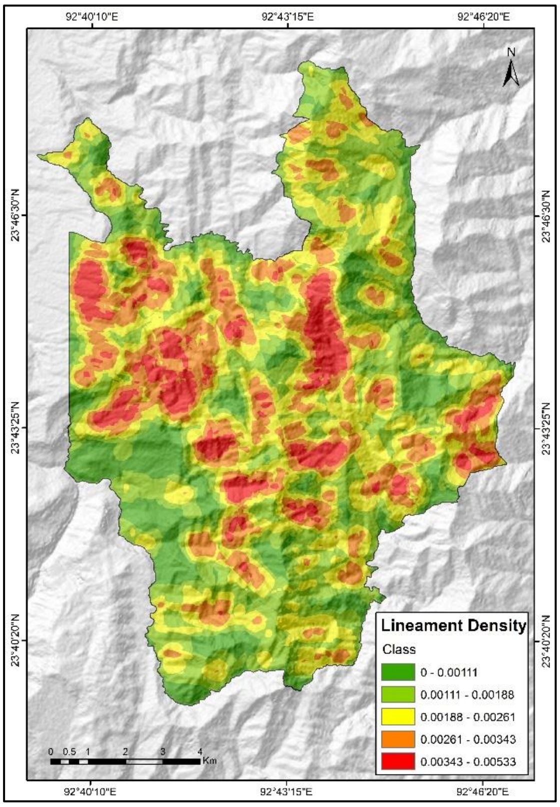

Fig. 4.7 *Lineament Density Map of the Study Area*

present study, drainage network was delineated from the satellite imagery from which the density map was subsequently generated using the following equation (Horton, 1932; 1945):

$$D_d = \frac{L_{\mathrm{T}}}{A} \tag{4.1}$$

where D_d is the drainage density, L_{T} represents the total length of streams, and A denotes the total area. The drainage density map was further classified into five classes, as shown in the Figure 4.8.

ii) Stream Power Index (SPI): This measures the potential flow erosion at a given topographic location, thereby regulating the erosive power of water flow. High SPI values indicate a greater propensity for erosion, and are linked to a higher potential for high-velocity earth flows and increased landslide probability. The SPI of the study area was generated from the Cartosat-1 DEM using the equation (Moore et al., 1991):

$$SPI = A_s \times \tan\beta \tag{4.2}$$

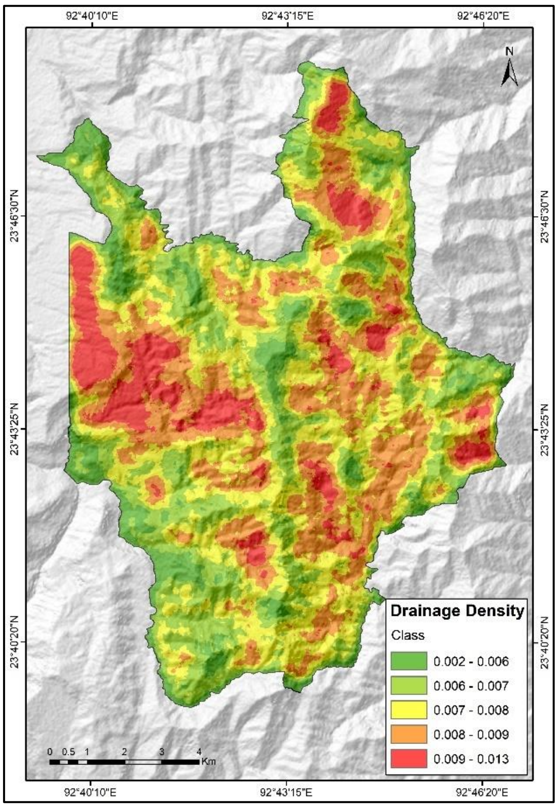

Fig. 4.8 *Drainage Density Map of the Study Area*

where A_s is the specific catchment area (also known as flow accumulation) expressed in m/m^2, and β represents the tangent of the local slope gradient (in degrees). The SPI of the study area was classified into five classes, as depicted in Figure 4.9.

iii) Topographic Wetness Index (TWI): This is a steady-state wetness index used to quantify the influence of topography on the location and size of saturated source areas for runoff generation. The mechanism by which TWI influences landslides is through its correlation with moisture content and hydrological processes. Areas with higher TWI values are generally associated with higher level of saturation in soil and rock layers which in turn reduces their shear strength and initiate slope failures. In the present study, the TWI was generated from the DEM using the following equation:

$$TWI = \mathrm{Ln}[A_s/tan(\beta)] \tag{4.3}$$

where Ln is the natural logarithm; A_s represents the specific catchment area measured in m/m^2, and $tan(\beta)$ is the local slope gradient, which is expressed in degrees. The TWI was divided into five classes, and the map is shown in Figure 4.10.

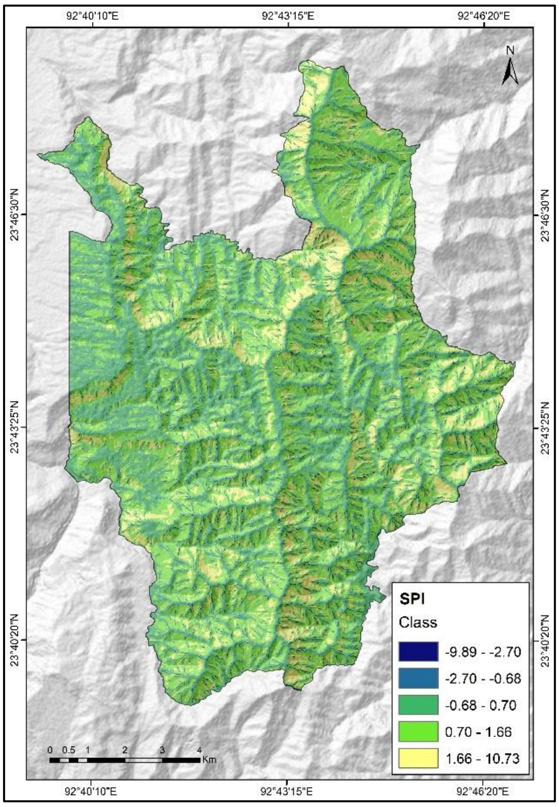

Fig. 4.9 *Stream Power Index Map of the Study Area*

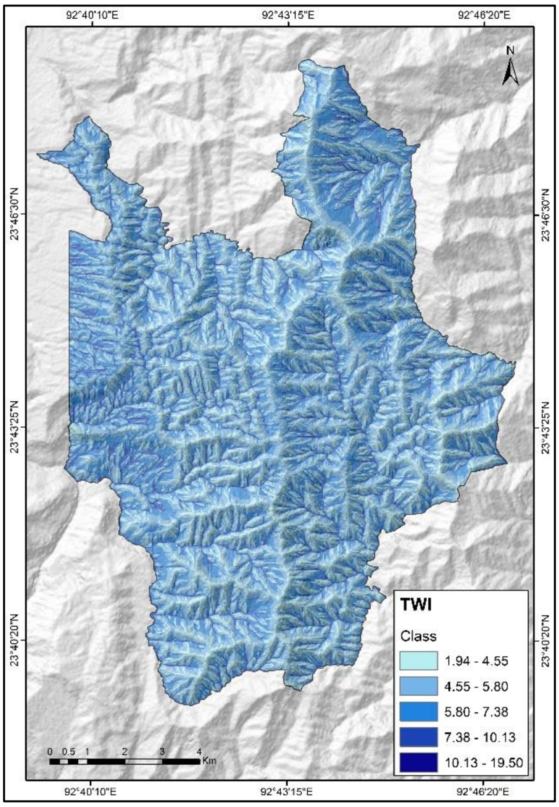

Fig. 4.10 *Topographic Wetness Index Map of the Study Area*

4.3.4 Land Cover Factors

Land cover characteristics govern the interaction between the land surface and atmospheric processes (Betts et al., 1996), with vegetation cover playing a vital role in enhancing slope stability and preventing erosion (Shen et al., 2017). Under this category, land use/land cover (LULC) and Normalized Difference Vegetation Index (NDVI) are the factors considered in the present study.

i) Land Use/Land Cover (LULC): The changes in LULC patterns are recognized as influential factors for rainfall-triggered landslides, as human activities on hillsides destabilize areas and induce slope failure. Barren lands and sparsely vegetated areas are generally more susceptible to landslides than densely vegetated ones. In the present study, the LULC map (Fig. 4.11) was prepared through visual interpretation of Google Earth® image, and was subsequently validated by field checks. The study area was divided into nine LULC classes, where the largest area was occupied by scrubland (30.44%), which was followed by open forest (24.22%) and built-up areas (21.10%), respectively.

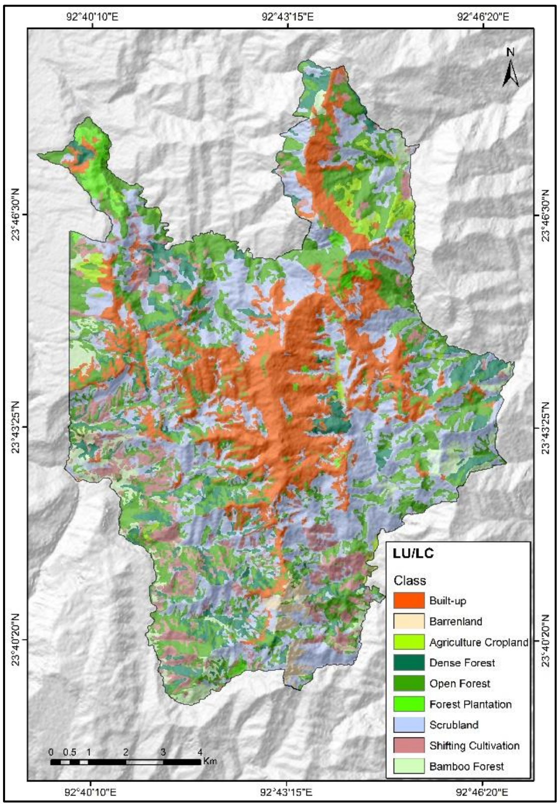

Fig. 4.11 *LULC Map of the Study Area*

ii) Normalized Difference Vegetation Index (NDVI): This is a standardized quantitative metric used to represent greenness or the relative density of vegetation and relative biomass. The NDVI values range from -1.0 to 1.0 where a higher value corresponds to a greater density of vegetation and vice versa. The NDVI is inversely associated with landslide density, indicating that greater vegetation density generally corresponds to lower landslide susceptibility. Thus, higher the NDVI values, lower is the chance of slope failure owing to dense vegetation. Conversely, deforested areas and barren lands are often associated with slope instability. In the present study, the NDVI was generated from Sentinel-2 data using the following equation (Rouse et al., 1974):

$$NDVI = \frac{(NIR - Red)}{(NIR + Red)} \tag{4.4}$$

where NIR indicates the reflectance in the near-infrared band and Red signifies the reflectance in the red band. By using the natural break method, the NDVI of the study area was classified into five classes whose values range from -0.25 to 0.91, and the map is shown in Fig. 4.12.

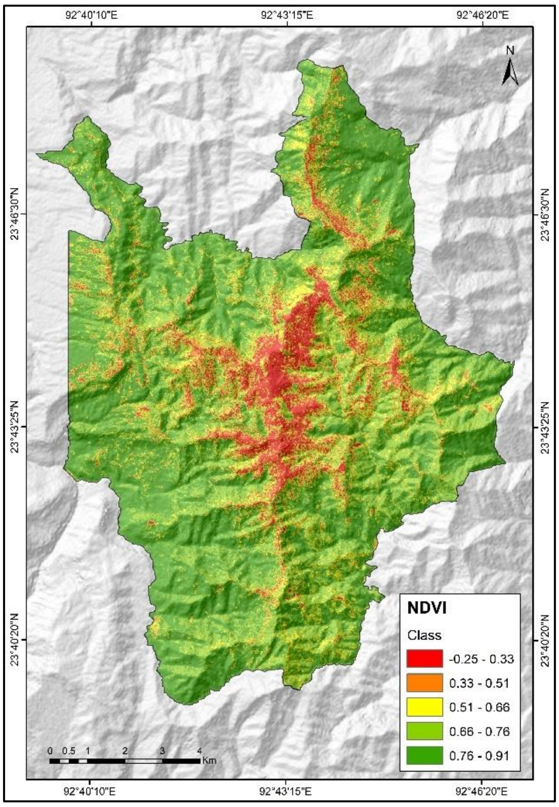

Fig. 4.12 *NDVI Map of the Study Area*

4.4 Landslide Susceptibility Models

In the present study, three bivariate statistical models, namely—Information Value (IV), Frequency Ratio (FR), and Weight of Evidence (WofE) were employed to generate the landslide susceptibility map of the Aizawl Municipal Area. These statistical data-driven models were selected due to their relative simplicity, adaptability, and proven effectiveness in various landslide settings.

4.4.1 Information Value (IV) Model

This model was originally introduced by Yin and Yan (1988) and later refined by van Westen (1993). The Information Value method determines the weight for each class of a factor layer based on the ratio of landslide density within that class to the landslide density of the total study area. It is defined by the following equation:

$$W_i = ln\frac{Npix(Si)/Npix(Ni)}{\sum Npix(Si)/\sum Npix(Ni)} \tag{4.5}$$

where W_i is the weight of a factor class; $Npix(Si)$ denotes the number of pixels of landslides within class i; $Npix(Ni)$ is the number of pixels of class i; $\sum Npix(Si)$ indicates number of pixels of landslide within the study area; and $\sum Npix(Ni)$ represents the number of pixels of the study area.

By using the above equation (4.5), the weight value was assigned for every class of a factor. A positive weight was assigned when the landslide density within a particular class of a factor is higher than the overall average, while a negative weight indicates a lower density than the normal. The natural logarithm (ln) was applied to account for wide variations in weights. A Landslide Susceptibility Index (LSI) map was then subsequently generated by summing the weighted values of all factor classes using the following equation:

$$LSI = \sum_{i=1}^{n} W_i \tag{4.6}$$

where i represents the class of a factor, with values ranging from 1 to n.

4.4.2 Frequency Ratio Model

This bivariate statistical model establishes a correlation between each landslide conditioning factor and the spatial distribution of landslides in the area. In this method, the frequency ratio for each class of a conditioning factor was derived by dividing the landslide occurrence ratio by the area ratio (Lee & Talib, 2005). This is defined by the following equation:

$$FR = \frac{Npix(Si)/\sum Npix(Si)}{Npix(Ni)/\sum Npix(Ni)} \tag{4.7}$$

where $Npix(Si)$ represents the number of pixels of landslides within class i of the factor; $\sum Npix(Si)$ is the total number of landslide pixels across the entire study area; $Npix(Ni)$ denotes the total number of pixels in class i of the factor; and $\sum Npix(Ni)$ signifies the total number of pixels in the entire study area.

The frequency values determined were utilized to correlate the spatial association between a particular class of a factor and landslide occurrences. An FR value of 1 represents the average correlation which implies that the density of landslides within the class is proportional to the areal extent of the factor class in the study area. When the value is greater than 1, it indicates a strong positive spatial association and a high propensity for landslide occurrence. If the value is less than 1, it signifies a low and negative correlation, indicating a low probability of landslide occurrence. The LSI map was generated by summing the FR values of all factor classes using the following equation:

$$LSI = \sum_{i=1}^{n} FR \tag{4.8}$$

where i denotes the class of a factor whose values range from 1 to n.

4.4.3 Weight of Evidence Model

This is a quantitative data-driven method initially developed for mineral potential mapping (Agterberg et al., 1993; Bonham-Carter, 1994). The technique has since been widely adopted for landslide susceptibility assessment due to its robust statistical framework (Mathew et al., 2007; Neuhäuser & Terhorst, 2007; Pradhan et al., 2010; Martha et al., 2013). This approach is based on the Bayesian probability model which employs a log-linear form that leverages prior and posterior probabilities (Pradhan et al., 2010). In this model, the input layers are assumed to be independent of one another (Neuhäuser & Terhorst, 2007). The model calculates both the positive and negative weights for each landslide conditioning factor based on the presence or absence of landslides within the study area as defined below:

$$W^{+} = ln\frac{P\{B|A\}}{P\{B|\bar{A}\}} \tag{4.9}$$

$$W^{-} = ln\frac{P\{\bar{B}|A\}}{P\{\bar{B}|\bar{A}\}} \tag{4.10}$$

where ln is the natural logarithm; P represents the probability ratio; B and $\bar{B}$ indicate the presence and absence of the desired class of the landslide conditioning factor, while A and $\bar{A}$ represent the presence and absence of landslides, respectively. A weight of contrast value (C) was then calculated from these positive and negative weights using the following equation:

$$C = W^{+} - W^{-} \tag{4.11}$$

This contrast value (C) establishes the spatial association between the classes of the predisposing factors and the landslide occurrences. A positive contrast value indicates a positive spatial correlation and higher susceptibility, while a negative value suggests a negative spatial association and lower susceptibility. A landslide susceptibility index (LSI) was subsequently generated by summing the contrast values (C) of all the factor classes by the equation:

$$LSI = \sum_{i=1}^{n} C \tag{4.12}$$

where i represents the class of a factor, with its values varying from 1 to n.

4.5 Validation of the Models

Validation of the generated landslide susceptibility map is an essential step to ascertain the reliability of the modeling process. This procedure facilitates a comparative analysis of the performance and predictive capabilities of the different models, and justification for the selection of the input parameters (Chung & Fabbri, 2003; Beguería, 2006). In the present study a Receiver Operating Characteristic (ROC) curve and its associated Area Under the Curve (AUC) was employed for the validation process. The ROC curve plots the True Positive Rate (the cumulative percentage of landslide occurrences) on the Y-axis against the False Positive Rate (the cumulative area percentage) on the X-axis. The True Positive Rate (TPR) and the False Positive Rate (FPR) were calculated using the following equations:

$$TPR = \frac{TP}{TP + FN} \tag{4.13}$$

$$FPR = \frac{FP}{TN + FP} \tag{4.14}$$

where TP (True Positives) is the number of actual landslides correctly predicted as landslides, while FN (False Negatives) denotes the number of actual landslides incorrectly predicted as non-landslides. FP (False Positives) indicates the number of non-landslides incorrectly identified as landslides by the model, and TN (True Negatives) represents the number of non-landslide areas correctly predicted as non-landslides by the model.

The overall performance of a particular model was evaluated by determining the Area Under the Curve (AUC) from the Receiver Operating Characteristic (ROC) analysis. The AUC provides an indication of both the success and prediction rates of the models (Brenning, 2005). The success rate curve was computed by comparing the predictive model against the training landslide dataset. Conversely, the prediction rate curve was determined by comparing the generated susceptibility map with the validation landslide dataset. The AUC value ranges from 0.5 to 1, where values close to 1 indicate higher accuracy and better predictive power. On the other hand, values near 0.5 represents poor performance and less accurate in prediction (Pradhan, 2013).

The overall methodology for generating landslide susceptibility maps is shown in Figure 4.13.

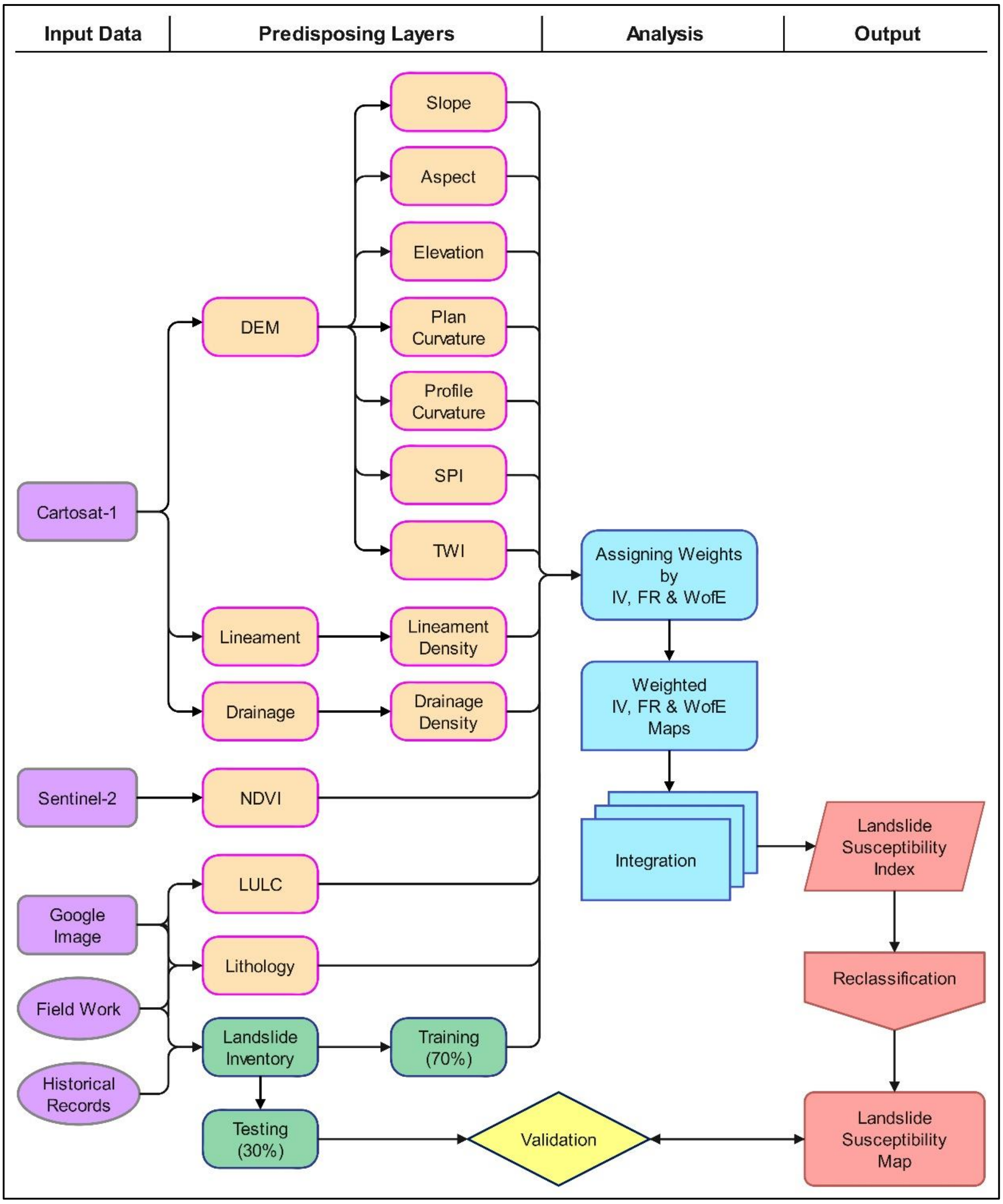

Fig. 4.13 *Flowchart of the Methodology for preparing Landslide Susceptibility Maps*

4.6 Summary

This chapter described the data and methodology employed for the quantitative assessment of landslide susceptibility for the Aizawl Municipal Area. Three bivariate statistical models, viz., Information Value (IV), Frequency Ratio (FR), and Weight of Evidence (WofE) were employed to generate the landslide susceptibility maps. A comprehensive inventory of 381 landslides was developed from historical records, satellite imagery, and field surveys. Twelve landslide conditioning factors, comprising topographical, geological, hydrological, and land cover variables were generated from satellite data such as Cartosat-1 and Sentinel-2 data. A 70% of the landslide data were used for model training and 30% for validation. Each of the three statistical models was used to calculate a Landslide Susceptibility Index (LSI) by assigning weights to the different classes within each factor map. The performance and reliability of the models were validated using the Receiver Operating Characteristic (ROC) curve and Area Under the Curve (AUC) analysis. The process involved comparing the generated susceptibility maps against both the training and validation landslide datasets to assess the success and prediction rates, respectively.

CHAPTER 5

VULNERABILITY AND RISK ASSESSMENTS

The methodologies for the assessments of landslide vulnerability and risk within the study area are presented in this chapter. The social vulnerability was evaluated based on a framework using the socio-economic and demographic characteristics from the 2011 Census data, while the physical vulnerability was assessed considering the buildings and road networks. These vulnerabilities were combined along with the landslide hazard map to generate the landslide risk index of the study area. This chapter is based on the work published in the *Journal of the Indian Society of Remote Sensing,* Vol. 53(12), 2025, pp. 4257–4279. https://doi.org/10.1007/s12524-025-02243-7.

5.1 Data

For the social vulnerability assessment, the demographic and socio-economic data derived from the Census of India (2011) were used which represented the most recent and reliable data available at the time of this research. Apart from these, data pertaining to the elderly population (65 years and above) were collected from the records maintained by the respective *Mizo Upa Pawl* (MUP) units (senior citizen organization) within the various local councils of the municipal area.

The data for the physical vulnerability assessment constitute the buildings and road networks which were extracted from manual digitization of high-resolution Google Earth® image. A total of 54,425 building polygons and 1,071 km length of road networks were delineated within the study area (Fig. 5.1). An extensive ground validation work was carried out to ensure the accuracy and reliability of these generated datasets. In addition, comprehensive interviews were conducted with the elected members of the local councils within the municipal area to cross-verify the results. Being the smallest administrative unit within the study area, the local council was used as the primary mapping unit in the social vulnerability assessment. In order to maintain consistency with the socio-economic and demographic data, the 76 local councils as recorded in the Census 2011 were used instead of the present 83 local councils.

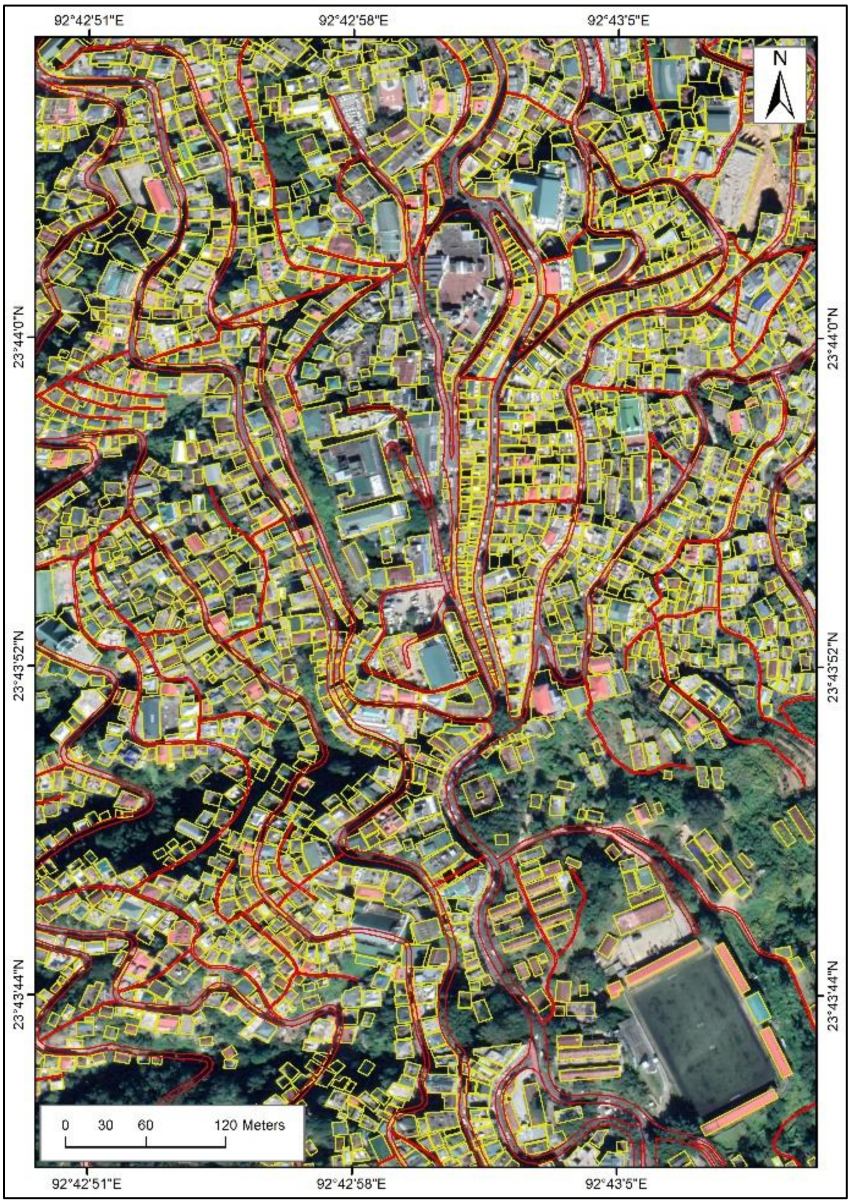

Fig. 5.1 *Building footprints (yellow) and roads (red) delineated from Google Image*

5.2 Social Vulnerability Assessment

Social vulnerability is conceptualized as a set of socio-economic factors influencing a population capacity to manage stress or adapt to changes (Blaikie et al., 1994; Birkmann, 2006b). It is defined as the susceptibility of individuals or communities to the harmful effects of hazardous processes, influenced by their demographic, geographical context, or social characteristics (Cutter et al., 2003; Yoon, 2012), and their capacity to manage, respond and recover from the adverse effects of the hazards (Eidsvig et al., 2014).

In the current research, the assessment of social vulnerability was conducted following a methodological framework adapted from Guillard-Gonçalves and Zêzere (2018), in which both the sensitivity and the lack of resilience of the resident population were considered. There are no strict standardized rules or guidelines regarding the number of variables or indicators for social vulnerability assessments, and various researchers have employed varying numbers. For instance, Clark et al. (1998) utilized 34 variables while Cutter et al. (2003) used 42 variables. In a study in Mexico, Murillo-Garcia et al. (2017) employed 14 indicators whereas Kaur et al. (2022) employed only 8 indicators in Sikkim. In the present study, the selection of indicators for both sensitivity and lack of resilience variables was based on their contextual relevance to the study area, data availability, and a thorough review of existing literatures. A total of 10 indicators, comprising 5 for sensitivity and 5 for lack of resilience, were chosen to represent the underlying socio-economic and demographic factors influencing the vulnerability of the residents. The indicators for both sensitivity and lack of resilience are shown in Tables 5.1 and 5.2, respectively.

Table 5.1 *Indicators for Sensitivity*

Sl. No.	Indicator	Description
1	CP	Children Population: Population under 6 years of age
2	EP	Elders Population: Population above 65 years of age
3	FP	Female Population: Number of Female Residents
4	IP	Illiterate Population: Number of populations who cannot read or write
5	DP	Population Density: Number of residents per square kilometre

Table 5.2 *Indicators for Lack of Resilience*

Sl. No.	Indicator	Description
1	RA	Rented Accommodation: Households living in rented houses
2	WE	Without Electricity: Households without electricity
3	WA	Without Assets: Households without basic assets
4	LI	Low Income: Households having low income/earnings
5	NW	Non-Workers: Number of persons without works/jobs

5.2.1 Sensitivity

Sensitivity is the degree to which particular population groups are disproportionately impacted by disasters owing to their inherent demographic and socio-economic characteristics (Birkmann, 2006b). The sensitivity index was calculated as the average of these five indicators, as given below:

$$Sensitivity = \frac{CP + EP + FP + IP + DP}{5} \tag{5.1}$$

where CP is the children population; EP denotes the elders population; FP represents the female population; IP is the illiterate population; and DP represents the population density. The maps of the indicators for sensitivity variable are shown in Figure 5.2.

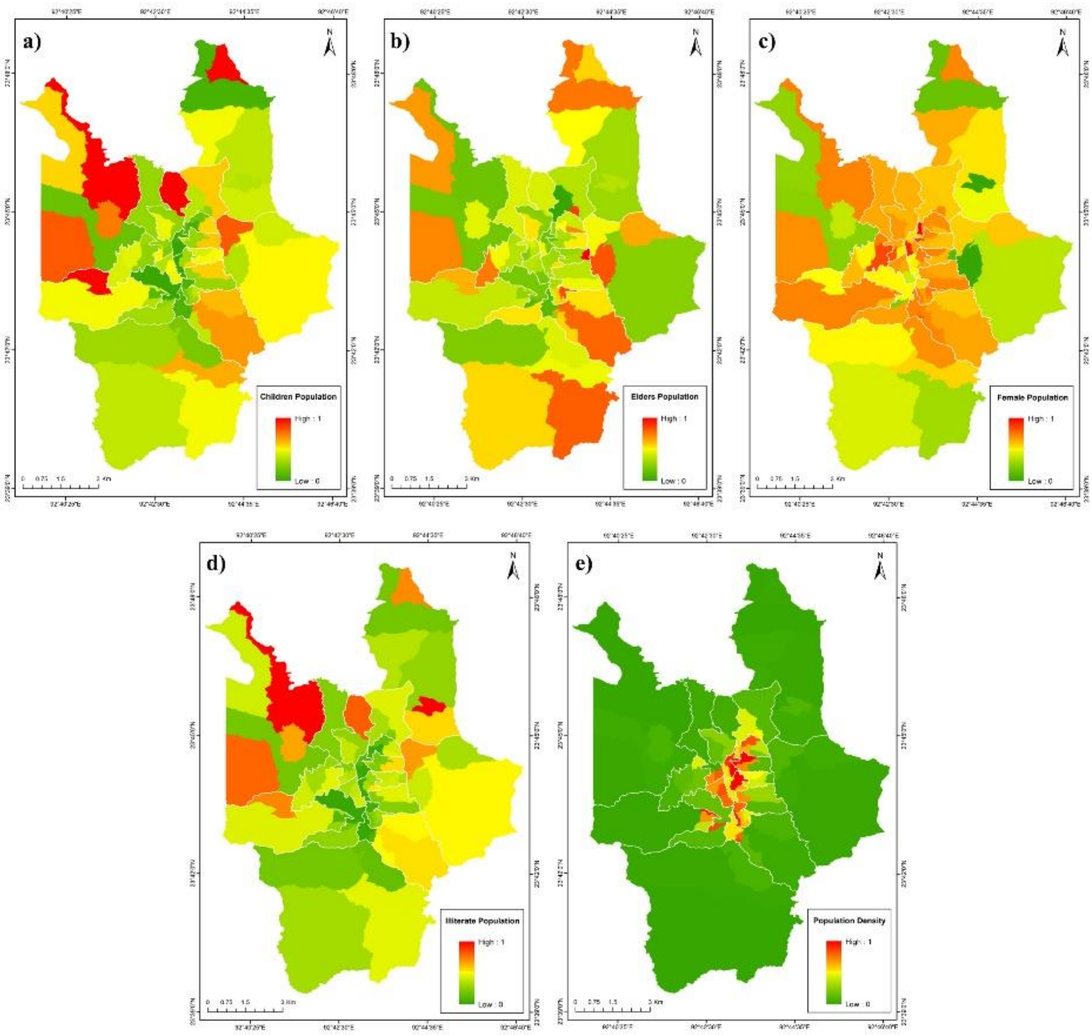

***Fig. 5.2** Indicators for Sensitivity. **a)** Children Population, **b)** Elders Population, **c)** Female Population, **d)** Illiterate Population, and **e)** Population Density*

Children below 6 years of age represent highly dependent population during disasters (Peek, 2008). They were considered vulnerable owing to their limited ability to rely on intuition or sense which made them less capable of protecting themselves or stay away from harm (Spencer & Thompson, 2024). The elders represent another dependent population due to declining physical functions and mobility, reduced adaptive capacity and health challenges (Cutter et al., 2000; Ngo, 2012). Women were considered as being mentally and physically weaker than men, apart from their caregiving responsibilities to children which made them more vulnerable during and after disasters (Blaikie et al., 1994; Fothergill, 1996). The literacy level is another important factor which is connected with access to resources and information in times of emergency. Illiterate people can face challenges to understand early warnings, recovery information and direction to evacuation routes (Brown et al., 2014). Higher population density implies greater exposure to hazards for a larger number of people in addition to increasing pressure on disaster response and recovery processes (Ehrlich et al., 2018).

5.2.2 Lack of Resilience

Lack of resilience refers to the inability of an individual or society to withstand or recover from the impacts of adverse effects due to their socio-economic status or present situation (Keck & Sakdapolrak, 2013; Vázquez-González et al., 2021). The lack of resilience index was determined as the mean or average of the five indicators, as given in the following equation:

$$Lack\ of\ Resilience = \frac{RA + WE + WA + LI + NW}{5} \tag{5.2}$$

where RA indicates the number of households residing in rented houses; WE denotes the number of households lacking electricity; WA represents the number of households without basic assets; LI is the number of households with low income or earnings; and NW indicates the number of persons without work or jobs. The maps of the lack of resilience indicators are shown in Figure 5.3.

Households living in rented accommodations were considered more vulnerable to displacement and economic insecurity during disasters due to lack of financial stability and social safety nets (Pardee, 2012; Lee & Van Zandt, 2019). Lack of electricity may

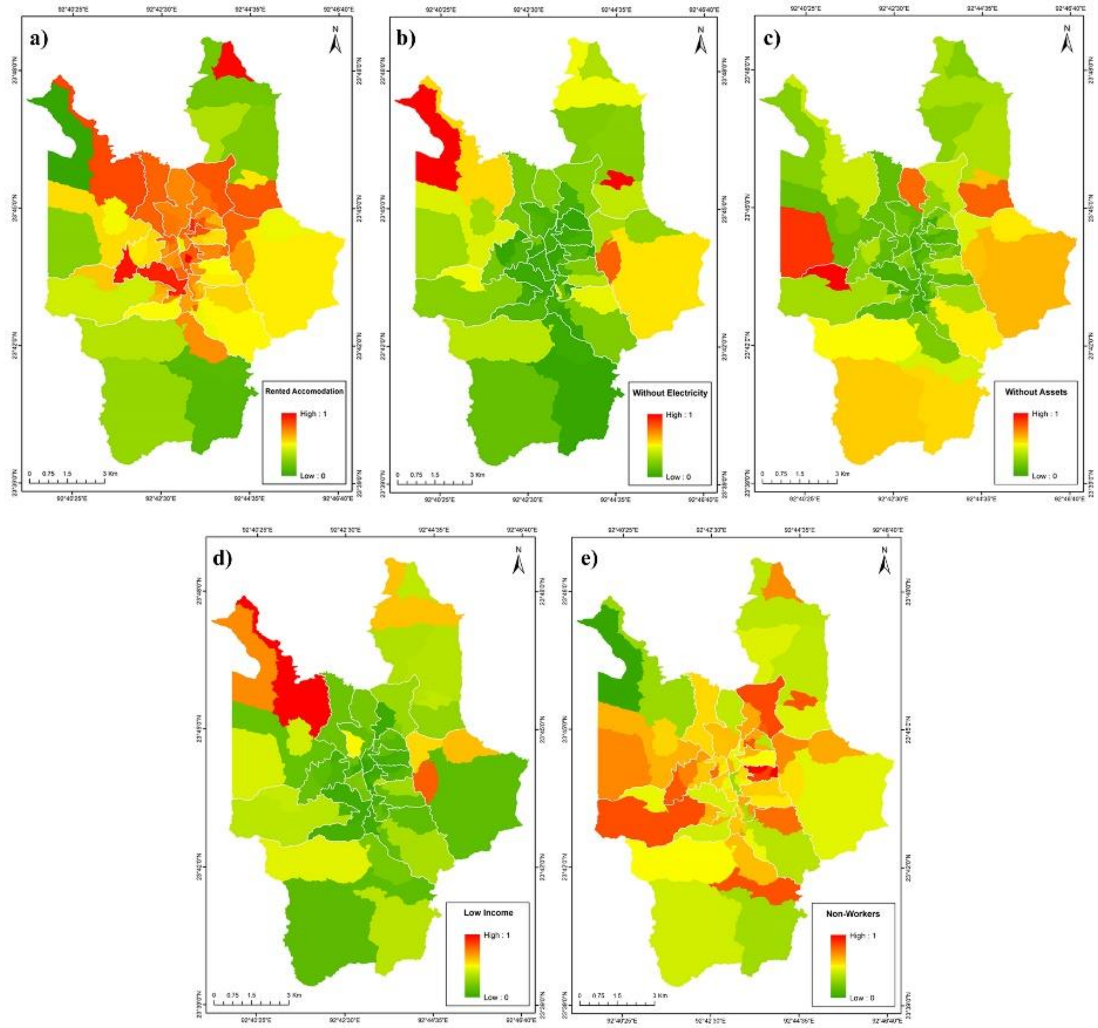

***Fig. 5.3** Indicators for Lack of Resilience. **a)** Rented Accommodation, **b)** Without Electricity, **c)** Without Assets, **d)** Low Income, and **e)** Non-Workers*

hinder access to essential services, communication and technology which are vital for effectively responding to the impacts of hazards (Sadath et al., 2017; Stock et al., 2023). Lack of basic household assets is an indicative of economic fragility that can weaken the capacity of a community to recover from a disaster (Zhang et al., 2020). The household income is another important factor that determine the vulnerability of a society. Low-income households have limited financial resources to invest in preparedness, recovery and mitigation measures for disasters, thereby elevating their vulnerability (Deria et al., 2020; Chowdhury & Parida, 2023). The ratio of non-workers to the population is an indicator of economic inactivity and dependency. Such high non-worker or unemployed numbers represent community constraints on economic contribution and adaptive capacities, thus raising vulnerability to hazards (Kablan et al., 2017).

5.2.3 Standardization and Social Vulnerability Index Calculation

Prior to conducting analyses, the values of each indicator were converted to their respective percentages. Subsequently, it was necessary to transform all indicators to a common, dimensionless scale in order to facilitate meaningful comparison and to minimize potential bias arising from differences in units of measurement. As all the selected indicators exhibit a consistent positive functional relationship, where higher values correspond to higher levels of vulnerability, they were standardized or normalized using a min-max technique to a scale of 0 to 1, using the following equation:

$$X_n = \frac{X - X_{min}}{X_{max} - X_{min}} \tag{5.3}$$

where X_n corresponds to the standardized value; X indicates the value of the indicator, and X_{max} and X_{min} represent the maximum and minimum values of the indicator, respectively. The maps showing sensitivity and lack of resilience variables are presented in Figures 5.4 (a and b).

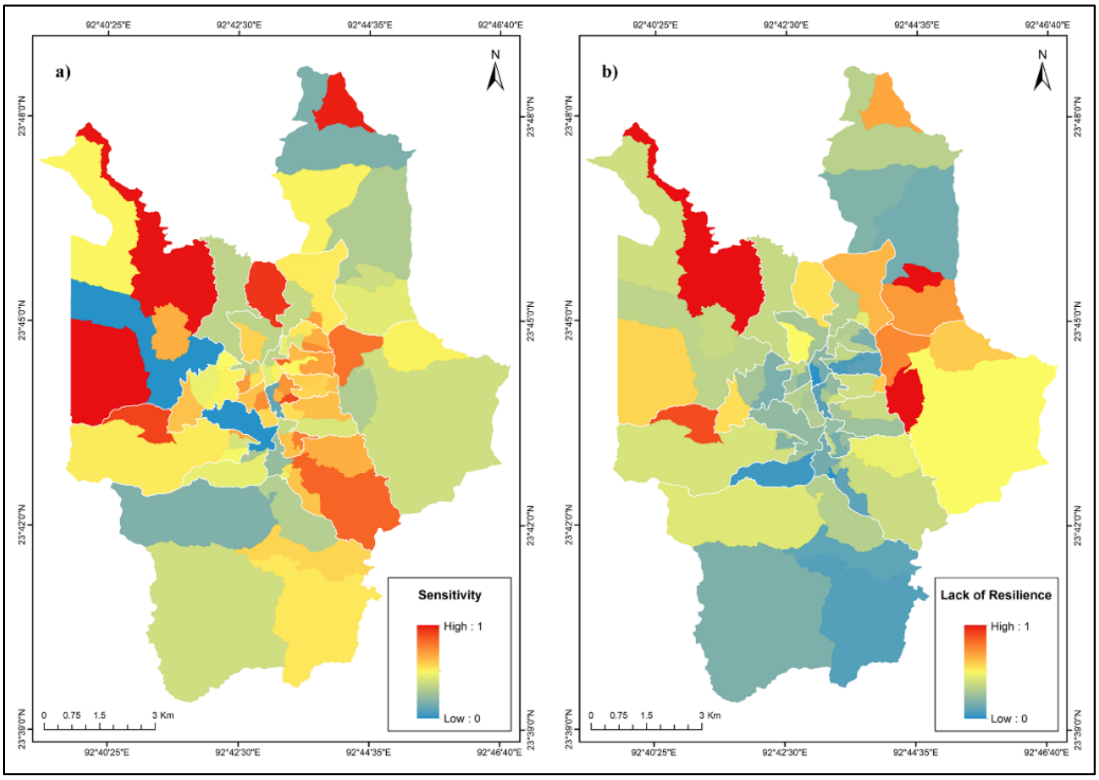

***Fig. 5.4** Maps showing **a)** Sensitivity and **b)** Lack of Resilience*

The social vulnerability index was then subsequently determined as the mean or average of the sensitivity of the population and lack of resilience using the equation (Guillard-Gonçalves & Zêzere, 2018):

$$Social\ Vulnerability\ Index = \frac{Sensitivity + Lack\ of\ Resilience}{2} \tag{5.4}$$

The resulting social vulnerability index values range between 0 and 1, where 0 and 1 represent the least and the maximum vulnerabilities, respectively. These values were reclassified into three classes using the natural break method, as shown in Table 5.3.

Table 5.3 *Social Vulnerability Class*

Social Vulnerability Value	Value of the Class	Social Vulnerability Level
0 – 0.31	1	Low
0.31 – 0.62	2	Moderate
0.62 – 1	3	High

5.3 Physical Vulnerability Assessment

Physical vulnerability is mainly concerned with the susceptibility of a structure, service, or infrastructure, to be damaged or disrupted resulting from a specific hazardous phenomenon. It is a functional relationship between the magnitude of a hazard and its potential impacts on the physical elements at risk, expressed on a scale from 0 (no loss) to 1 (total loss) (UNDRO, 1984). The assessment of physical vulnerability is guided by the principle of interaction between landslide intensity and the resistance of the built environment, such as buildings or roads (Li et al., 2010; Luo et al., 2023). When data on this aspect is unavailable, alternative methods or proxies are heuristically improvised (Ghosh et al., 2012; Sarkar, 2018; Ram & Gupta, 2022).

In the present study, the evaluation of physical vulnerability was undertaken focusing on the physical infrastructures, namely buildings and the road network present within the study area. The assessment involved assigning vulnerability scores to these elements on the basis of construction materials used and their degree of exposure to landslide hazards.

5.3.1 Classification of Buildings and Roads

The buildings within the study area were classified into three types based on their construction materials as Reinforced Cement Concrete (RCC), Semi-Reinforced Cement Concrete (Semi-RCC) and Assam-Type (AT) buildings. The RCC structures are built with cement concrete, steel reinforcement, and brick infill walls, and accounted for 54.82% (29,834 units) of the total building stock. The Semi-RCC buildings represent a hybrid construction type, which incorporate RCC components for columns and beams, while posts, wall panels, and roof trusses are made of wood. Infill walls are often made of asbestos cement tile or bamboo, with galvanized corrugated iron (GCI) sheets for roofing material. They constituted 19.65% (10,692 units) of the total buildings. The AT buildings exhibit similarity in construction pattern and materials with Semi-RCC buildings, but they are practically devoid of RCC materials. They comprised 25.54% (13,899 units) of the total buildings within the study area. The different building types within the study area are shown in Figure 5.5(a-c).

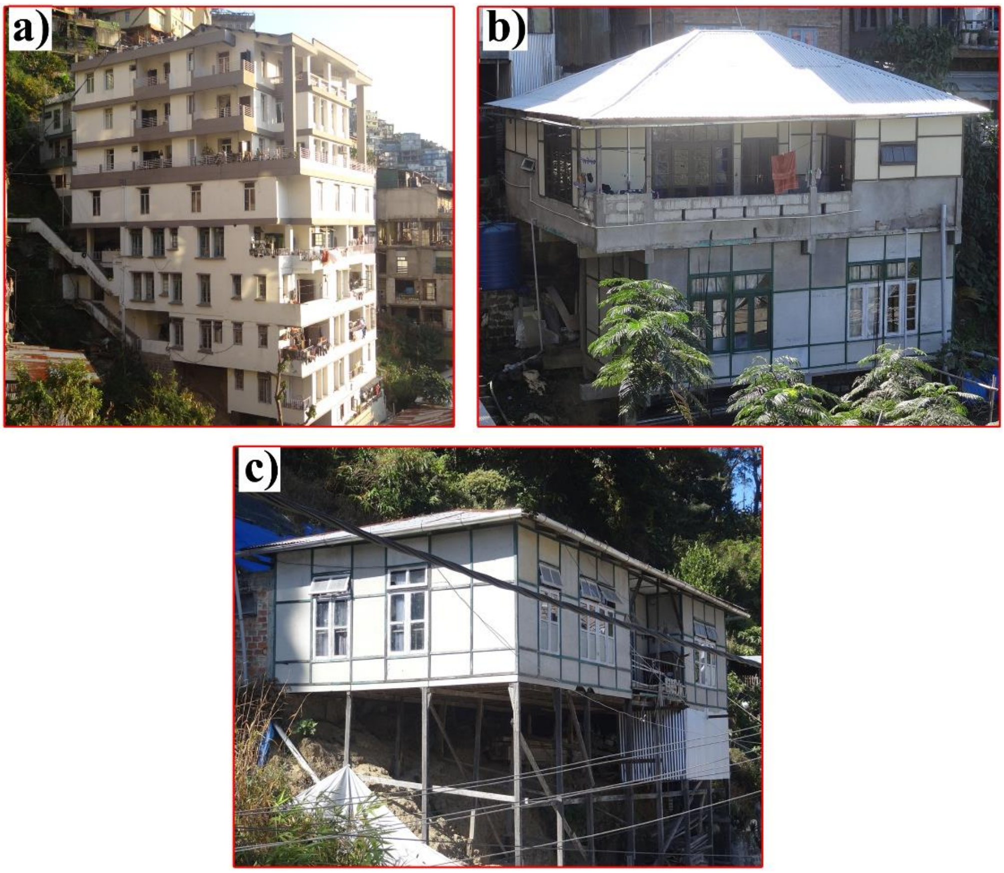

Fig. 5.5 *Typical buildings of the study area.* ***a)*** *RCC building,* ***b)*** *Semi-RCC building, and* ***c)*** *AT building*

Similarly, the road networks within the study area were also categorized into three types, namely metalled roads, bridges, and unmetalled roads. The metalled roads are constructed using a compacted base of boulders or stone chips, overlaid with bitumen or asphalt, and in some cases with reinforced cement concrete (RCC) surfaces to enhance durability and load-bearing capacity. The metalled roads represented 48.60% (520.89 km) of the total road network length. The bridges, although occupying a minimal proportion of the road network, play an important role in ensuring connectivity across streams and unstable terrains. They are relatively few in number and of short length, which are constructed using either reinforced cement concrete or steel/iron structures. They accounted for a minimal 0.04% (0.42 km) of the total length. As the name implies, the unmetalled roads are unpaved pathway lacking hard surfaces which are composed of sand, gravel, mud or bare earth materials. The unmetalled roads made up 51.36% (550.51 km) of the total road network length. The different road types within the study area are shown in Figure 5.6(a-c).

Fig. 5.6 *Different road types of the study area.* ***a)*** *Metalled Road,* ***b)*** *Bridge, and* ***c)*** *Unmetalled Road*

5.3.2 Assignment of Weights

In the study area, previous researches on the assessment of building damages due to landslides have not been conducted which results in the absence of empirical data on structural damage for reference. To overcome this limitation, the present assessment adopted the concept used by the Building Materials Technology Promotion Council (BMTPC, 2019), which utilizes the role of construction materials as a primary factor in influencing the potential damageability of buildings due to seismic events. Applying this principle, buildings within the study area, as per their construction materials, were used as indicators of their relative resistance to landslide impacts. Consequently, the RCC structures were regarded as the most resistant category, followed by Semi-RCC constructions, while the AT buildings were considered the least resistant. A similar principle was applied to road network, where the metalled roads were assumed to be more resilient and durable. The bridges, by virtue of their location, and materials used for their construction, were considered the second most resistant, while the unmetalled roads were ranked the least durable and resistant. Accordingly, numerical weights ranging from 1 to 3 were assigned to both building and road classes, with 3 denoting the lowest level of resistance and 1 representing the highest. Table 5.4 and 5.5 show the statistics of the building and road classes with the weights assigned.

Table 5.4 *Number of different building types and their weights*

Building Types	Number	Percent	Weight Assigned
RCC	29834	54.82	1
Semi-RCC	10692	19.65	2
Assam-Type	13899	25.54	3

Table 5.5 *Length of different road classes and their weights*

Road Types	Length (in Km)	Percent	Weight Assigned
Metalled	520.89	48.60	1
Bridges	0.42	0.04	2
Unmetalled	550.51	51.36	3

In actual practice, the temporal and magnitude probabilities of landslides are the prerequisites to convert landslide susceptibility maps into landslide hazard maps (Guzzetti et al., 1999; Fell et al., 2008; van Westen et al., 2008). However, owing to lack of data on these characteristics within the study area, the landslide susceptibility map was alternatively utilized as proxy for the hazard map in the present study. This approach was adopted by several researchers in their studies, especially in data-scarce situations (Kanungo et al., 2008; Guillard-Gonçalves & Zêzere, 2018; Arrogante-Funes et al., 2021; Singh et al., 2021; Ram & Gupta, 2022; Regmi & Agrawal, 2022; Sangeeta & Maheshwari, 2022). The landslide susceptibility map prepared using the Information Value (IV) method was selected for the present vulnerability and risk analyses. Accordingly, numerical weights were also assigned on a scale of 1 to 3, where the high hazard zone was given a weight of 3, the moderate hazard zone a weight of 2, and the low hazard was assigned a weight of 1.

5.3.3 GIS-based intersection and Vulnerability index calculation

The weighted buildings and road networks were spatially analyzed in a GIS environment by intersecting them with the landslide hazard map. This spatial intersection allowed the computation of different vulnerability scores based on the location of these assets within the different zones of the landslide hazard map. This process ensured that both the structural characteristics and the degree of exposure were simultaneously considered. A matrix-based approach (Fig. 5.7) was utilized for the qualitative cross-addition of the weights of the assets and the weights of the landslide hazard zones.

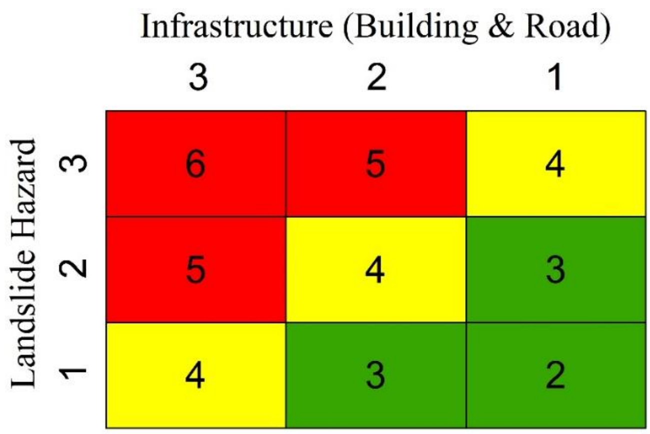

Fig. 5.7 Vulnerability Matrix. Red colour indicates high, yellow colour represents moderate, and green colour indicates low classes

The composite physical vulnerability index was then generated by summation of the vulnerability scores. It is represented mathematically as:

$$V_p = \begin{bmatrix} a_3 + b_3 & a_3 + b_2 & a_3 + b_1 \\ a_2 + b_3 & a_2 + b_2 & a_2 + b_1 \\ a_1 + b_3 & a_1 + b_2 & a_1 + b_1 \end{bmatrix} \tag{5.5}$$

where V_p indicates the physical vulnerability index; a is the landslide hazard zones; and b represents the classes of the assets. Substituting the values for a and b, we get:

$$V_p = \begin{bmatrix} 3+3 & 3+2 & 3+1 \\ 2+3 & 2+2 & 2+1 \\ 1+3 & 1+2 & 1+1 \end{bmatrix} = \begin{bmatrix} 6 & 5 & 4 \\ 5 & 4 & 3 \\ 4 & 3 & 2 \end{bmatrix} \tag{5.6}$$

The resulting physical vulnerability scores or values, ranging from 2 to 6, were then reclassified into three vulnerability levels, where the highest values (6 and 5) were designated as high vulnerability, while the intermediate score (4) was classified as moderate vulnerability. The lowest values (3 and 2) were grouped under low vulnerability in the vulnerability index, as shown in Table 5.6.

Table 5.6 *Physical Vulnerability Classes*

Physical Vulnerability Value	**Value of the Class**	**Physical Vulnerability Level**
2 and 3	1	Low
4	2	Moderate
5 and 6	3	High

5.4 Combination of Social and Physical Vulnerabilities

For the purpose of risk assessment, it is necessary to derive a single composite measure that reflects the overall vulnerability of the study area. To achieve this, the social and physical vulnerabilities were combined through direct summation of their respective class values (Tables 5.3 and 5.6), as expressed by the equation:

$$V = \sum V_s + V_p \tag{5.7}$$

where V represents the combined vulnerability; V_s is the social vulnerability; and V_p indicates the physical vulnerability. The resulting combined vulnerability values were also classified into three classes, as presented in Table 5.7.

Table 5.7 *Combined Vulnerability Class*

Combined Vulnerability Value	Value of the Class	Combined Vulnerability Class
2 - 3	1	Low
4	2	Moderate
5 - 6	3	High

5.5 Risk Assessment

Risk assessment constitutes the ultimate goal of landslide research which aimed at minimizing the adverse effects of landslide hazard (Guzzetti, 2005). It is a "function of the hazard and the vulnerability of exposed elements at risk" (Fell et al., 2005). Landslide risk is defined as "the expected number of lives lost, persons injured, damage to properties and disruption of economic activities due to landslides for a given area and a reference period" (Varnes, 1984). In the present study, landslide risk assessment was carried out using the following equation:

$$R = H \times V \tag{5.8}$$

where R is the landslide risk index; H indicates the landslide hazard; and V represents the combined vulnerability index.

The absence of detailed information on the distribution of occupants within individual buildings constrained the assessment of risk to human populations. As a result, the assessment was limited to the physical infrastructures, particularly to buildings and road networks. Furthermore, the lack of references for the construction or repair costs of these infrastructures within the study area prevented the incorporation of economic values into the risk assessment. These limitations imply that the present study reflects the risk of physical assets to landslides, while the potential risks on human lives and associated economic losses remain unquantified. The overall methodology for the vulnerability and risk assessments is presented in the Figure 5.8.

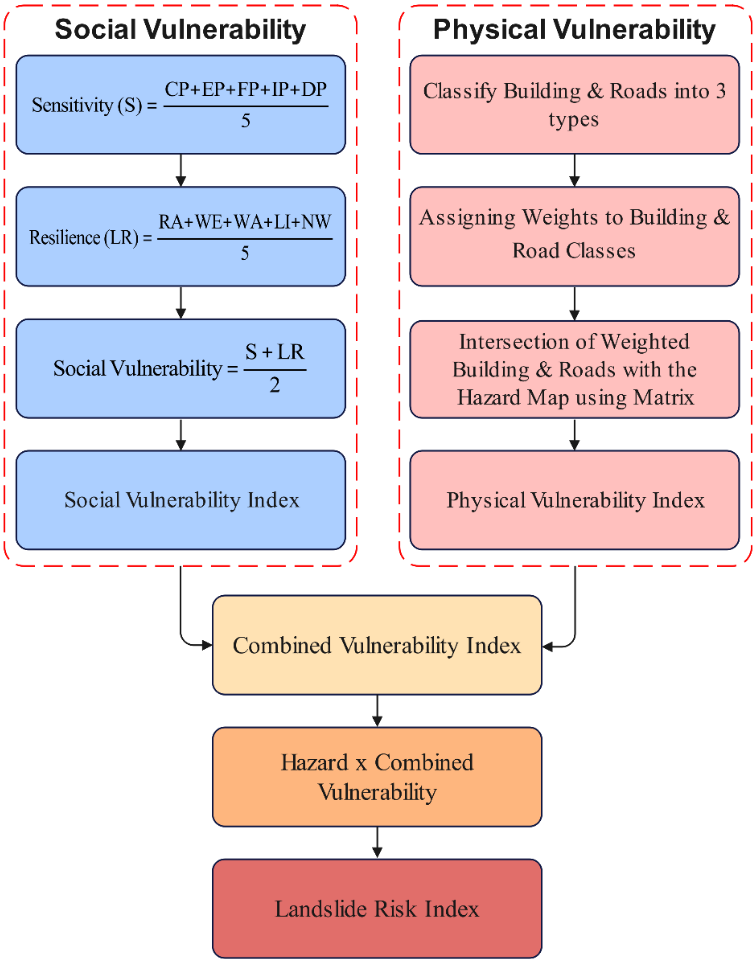

Fig. 5.8 *Methodological flowchart of the Landslide Risk Assessment*

5.6 Summary

This chapter presented an integrated assessment of landslide vulnerability and risk in the study area by combining both social and physical vulnerabilities. The social vulnerability was assessed using demographic and socio-economic indicators representing sensitivity and lack of resilience, while the physical vulnerability was evaluated based on the structural characteristics of buildings and road networks, and their exposures to landslide hazard. The landslide susceptibility map prepared using Information Value method was utilized as proxy for landslide hazard map. These individual components were standardized, spatially analyzed, and combined to generate a combined vulnerability index. Subsequently, the risk assessment was carried out by integrating the combined vulnerability with the landslide hazard map to generate the landslide risk index.

CHAPTER 6

RESULTS AND DISCUSSION

This chapter firstly presents the results of the landslide susceptibility mapping using the three bivariate statistical models. It provides the results and discussion on the spatial distribution of different susceptibility zones, the performance and validation of the models, and the spatial correlation of the various predisposing factors with landslide occurrences. It also describes the findings on the evaluations of the social and physical vulnerabilities, the combined vulnerability generated, and the generation of the final landslide risk index for the study area. The chapter also presents a comprehensive discussion on the analysis and results of the social, physical and combined vulnerabilities, along with those of the landslide risk index. The contents of this chapter are based on the works published in the *Himalayan Geology,* Vol. 45(1), 2024, pp. 39–57, and *Journal of the Indian Society of Remote Sensing,* Vol. 53(12), 2025, pp. 4257–4279. https://doi.org/10.1007/s12524-025-02243-7.

6.1 Landslide Susceptibility Map Generation and Classification

The landslide susceptibility maps for the Aizawl Municipal Area were generated from the Landslide Susceptibility Index (LSI) values derived from the IV, FR, and WofE equations. These maps were then classified into high, moderate, and low susceptibility zones based on the defined threshold values through the analysis of the respective success rate curves. The resulting landslide susceptibility maps are shown in Figures 6.1, 6.2 and 6.3. A more or less similarity in the general distribution pattern of these zones was observed across all the three models. The high susceptibility zone was more concentrated along the central longitudinal portion of the study area, with additional occurrences forming clusters in the eastern and western peripheries. Conversely, the moderate susceptibility zone is more uniformly distributed throughout the area, while the low susceptibility zone is predominantly found to stretch along the western part. At the same time, however, the areal extent of the different susceptibility zones showed certain variations among the models. In the IV model, an area of 20.46 km^2 (17.30%) was occupied by high susceptibility, the moderate zone extended over an area of 78.70

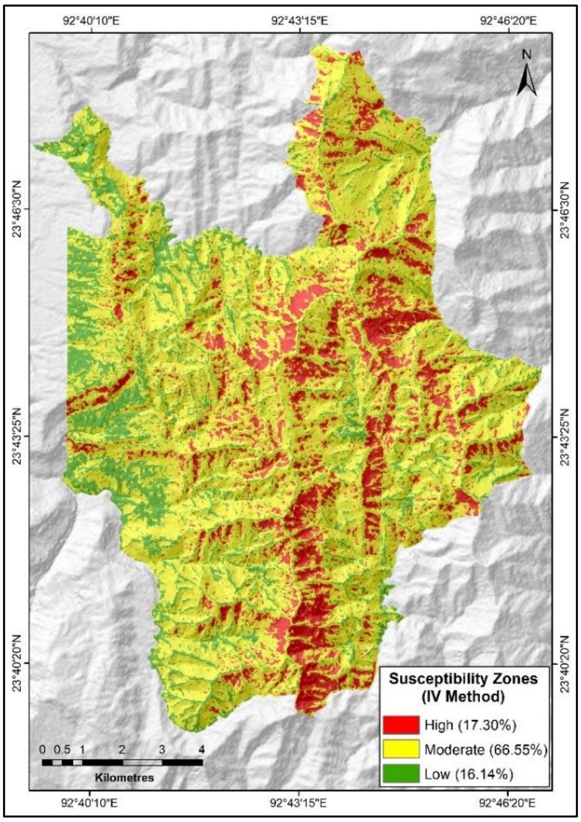

Fig. 6.1 *Landslide Susceptibility Map prepared using IV Method*

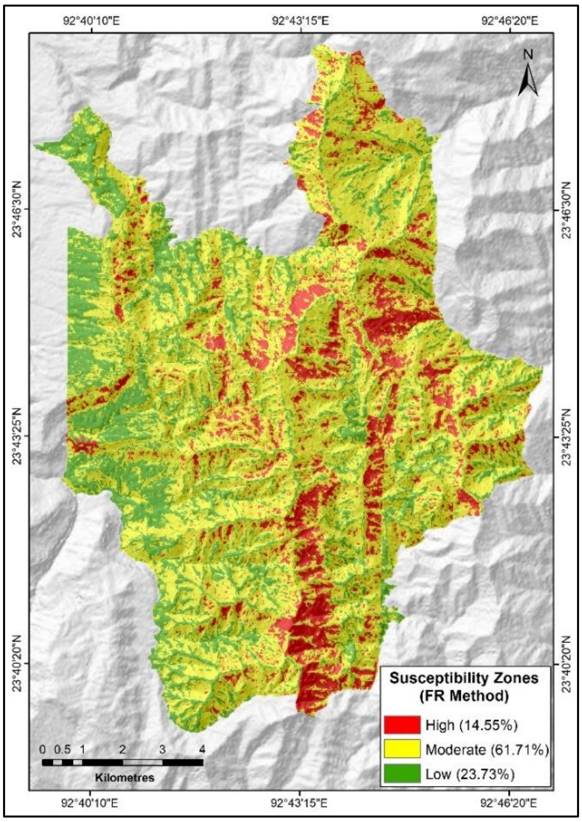

Fig. 6.2 *Landslide Susceptibility Map prepared using FR Method*

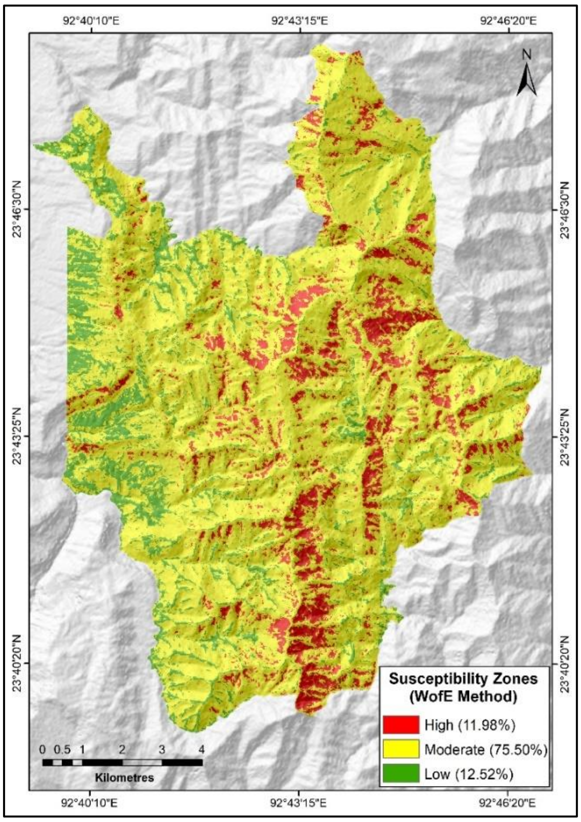

Fig.6.3 *Landslide Susceptibility Map prepared using WofE Method*

km^2 (66.55%), and the low susceptibility zone occupied 19.09 km^2 (16.14%). The FR model assigned 17.21 km^2 (14.56%) as high susceptibility zone, 72.97 km^2 (61.71%) as moderate zone, and 28.06 km^2 (23.73%) as low susceptibility zone. In the WofE model, the high susceptibility zone covered 14.17 km^2 (11.98%), the moderate zone dominated an area of 89.28 km^2 (75.50%), and the low susceptibility zone spanned over an area of 14.80 km^2 (12.52%). The statistics of the spatial distribution of the different susceptibility zones across the study area produced from the three models are shown in Table 6.1, and in Figure 6.4.

Table 6.1 *Area occupied by different susceptibility zones*

Susceptibility Zones	IV Model		FR Model		WofE Model	
	Area (km^2)	Area (%)	Area (km^2)	Area (%)	Area (km^2)	Area (%)
High	20.46	17.3	17.21	14.5	14.17	11.9
Moderate	78.7	66.5	72.97	61.7	89.28	75.5
Low	19.09	16.1	28.06	23.7	14.8	12.5

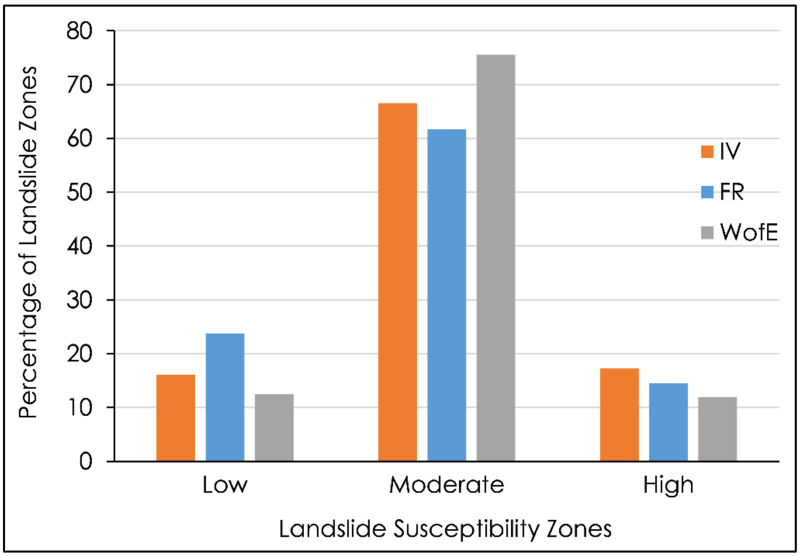

Fig. 6.4 *Area occupied by different landslide susceptibility zones*

In addition, the proportion of total landslides falling within each susceptibility zone also varied among the different models. In the case of IV model, it was observed that 65.72% of the total landslides were located in the high susceptibility zone, 33.05% in the moderate, and 1.23% in the low susceptibility zone (Fig. 6.5a). The distribution of landslides in the high, moderate and low susceptibility zones in FR model were found to be 61.03%, 36.81% and 2.16%, respectively (Fig. 6.5b). The high, moderate and low susceptibility zones of the WofE model respectively contained 57.13%, 42.02% and 0.85% of the total landslides (Fig. 6.5c).

6.2 Validation of Landslide Susceptibility Models

The generated landslide susceptibility maps were validated using the Area Under the Receiver Operating Characteristic curve (AUC-ROC) method. This validation involved calculating both the success rate, which represents how well the model fits the training data; and the prediction rate, which evaluates the model ability to predict landslides using the validation dataset. The results indicated more or less similarity in the performance of the three models evaluated. Among them, the WofE model achieved the highest success rate of 83.93%, followed closely by the IV model with 83.85% and the FR model with 83.72%. In terms of predictive ability, the WofE model again showed superior capability with a prediction rate of 83.79%, compared to 83.71% for the IV model, and 83.58% for the FR model. The validation results revealed that all

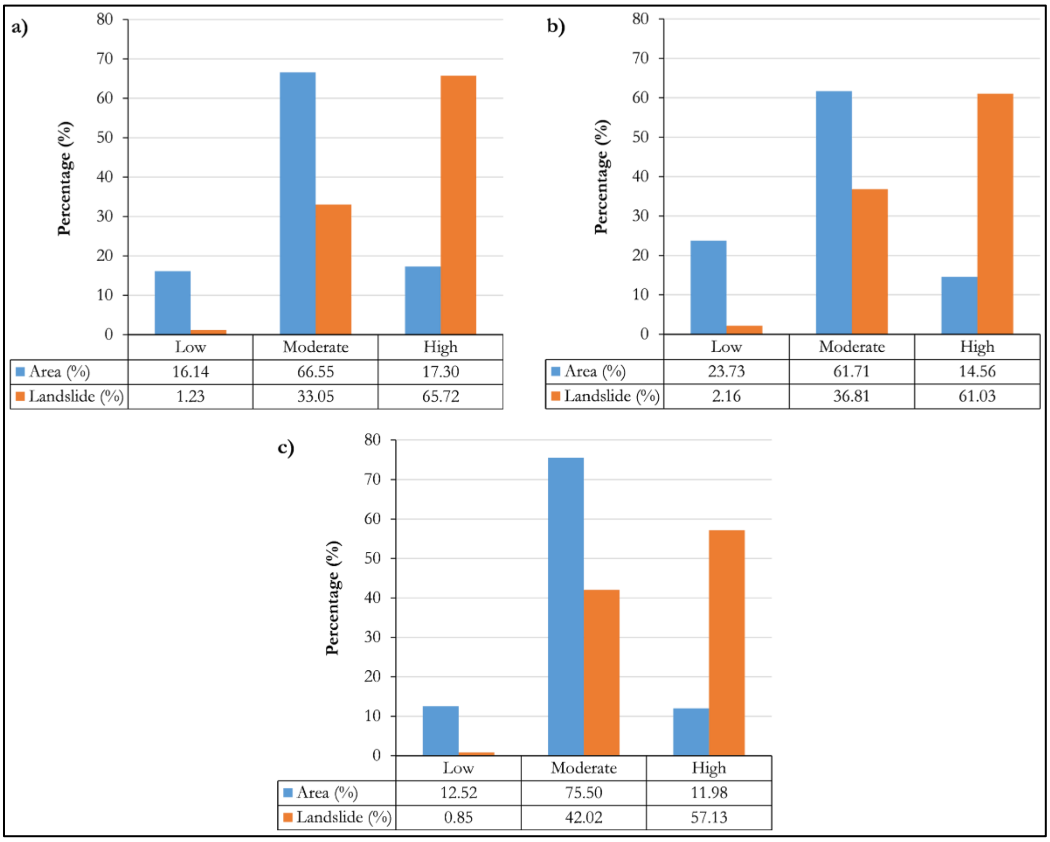

Fig. 6.5 *Distribution of landslides falling into different susceptibility zones.* ***a)*** *IV Method,* ***b)*** *FR Method, and* ***c)*** *WofE Method*

the three models performed satisfactorily in producing reliable landslide susceptibility maps for the study area. The success and prediction rate curves for the three models are shown in Figure 6.6 (a and b).

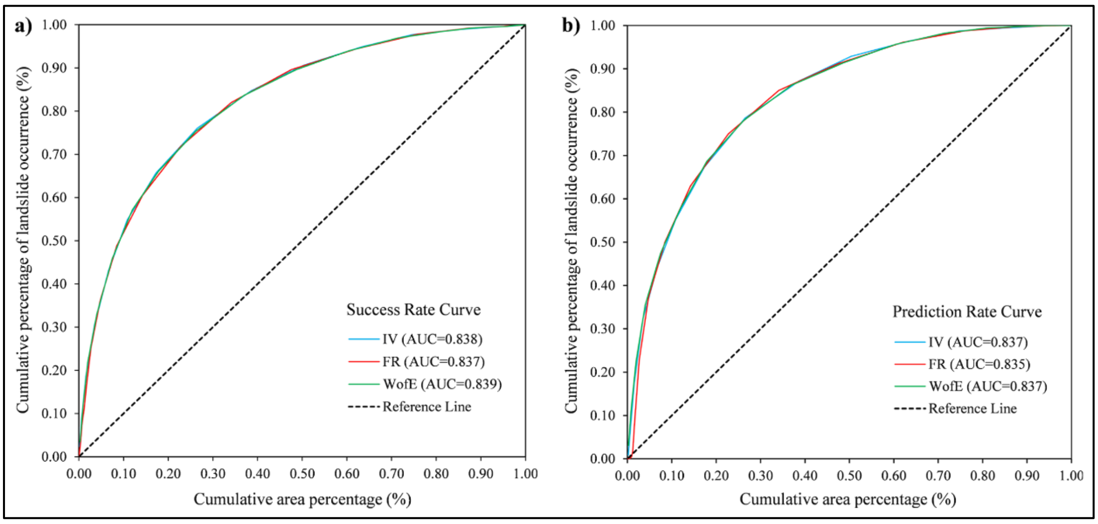

Fig. 6.6 *Curves showing* ***a)*** *Success rate of the landslide susceptibility models,* ***b)*** *Prediction rate of the landslide susceptibility models*

6.3 Spatial Correlation of Predisposing Factors and Landslide Occurrence

The analysis of spatial correlation between the twelve predisposing factors and landslide occurrences provided insights into their influence on slope instability within the study area. The classes of the predisposing factors were objectively assigned weights as per the IV, FR, and WofE methodologies. A more or less similarity of relative susceptibility was observed across all the three models for each class of the predisposing factors. This indicates that classes with higher or lower weight values generally correspond to higher or lower susceptibility, respectively. The spatial relationship between predisposing factors and landslide occurrence is determined by the respective weights of the models employed. In the IV and WofE models, positive weight values indicated a high correlation with landslide occurrence, while negative values suggested a low correlation. For the FR model, values greater than 1 indicated a strong positive correlation, and values less than 1 indicated a low correlation with landslide occurrence. The spatial associations between the various classes of predisposing factors and landslide occurrence, as derived from the three models, are presented in Table 6.2.

There existed certain variations in the spatial association of the predisposing factors and landslides. In the case of slope aspect, the east, south-east and south-facing slopes showed high or positive weight values across all the models, which indicated a higher probability of landslides. This is mainly attributed to more solar insolation in these classes which often led to increase in weathering and erosional processes (Fang & Guo, 2015). The remaining slope aspect classes including flatland showed no association with landslide occurrences. Some classes of drainage density exhibited a strong correlation with landslides. It was observed that the drainage density classes of 0.007–0.008 in the IV and WofE models, and 0.002–0.006 in the IV and FR models, particularly exhibited higher correlations with landslides compared to other classes. Contrary to a general belief that elevation may not directly influence landslides (Vakhshoori & Zare, 2016; Çellek, 2020; Sweta et al., 2022), a stronger relationship between landslides and higher elevations was observed in the present study. The elevation range of 800–1000 m showed higher weight values (0.33 for IV, 1.39 for FR, and 0.57 for WofE), followed by the highest elevation class, which exceeds 1000 m.

Table 6.2 *Spatial association of factor classes with landslides in the IV, FR & WofE models*

Factor	**Class**	**No. of pixel in class**	**Land-slide pixel in class**	**% of pixel in class**	**% of Land-slide pixel in class**	***IV***	***FR***	W^{+}	W^{-}	***C***
Aspect	Flat	3	0	0.00	0.00	0.00	0.00	0.00	0.00	0.00
	North	145033	957	12.25	9.10	-0.30	0.74	-0.30	0.04	-0.34
	North-East	156094	1347	13.19	12.81	-0.03	0.97	-0.03	0.00	-0.03
	East	167600	1650	14.16	15.69	0.10	1.11	0.10	-0.02	0.12
	South-East	136497	2128	11.53	20.23	0.56	1.75	0.57	-0.10	0.67
	South	123822	1416	10.46	13.46	0.25	1.29	0.25	-0.03	0.29
	South-West	158951	1000	13.43	9.51	-0.35	0.71	-0.35	0.04	-0.39
	West	161396	1345	13.63	12.79	-0.06	0.94	-0.06	0.01	-0.07
	North-West	134365	676	11.35	6.43	-0.57	0.57	-0.57	0.05	-0.63
Drainage Density	0.002 – 0.006	129450	1425	10.94	13.55	0.21	1.24	0.22	-0.03	0.25
	0.006 – 0.007	287930	2259	24.32	21.48	-0.12	0.88	-0.13	0.04	-0.16
	0.007 – 0.008	341978	3752	28.89	35.67	0.21	1.23	0.21	-0.10	0.31
	0.008 – 0.009	304591	2282	25.73	21.69	-0.17	0.84	-0.17	0.05	-0.23
	0.009 – 0.013	119812	801	10.12	7.61	-0.28	0.75	-0.29	0.03	-0.31
Elevation (m)	<300	11777	27	0.99	0.26	-1.35	0.26	-1.36	0.01	-1.37
	300 – 500	102918	390	8.69	3.71	-0.85	0.43	-0.86	0.05	-0.91
	500 – 800	482255	3029	40.74	28.80	-0.35	0.71	-0.35	0.19	-0.54
	800 – 1000	417959	5151	35.31	48.97	0.33	1.39	0.33	-0.24	0.57
	>1000	168852	1922	14.26	18.27	0.25	1.28	0.25	-0.05	0.30
Lineament Density	0 – 0.0011	179164	1672	15.14	15.90	0.05	1.05	0.05	-0.01	0.06
	0.0011 – 0.0018	336211	4279	28.40	40.68	0.36	1.43	0.36	-0.19	0.55
	0.0018 – 0.0026	334277	2298	28.24	21.85	-0.26	0.77	-0.26	0.09	-0.34
	0.0026 – 0.0034	233810	1763	19.75	16.76	-0.16	0.85	-0.17	0.04	-0.20
	0.0034 – 0.0053	100299	507	8.47	4.82	-0.56	0.57	-0.57	0.04	-0.61
Lithology	Sandstone	243505	1978	20.57	18.80	-0.09	0.91	-0.09	0.02	-0.11
	Shale + Sandstone	324688	1981	27.43	18.83	-0.38	0.69	-0.38	0.11	-0.49
	Shale + Siltstone	261907	1353	22.12	12.86	-0.54	0.58	-0.55	0.11	-0.66
	Shale	192897	4412	16.30	41.94	0.95	2.57	0.96	-0.37	1.33
	Siltstone + Shale	156395	759	13.21	7.22	-0.60	0.55	-0.61	0.07	-0.68
	Gravel, Sand + Silt	4369	36	0.37	0.34	-0.08	0.93	-0.08	0.00	-0.08
Land use/ Land cover	Built-up	249737	2247	21.10	21.36	0.01	1.01	0.01	0.00	0.02
	Barren land	15363	1117	1.30	10.62	2.10	8.18	2.17	-0.10	2.27
	Agri crop/Planta-tion	19742	55	1.67	0.52	-1.16	0.31	-1.17	0.01	-1.18
	Dense Forest	88736	142	7.50	1.35	-1.71	0.18	-1.72	0.06	-1.79
	Open Forest	286727	1060	24.22	10.08	-0.88	0.42	-0.88	0.17	-1.06

Table 6.2 (continued)

Factor	Class	No. of pixel in class	Land-slide pixel in class	% of pixel in class	% of Land-slide pixel in class	*IV*	*FR*	W^+	W^-	*C*
Land use/ Land cover	Forest Plantation	18963	49	1.60	0.47	-1.24	0.29	-1.24	0.01	-1.25
	Scrubland	360370	5489	30.44	52.18	0.54	1.71	0.55	-0.38	0.92
	Shifting Cultivation	98399	296	8.31	2.81	-1.08	0.34	-1.09	0.06	-1.15
	Bamboo Forest	45724	64	3.86	0.61	-1.85	0.16	-1.86	0.03	-1.89
NDVI	-0.25 – 0.33	68830	693	5.81	6.59	0.12	1.13	0.13	-0.01	0.13
	0.33 – 0.51	82473	1298	6.97	12.34	0.57	1.77	0.58	-0.06	0.64
	0.51 – 0.66	131651	2286	11.12	21.73	0.67	1.95	0.68	-0.13	0.81
	0.66 – 0.76	348296	2953	29.42	28.07	-0.05	0.95	-0.05	0.02	-0.07
	0.76 – 0.91	552511	3289	46.67	31.27	-0.40	0.67	-0.40	0.26	-0.66
Plan Curvature	-4.17 – -0.68	74777	1329	6.32	12.63	0.69	2.00	0.70	-0.07	0.77
	-0.68 – -0.23	267729	3634	22.62	34.55	0.42	1.53	0.43	-0.17	0.60
	-0.23 – 0.13	422157	3504	35.66	33.31	-0.07	0.93	-0.07	0.04	-0.11
	0.13 – 0.58	313989	1723	26.52	16.38	-0.48	0.62	-0.49	0.13	-0.62
	0.58 – 3.60	105109	329	8.88	3.13	-1.04	0.35	-1.05	0.06	-1.11
Profile Curvature	-3.74 – -0.68	64680	368	5.46	3.50	-0.45	0.64	-0.45	0.02	-0.47
	-0.68 – -0.21	254170	1856	21.47	17.64	-0.20	0.82	-0.20	0.05	-0.25
	-0.21 – 0.12	439602	3639	37.14	34.59	-0.07	0.93	-0.07	0.04	-0.11
	0.12 – 0.57	341772	3697	28.87	35.15	0.20	1.22	0.20	-0.09	0.29
	0.57 – 3.92	83537	959	7.06	9.12	0.26	1.29	0.26	-0.02	0.28
Slope (degree)	0 – 15	229691	458	19.40	4.35	-1.49	0.22	-1.50	0.17	-1.67
	15 – 25	453515	3146	38.31	29.91	-0.25	0.78	-0.25	0.13	-0.38
	25 – 35	390678	5334	33.00	50.71	0.43	1.54	0.43	-0.31	0.74
	35 – 45	98387	1443	8.31	13.72	0.50	1.65	0.51	-0.06	0.57
	>45	11490	138	0.97	1.31	0.30	1.35	0.30	0.00	0.31
SPI	-9.90 – -2.70	26380	155	2.23	1.47	-0.41	0.66	-0.42	0.01	-0.42
	-2.70 – -0.67	43546	62	3.68	0.59	-1.83	0.16	-1.84	0.03	-1.87
	-0.67 – 0.70	396448	1380	33.49	13.12	-0.94	0.39	-0.94	0.27	-1.21
	0.70 – 1.66	543454	5467	45.91	51.97	0.12	1.13	0.13	-0.12	0.25
	1.66 – 10.73	173933	3455	14.69	32.85	0.80	2.24	0.82	-0.24	1.06
TWI	1.94 – 4.56	262492	1532	22.17	14.56	-0.42	0.66	-0.42	0.09	-0.52
	4.56 – 5.80	496678	4725	41.96	44.92	0.07	1.07	0.07	-0.05	0.12
	5.80 – 7.38	324478	3169	27.41	30.13	0.09	1.10	0.10	-0.04	0.13
	7.38 – 10.13	78356	973	6.62	9.25	0.33	1.40	0.34	-0.03	0.37
	10.13 – 19.50	21757	120	1.84	1.14	-0.48	0.62	-0.48	0.01	-0.49

A surprising observation was the higher propensity for slope failure in lower lineament density classes compared to the higher density classes within the study area. This was probably due to the stronger effect of other factors since the concentration of higher lineament density was mostly observed in areas with low slope angles, where landslide activities are naturally less frequent or absent. Therefore, it can be inferred that lineament density have limited direct influence on landslide occurrences within the study area. Among the various lithological units, shale emerged as the most susceptible to landslides, as indicated by the higher and positive weight values in all the three models. Also, it is the only rock type that showed spatial association with landslide occurrence. The shale units within the study area were mostly soft, crumpled, highly-weathered, thinly bedded and friable which make them more prone to failure than the comparatively compact and massive sandstone unit (Mazumder et al., 2025). Other lithological classes, including gravel, sand, and silt found along major streams, showed no association with landslide occurrences.

In the case of LULC, a very strong correlation was observed between barren land and landslide, particularly in the FR model with a high value of 8.18. The weight values of barren land in the other two models were also relatively high compared to those of other classes. Within the study area, barren lands lacked vegetative cover, and are more exposed to weathering and erosion, which make them highly susceptible to slope failure (Sarkar et al., 1995; Gupta et al., 1999). Similarly, built-up areas and scrubland also showed higher probability of landslide occurrence. This is mainly attributed to extensive anthropogenic activities within the settlement area, and the absence of large trees whose root systems stabilize the slopes against erosion and landslides (Reubens et al., 2007; Cohen & Schwarz, 2017). An indirect relationship between NDVI and landslide occurrence was observed in the present study. It is known that the higher NDVI values corresponds to an increase in vegetative cover density. Positive or higher weight values were consistently observed for lower NDVI classes in all the three models, indicating that landslides were more prevalent in areas with sparse vegetation. Conversely, highly vegetated areas represented by higher NDVI values showed negative spatial associations which further suggested that vegetation provides natural anchorage and stability to slope materials (Dorairaj & Osman, 2021).

The study area was characterized by the presence of several convex and concave slopes, both oriented in transverse and longitudinal directions. These are known respectively as profile and plan curvatures. Both the convex slopes in the profile curvature class and the concave slopes in the plan curvature class in the study area were identified as relatively favourable for landslide occurrences, as evidenced by the positive weight values across all the models. Conversely, the convex plan curvatures and concave profile curvatures showed no association with landslides, and were therefore, free from landslide activities. A similar pattern was also observed from other studies in the Himalayan region (Devkota et al., 2013; Guri et al., 2015; Kumar & Gupta, 2021).

The slope angle factor analysis indicated that landslide occurrences were more frequent within specific slope classes. The 35–45° slope angle showed the highest number of landslide occurrences in both the IV and FR models, while the 25–35° slope angle was the most associated with landslides in the WofE model. Interestingly, the highest slope class, i.e., >45° showed no spatial association with landslides. This pattern was observed in some studies in which landslide activity increases to a certain extent as the slope angle increases, and gradually decreases till no further activity was observed in the highest slope class (Jaafari et al., 2014; Wang et al., 2015; Vakhshoori & Zare, 2016; Wang et al., 2019b). Within the study area, the maximum slope class was mostly characterized by escarpments and cliffs where the weathered materials fell off quickly. Besides, the cliffs and escarpments were generally composed of hard rocky outcrops which were resistant to weathering and erosional processes. Therefore, the highest slope class showed negative spatial association with landslides.

The SPI represented the erosive power of water flow whose higher value classes showed strong correlation with increased landslide activity. It was observed that the highest class range of SPI (1.66–10.73) recorded maximum weight values across all the three models (0.80 for IV, 2.24 for FR, and 1.06 for WofE). This suggested a positive influence of SPI on landslide occurrences. The lower classes, on the other hand, showed no association with landslide. The TWI is another important factor influencing landslide occurrences. The TWI class range of 7.38–10.13 exhibited a strong correlation with landslides, showing high weight values of 0.33 for IV, 1.40 for FR, and 0.37 for WofE. However, both the highest and lowest TWI classes showed no significant association with landslide occurrence.

From the foregoing discussion, a more or less similarity on the spatial association of the predisposing factors and landslide occurrences in all the three models can be observed. With the exception of drainage density, profile curvature and slope factors, the remaining factors uniformly have identical highest weight values in their respective classes in all the three models. However, a closer and more detailed analysis of the relationships between landslides and individual factor classes showed some variations in their relative influence on slope instability within the study area. The LULC factor indicated a strong positive correlation with landslide occurrences, as all the classes considered susceptible consistently showed high or positive weight values across all the three models. A similar correlation can be observed among the classes of lithology, SPI, NDVI, slope and TWI factors, and thus they may be considered the most significant and influential factors in influencing mass movements. In contrast, factors such as aspect, lineament density, and drainage density were found to have a relatively little influence on landslide susceptibility within the study area.

6.4 Social Vulnerability

The social vulnerability was assessed based on the existing framework using the socio-economic and demographic data obtained from the Census 2011 which were divided into sensitivity and lack of resilience variables. The results of this assessment revealed a distinct spatial distribution of social vulnerability across the study area. The highest social vulnerability level, indicated by index values between 0.62 and 1, extended over 16.27 km^2, representing 13.75% of the total study area. The highest social vulnerability class was mostly observed in the peripheral areas, comprising seven local councils, with one local council located in the central area. A moderate social vulnerability class, having index values ranging from 0.31 to 0.62, stretched over 43.73 km^2 with 36.98% of the total study area. This particular class was distributed across the middle sections of the study area, and covered 37 local councils. The lowest vulnerability level, with index values from 0 to 0.31, dominated the municipal area which spanned over an area of 58.25 km^2 which is 49.26% of the total study area. This low vulnerability was mainly concentrated in the southern and northern portions, including the core of the area covering 31 local councils. The social vulnerability map and the local council-wise distribution of the different classes are shown in Figure 6.7 and Table 6.3, respectively.

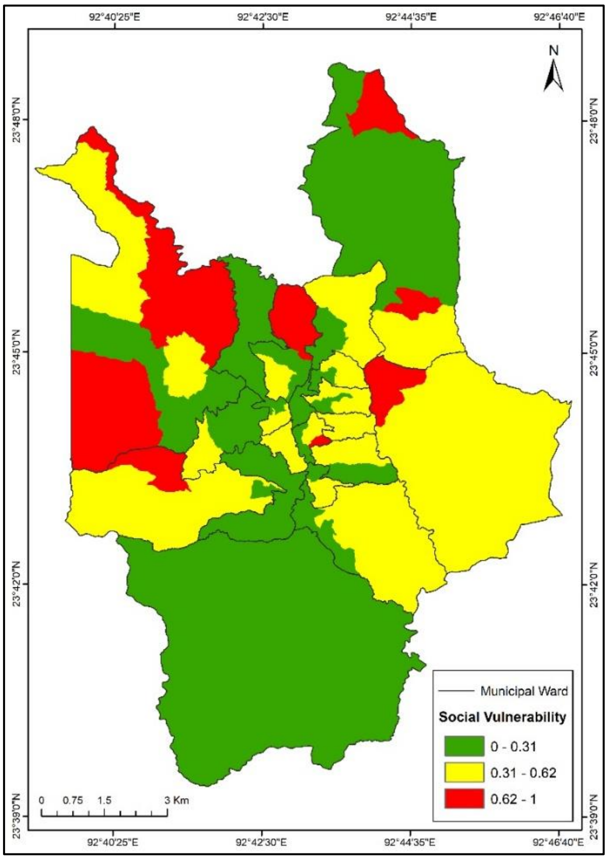

Fig. 6.7 *Social Vulnerability Map of the Study Area*

Table 6.3 *Distribution of social vulnerability class across various local councils*

Sl. No.	Class	Local Councils
1	Low	Bungkawn, Chaltlang, Chanmari, Chanmari West, Chawnpui, College Veng, Dawrpui, Durtlang, Durtlang Leitan, Durtlang Vengthar, Electric Veng, Hlimen, Khatla, Khatla South, Kulikawn, Laipuitlang, Luangmual, Melthum, Mission Veng, Mission Vengthlang, Ramhlun Venglai, Ramthar Veng, Saikhamakawn, Thakthing, Tlangnuam, Vaivakawn, Venghlui, Venghnuai, Zarkawt, Zonuam, Zotlang
2	Moderate	Aizawl Venglai, Armed Veng, Armed Veng South, Bawngkawn, Bawngkawn South, Bethlehem Veng, Bethlehem Vengthlang, Bungkawn Vengthar, Chawlhhmun, Chhinga Veng, Chite, Dam Veng, Dawrpui Vengthar, Dinthar, Falkland, Govt Complex, Hunthar Veng, ITI Veng, Kanaan Veng, Maubawk, Nursery, Ramhlun North, Ramhlun South, Ramhlun Sports Complex, Ramhlun Vengthar, Ramthar North, Republic Veng, Republic Vengthlang, Sakawrtuichhun, Salem Veng, Sarawn Veng, Tuikual North, Tuikual South, Upper Republic, Zemabawk, Zemabawk North, Zuangtui
3	High	Edenthar, Lawipu, Muanna Veng, Rangvamual, Selesih, Thuampui, Tanhril, Tuithiang

The averaging of the 10 indicators of the sensitivity and lack of resilience variables was portrayed in the form of social vulnerability of the residents of the Aizawl municipal area. The reasons for the elevated vulnerability in the highest class could be due to the fact that this class was characterized by the convergence of high sensitivity and lack of resilience scores. This included higher concentrations of low-income households, non-workers and rented accommodations including high dependency ratios. This resulted in the limited access to resources and economic insecurity which exacerbate the vulnerability to various hazards and impedes coping mechanisms for the residents (Adger, 1999; Biswas & Nautiyal, 2023).

The moderate vulnerability class was characterized by a composite interaction of vulnerabilities. For instance, while the areas falling within this class may exhibit certain degree of economic stability, other indicators such as population density and the high percentage of households living in rented accommodations still contribute to their vulnerability. The areas within the low vulnerability level have shown better resilience due to higher income levels, more robust infrastructure and improved socio-economic conditions. Consequently, these areas have higher literacy rates, better access to services and other opportunities (Saitluanga, 2018) which can help in mitigating the adverse consequences of disasters.

The contributions of all the indicators to the overall social vulnerability of the study area was further analyzed which provided important insights into the drivers of social vulnerability within the study area, and is shown in Figure 6.8. The analysis revealed that the female population was the most significant contributor, accounting for 19.56% of the overall social vulnerability. This indicated that gender-related vulnerabilities were the major influence of the social vulnerability. Within the study area, gender disparity is negligible, with women enjoying relatively equal opportunities. They contributed significantly to household income and are dominating in both the entrepreneurship and government employment sectors (Guha & Adak, 2014; Lalremruati & Ramaswamy, 2014). However, their perceived inherent physical and mental frailties, with caregiving responsibilities, still rendered them more vulnerable. Another important contributor was households living in rented accommodations, with 17.72% to the overall social vulnerability. Renters within the study area were composed of a mix of the indigenous Mizos from other parts of the state, and those non-Mizos who tempora-

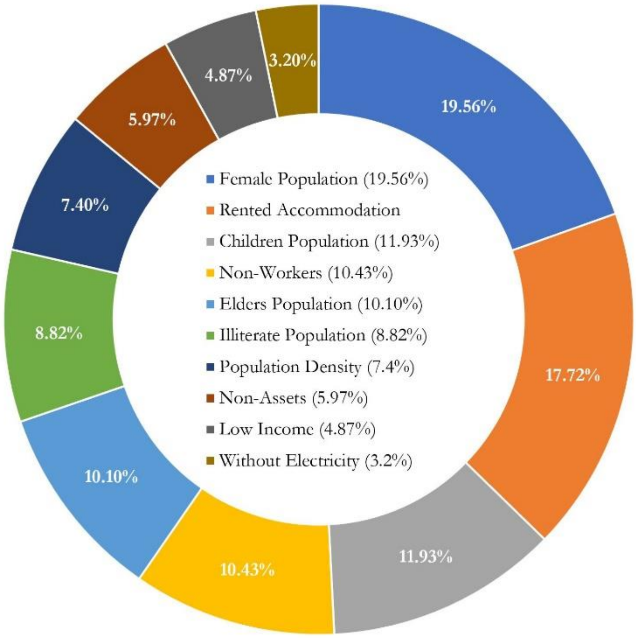

Fig. 6.8 *Contributions of the indicators to the Social Vulnerability*

rily residing from other parts of the country and neighbouring countries as well. Demographic indicators played a considerable role in shaping social vulnerability. The children population (under 6 years) contributed to 11.93%, non-workers (persons without work/jobs) contributed to 10.44%, and the elders population (above 65 years) contributed to 10.10% of the total social vulnerability. These groups of people collectively led to higher dependency ratios, limited economic participation, and reduced resilience capacities, which further necessitated targeted interventions.

Moderate contributions to social vulnerability were observed from illiteracy (8.82%), population density (7.40%), and households without assets (5.97%) indicators. Illiteracy restricts access to information and job opportunities, while high population density in urban areas can lead to resource scarcity and overburdened infrastructure. The absence of household assets reflects economic fragility, which directly reduces the ability to cope with disasters (Vatsa, 2004). The least contributing indicators to the overall social vulnerability were households with low income (4.87%) and those without electricity (3.19%). Although their influence on the total social vulnerability index was relatively lower in this assessment, these figures indicated the presence of urban poor sections within the municipality that warrant sustained attention for long-term development efforts.

6.5 Physical Vulnerability

In the present study, the assessment of physical vulnerability focused on the built infrastructures, namely buildings and road networks within the study area considering the materials used for construction and their exposure to landslide intensities. The resulting physical vulnerability map is shown in Figure 6.9.

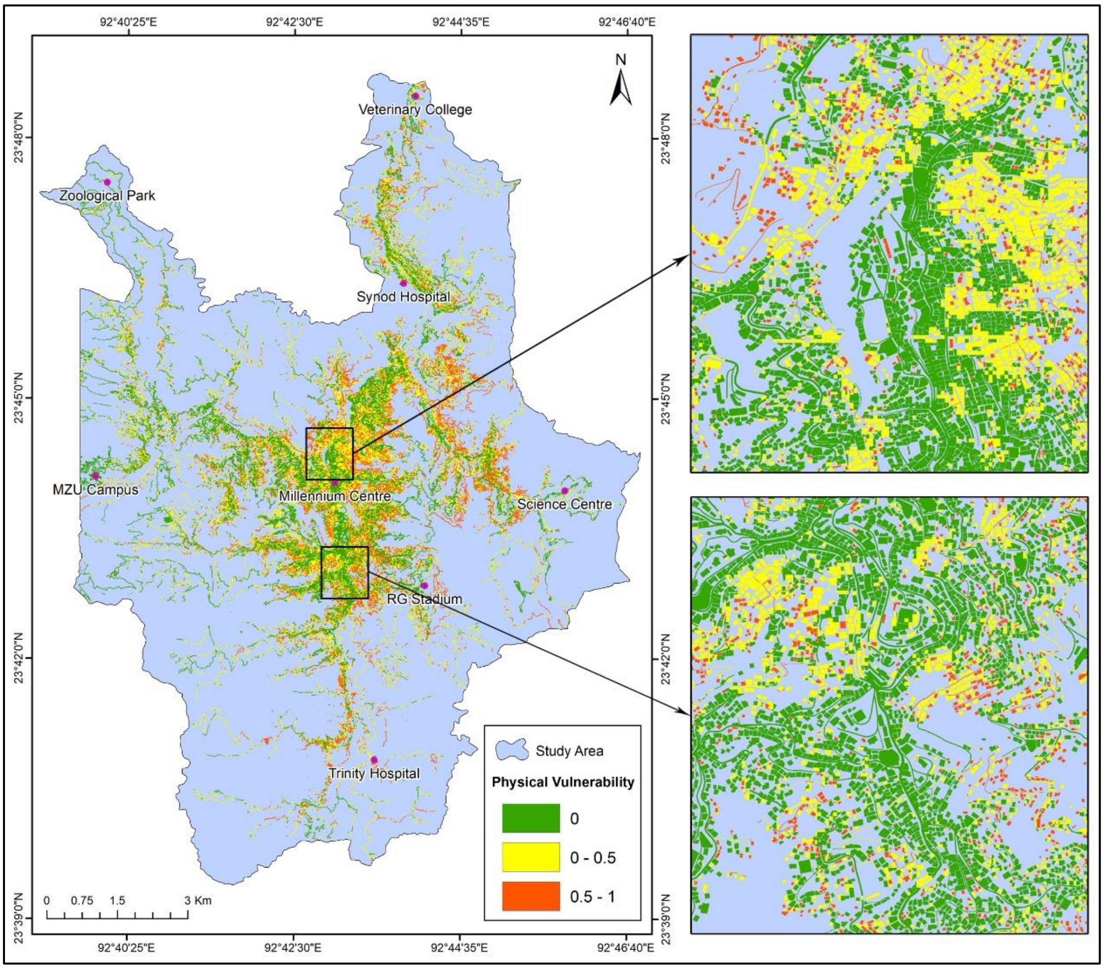

Fig. 6.9 *Physical Vulnerability Map of the Study Area*

Among the building types, the RCC structures showed the highest resilience, with the majority of their area comprising of 317.72 ha (57.8% of the total building area) falling under the low vulnerability class, and a considerable portion of 89.74 ha (16.32%) located under the moderate vulnerability class. The Semi-RCC buildings were distributed across all the vulnerability classes, with an area of 6.62 ha (1.2%), 52.84 ha (9.61%) and 20.91 ha (3.80%) situated under the low, moderate and high vulnerability classes, respectively. The AT buildings, regarded to be the least resistant, predominantly contributed to the high vulnerability class with an area of 56.75 ha (10.32%), and a smaller portion of 5.15 ha area (0.94%) located in the moderate vulnerability class. Table 6.4 shows the distribution of buildings across the different vulnerability classes.

Table 6.4 *Distribution of building vulnerability class*

Sl. No.	Building Class	Vulnerability	Area in hectare	Area in %
1	RCC	Low	317.72	57.8
		Moderate	89.74	16.32
2	Semi-RCC	Low	6.62	1.2
		Moderate	52.84	9.61
		High	20.91	3.8
3	Assam-Type	Moderate	5.15	0.94
		High	56.75	10.32
Total			**549.72**	**100**

In the case of road network, metalled roads exhibited high resilience, dominating the low vulnerability zone with 396.10 km which is 36.95% of the total network length. A total length of 126.04 km (11.76%) was under the moderate vulnerability class. The unmetalled roads, due to their inherent fragility, dominated the high vulnerability class with 472.97 km, comprising 44.13% of the total network length. A considerable length of 76.36 km (7.12%) was within the moderate vulnerability class. The bridges which constituted only a small fraction of the total road length, were distributed across all the vulnerability classes. A minimal length of 0.12 km (0.01%) was located within the low vulnerability class. A small stretch of 0.22 km, constituting 0.02% of the total network length was under the moderate class while the high vulnerability class accommodated only 0.05 km length. The distribution of the road classes across the different vulnerability zones are shown in Table 6.5.

The classification of physical vulnerability was derived from the GIS-based analysis of the characteristics of the infrastructure and the landslide hazard zones using the matrix-based approach. The results showed that when infrastructure with the lowest weight (RCC buildings and metalled roads) intersected with the highest hazard zone, the maximum vulnerability score attained was 4, which corresponds to the moderate

Table 6.5 *Distribution of road vulnerability class*

Sl. No.	Road Class	Vulnerability	Length in km	Length in %
1	Metalled	Low	396.10	36.95
		Moderate	126.04	11.76
2	Bridge	Low	0.12	0.01
		Moderate	0.22	0.02
		High	0.05	0.00
3	Unmetalled	Moderate	76.36	7.12
		High	472.97	44.13
Total			**1071.86**	**100**

vulnerability class. Since the high vulnerability class was defined by scores of 5 and 6, the RCC buildings and metalled roads did not fall into this category even when located within the high hazard zone. This outcome indicated their inherent structural resilience, which minimized their vulnerability to severe structural damage from landslide impact. Conversely, when infrastructures with the highest weights (AT buildings and unmetalled roads) intersected with the lowest weight of landslide hazard zone, the matrix produced a minimum vulnerability score of 4 which is the moderate class. The analysis further allowed these infrastructures to attain higher scores of 5 or 6, which is the highest vulnerability class. Consequently, these scores allocated the AT buildings and unmetalled roads either in the high or moderate vulnerability classes, but not in the low class even when they were in the low hazard zone. This indicated that these infrastructures were intrinsically vulnerable to damage or failure to landslide impacts owing to their inherent structural fragility and the absence of reinforced materials.

The present study highlighted the importance of construction materials and structural integrity in determining the physical vulnerability of buildings and roads to landslide hazard. The RCC buildings and the metalled roads, constructed respectively with cement concrete and steel reinforcement, and hard rocks with bitumen or asphalt, have the highest resistance. The combination of cement concrete and steel structure reinforcement used in RCC buildings gives the structure more tensile strength as well as compressive strength, and enhances the overall structural integrity (Reynolds et al., 2007), and are therefore, generally less vulnerable to landslides (Cardoso et al., 2023; Shi et al., 2024). It was observed that RCC buildings suffered slight damage from landslide impact pressure below 35 kPa while the non-RCC buildings were found to be completely destroyed at pressure above 30 kPa (Kang & Kim, 2016). Likewise, the metalled roads have better drainage and structural support, and reduce the risk of landslides compared to unmetalled roads which are considered to be more susceptible to erosion and instability. Thus, the design and the materials used in RCC buildings and metalled roads contribute to their enhanced durability against landslide phenomena.

Most of the bridges, although very few in number and small-length within the study area were constructed across small streams perpendicular to the slope of the terrain. The inherent instability nature of the slope coupled with heavy rainfall and unstable foundations were significant factors for their vulnerability to landslides. In addition, the foundations on which the abutments were constructed are often subjected to frequent toe-erosion due to torrential flow of water, and were rendered vulnerable. The unmetalled roads were considered the least resistant owing to direct exposure to landslide hazard without any reinforced materials on the surface. Further, they were usually devoid of proper drainage which can facilitate efficient surface runoff. This often results in surface water accumulation and subsequent seepage underneath. This rendered them relatively more vulnerable to failure, particularly along the hill slope.

A notable observation regarding the distribution of building types is the increasing prevalence of RCC buildings within the study area. This trend suggested a shift towards more robust and resilient construction practices as far as landslide hazard is concerned. Apart from its structural durability, RCC buildings are preferred in the study area for high-density housing to meet the growing urban population (Saitluanga, 2017b). Historically, traditional timber construction was common, but it is progressively being replaced by modern construction practices that utilize RCC materials. According to Welsh-Huggins et al. (2017), approximately 47% of the buildings in Aizawl city were constructed using RCC materials. However, the present study revealed that this proportion has now risen to over 50% of the total building stock. This suggested that as urbanization progresses within the Aizawl municipal area, RCC construction, with its prominent durability and strength, is likely to further dominate the built environment.

6.6 Combined Vulnerability

By integrating the social and physical vulnerabilities, the combined vulnerability was generated which represents the overall vulnerability of the study area. Figure 6.10 shows the resulting combined vulnerability map. The map showed a more comprehensive understanding of the overall vulnerability to recognize that it is not solely determined by either social or physical factors, but rather by their complex interaction. The different classes of the combined vulnerability showed certain variations in spatial extent. The high vulnerability class covered the smallest area, occupying 83.91 ha which accounts for 10.22% of the area. This was followed by the moderate class which covered an area of 193.82 ha, comprising 23.60% of the total area. The low vulnerability class constituted the largest portion with an area of 543.45 ha which represents 66.18% of the total area. Table 6.6 shows the distribution of the different combined vulnerability classes in the study area.

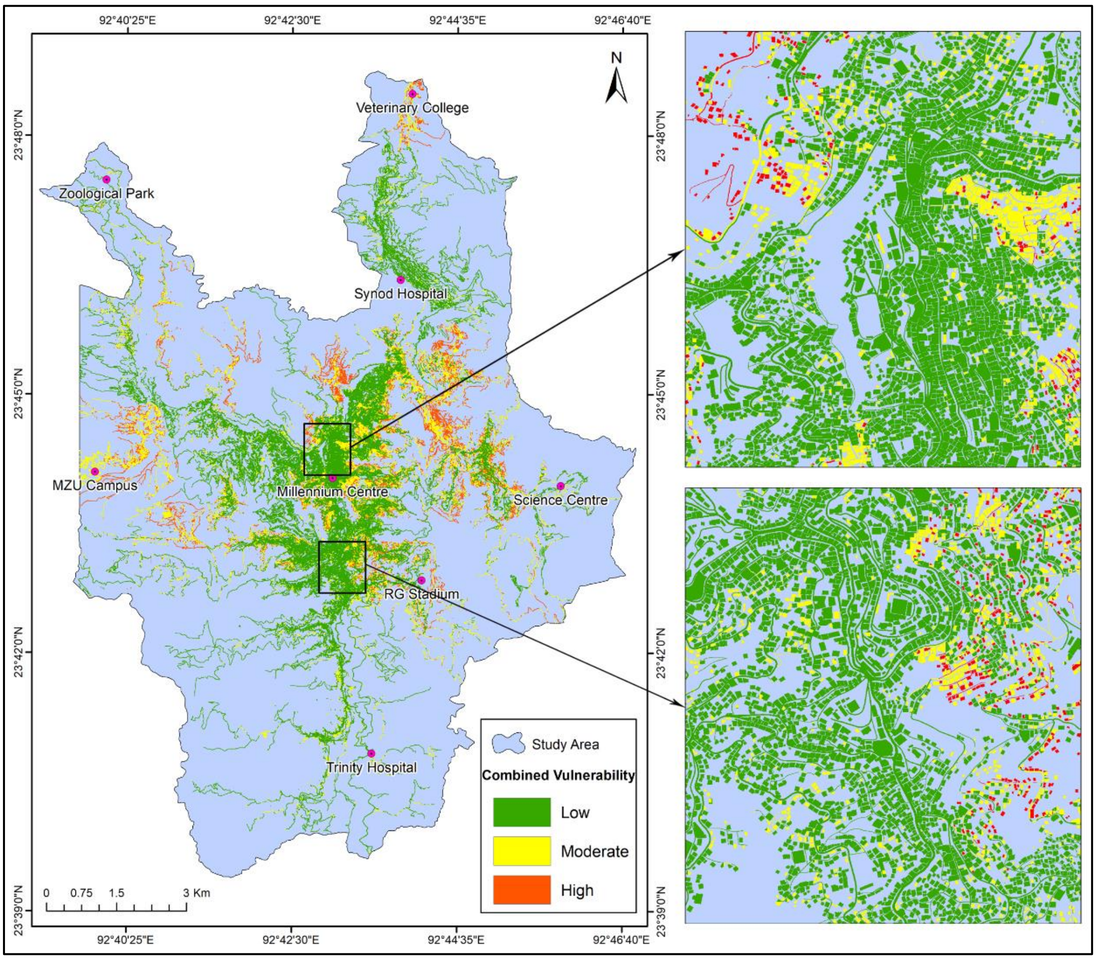

Fig. 6.10 *Combined Vulnerability Map of the Study Area*

Table 6.6 *Distribution of combined vulnerability class*

Sl. No.	Vulnerability	Area in hectare	Area in %
1	Low	543.45	66.18
2	Moderate	193.82	23.6
3	High	83.91	10.22
	Total	**821.19**	**100**

The spatial distribution of combined vulnerability levels showed distinct patterns that reflected the interaction between the social and physical factors in determining the overall vulnerability profile of the Aizawl Municipality. It can be observed that areas with high physical vulnerability, such as those with a predominance of AT buildings and unmetalled roads, do not necessarily coincide with areas of high social vulnerability. However, when these two factors do converge, it resulted in the high combined vulnerability class, which were mostly located in the peripheral areas of the study area. This is suggestive of a compounding effect where socio-economic challenges intersected with infrastructural fragilities which proportionately increased the overall vulnerability to landslide hazards. This is particularly relevant considering the rapid urbanization and the proportional increase in population density, which exerted additional pressure on the infrastructure and resources, particularly in areas already characterized by high vulnerability. The moderate vulnerability class, which occupied the second largest area, was spread across areas where either the social or physical vulnerability showed higher levels while the other remained relatively lower which subsequently generated a balanced effect on the overall vulnerability. This class was characterized by mixed development patterns and varying socio-economic conditions of the study area.

The low combined vulnerability class was mainly concentrated in the central part of the municipality. This is due to the presence of more robust building construction, better infrastructure and populations with greater socio-economic resources and coping capacities. The relative dominance of this vulnerability class (66.18%) suggested that a considerable portion of the municipality has developed some degree of resilience through infrastructural improvements and social development. However, it is important to keep in mind that this is an indicative of lower degree of combined vulnerability when compared to other areas with high and moderate classes, and does not necessarily imply complete absence of the vulnerability.

The combined vulnerability showed varying distribution of vulnerability levels across the study area. The peripheral areas were showing comparatively higher vulnerability levels than the central core areas. This pattern is consistent with typical urban development trends, where the new and less-planned developments usually concentrate at the peripheries, while the core area remains more well-established and developed in terms of services and infrastructures. The present study also emphasized the necessity of considering both physical and social aspects in vulnerability assessment, since areas with similar physical characteristics revealed different combined vulnerability levels based on their social characteristics and vice versa.

6.7 Landslide Risk

The assessments of landslide risk for exposed elements of risk, i.e., buildings and roads within the study area were carried out by integrating the combined vulnerability and the landslide hazard. Figure 6.11 shows the resulting landslide risk index map of the study area. The landslide risk evaluation for building revealed varying degrees of risk within the different building types. In spite of their inherent structural resistance, the RCC buildings showed wide distribution across all the risk classes. A considerable portion of 45.70 ha (8.31%) was falling within the high risk zone, while the moderate risk class accommodated an area of 64.59 ha (11.75%). Majority of the RCC buildings, which comprised an area of 297.23 ha (54.07%) were within the low risk class. The Semi-RCC buildings exhibited a more evenly distributed risk pattern. About 20.85 ha (3.80%) fell into the high risk class, 31.44 ha (5.72%) into the moderate risk class, and 28.06 ha (5.10%) were located under the low risk class. Although structurally less-resilient, the AT buildings showed lower occurrences in the high risk class with an area of 16.55 ha (3.01%). However, a substantial portion, comprising 40.76 ha (7.42%) was within the moderate risk class, and a smaller area of 4.56 ha (0.83%) fell into the low risk class. The distribution of the different risk classes for buildings are shown in the Table 6.7.

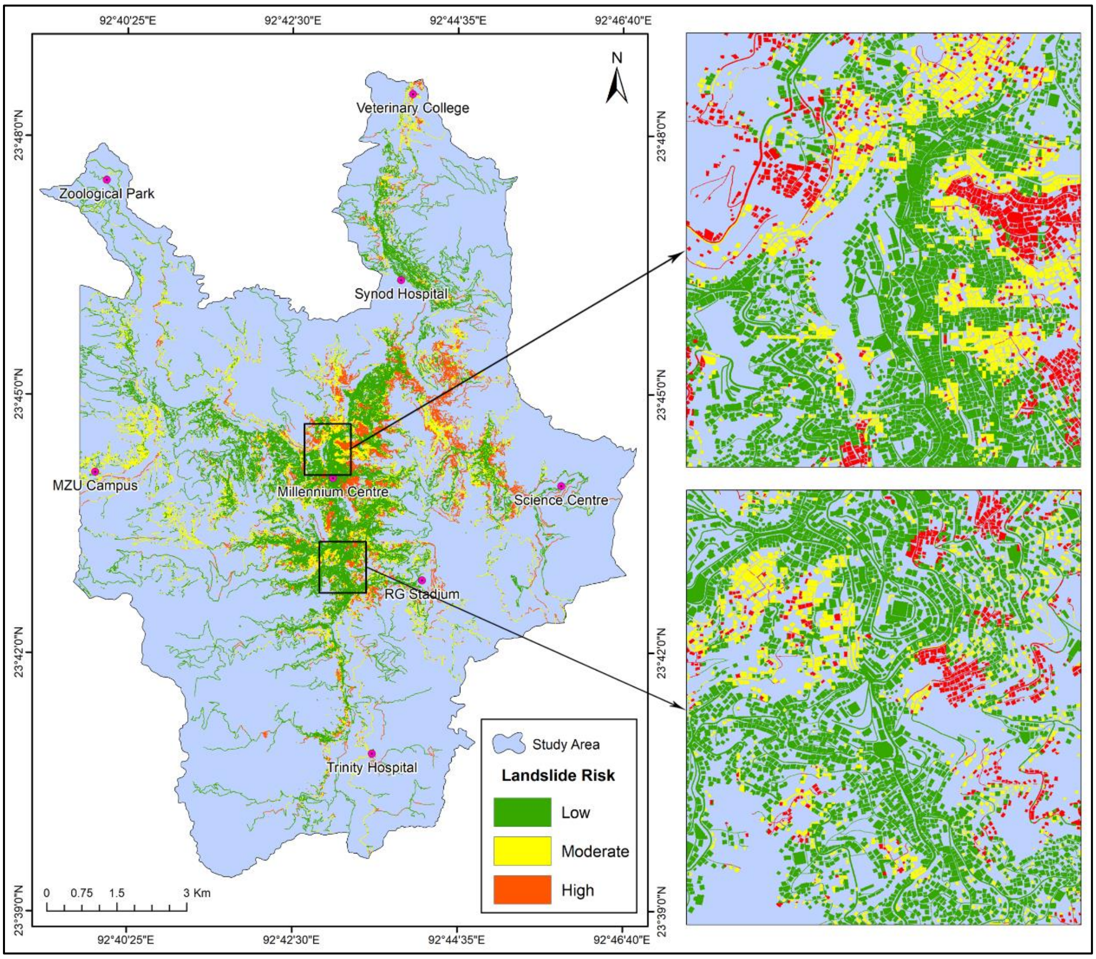

__Fig. 6.11__ Landslide Risk Map of the Study Area

__Table 6.7__ Distribution of building risk class

Sl. No.	Building Class	Risk Class	Area in hectare	Area in %
1	RCC	Low	297.23	54.07
		Moderate	64.59	11.75
		High	45.7	8.31
2	Semi-RCC	Low	28.06	5.1
		Moderate	31.44	5.72
		High	20.85	3.8
3	Assam-Type	Low	4.56	0.83
		Moderate	40.76	7.42
		High	16.55	3.01
Total			**549.72**	**100**

With respect to the road network, the metalled roads, despite being the most resistant, still showed notable exposure to risk, with a length of 64.30 km (6.00%) falling under the high risk class. A length of 101.66 km (9.48%) was classified as moderate risk, while the low risk class dominated the total network length with 358.96 km (33.49%). The unmetalled roads, due to their inherent fragility, exhibited the highest risk among all road types, with 112.83 km (10.53%) falling into the high risk class. Furthermore, a stretch of 194.53 km (18.15%) was within the moderate risk class, and a length of 239.21 km, constituting 22.32% of the total length was in the low risk class. As expected, the bridges showed a comparatively lower risk among all the road classes due to their minimal length. A negligibly small length of 0.05 km was within the high risk class. The moderate and low risk classes respectively covered 0.23 km and 0.11 km of the total road network. Table 6.8 presents the distribution of risk classes for road network.

Table 6.8 *Distribution of road risk class*

Sl. No.	Road Class	Risk Class	Length in km	Length in %
1	Metalled	Low	358.96	33.49
		Moderate	101.66	9.48
		High	64.30	6.00
2	Bridge	Low	0.11	0.01
		Moderate	0.23	0.02
		High	0.05	0.00
3	Unmetalled	Low	239.21	22.32
		Moderate	194.53	18.15
		High	112.83	10.53
Total			**1071.86**	**100**

The fundamental principle guiding this assessment was that landslide risk is a function of the hazard and the vulnerability of exposed elements at risk. The assessment extend beyond the conventional hazard-centric viewpoint to a more holistic understanding, which demonstrated that risk results from the intersection of natural processes and vulnerable built environment. It is the characteristics of the buildings and infrastructure exposed to the hazard that ultimately influence the landslide risk in the study area.

The present risk assessment showed that landslide risk is not only determined by the hazard intensity but is also considerably influenced by the vulnerability of the exposed elements. The analysis revealed a clear spatial variability between the hazard and risk which illustrated that the moderate hazard zones can still experience high landslide risk when intersected with elements characterized by high combined vulnerability. For example, the AT buildings and unmetalled roads, when located within moderate hazard zones but exhibiting high combined vulnerability (as determined by the integration of social and physical vulnerability indices), were classified as belonging to the high risk category. This indicated that the intrinsic structural fragility of certain building types, such as AT constructions, and the structural inadequacy of unmetalled roads, increased the risk even in areas not classified under the highest hazard zones.

Conversely, the assessment also revealed that areas situated within high hazard zones may exhibit comparatively lower landslide risk if they are predominantly occupied by elements with low combined vulnerability. For instance, the RCC buildings and metalled roads, due to their inherent structural resilience and construction quality, were frequently classified under low or moderate risk classes, despite being exposed to high hazard intensities. This finding revealed the protecting role of the physical strength and infrastructure quality in reducing the potential risk even under adverse hazard conditions.

The risk evaluation further illustrated the diverse risk profiles associated with different building and road types across the municipal area. While the majority of RCC buildings (54.07%) were found in the low risk class, a non-negligible proportion (8.31%) still appeared in the high risk class. This showed the spatial variability and interaction between the hazard and the combined vulnerability. The pattern for the unmetalled roads was even more prominent, with over 10% classified under high risk, as opposed to the metalled roads which accommodated only 6% of the total length within the high risk category.

These results collectively revealed the necessity of integrating both hazard and vulnerability dimensions in the risk assessment framework. Relying solely on hazard intensity can underestimate the actual risk posed to certain infrastructure, particularly in rapidly urbanizing settlements with varying social and physical vulnerabilities. The present findings also emphasized the urgent need for taking up effective landslide risk reduction measures within the study area by reducing the hazard exposure wherever feasible. Equally important is the strengthening of the resilience of vulnerable elements such as upgrading construction materials, improving road infrastructure, and targeting social vulnerability hotspots. This holistic approach is essential for the development and implementation of evidence-based policies aimed at minimizing landslide impacts and safeguarding both lives and assets within the Aizawl municipal area.

6.8 Limitations of the Study

The present study acknowledges several limitations, which are important for interpreting the findings and for guiding future research and policy recommendations. These limitations mainly constitute data availability, methodological constraints, and the dynamic nature of the studied phenomena. With regard to the landslide susceptibility assessment, the landslide inventory dataset, which formed a fundamental basis for the susceptibility mapping, do not represent the complete landslide events within the area, particularly those of historical events. This is primarily due to lack of recorded data and the characteristics of the inventory data such as date of occurrence, geographical location, size, etc. This limitation could influence the spatial distribution of the different susceptibility zones and the overall accuracy of the resulting maps. Another limitation is the selection of predisposing factors for the assessment, which was mainly based on data availability. The assessment may fail to include other important influencing parameters for landslide occurrences in the study area.

Another significant and obvious limitation is the use of the 2011 Census data for the social vulnerability assessment. The data was more than a decade old, and considerable changes in population dynamics, socio-economic conditions, and spatial distribution patterns could have happened since then. This may lead to an inaccurate representation of the current social vulnerability status of the resident population. Furthermore, the choice of the indicators, which was primarily guided by the availability of data, may not capture all relevant aspects such as access to healthcare, community participation and coping strategies which are important for social vulnerability evaluation (Rufat et al., 2015). Regarding the assessment of physical vulnerability, the study utilized construction materials as a proxy for structural resistance due to constraints in data availability. This approach overlooked several other critical factors such as building age, the number of floors, geographic location, and the state of maintenance which were not incorporated into the analysis. Besides, the subjectivity in numerical weight assignments may also introduce bias in the analyses which could affect the overall results.

The lack of reference data for infrastructure damages within the study area limits the validation for the landslide risk assessment results which may introduce a degree of uncertainty. Due to the absence of the temporal and magnitude information on landslide events, the susceptibility map was utilized as a substitute for the landslide hazard map. This may not fully represent the actual landslide hazard potential which could further lead to either an underestimation or overestimation of the actual risk levels. Lastly, the study was unable to perform risk assessment specifically for the population due to data constraints on the distribution of persons within each building which further adds to another major limitation of the assessment.

These limitations, particularly those arising from data scarcity and the temporal aspects of some datasets, highlighted areas for future research. Addressing these aspects by incorporating more recent and relevant data, along with refining methodological approaches to include a broader range of vulnerability factors and population risk, would greatly enhance the comprehensiveness and accuracy of landslide risk assessment within the Aizawl municipal area.

CHAPTER 7

CONCLUSION AND RECOMMENDATIONS

The present research carried out a comprehensive assessment of landslide susceptibility, vulnerability and risk within the Aizawl municipal area. The study employed a methodological framework that integrated geospatial techniques, quantitative bivariate statistical models, and socio-economic and physical infrastructure data, and sought to evaluate the interaction of these factors in contributing to landslide hazards and the subsequent risk posed by them. The study utilized an inventory of 381 rainfall-induced shallow landslides and twelve conditioning factors to generate the susceptibility maps. The assessment for social vulnerability was conducted using the socio-economic and demographic indicators derived from Census 2011 data, while the physical vulnerability was evaluated using the buildings and road networks obtained through manual digitization of high-resolution Google Earth® images. A landslide risk index for the study area was ultimately generated from the product of the hazard and combined vulnerability. This chapter summarizes the main findings of the research, and provides recommendations for enhanced landslide risk management and future research directions.

7.1 Landslide Susceptibility

The landslide susceptibility mapping utilized three bivariate statistical models, namely, Information Value (IV), Frequency Ratio (FR), and Weight of Evidence (WofE). The resulting susceptibility maps were classified into High, Moderate and Low zones. All the three models performed satisfactorily in producing reliable landslide susceptibility maps, with the WofE model showing slightly higher success rate (83.93%) and prediction rate (83.79%) compared to the IV and FR models with the success rates of 83.85% and 83.72%, and prediction rates of 83.71% and 83.58%, respectively.

A general similarity was observed in the spatial distribution of susceptibility zones across the models. However, the areal extent of these zones showed certain variations among the models. The moderate zone occupied maximum area in all the three models which was followed by the low susceptibility zone in both the FR and WofE models. The low susceptibility zone occupied the smallest area in the IV model. Naturally, a majority of landslides were located in the high susceptibility zone, with the IV model having 65.72%, FR with 61.03%, and WofE having 57.13% of total landslides in the high susceptibility zone.

The analysis of the spatial correlation between the predisposing factors and landslide occurrences provided insights into their influence on slope instability. The east, south-east, and south-facing slopes, shale unit, higher elevation, built-up, scrubland, barren land, and high slope angles showed positive influence among the various factor classes. On the other hand, LULC, lithology, SPI, NDVI, slope angle, and TWI were identified as the most significant and influential factors for mass movements, while aspect, lineament density, and drainage density had relatively less influence. The present landslide susceptibility assessment showed that the bivariate statistical models, specifically the IV, FR and WofE can be employed successfully to produce reliable and highly accurate results, which can further be suitably utilized for the implementation of future land use planning within the study area.

7.2 Social Vulnerability

The social vulnerability assessment was carried out using five indicators each for the sensitivity and lack of resilience variables using Census 2011 data at the local council level. The highest social vulnerability class was mainly observed in the peripheral areas which is represented by higher concentrations of low-income households, non-workers, and rented accommodations, along with high dependency ratios. The moderate social vulnerability class was mostly concentrated in the central part of the municipal area which exhibited mixed vulnerabilities where economic stability might be present but factors like population density or rented accommodation still contributed to vulnerability. The lowest social vulnerability level dominated the Aizawl municipal area which spread across the southern, northern, and the central portions. This class was mainly attributed to better resilience factors such as higher income levels, robust infrastructure, and improved socio-economic conditions.

Analysis of individual indicator contributions revealed that the female population was the most significant contributor to the overall social vulnerability. Households in rented accommodations also highly contributed, indicating vulnerability due to potential displacement and economic insecurity. Demographic indicators like children population, non-workers, and elders population also collectively influenced the social vulnerability to a considerable extent due to higher dependency ratios and reduced resilience capacities. Moderate contributions came from illiteracy, population density, and households without assets. Low income and lack of electricity were the least contributing indicators, which highlighted the presence of urban poor sections that warrant attention and targeted support.

7.3 Physical Vulnerability

The physical vulnerability assessment focused on the built infrastructures such as buildings and road networks. Among the building types, the RCC structures showed the highest resilience, with the majority of the area falling under the low vulnerability class. The semi-RCC buildings were distributed across all the classes, with smaller portions in the low and in the moderate classes, and a notable portion in the high vulnerability class. The AT buildings were the least resistant buildings, predominantly contributing to the high vulnerability class and a smaller portion to the moderate vulnerability zone.

In case of the road networks, the metalled roads exhibited high resilience, dominating the low vulnerability zone. The bridges, though minimal in length, were distributed across all vulnerability classes, due to their location across streams and unstable terrains, and susceptibility to toe-erosion. The unmetalled roads were inherently fragile, with their considerable length in the high vulnerability class, and a notable length in the moderate vulnerability zone.

The present study revealed that both the RCC buildings and metalled roads showed inherent structural resilience, which can potentially minimize severe damage even when located in the highest hazard situations. Conversely, the AT buildings and unmetalled roads were intrinsically vulnerable, most of which were classified in the moderate or the high vulnerability class due to their structural fragility and absence of reinforced materials. As far as landslide hazard is concerned, the present study noted increasing shift towards more resilient construction practices in the study area, with the RCC buildings being preferred over the traditional timber construction.

7.4 Combined Vulnerability

The integration of social and physical vulnerabilities provided a comprehensive understanding of the overall vulnerability profile of the Aizawl municipal area. The low combined vulnerability class constituted the largest portion, and is predominantly concentrated in the central part of the municipality. This is characterized by more resilient buildings, better infrastructure, and relatively better socio-economic resources. The moderate class spread across areas where either social or physical vulnerability was higher which created a balanced overall effect, and is characterized by mixed development patterns. The high combined vulnerability class covered the smallest area, mostly located in peripheral areas where high physical and social vulnerabilities converged which indicated a compounding effect of socio-economic challenges and infrastructural fragilities. This assessment highlighted that the overall vulnerability is an interaction of both the social and physical factors, and not determined by only one factor. The peripheral areas exhibited higher combined vulnerability levels compared to the core area, which is consistent with typical urban development patterns where new and less-planned developments occur at the peripheries.

7.5 Landslide Risk

Landslide risk was assessed as a function of the landslide hazard and the combined vulnerability index. The assessment was limited to the physical infrastructures due to constraints on data for building occupants and economic costs. The landslide risk assessment revealed varying degrees of risk within different building types and road networks. Although the RCC buildings showed wide distribution across all risk classes, majority of their areas fell under the low risk class, which revealed the spatial variability of the hazard and vulnerability. The semi-RCC buildings exhibited a more evenly distributed risk pattern across the high, the moderate, and the low risk classes. The AT buildings, being structurally less resilient, showed relatively higher occurrences in the moderate and the high risk classes, and a small portion in the low risk class.

Regarding the road networks, the metalled roads, despite high resistance, still showed notable exposure to risk, but majority of the total length occurred in the low risk class. Owing to their inherent fragility, the unmetalled roads exhibited the highest risk among all road types, but still showed higher occurrences in the low and the moderate classes. The bridges showed comparatively lower overall risk due to their negligible length.

The study highlighted that landslide risk is not solely determined by hazard intensity but is considerably influenced by the vulnerability of exposed elements. This implies the necessity of integrating both hazard and vulnerability dimensions in the risk assessment framework to avoid under- or over-estimation of the actual risk. It also showed that risk mitigation measures should address both the socio-economic aspects and the resilience of the physical infrastructures to minimize the disasters caused by landslides. The results further showed the protective role of physical strength and infrastructure quality in reducing potential risk even under adverse hazard conditions.

The present study successfully developed and validated a comprehensive methodology for landslide susceptibility, vulnerability, and risk assessment in the Aizawl municipal area. By integrating geospatial data, statistical models, and detailed socio-economic and infrastructural characteristics, the study provides valuable insights into the spatial patterns and underlying factors of landslide risk. An important conclusion is that risk is a multifaceted phenomenon which arises from the intricate interaction between natural hazards and the social and physical vulnerabilities of the exposed elements. This concept goes beyond a hazard-centric view which emphasized that both the intensity of the natural process and the inherent resilience or fragility of human communities and their built environment collectively determine the ultimate risk. The spatial variability revealed, with peripheral areas generally exhibiting higher combined vulnerability and risk, points towards the dynamic challenges of urban expansion in hilly terrains.

7.6 Recommendations

Based on the findings of this study, the following recommendations are proposed for effective landslide risk reduction, sustainable development, and future research within the Aizawl municipal area:

7.6.1 For Landslide Risk Reduction and Management

1. Prioritizing Targeted Interventions in High Risk Zones: Resources and mitigation efforts should be focused on the identified high susceptibility and high risk zones, particularly in the central longitudinal portion and the peripheral areas where there were convergence of high social and physical vulnerabilities. It is also strongly recommended to develop and implement landslide early warning systems, and formulation of evacuation plans specifically designed for these areas.

2. Strengthening Regulatory Frameworks and Land Use Planning: Although the present Slope Development and Slope Modification (SD&SM) Regulation 2017 is being enforced, there is still a need to enforce stricter zoning regulations and building codes, especially in the identified high susceptibility and high risk zones, and to restrict new constructions in areas which are currently susceptible and vulnerable. Promoting sustainable land use practices that discourage extensive anthropogenic activities along unstable slopes, particularly in barren lands and scrublands which show a high correlation with landslides, is also necessary for long-term stability.

3. Upgrading Vulnerable Infrastructure: Investment is required to improve the structural integrity of the unmetalled roads and the AT/Semi-RCC buildings, especially those located in the moderate to high hazard zones. This could involve reinforcing construction materials, and mandating geotechnical evaluation and engineered/architectural design for construction of any infrastructure. Strengthening of foundations of the bridges against toe-erosion and subsidence is important in view of their vulnerability to torrential water flow and seepage underneath.

4. Implementing Integrated Environmental Management Strategies: Comprehensive afforestation schemes should be initiated especially in barren lands and sparsely vegetated areas to enhance slope stability and reduce erosion. Improving and maintaining drainage networks, particularly in high drainage density areas is necessary to manage surface runoff and prevent water seepage that can reduce shear strength.

5. Addressing Social Vulnerability Hotspots: Targeted social development and protection initiatives are needed especially for the peripheral areas and local councils identified with high social vulnerability. These initiatives should focus on improving access to resources, enhancing economic security for low-income households and non-workers, and providing specific support mechanisms for vulnerable groups such as women, children, and the elderly. Support for community-based disaster preparedness and resilience-building initiatives are also highly recommended.

6. Fostering Holistic and Integrated Policy Development: Policy-making should emphasize an integrated approach that considers both the physical (infrastructure quality and land use) and the social (demographics and socio-economic status) dimensions of vulnerability. Moving beyond hazard-centric disaster management to a comprehensive risk reduction framework that incorporates vulnerability assessments is required to safeguard lives and the assets.

7.6.2 For Future Research and Methodological Improvements

1. Landslide Inventory Data: Future research should prioritize systematic landslide inventory mapping to capture complete landslide events, including accurate geographical coordinates, exact dates of occurrence, failure types, and sizes of the landslide. This would considerably improve the accuracy of susceptibility models and allow for spatio-temporal analysis of landslide triggers.

2. Rainfall Data: Since rainfall is the major triggering factor for landslides in the study area, incorporating accurate and comprehensive rainfall data is required, particularly for intensity-duration thresholds evaluation. This will enable to include the temporal probability of a landslide event for developing *actual* landslide hazard maps for the Aizawl municipal area. For this, it is important to invest in and install a network of additional rain gauge stations throughout the study area to capture the spatial and temporal variability of rainfall. This will provide high-resolution data on intensity, duration, and cumulative precipitation for accurate landslide hazard assessment.

3. Vulnerability Data: For social vulnerability, a new and more recent socio-economic and demographic data is essential to accurately reflect current population dynamics and social vulnerability status. Additional relevant indicators such as access to healthcare, coping strategies and community participation may be incorporated to provide a more comprehensive assessment. For physical vulnerability evaluation, detailed data on other critical factors like building age, number of floors, construction quality, and maintenance status may be included which would allow moving beyond construction materials as a sole proxy for structural resistance. Data on the distribution and density of occupants within individual buildings is needed to enable a specific assessment of risk to human lives, which was a limitation in the current study. Furthermore, collecting data on construction and repair costs of infrastructures within the study area is necessary to quantify potential economic losses due to landslides which will provide a more complete picture of landslide impacts.

4. Refining Methodological Approaches: Exploring alternative methods such as AI-driven models (ML, DL, XAI, etc) for susceptibility mapping could provide comparisons of predictive performances. The subjectivity in numerical weight assignments for physical vulnerability components could be reduced by developing more data-driven or expert-validated weighting schemes to enhance objectivity. It is also necessary to incorporate temporal and magnitude probabilities of landslide events to transform susceptibility maps into actual landslide hazard maps for providing a more accurate representation of hazard potential and risk levels.

5. Integration of Dynamic Factors: Future studies should consider the dynamic nature of landslide occurrences by integrating factors like climate change projections (e.g., changes in rainfall patterns). Equally important is the incorporation of future urbanization growth scenarios into the susceptibility and risk models to account for the rapidly evolving conditions.

6. Monitoring and Validation: Establishing a framework for continuous monitoring and data collection is essential to enable studies that identify changes in susceptibility or hazard, vulnerability, and risk over time. In addition, conducting empirical validation of risk assessment results through post-disaster damage surveys would help calibrate and improve the accuracy of the models.

7. Continual Updating of Landslide Susceptibility/Hazard Zonation Map: In a rapidly urbanizing settlement like Aizawl, it is important to regularly update the landslide susceptibility/hazard zonation maps prepared for the study area to account for the changes in land use pattern, anthropogenies, and the climatic extremes. This will help in getting an updated and real-time landslide hazard potential for taking suitable mitigation measures by the authorities concerned.

This research has provided a foundational understanding of landslide risk in the Aizawl Municipal Area, offering critical insights into the spatial dynamics of hazard and vulnerability. The findings and recommendations herein are intended to serve as a vital resource for policymakers, urban planners, and disaster management authorities. By adopting a holistic and integrated approach to landslide risk reduction, focusing on both the natural processes and the socio-physical characteristics of the exposed environment, the Aizawl municipal area can move towards a more resilient and sustainable future, and safeguarding its population and assets from the devastating impacts of landslides.

REFERENCES

Abdallah, C., Chorowicz, J., Boukheir, R., & Dhont, D. (2007). Comparative use of processed satellite images in remote sensing of mass movements: Lebanon as a case study. *International Journal of Remote Sensing*, *28*(19), 4409–4427. https://doi.org/10.1080/01431160701241761

Abdelkader, M. M., & Csámer, Á. (2025). Comparative assessment of machine learning models for landslide susceptibility mapping: A focus on validation and accuracy. *Natural Hazards*. https://doi.org/10.1007/s11069-025-07197-0

Abdulwahid, W. M., & Pradhan, B. (2017). Landslide vulnerability and risk assessment for multi-hazard scenarios using airborne laser scanning data (LiDAR). *Landslides, 14*(3), 1057–1076. https://doi.org/10.1007/s10346-016-0744-0

Abella, E. A. C., & van Westen, C. J. (2007). Generation of a landslide risk index map for Cuba using spatial multi-criteria evaluation. *Landslides, 4*(4), 311–325. https://doi.org/10.1007/s10346-007-0087-y

Abraham, M. T., Satyam, N., Jain, P., Pradhan, B., & Alamri, A. (2021). Effect of spatial resolution and data splitting on landslide susceptibility mapping using different machine learning algorithms. *Geomatics, Natural Hazards and Risk*, *12*(1), 3381–3408. https://doi.org/10.1080/19475705.2021.2011791

Acosta-Quesada, M., & Quesada-Román, A. (2025). Landslide and flood risk assessment in a rapidly urbanizing municipality of Costa Rica. *Journal of South American Earth Sciences, 152*, 105330. https://doi.org/10.1016/j.jsames.2024.105330

Addis, A. (2023). GIS-based landslide susceptibility mapping using frequency ratio and Shannon Entropy Models in Dejen District, Northwestern Ethiopia. *Journal of Engineering*, *2023*(1), 1062388. https://doi.org/10.1155/2023/1062388

Adger, W. N. (1999). Social vulnerability to climate change and extremes in coastal Vietnam. *World Development*, *27*(2), 249–269. https://doi.org/10.1016/S0305-750X(98)00136-3

Adger, W. N. (2003). Social capital, collective action, and adaptation to climate change. *Economic Geography*, *79*(4), 387–404. https://doi.org/10.1111/j.1944-8287.2003.tb00220.x

Adger, W. N. (2006). Vulnerability. *Global Environmental Change*, *16*(3), 268–281. https://doi.org/10.1016/j.gloenvcha.2006.02.006

Adger, W. N., & Kelly, P. M. (2001). Social vulnerability and resilience. In W. N. Adger, P. M. Kelly, & N. H. Ninh (Eds.), *Living with environmental change* (1st ed., pp. 19–34). Routledge. https://doi.org/10.4324/9780203995570-3

Adla, K., K., Dejan, D., Neira, & Š., Dragana. (2022). Degradation of ecosystems and loss of ecosystem services. In J. C. Prata, A. I. Ribeiro, & T. Rocha-Santos (Eds.), *One health: Integrated approach to 21st century challenges to health* (pp. 281–327). Elsevier Science. https://doi.org/10.1016/B978-0-12-822794-7.00008-3

Adnan, M. S. G., Siam, Z. S., Chakma, S., Rahman, R. M., & Dewan, A. (2025). Landslide susceptibility mapping using machine-learning algorithms and earth observation data. In I. Șandric, V. Ilinca, & Z. Chitu (Eds.), *Earth observation applications to landslide mapping, monitoring and modeling* (pp. 313–333). Elsevier. https://doi.org/10.1016/B978-0-12-823868-4.00015-5

Ado, M., Amitab, K., Maji, A. K., Jasińska, E., Gono, R., Leonowicz, Z., & Jasiński, M. (2022). Landslide susceptibility mapping using machine learning: A literature survey. *Remote Sensing*, *14*(13), 3029. https://doi.org/10.3390/rs14133029

Agliata, R., Bortone, A., & Mollo, L. (2021). Indicator-based approach for the assessment of intrinsic physical vulnerability of the built environment to hydro-meteorological hazards: Review of indicators and example of parameters selection for a sample area. *International Journal of Disaster Risk Reduction*, *58*, 102199. https://doi.org/10.1016/j.ijdrr.2021.102199

Agrawal, N., & Dixit, J. (2023). GIS-based landslide susceptibility mapping of the Meghalaya-Shillong Plateau region using machine learning algorithms. *Bulletin of Engineering Geology and the Environment*, *82*(5), 170. https://doi.org/10.1007/s10064-023-03188-2

AGS (Australian Geomechanics Society). (2000). Landslide risk management concepts and guidelines. *Australian Geomechanics, 35*(1), 49–52.

AGS (Australian Geomechanics Society). (2002). Landslide risk management concepts and guidelines. *Australian Geomechanics*, *37*(2), 1–44. https://search.informit.org/doi/10.3316/informit.809857183323774

Agterberg, F. P., Bonham-Carter, G. F., Cheng, Q., & Wright, D. F. (1993). Weights of evidence modeling and weighted logistic regression for mineral potential mapping. In J. C. Davis & U. C. Herzfeld (Eds.), *Computers in geology—25 years of progress* (pp. 13–32). Oxford University Press. https://doi.org/10.1093/oso/9780195085938.003.0007

Ahmed, B. (2015). Landslide susceptibility mapping using multi-criteria evaluation techniques in Chittagong Metropolitan Area, Bangladesh. *Landslides*, *12*(6), 1077–1095. https://doi.org/10.1007/s10346-014-0521-x

Ahmed, B. (2021). The root causes of landslide vulnerability in Bangladesh. *Landslides*, *18*(5), 1707–120. https://doi.org/10.1007/s10346-020-01606-0

Ahmed, B., & Kelman, I. (2018). Measuring community vulnerability to environmental hazards: A method for combining quantitative and qualitative data. *Natural Hazards Review*, *19*(3), 04018008. https://doi.org/10.1061/(ASCE)NH.1527-6996.0000290

Akbas, S. O., Blahut, J., & Sterlacchini, S. (2009). Critical assessment of existing physical vulnerability estimation approaches for debris flows. In J. Malet, A. Remaître, & T. Bogaard (Eds.), *Landslide processes: From geomorphological mapping to dynamic modelling* (pp. 229–233). CERG Editions.

Akinci, H., Kilicoglu, C., & Dogan, S. (2020). Random Forest-based landslide susceptibility mapping in coastal regions of Artvin, Turkey. *ISPRS International Journal of Geo-Information*, *9*(9), 553. https://doi.org/10.3390/ijgi9090553

Akosah, S., Gratchev, I., Kim, D.-H., & Ohn, S.-Y. (2024). Application of artificial intelligence and remote sensing for landslide detection and prediction: Systematic review. *Remote Sensing*, *16*(16), 2947. https://doi.org/10.3390/rs16162947

Aksha, S. K., Juran, L., Resler, L. M., & Zhang, Y. (2019). An analysis of social vulnerability to natural hazards in Nepal using a modified social vulnerability index. *International Journal of Disaster Risk Science*, *10*(1), 103–116. https://doi.org/10.1007/s13753-018-0192-7

Aleotti, P., & Chowdhury, R. (1999). Landslide hazard assessment: Summary review and new perspectives. *Bulletin of Engineering Geology and the Environment*, *58*, 21–44. https://doi.org/10.1007/s100640050066

Alexander, D. (1992). On the causes of landslides: Human activities, perception, and natural processes. *Environmental Geology and Water Sciences*, *20*(3), 165–179. https://doi.org/10.1007/BF01706160

Alexander, D. (2005). Vulnerability to landslides. In T. Glade, M. Anderson, & M. J. Crozier (Eds.), *Landslide Hazard and Risk* (pp. 175–198). John Wiley & Sons Ltd. https://doi.org/10.1002/9780470012659.ch5

Alexander, D. E. (2002). *Principles of emergency planning and management*. Terra Publishing.

Al-Najjar, H. A., Pradhan, B., He, X., Sheng, D., Alamri, A., Gite, S., & Park, H. J. (2024). Integrating physical and machine learning models for enhanced landslide prediction in data-scarce environments. *Earth Systems and Environment*, 1–28. https://doi.org/10.1007/s41748-024-00508-8

Althuwaynee, O. F., & Pradhan, B. (2017). Semi-quantitative landslide risk assessment using GIS-based exposure analysis in Kuala Lumpur City. *Geomatics, Natural Hazards and Risk, 8*(2), 706–732. https://doi.org/10.1080/19475705.2016.1255670

Althuwaynee, O. F., Pradhan, B., & Lee, S. (2012). Application of an evidential belief function model in landslide susceptibility mapping. *Computers & Geosciences*, *44*, 120–135. https://doi.org/10.1016/j.cageo.2012.03.003

Alvioli, M., & Baum, R. L. (2016). Parallelization of the TRIGRS model for rainfall-induced landslides using the message passing interface. *Environmental Modelling & Software*, *81*, 122–135. https://doi.org/10.1016/j.envsoft.2016.04.002

Alvioli, M., Loche, M., Jacobs, L., Grohmann, C. H., et al. (2024). A benchmark dataset and workflow for landslide susceptibility zonation. *Earth-Science Reviews*, *258*, 104927. https://doi.org/10.1016/j.earscirev.2024.104927

Alvioli, M., Marchesini, I., Reichenbach, P., Rossi, M., Ardizzone, F., Fiorucci, F., & Guzzetti, F. (2016). Automatic delineation of geomorphological slope units with r.slopeunits v1.0 and their optimization for landslide susceptibility modeling. *Geoscientific Model Development*, *9*(11), 3975–3991. https://doi.org/10.5194/gmd-9-3975-2016

Amarasinghe, M. P., Kulathilaka, S. A. S., Robert, D. J., Zhou, A., & Jayathissa, H. A. G. (2024). Risk assessment and management of rainfall-induced landslides in tropical regions: A review. *Natural Hazards, 120*(3), 2179–2231. https://doi.org/10.1007/s11069-023-06277-3

Amatya, P., Kirschbaum, D., Stanley, T., & Tanyas, H. (2021). Landslide mapping using object-based image analysis and open source tools. *Engineering Geology*, *282*, 106000. https://doi.org/10.1016/j.enggeo.2021.106000

Anbalagan, R. (1992). Landslide hazard evaluation and zonation mapping in mountainous terrain. *Engineering Geology*, *32*(4), 269–277. https://doi.org/10.1016/0013-7952(92)90053-2

Anbalagan, R., & Singh, B. (1996). Landslide hazard and risk assessment mapping of mountainous terrains—a case study from Kumaun Himalaya, India. *Engineering Geology, 43*(4), 237–246. https://doi.org/10.1016/S0013-7952(96)00033-6

Andharia, J. (2022). Vulnerability: Its discursive and material nature. In T. K. McGee & E. C. Penning-Rowsell (Eds.), *Routledge handbook of environmental hazards and society* (pp. 185–200). Routledge. https://doi.org/10.4324/9780367854584-17

Antonini, G., Ardizzone, F., Cardinali, M., Galli, M., Guzzetti, F., & Reichenbach, P. (2002). Surface deposits and landslide inventory map of the area affected by the 1997 Umbria-Marche earthquakes. *Bollettino della Societa Geologica Italiana*, *1*(2), 843–853.

Aristizábal, E., & Sánchez, O. (2020). Spatial and temporal patterns and the socioeconomic impacts of landslides in the tropical and mountainous Colombian Andes. *Disasters*, *44*(3), 596–618. https://doi.org/10.1111/disa.12391

Arrogante-Funes, P., Bruzón, A. G., Arrogante-Funes, F., Ramos-Bernal, R. N., & Vázquez-Jiménez, R. (2021). Integration of vulnerability and hazard factors for landslide risk assessment. *International Journal of Environmental Research and Public Health, 18*(22), 11987. https://doi.org/10.3390/ijerph182211987

Arshid, M. U., Akbar, M., Zohaib, M., Huali, P., Salih, R., Khan, M. A., Alkahtani, M. Q., Badar, J., Mursaleen, M., Soudagar, M. E., & Islam, S. (2024). Landslide susceptibility analysis and hazard zonation of Koh-e-Suleman range using weighted overlay technique. *Geomatics, Natural Hazards and Risk*, *15*(1), 2389861. https://doi.org/10.1080/19475705.2024.2389861

Aslam, B., Zafar, A., & Khalil, U. (2023). Comparative analysis of multiple conventional neural networks for landslide susceptibility mapping. *Natural Hazards*, *115*(1), 673–707. https://doi.org/10.1007/s11069-022-05570-x

Atkinson, P. M., & Massari, R. (1998). Generalised linear modelling of susceptibility to landsliding in the central Apennines, Italy. *Computers & Geosciences*, *24*(4), 373–385. https://doi.org/10.1016/S0098-3004(97)00117-9

Ayalew, L., & Yamagishi, H. (2005). The application of GIS-based logistic regression for landslide susceptibility mapping in the Kakuda-Yahiko Mountains, Central Japan. *Geomorphology*, *65*(1-2), 15–31. https://doi.org/10.1016/j.geomorph.2004.06.010

Ayalew, L., Yamagishi, H., & Ugawa, N. (2004). Landslide susceptibility mapping using GIS-based weighted linear combination, the case in Tsugawa area of Agano River, Niigata Prefecture, Japan. *Landslides*, *1*, 73–81. https://doi.org/10.1007/s10346-003-0006-9

Ba, Q., Chen, Y., Deng, S., Yang, J., & Li, H. (2018). A comparison of slope units and grid cells as mapping units for landslide susceptibility assessment. *Earth Science Informatics*, *11*, 373–388. https://doi.org/10.1007/s12145-018-0335-9

Baeza, C., & Corominas, J. (2001). Assessment of shallow landslide susceptibility by means of multivariate statistical techniques. *Earth Surface Processes and Landforms*, *26*(12), 1251–1263. https://doi.org/10.1002/esp.263

Baiges, J., & Codina, R. (2010). The fixed-mesh ALE approach applied to solid mechanics and fluid-structure interaction problems. *International Journal for Numerical Methods in Engineering*, *81*(12), 1529–1557. https://doi.org/10.1002/nme.2740

Baltzer, A. (1875). Über bergstürze in den Alpen [About landslides in the Alps]. *Schweizer Alpen Club Bern Jahrbuch, 10*, 409–456.

Barman, B. K., Rao, K. S., & Saikia, I. J. (2019). Delineation of potential landslide prone zones using remote sensing and GIS techniques: A case study from north western part of Aizawl city, Mizoram, India. *International Journal of Multidisciplinary*, *4*(4), 1395–1400.

Barredo, J., Benavides, A., Hervás, J., & van Westen, C. J. (2000). Comparing heuristic landslide hazard assessment techniques using GIS in the Tirajana basin, Gran Canaria Island, Spain. *International Journal of Applied Earth Observation and Geoinformation*, *2*(1), 9–23. https://doi.org/10.1016/S0303-2434(00)85022-9

Baum, R. L., Savage, W. Z., & Godt, J. W. (2008). *TRIGRS: A Fortran program for transient rainfall infiltration and grid-based regional slope-stability analysis, version 2.0* (U.S. Geological Survey Open-File Report 2008-1159). U.S. Geological Survey.

Bednarik, M., Yilmaz, I., & Kralovičová, L. (2024). Deterministic approach to assess landslide susceptibility and landslide activity in the Central-Western Region of Slovakia. *Bulletin of Engineering Geology and the Environment*, *83*(8), 327. https://doi.org/10.1007/s10064-024-03795-7

Beguería, S. (2006). Validation and evaluation of predictive models in hazard assessment and risk management. *Natural Hazards, 37*(3), 315–329. https://doi.org/10.1007/s11069-005-5182-6

Beingachhi, B., & Deka, G. (2013). Landslide and associated environmental problems: A case study of Hlimen in Aizawl City. In *Proceedings of BICON 2013* (pp. 390–396).

Beingachhi, B., & Vanlalhmangaihsangi, F. (2017). Slope instability and its related problems: A case study of South Hlimen landslide. *Senhri Journal of Multidisciplinary Studies, 2*(1), 88–99.

Bell, R., & Glade, T. (2004). Quantitative risk analysis for landslides: Examples from Bíldudalur, NW-Iceland. *Natural Hazards and Earth System Sciences*, *4*(1), 117–131. https://doi.org/10.5194/nhess-4-117-2004

Ben-Zion, Y., & Sammis, C. G. (2003). Characterization of fault zones. *Pure and Applied Geophysics, 160*(3), 677–715. https://doi.org/10.1007/PL00012554

Bera, S., Guru, B., & Oommen, T. (2020). Indicator-based approach for assigning physical vulnerability of the houses to landslide hazard in the Himalayan region of India. *International Journal of Disaster Risk Reduction*, *50*, 101891. https://doi.org/10.1016/j.ijdrr.2020.101891

Bergstrand, K., Mayer, B., Brumback, B., & Zhang, Y. (2015). Assessing the relationship between social vulnerability and community resilience to hazards. *Social Indicators Research*, *122*(2), 391–409. https://doi.org/10.1007/s11205-014-0698-3

Bertani, A., Di Paola, G., Russo, E., & Tuzzolino, F. (2018). How to describe bivariate data. *Journal of Thoracic Disease*, *10*(2), 1133–1137. https://doi.org/10.21037/jtd.2018.01.134

Betts, A. K., Ball, J. H., Beljaars, A. C., Miller, M. J., & Viterbo, P. A. (1996). The land surface-atmosphere interaction: A review based on observational and global modeling perspectives. *Journal of Geophysical Research: Atmospheres*, *101*(D3), 7209–7225. https://doi.org/10.1029/95JD02135

Bhat, G. M. (2024). Landslide Scenario in India with Special Reference to the Himalaya and Community Resilience to Hazards. *Journal of the Geological Society of India*, *100*(11), 1507–1510. https://doi.org/10.17491/jgsi/2024/174010

Bhuyan, K., Tanyaş, H., Nava, L., Puliero, S., Meena, S. R., Floris, M., van Westen, C., & Catani, F. (2023). Generating multi-temporal landslide inventories through a general deep transfer learning strategy using HR EO data. *Scientific Reports*, *13*(1), 162. https://doi.org/10.1038/s41598-022-27352-y

Biçer, Ç. T., & Ercanoglu, M. (2020). A semi-quantitative landslide risk assessment of central Kahramanmaraş City in the Eastern Mediterranean region of Turkey. *Arabian Journal of Geosciences, 13*(15), 732. https://doi.org/10.1007/s12517-020-05697-w

Bilboe, W. (1998). The Thredbo landslide: was it only media ethics that came tumbling down? *Australian Journalism Review, 20*(2), 88–110. https://search.informit.org/doi/10.3316/ielapa.200006137

Birkmann, J. (2006a). Indicators and criteria for measuring vulnerability: Theoretical bases and requirements. In J. Birkmann (Ed.), *Measuring vulnerability to natural hazards: Towards disaster resilient societies* (1st ed., pp. 55–77). United Nations University Press.

Birkmann, J. (2006b). Measuring vulnerability to promote disaster-resilient societies: Conceptual frameworks and definitions. In J. Birkmann (Ed.), *Measuring vulnerability to natural hazards: Towards disaster resilient societies* (1st ed., pp. 9–54). United Nations University Press.

Birkmann, J. (2011). First- and second-order adaptation to natural hazards and extreme events in the context of climate change. *Natural Hazards*, *58*(2), 811–840. https://doi.org/10.1007/s11069-011-9806-8

Birkmann, J. (2013). Measuring vulnerability to promote disaster-resilient societies and to enhance adaptation: Discussion of conceptual frameworks and definitions. In J. Birkmann (Ed.), *Measuring vulnerability to natural hazards: Towards disaster resilient societies* (2nd ed., pp. 9–79). United Nations University Press.

Birkmann, J., Cardona, O. D., Carreño, M. L., Barbat, A. H., Pelling, M., Schneiderbauer, S., Kienberger, S., Keiler, M., Alexander, D., Zeil, P., & Welle, T. (2014). Theoretical and conceptual framework for the assessment of vulnerability to natural hazards and climate change in Europe: The MOVE framework. In J. Birkmann, S. Kienberger, & D. E. Alexander (Eds.), *Assessment of vulnerability to natural hazards: A European perspective* (pp. 1–19). Elsevier. https://doi.org/10.1016/B978-0-12-410528-7.00001-1

Birkmann, J., Cutter, S. L., Rothman, D. S., Welle, T., Garschagen, M., van Ruijven, B., O'Neill, B., Preston, B. L., Kienberger, S., Cordona, O. D., Siagian, T., Hidayati, D., Setiadi, N., Binder, C. R., Hughes, B., & Pulwarty, R. (2015). Scenarios for vulnerability: Opportunities and constraints in the context of climate change and disaster risk. *Climatic Change*, *133*, 53–68. https://doi.org/10.1007/s10584-013-0913-2

Birkmann, J., Garschagen, M., Fernando, N., Tuan, V. V., Oliver-Smith, A., & Hettige, S. (2013). Dynamics of vulnerability: Relocation in the context of natural hazards and disasters. In J. Birkmann (Ed.), *Measuring vulnerability to natural hazards: Towards disaster resilient societies* (2nd ed., pp. 505–550). United Nations University Press.

Birkmann, J., Sorg, L., & Welle, T. (2017). Disaster vulnerability. In M. Pompella & N. A. Scordis (Eds.), *The Palgrave handbook of unconventional risk transfer* (pp. 329–356). Palgrave Macmillan. https://doi.org/10.1007/978-3-319-59297-8_11

Biswas, S., & Nautiyal, S. (2023). A review of socio-economic vulnerability: The emergence of its theoretical concepts, models and methodologies. *Natural Hazards Research*, *3*(3), 563–571. https://doi.org/10.1016/j.nhres.2023.05.005

Blaikie, P., Cannon, T., Davis, I., & Wisner, B. (1994). *At risk: Natural hazards, people's vulnerability and disasters* (1st ed.). Routledge. https://doi.org/10.4324/9780203 974575

Blais-Stevens, A., & Septer, D. (2008). *Historical accounts of landslides and flooding events along the Sea to Sky Corridor, British Columbia, from 1855–2007* (Geological Survey of Canada Open File Report 5741). Geological Survey of Canada.

Blong, R. J. (1973). A numerical classification of selected landslides of the debris slide-avalanche-flow type. *Engineering Geology*, *7*(2), 99–114. https://doi.org/10.1016/0013-7952(73)90040-9

BMTPC (Building Materials and Technology Promotion Council). (2019). *Vulnerability atlas of India* (3rd ed.). Ministry of Housing and Urban Affairs, Government of India.

Bogaard, T. A., & Greco, R. (2016). Landslide hydrology: From hydrology to pore pressure. *Wiley Interdisciplinary Reviews: Water*, *3*(3), 439–459. https://doi.org/10.1002/wat2.1126

Bohle, H. G., Downing, T. E., & Watts, M. J. (1994). Climate change and social vulnerability: Toward a sociology and geography of food insecurity. *Global Environmental Change*, *4*(1), 37–48. https://doi.org/10.1016/0959-3780(94)90020-5

Bonham-Carter, G. (1994). *Geographic information systems for geoscientists: Modelling with GIS*. Elsevier. https://doi.org/10.1016/C2013-0-03864-9

Boruff, B. J., Emrich, C., & Cutter, S. L. (2005). Erosion hazard vulnerability of US coastal counties. *Journal of Coastal Research*, *21*(5), 932–942. https://doi.org/10.2112/04-0172.1

Brabb, E. E. (1984). Innovative approaches to landslide hazard mapping. *Proceedings of the 4th International Symposium on Landslides*, *1*, 307–324.

Brabb, E. E. (1995). The San Mateo County California GIS project for predicting the consequences of hazardous geologic processes. In A. Carrara & F. Guzzetti (Eds.), *Geographical information systems in assessing natural hazards* (pp. 299–334). Springer. https://doi.org/10.1007/978-94-015-8404-3_15

Brabb, E. E., & Pampeyan, E. H. (1972). *Preliminary map of landslide deposits in San Mateo County, California* (US Geological Survey Miscellaneous Field Studies Map 344). https://doi.org/10.3133/mf344

Brenning, A. (2005). Spatial prediction models for landslide hazards: Review, comparison and evaluation. *Natural Hazards and Earth System Sciences*, *5*(6), 853–862. https://doi.org/10.5194/nhess-5-853-2005

Brenning, A. (2012). Spatial cross-validation and bootstrap for the assessment of prediction rules in remote sensing: The R package sperrorest. *2012 IEEE International Geoscience and Remote Sensing Symposium*, 5372–5375. https://doi.org/10.1109/IGARSS.2012.6352393

Brooks, N. (2003). *Vulnerability, risk and adaptation: A conceptual framework* (Tyndall Centre Working Paper No. 38). Tyndall Centre for Climate Change Research.

Brown, C. D., & Davis, H. T. (2006). Receiver operating characteristics curves and related decision measures: A tutorial. *Chemometrics and Intelligent Laboratory Systems*, *80*(1), 24–38. https://doi.org/10.1016/j.chemolab.2005.05.004

Brown, L. M., Haun, J. N., & Peterson, L. (2014). A proposed disaster literacy model. *Disaster Medicine and Public Health Preparedness, 8*(3), 267–275. https://doi.org/10.1017/dmp.2014.43

Brunsden, D. (1984). Mudslides. In D. Brunsden & D. B. Prior (Eds.), *Slope instability* (pp. 363–418). John Wiley and Sons.

Buckle, P., Mars, G., & Smale, S. (2000). New approaches to assessing vulnerability and resilience. *The Australian Journal of Emergency Management*, *15*(2), 8–14. https://search.informit.org/doi/10.3316/ielapa.369155833780624

Bui, D. T, Pradhan, B., Lofman, O., & Revhaug, I. (2012a). Landslide susceptibility assessment in Vietnam using support vector machines, decision tree, and Naive Bayes models. *Mathematical Problems in Engineering*, *2012*(1), 974638. https://doi.org/10.1155/2012/974638

Bui, D. T., Lofman, O., Revhaug, I., & Dick, O. (2011). Landslide susceptibility analysis in the Hoa Binh province of Vietnam using statistical index and logistic regression. *Natural Hazards*, *59*, 1413–1444. https://doi.org/10.1007/s11069-011-9844-2

Bui, D. T., Pradhan, B., Lofman, O., Revhaug, I., & Dick, O. B. (2012b). Spatial prediction of landslide hazards in Hoa Binh province (Vietnam): A comparative assessment of the efficacy of evidential belief functions and fuzzy logic models. *CATENA*, *96*, 28–40. https://doi.org/10.1016/j.catena.2012.04.001

Bui, D. T., Pradhan, B., Lofman, O., Revhaug, I., & Dick, Ø. B. (2013). Regional prediction of landslide hazard using probability analysis of intense rainfall in the Hoa Binh province, Vietnam. *Natural Hazards, 66*(2), 707–730. https://doi.org/10.1007/s11069-012-0510-0

Bui, D. T., Tsangaratos, P., Nguyen, V. T., Van Liem, N., & Trinh, P. T. (2020). Comparing the prediction performance of a deep learning neural network model with conventional machine learning models in landslide susceptibility assessment. *CATENA*, *188*, 104426. https://doi.org/10.1016/j.catena.2019.104426

Burton, A., & Bathurst, J. C. (1998). Physically based modelling of shallow landslide sediment yield at a catchment scale. *Environmental Geology*, *35*, 89–99. https://doi.org/10.1007/s002540050296

Burton, C., Rufat, S., & Tate, E. (2018). Social vulnerability. In S. Fuchs & T. Thaler (Eds.), *Vulnerability and resilience to natural hazards* (pp. 53–81). Cambridge University Press. https://doi.org/10.1017/9781316651148

Burton, I., Kates, R. W., & White, G. F. (1993). *The environment as hazard* (2nd ed.). The Guilford Press.

Caleca, F., Lombardo, L., Steger, S., Tanyas, H., Raspini, F., Dahal, A., Nefros, C., Mărgărint, M. C., Drouin, V., Jemec-Auflič, M., Novellino, A., Tonini, M., Loche, M., Casagli, N., & Tofani, V. (2025). Pan-European landslide risk assessment: From theory to practice. *Reviews of Geophysics*, *63*(1), e2023RG000825. https://doi.org/10.1029/2023RG000825

Caleca, F., Scaini, C., Frodella, W., & Tofani, V. (2024). Regional-scale landslide risk assessment in Central Asia. *Natural Hazards and Earth System Sciences, 24*(1), 13–27. https://doi.org/10.5194/nhess-24-13-2024

Caleca, F., Tofani, V., Segoni, S., Raspini, F., Franceschini, R., & Rosi, A. (2022). How can landslide risk maps be validated? Potential solutions with open-source databases. *Frontiers in Earth Science*, *10*, 998885. https://doi.org/10.3389/feart.2022.998885

Caleca, F., Tofani, V., Segoni, S., Raspini, F., Rosi, A., Natali, M., Catani, F., & Casagli, N. (2022). A methodological approach of QRA for slow-moving landslides at a regional scale. *Landslides, 19*(7), 1539–1561. https://doi.org/10.1007/s10346-022-01875-x

Cao, Y., Wei, X., Fan, W., Nan, Y., Xiong, W., & Zhang, S. (2021). Landslide susceptibility assessment using the Weight of Evidence method: A case study in Xunyang area, China. *PLoS ONE*, *16*(1), e0245668. https://doi.org/10.1371/journal.pone.0245668

Cardellicchio, A., Ruggieri, S., Nettis, A., Renò, V., & Uva, G. (2023). Physical interpretation of machine learning-based recognition of defects for the risk management of existing bridge heritage. *Engineering Failure Analysis*, *149*, 107237. https://doi.org/10.1016/j.engfailanal.2023.107237

Cardinali, M., Reichenbach, P., Guzzetti, F., Ardizzone, F., Antonini, G., Galli, M., Cacciano, M., Castellani, M., & Salvati, P. (2002). A geomorphological approach to the estimation of landslide hazards and risks in Umbria, Central Italy. *Natural Hazards and Earth System Sciences*, *2*(1/2), 57–72. https://doi.org/10.5194/nhess-2-57-2002

Cardona, O. D. (1999). Environmental management and disaster prevention: Two related topics: A holistic risk assessment and management approach. In J. Ingleton (Ed.), *Natural disaster management* (pp. 151–153). Tudor Rose Holdings.

Cardona, O. D. (2004). The need for rethinking the concepts of vulnerability and risk from a holistic perspective: A necessary review and criticism for effective risk management. In G. Bankoff, G. Frerks, & D. Hilhorst (Eds.), *Mapping vulnerability: Disasters, development and people* (pp. 37–51). Routledge. https://doi.org/10.4324/9781849771924-4

Cardona, O. D., & Barbat, A. H. (2000). *El riesgo sísmico y su prevención* (Cuaderno Técnico 5). Calidad Siderúrgica.

Cardoso, A., Pereira, S., Ferreira, T. M., Zêzere, J. L., Melo, R., Vaz, T., Oliveira, S. C., Garcia, R. A. C., Santos, P. P., & Reis, E. (2023). On the physical vulnerability of buildings exposed to landslide hazards in the Lisbon Metropolitan Area. In T. M. Ferreira (Ed.), *Multi-risk interactions towards resilient and sustainable cities* (pp. 117–144). Springer. https://doi.org/10.1007/978-981-99-0745-8_7

Carrara, A. (1983). Multivariate models for landslide hazard evaluation. *Mathematical Geology*, *15*, 403–426. https://doi.org/10.1007/BF01031290

Carrara, A., Cardinali, M., Detti, R., Guzzetti, F., Pasqui, V., & Reichenbach, P. (1991). GIS techniques and statistical models in evaluating landslide hazard. *Earth Surface Processes and Landforms*, *16*(5), 427–445. https://doi.org/10.1002/esp.3290160505

Carrara, A., Cardinali, M., Guzzetti, F., & Reichenbach, P. (1995). GIS technology in mapping landslide hazard. In A. Carrara & F. Guzzetti (Eds.), *Geographical information systems in assessing natural hazards* (pp. 135–175). Springer. https://doi.org/10.1007/978-94-015-8404-3_8

Carson, M. A., & Kirkby, M. J. (1972). *Hillslope form and process*. Cambridge University Press.

Casagli, N., Frodella, W., Morelli, S., Tofani, V., Ciampalini, A., Intrieri, E., Raspini, F., Rossi, G., Tanteri, L., & Lu, P. (2017). Spaceborne, UAV and ground-based remote sensing techniques for landslide mapping, monitoring and early warning. *Geoenvironmental Disasters*, *4*, 9. https://doi.org/10.1186/s40677-017-0073-1

Casagli, N., Intrieri, E., Tofani, V., Gigli, G., & Raspini, F. (2023). Landslide detection, monitoring and prediction with remote-sensing techniques. *Nature Reviews Earth & Environment*, *4*(1), 51–64. https://doi.org/10.1038/s43017-022-00373-x

Cascini, L. (2008). Applicability of landslide susceptibility and hazard zoning at different scales. *Engineering Geology*, *102*(3-4), 164–177. https://doi.org/10.1016/j.enggeo.20 08.03.016

Cascini, L., Bonnard, C., Corominas, J., Jibson, R., & Montero-Olarte, J. (2005). Landslide hazard and risk zoning for urban planning and development. In O. Hungr, R. Fell, R. Couture, & E. Eberhardt (Eds.), *Landslide risk management* (1st ed., pp. 209–246). CRC Press. https://doi.org/10.1201/9781439833711-10

Catani, F., Lagomarsino, D., Segoni, S., & Tofani, V. (2013). Landslide susceptibility estimation by random forests technique: Sensitivity and scaling issues. *Natural Hazards and Earth System Sciences*, *13*(11), 2815–2831. https://doi.org/10.5194/nhess-13-2815-2013

Catani, F., Nava, L., & Bhuyan, K. (2025). Artificial intelligence applications for landslide mapping and monitoring on EO data. In I. Șandric, V. Ilinca, & Z. Chitu (Eds.), *Earth observation applications to landslide mapping, monitoring and modeling* (pp. 119–145). Elsevier. https://doi.org/10.1016/B978-0-12-823868-4.00007-6

Çellek, S. (2020). Morphological parameters causing landslides: A case study of elevation. *Bulletin of the Mineral Research and Exploration*, *162*(162), 197–224. https://doi.org/10.19111/bulletinofmre.649758

Census of India. (2011). *District census handbook: Aizawl*. Directorate of Census Operations, Government of India.

Chacón, J., Irigaray, C., Fernández, T., & El Hamdouni, R. (2006). Engineering geology maps: Landslides and geographical information systems. *Bulletin of Engineering Geology and the Environment*, *65*, 341–411. https://doi.org/10.1007/s10064-006-0064-z

Chakraborty, J., Tobin, G. A., & Montz, B. E. (2005). Population evacuation: Assessing spatial variability in geophysical risk and social vulnerability to natural hazards. *Natural Hazards Review*, *6*(1), 23–33. https://doi.org/10.1061/(ASCE)1527-6988(2005)6:1(23

Champati Ray, P. K., & Lakhera, R. C. (2004). *Landslide Hazards in India* [Paper presentation]. Asian Workshop on Regional Capacity Enhancement for Landslide Mitigation (RECLAIM), Bangkok, Thailand.

Chatterjee, B. (2009). Engineering geological aspect for urban development in three capital cities in North Eastern India. In M. G. Culshaw, H. J. Reeves, I. Jefferson, & T. W. Spink (Eds.), *Engineering geology for tomorrow's cities* (Paper No. 833). *Engineering Geology Special Publications*, *22*. Geological Society.

Chawla, A., Chawla, S., Pasupuleti, S., Rao, A. C. S., Sarkar, K., & Dwivedi, R. (2018). Landslide susceptibility mapping in Darjeeling Himalayas, India. *Advances in Civil Engineering*, *2018*(1), 6416492. https://doi.org/10.1155/2018/6416492

Chen, L., Xiang, X., Wen, H., Xiao, J., Song, C., Zhou, X., & Yu, J. (2024). Improve unsupervised learning-based landslides detection by band ratio processing of RGB optical images: A case study on rainfall-induced landslide clusters. *Geomatics, Natural Hazards and Risk*, *15*(1), 2363406. https://doi.org/10.1080/19475705.2024.2363406

Chen, Q., Chen, L., Gui, L., Yin, K., Shrestha, D. P., Du, J., & Cao, X. (2020). Assessment of the physical vulnerability of buildings affected by slow-moving landslides. *Natural Hazards and Earth System Sciences*, *20*(9), 2547–2565. https://doi.org/10.5194/nhess-20-2547-2020

Chen, W., Cutter, S. L., Emrich, C. T., & Shi, P. (2013). Measuring social vulnerability to natural hazards in the Yangtze River Delta region, China. *International Journal of Disaster Risk Science*, *4*(4), 169–181. https://doi.org/10.1007/s13753-013-0018-6

Chenkual, L. (2015). Some issues and concern from 2013 rockslide disaster at Laipuitlang, Aizawl, Mizoram, India. *Science Vision*, *15*(1), 34–38.

Chiarelli, D. D., Galizzi, M., Bocchiola, D., Rosso, R., & Rulli, M. C. (2023). Modeling snowmelt influence on shallow landslides in Tartano valley, Italian Alps. *Science of The Total Environment*, *856*(1), 158772. https://doi.org/10.1016/j.scitotenv.2022.158772

Chimidi, G., Raghuvanshi, T. K., & Suryabhagavan, K. V. (2017). Landslide hazard evaluation and zonation in and around Gimbi town, western Ethiopia—A GIS-based statistical approach. *Applied Geomatics*, *9*, 219–236. https://doi.org/10.1007/s12518-017-0195-x

Chorley, R. J., Schumm, S. A., & Sugden, D. E. (1984). *Geomorphology* (1st ed.). Routledge. https://doi.org/10.4324/9780429273636

Choubey, V. D. (1992). Landslide hazards and their mitigation in the Himalayan region. In D. H. Bell (Ed.), *Proceedings of the 6th International Symposium on Landslides*, (pp. 1849–1869). A. A. Balkema.

Chowdhury, J. R., & Parida, Y. (2023). Flood shocks and post-disaster recovery of households: An empirical analysis from rural Odisha, India. *International Journal of Disaster Risk Reduction, 97*, 104070. https://doi.org/10.1016/j.ijdrr.2023.104070

Chowdhury, R., & Flentje, P. (2003). Role of slope reliability analysis in landslide risk management. *Bulletin of Engineering Geology and the Environment, 62*(1), 41–46. https://doi.org/10.1007/s10064-002-0166-1

Chung, C.-J. F., & Fabbri, A. G. (1993). The representation of geoscience information for data integration. *Natural Resources Research*, *2*, 122–139. https://doi.org/10.1007/BF02272809

Chung, C.-J. F., & Fabbri, A. G. (1999). Probabilistic prediction models for landslide hazard mapping. *Photogrammetric Engineering and Remote Sensing*, *65*(12), 1389–1399.

Chung, C.-J. F., & Fabbri, A. G. (2003). Validation of spatial prediction models for landslide hazard mapping. *Natural Hazards, 30*, 451–472. https://doi.org/10.1023/B:NHAZ.0000007172.62651.2b

Chung, C.-J. F., & Fabbri, A. G. (2005). Systematic procedures of landslide hazard mapping for risk assessment using spatial prediction models. In T. Glade, M. G. Anderson, & M. J. Crozier (Eds.), *Landslide hazard and risk* (pp. 139–174). John Wiley & Sons Ltd. https://doi.org/10.1002/9780470012659.ch4

Ciurean, R. L., Schröter, D., & Glade, T. (2013). Conceptual frameworks of vulnerability assessments for natural disasters reduction. In J. P. Tiefenbacher (Ed.), *Approaches to disaster management - Examining the implications of hazards, emergencies and disasters* (pp. 1–32). Intech. https://doi.org/10.5772/55538

Clark, G. E., Moser, S. C., Ratick, S. J., Dow, K., Meyer, W. B., Emani, S., Jin, W., Kasperson, J. X., Kasperson, R. E., & Schwarz, H. E. (1998). Assessing the vulnerability of coastal communities to extreme storms: The case of Revere, MA., USA. *Mitigation and Adaptation Strategies for Global Change, 3*(1), 59–82. https://doi.org/10.1023/A:1009609710795

Coates, D. R. (1977). Landslide perspectives. In D. R. Coates (Ed.), *Reviews in engineering geology* (Vol. 3, pp. 3–28). Geological Society of America. https://doi.org/10.1130/REG3-p3

Cohen, D., & Schwarz, M. (2017). Tree-root control of shallow landslides. *Earth Surface Dynamics*, *5*(3), 451–477. https://doi.org/10.5194/esurf-5-451-2017

Cohen, J. (1960). A coefficient of agreement for nominal scales. *Educational and Psychological Measurement*, *20*(1), 37–46. https://doi.org/10.1177/001316446002000104

Collini, E., Palesi, L. I., Nesi, P., Pantaleo, G., Nocentini, N., & Rosi, A. (2022). Predicting and understanding landslide events with explainable AI. *IEEE Access*, *10*, 31175–31189. https://doi.org/10.1109/ACCESS.2022.3158328

Coluzzi, R., Perrone, A., Samela, C., Imbrenda, V., Manfreda, S., Pace, L., & Lanfredi, M. (2025). Rapid landslide detection from free optical satellite imagery using a robust change detection technique. *Scientific Reports*, *15*(1), 4697. https://doi.org/10.1038/s41598-025-89542-8

Corominas, J., Einstein, H., Davis, T., Strom, A., Zuccaro, G., Nadim, F., & Verdel, T. (2015). Glossary of terms on landslide hazard and risk. In G. Lollino, D. Giordan, G. B. Crosta, J. Corominas, R. Azzam, J. Wasowski, & N. Sciarra (Eds.), *Engineering Geology for Society and Territory* (Volume 2, pp. 1775–1779). Springer. https://doi.org/10.1007/978-3-319-09057-3_314

Corominas, J., Guzzetti, F., Lan, H., Macciotta, R., Marunteranu, C., McDougall, S., & Strom, A. (2023). Revisiting landslide risk terms: IAEG commission C-37 working group on landslide risk nomenclature. *Bulletin of Engineering Geology and the Environment*, *82*(12), 450. https://doi.org/10.1007/s10064-023-03474-z

Corominas, J., van Westen, C., Frattini, P., Cascini, L., Malet, J. -P., Fotopoulou, S., Catani, F., van Den Eeckhaut, M., Mavrouli, O., Agliardi, F., Pitilakis, K., Winter, M. G., Pastor, M., Ferlisi, S., Tofani, V., Hervás, J., & Smith, J. T. (2014). Recommendations for the quantitative analysis of landslide risk. *Bulletin of Engineering Geology and the Environment*, *73*, 209–263. https://doi.org/10.1007/s10064-013-0538-8

Crawford, M. M., Dortch, J. M., Koch, H. J., Zhu, Y., Haneberg, W. C., Wang, Z., & Bryson, L. S. (2022). Landslide risk assessment in Eastern Kentucky, USA: Developing a regional scale, limited resource approach. *Remote Sensing, 14*(24), 6246. https://doi.org/10.3390/rs14246246

Cross, M. (1998). Landslide susceptibility mapping using the matrix assessment approach: A Derbyshire case study. In J. G. Maund & M. Eddleston (Eds.), *Geohazards in engineering geology* (Vol. 15, pp. 247–261). The Geological Society. https://doi.org/10.1144/GSL.ENG.1998.015.01.26

Crosta, G. B., & Frattini, P. (2003). Distributed modelling of shallow landslides triggered by intense rainfall. *Natural Hazards and Earth System Sciences*, *3*(1/2), 81–93. https://doi.org/10.5194/nhess-3-81-2003

Crozier, M. J. (1973). Techniques for the morphometric analysis of landslips. *Zeitschrift für Geomorphologie*, *17*(1), 78–101. https://doi.org/10.1127/zfg/17/1973/78

Crozier, M. J. (1986). *Landslides: Causes, consequences and environment*. Croom Helm. https://doi.org/10.5555/19871915008

Crozier, M. J. (2005). Management frameworks for landslide hazard and risk: Issues and options. In T. Glade, M. Anderson, & M. J. Crozier (Eds.), *Landslide hazard and risk* (pp. 329–350). John Wiley & Sons Ltd. https://doi.org/10.1002/9780470012659.ch11

Crozier, M. J., & Glade, T. (2005). Landslide hazard and risk: Issues, concepts and approach. In T. Glade, M. Anderson, & M. J. Crozier (Eds.), *Landslide hazard and risk* (pp. 1–40). John Wiley & Sons Ltd. https://doi.org/10.1002/9780470012659.ch1

Cruden, D. M. (1991). A simple definition of a landslide. *Bulletin of the International Association of Engineering Geology*, *43*, 27–29. https://doi.org/10.1007/BF02590167

Cruden, D. M. (1997). Estimating the risks from landslides using historical data. In D. M. Cruden & R. Fell (Eds.), *Landslide risk assessment* (1st ed., pp. 177–184). Routledge. https://doi.org/10.1201/9780203749524-8

Cruden, D. M. (2003). The first classification of landslides? *Environmental & Engineering Geoscience*, *9*(3), 197–200. https://doi.org/10.2113/9.3.197

Cruden, D. M., & Varnes, D. J. (1996). Landslide types and processes. In A. K. Turner & R. L. Schuster (Eds.), *Landslides: Investigation and mitigation* (Transportation Research Board Special Report 247, pp. 36–75). National Academy of Sciences.

Cutter, S. L. (1993). *Living with risk: The geography of technological hazards*. Edward Arnold.

Cutter, S. L. (1996). Vulnerability to environmental hazards. *Progress in Human Geography*, *20*(4), 529–539. https://doi.org/10.1177/030913259602000407

Cutter, S. L. (2024). The origin and diffusion of the social vulnerability index (SoVI). *International Journal of Disaster Risk Reduction*, *109*, 104576. https://doi.org/10.1016/j.ijdrr.2024.104576

Cutter, S. L., & Emrich, C. T. (2006). Moral hazard, social catastrophe: The changing face of vulnerability along the hurricane coasts. *The ANNALS of the American Academy of Political and Social Science*, *604*(1), 102–112. https://doi.org/10.1177/0002716205285515

Cutter, S. L., & Finch, C. (2008). Temporal and spatial changes in social vulnerability to natural hazards. *Proceedings of the National Academy of Sciences*, *105*(7), 2301–2306. https://doi.org/10.1073/pnas.0710375105

Cutter, S. L., & Morath, D. P. (2013). The evolution of the Social Vulnerability Index (SoVI). In J. Birkmann (Ed.), *Measuring vulnerability to natural hazards: Towards disaster resilient societies* (2nd ed., pp. 304–321). United Nations University Press.

Cutter, S. L., Boruff, B. J., & Shirley, W. L. (2003). Social vulnerability to environmental hazards. *Social Science Quarterly*, *84*(2), 242–261. https://doi.org/10.1111/1540-6237.8402002

Cutter, S. L., Mitchell, J. T., & Scott, M. S. (2000). Revealing the vulnerability of people and places: A case study of Georgetown County, South Carolina. *Annals of the Association of American Geographers*, *90*(4), 713–737. https://doi.org/10.1111/0004-5608.00219

Dahal, A., & Lombardo, L. (2023). Explainable artificial intelligence in geoscience: A glimpse into the future of landslide susceptibility modeling. *Computers & Geosciences*, *176*, 105364. https://doi.org/10.1016/j.cageo.2023.105364

Dahal, A., Tanyas, H., van Westen, C., van der Meijde, M., Mai, P. M., Huser, R., & Lombardo, L. (2024). Space–time landslide hazard modeling via Ensemble Neural Networks. *Natural Hazards and Earth System Sciences*, *24*(3), 823–845. https://doi.org/10.5194/nhess-24-823-2024

Dai, F. C., & Lee, C. F. (2002). Landslide characteristics and slope instability modeling using GIS, Lantau Island, Hong Kong. *Geomorphology*, *42*(3-4), 213–228. https://doi.org/10.1016/S0169-555X(01)00087-3

Dai, F. C., Lee, C. F., & Ngai, Y. Y. (2002). Landslide risk assessment and management: An overview. *Engineering Geology*, *64*(1), 65–87. https://doi.org/10.1016/S0013-7952(01)00093-X

Dai, F. C., Lee, C. F., Li, J., & Xu, Z. W. (2001). Assessment of landslide susceptibility on the natural terrain of Lantau Island, Hong Kong. *Environmental Geology*, *40*, 381–391. https://doi.org/10.1007/s002540000163

Das, S., Sarkar, S., & Kanungo, D. P. (2022). GIS-based landslide susceptibility zonation mapping using the analytic hierarchy process (AHP) method in parts of Kalimpong Region of Darjeeling Himalaya. *Environmental Monitoring and Assessment*, *194*(4), 234. https://doi.org/10.1007/s10661-022-09851-7

Das, S., Sarkar, S., & Kanungo, D. P. (2023). A critical review on landslide susceptibility zonation: Recent trends, techniques, and practices in Indian Himalaya. *Natural Hazards*, *115*(1), 23–72. https://doi.org/10.1007/s11069-022-05554-x

De Graff, J. V., Romesburg, H. C., Ahmad, R., & McCalpin, J. P. (2012). Producing landslide-susceptibility maps for regional planning in data-scarce regions. *Natural Hazards*, *64*, 729–749. https://doi.org/10.1007/s11069-012-0267-5

de León, J. C. V. (2007). Vulnerability assessment: The sector approach. In J. Birkmann (Ed.), *Measuring vulnerability to natural hazards: Towards disaster resilient societies* (1st ed., pp. 300–315). United Nations University Press.

de Loyola Hummell, B. M., Cutter, S. L., & Emrich, C. T. (2016). Social vulnerability to natural hazards in Brazil. *International Journal of Disaster Risk Science*, *7*(2), 111–122. https://doi.org/10.1007/s13753-016-0090-9

de Oliveira Mendes, J. M. (2009). Social vulnerability indexes as planning tools: Beyond the preparedness paradigm. *Journal of Risk Research*, *12*(1), 43–58. https://doi.org/10.1080/13669870802447962

Del Zoppo, M., Di Ludovico, M., & Prota, A. (2022). A mechanics-based method towards risk assessment of RC buildings under tsunami and flow-type hazards. *Engineering Structures*, *264*, 114452. https://doi.org/10.1016/j.engstruct.2022.114452

Deng, X., Li, L., & Tan, Y. (2017). Validation of spatial prediction models for landslide susceptibility mapping by considering structural similarity. *ISPRS International Journal of Geo-Information*, *6*(4), 103. https://doi.org/10.3390/ijgi6040103

Deria, A., Ghannad, P., & Lee, Y. C. (2020). Evaluating implications of flood vulnerability factors with respect to income levels for building long-term disaster resilience of low-income communities. *International Journal of Disaster Risk Reduction, 48*, 101608. https://doi.org/10.1016/j.ijdrr.2020.101608

Devkota, K. C., Regmi, A. D., Pourghasemi, H. R., Yoshida, K., Pradhan, B., Ryu, I. C., Dhital, M. R., & Althuwaynee, O. F. (2013). Landslide susceptibility mapping using certainty factor, index of entropy and logistic regression models in GIS and their comparison at Mugling–Narayanghat road section in Nepal Himalaya. *Natural Hazards*, *65*, 135–165. https://doi.org/10.1007/s11069-012-0347-6

Dietrich, W. E., Reiss, R., Hsu, M.-L., & Montgomery, D. R. (1995). A process-based model for colluvial soil depth and shallow landsliding using digital elevation data. *Hydrological Processes*, *9*, 383–400. https://doi.org/10.1002/hyp.3360090311

Dikau, R., Brunsden, D., Schrott, L., & Ibsen, M.-L. (1996). *Landslide recognition, identification, movement and causes*. John Wiley and Sons.

Dikshit, A., Sarkar, R., Pradhan, B., Acharya, S., & Alamri, A. M. (2020b). Spatial landslide risk assessment at Phuentsholing, Bhutan. *Geosciences, 10*(4), 131. https://doi.org/10.3390/geosciences10040131

Dikshit, A., Sarkar, R., Pradhan, B., Segoni, S., & Alamri, A. M. (2020a). Rainfall Induced Landslide Studies in Indian Himalayan Region: A Critical Review. *Applied Sciences*, *10*(7), 2466. https://doi.org/10.3390/app10072466

Ding, D., Wu, Y., Wu, T., & Gong, C. (2025). Landslide susceptibility assessment in Tongguan District Anhui China using information value and certainty factor models. *Scientific Reports*, *15*(1), 12275. https://doi.org/10.1038/s41598-025-93704-z

Dinpuia, L. (2019). Cut slope stability analysis of Rangvamual landslide along Aizawl Airport Road, Northeast India. In S. Hemeda & M. Bouassida (Eds.), *Contemporary issues in soil mechanics* (pp. 185–193). Springer. https://doi.org/10.1007/978-3-030-01941-9_16

DM&R. (2020). *State Disaster Management Plan (SDMP) 2020*. Directorate of Disaster Management & Rehabilitation, Government of Mizoram.

DM&R. (2023). *State Disaster Management Plan (SDMP) 2023*. Directorate of Disaster Management & Rehabilitation, Government of Mizoram.

DoE (Department of the Environment). (1995). *A guide to risk assessment and risk management for environmental protection*. H.M. Stationery Office.

Domakinis, C., Oikonomidis, D., & Astaras, T. (2008). Landslide mapping in the coastal area between the Strymonic Gulf and Kavala (Macedonia, Greece) with the aid of remote sensing and geographical information systems. *International Journal of Remote Sensing*, *29*(23), 6893–6915. https://doi.org/10.1080/01431160802082130

Dorairaj, D., & Osman, N. (2021). Present practices and emerging opportunities in bioengineering for slope stabilization in Malaysia: An overview. *PeerJ*, *9*, e10477. https://doi.org/10.7717/peerj.10477

Dou, J., Yunus, A. P., Bui, D. T., Merghadi, A., Sahana, M., Zhu, Z., Chen, C. W., Khosravi, K., Yang, Y., & Pham, B. T. (2019). Assessment of advanced random forest and decision tree algorithms for modeling rainfall-induced landslide susceptibility in the Izu-Oshima Volcanic Island, Japan. *Science of The Total Environment*, *662*, 332–346. https://doi.org/10.1016/j.scitotenv.2019.01.221

Douglas, J. (2007). Physical vulnerability modelling in natural hazard risk assessment. *Natural Hazards and Earth System Sciences*, *7*(2), 283–288. https://doi.org/10.5194/nhess-7-283-2007

Dow, K. (1992). Exploring differences in our common future(s): The meaning of vulnerability to global environmental change. *Geoforum*, *23*(3), 417–436. https://doi.org/10.1016/0016-7185(92)90052-6

Drakes, O., & Tate, E. (2022). Social vulnerability in a multi-hazard context: A systematic review. *Environmental Research Letters*, *17*(3), 033001. https://doi.org/10.1088/1748-9326/ac5140

Dwyer, A., Zoppou, C., Nielsen, O., Day, S., & Roberts, S. (2004). *Quantifying social vulnerability: A methodology for identifying those at risk to natural hazards* (Record 2004/14). Geoscience Australia.

Eakin, H., & Luers, A. L. (2006). Assessing the vulnerability of social-environmental systems. *Annual Review of Environment and Resources*, *31*(1), 365–394. https://doi.org/10.1146/annurev.energy.30.050504.144352

Ebrahim, K. M. P., Gomaa, S. M. M. H., Zayed, T., & Alfalah, G. (2024). Rainfall-induced landslide prediction models, part II: Deterministic physical and phenomenologically models. *Bulletin of Engineering Geology and the Environment*, *83*(3), 85. https://doi.org/10.1007/s10064-024-03563-7

Ehrlich, D., Kemper, T., Pesaresi, M., & Corbane, C. (2018). Built-up area and population density: Two essential societal variables to address climate hazard impact. *Environmental Science & Policy, 90*, 73–82. https://doi.org/10.1016/j.envsci.2018.10.001

Eidsvig, U. M. K., McLean, A., Vangelsten, B. V., Kalsnes, B., Ciurean, R. L., Argyroudis, S., Winter, M. G., Mavrouli, O. C., Fotopoulou, S., Pitilakis, K., Baills, A., Malet, J.-P., & Kaiser, G. (2014). Assessment of socioeconomic vulnerability to landslides using an indicator-based approach: Methodology and case studies. *Bulletin of Engineering Geology and the Environment*, *73*(2), 307–324. https://doi.org/10.1007/s10064-014-0571-2

Einstein, H. H. (1988). Landslide risk assessment procedure. In C. Bonnard (Ed.), *Proceedings of the Fifth International Symposium on Landslides* (Vol. 2, pp. 1075–1089). A.A. Balkema.

EM-DAT. (2025). The OFDA/CRED International Disaster Database. Centre for Research on the Epidemiology of Disasters (CRED), Université catholique de Louvain. https://www.emdat.be (retrieved on 22 January, 2025).

Ercanoglu, M., & Gokceoglu, C. (2002). Assessment of landslide susceptibility for a landslide-prone area (north of Yenice, NW Turkey) by fuzzy approach. *Environmental Geology*, *41*, 720–730. https://doi.org/10.1007/s00254-001-0454-2

Ercanoglu, M., & Sonmez, H. (2018). General trends and new perspectives on landslide mapping and assessment methods. In N. Ceryan (Ed.), *Handbook of research on trends and digital advances in engineering geology* (pp. 350–379). IGI Global. https://doi.org/10.4018/978-1-5225-2709-1.ch010

Erener, A., & Düzgün, H. S. B. (2012). Landslide susceptibility assessment: What are the effects of mapping unit and mapping method? *Environmental Earth Sciences*, *66*, 859–877. https://doi.org/10.1007/s12665-011-1297-0

Erener, A., Mutlu, A., & Düzgün, H. S. (2016). A comparative study for landslide susceptibility mapping using GIS-based multi-criteria decision analysis (MCDA), logistic regression (LR) and association rule mining (ARM). *Engineering Geology*, *203*, 45–55. https://doi.org/10.1016/j.enggeo.2015.09.007

Ermini, L., Catani, F., & Casagli, N. (2005). Artificial neural networks applied to landslide susceptibility assessment. *Geomorphology*, *66*(1-4), 327–343. https://doi.org/10.1016/j.geomorph.2004.09.025

Erskine, C. F. (1973). *Landslides in the vicinity of the Fort Randall Reservoir, South Dakota* (Geological Survey Professional Paper 675). U.S. Government Printing Office.

Espizua, L. E., & Bengochea, J. D. (2002). Landslide hazard and risk zonation mapping in the Rio Grande Basin, Central Andes of Mendoza, Argentina. *Mountain Research and Development*, *22*(2), 177–185. https://doi.org/10.1659/0276-4741(2002)022[0177:LHARZM]2.0.CO;2

Fan, L., Kuang, X., Ouyang, C., Chen, K., & Zheng, C. (2025). Climatic controls on hydrological landslide triggering in the northern Himalayas. *Water Resources Research*, *61*(2), e2024WR039611. https://doi.org/10.1029/2024WR039611

Fang, H. Y., & Guo, M. (2015). Aspect-induced differences in soil erosion intensity in a gullied hilly region on the Chinese Loess Plateau. *Environmental Earth Sciences*, *74*(7), 5677–5685. https://doi.org/10.1007/s12665-015-4648-4

Fekete, A., & Montz, B. (2018). Vulnerability: An introduction. In S. Fuchs & T. Thaler (Eds.), *Vulnerability and resilience to natural hazards* (pp. 14–31). Cambridge University Press. https://doi.org/10.1017/9781316651148

Fekete, A., Hufschmidt, G., & Kruse, S. (2014). Benefits and challenges of resilience and vulnerability for disaster risk management. *International Journal of Disaster Risk Science*, *5*, 3–20. https://doi.org/10.1007/s13753-014-0008-3

Fell, R. (1994). Landslide risk assessment and acceptable risk. *Canadian Geotechnical Journal*, *31*(2), 261–272. https://doi.org/10.1139/t94-031

Fell, R., & Hartford, D. (1997). Landslide risk management. In D. Cruden & R. Fell (Eds.), *Landslide Risk Assessment* (pp. 51–109). Routledge. https://doi.org/10.1201/97802 03749524-4

Fell, R., Chapman, T. G., & Maguire, P. K. (1991). A model for prediction of piezometric levels in landslides. In R. J. Chandler (Ed.), *Slope stability engineering developments and applications: Proceedings of the international conference on slope stability* (pp. 37–42). Thomas Telford Publishing. https://doi.org/10.1680/ssedaa.16606.0007

Fell, R., Corominas, J., Bonnard, C., Cascini, L., Leroi, E., Savage, W. Z., & JTC-1 Joint Technical Committee on Landslides and Engineered Slopes. (2008). Guidelines for landslide susceptibility, hazard and risk zoning for land use planning. *Engineering Geology*, *102*(3-4), 85–98. https://doi.org/10.1016/j.enggeo.2008.03.022

Fell, R., Ho, K. K. S., Lacasse, S., & Leroi, E. (2005). A framework for landslide risk assessment and management. In O. Hungr, R. Fell, R. Couture, & E. Eberhardt (Eds.), *Landslide risk management* (1st ed., pp. 13–36). CRC Press. https://doi.org/10.1201/9781439833711-4

Fernández, T., Irigaray, C., El Hamdouni, R., & Chacón, J. (2003). Methodology for landslide susceptibility mapping by means of a GIS. Application to the Contraviesa area (Granada, Spain). *Natural Hazards*, *30*, 297–308. https://doi.org/10.1023/B:NHAZ.0000007092.51910.3f

Fernández, T., Pérez-García, J. L., Gómez-López, J. M., Cardenal, J., Moya, F., & Delgado, J. (2021). Multitemporal landslide inventory and activity analysis by means of aerial photogrammetry and LiDAR techniques in an area of southern Spain. *Remote Sensing*, *13*(11), 2110. https://doi.org/10.3390/rs13112110

Few, R. (2007). Health and climatic hazards: Framing social research on vulnerability, response and adaptation. *Global Environmental Change*, *17*(2), 281–295. https://doi.org/10.1016/j.gloenvcha.2006.11.001

Finch, C., Emrich, C. T., & Cutter, S. L. (2010). Disaster disparities and differential recovery in New Orleans. *Population and Environment*, *31*(4), 179–202. https://doi.org/10.1007/s11111-009-0099-8

Fiorucci, F., Cardinali, M., Carlà, R., Rossi, M., Mondini, A. C., Santurri, L., Ardizzone, F., & Guzzetti, F. (2011). Seasonal landslide mapping and estimation of landslide mobilization rates using aerial and satellite images. *Geomorphology*, *129*(1-2), 59–70. https://doi.org/10.1016/j.geomorph.2011.01.013

Fleuchaus, P., Blum, P., Wilde, M., Terhorst, B., & Butscher, C. (2021). Retrospective evaluation of landslide susceptibility maps and review of validation practice. *Environmental Earth Sciences*, *80*, 485. https://doi.org/10.1007/s12665-021-09770-9

Fothergill, A. (1996). Gender, risk, and disaster. *International Journal of Mass Emergencies & Disasters, 14*(1), 33–56. https://doi.org/10.1177/028072709601400103

Fotopoulou, S. D., & Pitilakis, K. D. (2017). Vulnerability assessment of reinforced concrete buildings at precarious slopes subjected to combined ground shaking and earthquake induced landslide. *Soil Dynamics and Earthquake Engineering*, *93*, 84–98. https://doi.org/10.1016/j.soildyn.2016.12.007

Frattini, P., Crosta, G., & Carrara, A. (2010). Techniques for evaluating the performance of landslide susceptibility models. *Engineering Geology*, *111*(1-4), 62–72. https://doi.org/10.1016/j.enggeo.2009.12.004

Frerks, G., Warner, J., & Weijs, B. (2011). The politics of vulnerability and resilience. *Ambiente & Sociedade*, *14*(2), 105–122. https://doi.org/10.1590/S1414-753X2011000200008

Frigerio, I., & De Amicis, M. (2016). Mapping social vulnerability to natural hazards in Italy: A suitable tool for risk mitigation strategies. *Environmental Science & Policy*, *63*, 187–196. https://doi.org/10.1016/j.envsci.2016.06.001

Froude, M. J., & Petley, D. N. (2018). Global fatal landslide occurrence from 2004 to 2016. *Natural Hazards and Earth System Sciences*, *18*(8), 2161–2181. https://doi.org/10.5194/nhess-18-2161-2018

Fuchs, S. (2009). Susceptibility versus resilience to mountain hazards in Austria—paradigms of vulnerability revisited. *Natural Hazards and Earth System Sciences*, *9*(2), 337–352. https://doi.org/10.5194/nhess-9-337-2009

Fuchs, S., & Thaler, T. (Eds.). (2018). *Vulnerability and resilience to natural hazards*. Cambridge University Press.

Fuchs, S., Birkmann, J., & Glade, T. (2012). Vulnerability assessment in natural hazard and risk analysis: Current approaches and future challenges. *Natural Hazards*, *64*, 1969–1975. https://doi.org/10.1007/s11069-012-0352-9

Fuchs, S., Frazier, T., & Siebeneck, L. (2018). Physical vulnerability. In S. Fuchs & T. Thaler (Eds.), *Vulnerability and resilience to natural hazards* (pp. 32–52). Cambridge University Press. https://doi.org/10.1017/9781316651148

Fuchs, S., Heiss, K., & Hübl, J. (2007). Towards an empirical vulnerability function for use in debris flow risk assessment. *Natural Hazards and Earth System Sciences*, *7*(5), 495–506. https://doi.org/10.5194/nhess-7-495-2007

Fuchs, S., Keiler, M., Ortlepp, R., Schinke, R., & Papathoma-Köhle, M. (2019). Recent advances in vulnerability assessment for the built environment exposed to torrential hazards: Challenges and the way forward. *Journal of Hydrology*, *575*, 587–595. https://doi.org/10.1016/j.jhydrol.2019.05.067

Fuchs, S., Kuhlicke, C., & Meyer, V. (2011). Editorial for the special issue: Vulnerability to natural hazards—the challenge of integration. *Natural Hazards*, *58*, 609–619. https://doi.org/10.1007/s11069-011-9825-5

Füssel, H. M. (2007). Vulnerability: A generally applicable conceptual framework for climate change research. *Global Environmental Change*, *17*(2), 155–167. https://doi.org/10.1016/j.gloenvcha.2006.05.002

Gabor, T., & Griffith, T. K. (1980). The assessment of community vulnerability to acute hazardous materials incidents. *Journal of Hazardous Materials*, *3*(4), 323–333. https://doi.org/10.1016/0304-3894(80)80004-5

Galli, M., & Guzzetti, F. (2007). Landslide vulnerability criteria: A case study from Umbria, Central Italy. *Environmental Management*, *40*(4), 649–665. https://doi.org/10.1007/s00267-006-0325-4

Galli, M., Ardizzone, F., Cardinali, M., Guzzetti, F., & Reichenbach, P. (2008). Comparing landslide inventory maps. *Geomorphology*, *94*(3-4), 268–289. https://doi.org/10.1016/j.geomorph.2006.09.023

Ganesh, B., Vincent, S., Pathan, S., & Benitez, S. R. G. (2023). Machine learning based landslide susceptibility mapping models and GB-SAR based landslide deformation monitoring systems: Growth and evolution. *Remote Sensing Applications: Society and Environment*, *29*, 100905. https://doi.org/10.1016/j.rsase.2022.100905

Gee, M. D. (1992). Classification of landslide hazard zonation methods and a test of predictive capability. In D. H. Bell (Ed.), *Proceedings of the 6th International Symposium on Landslides*, (Vol. 2, pp. 947–952). A. A. Balkema.

Gems, B., Mazzorana, B., Hofer, T., Sturm, M., Gabl, R., & Aufleger, M. (2016). 3-D hydrodynamic modelling of flood impacts on a building and indoor flooding processes. *Natural Hazards and Earth System Sciences*, *16*(6), 1351–1368. https://doi.org/10.5194/nhess-16-1351-2016

Ghorbanzadeh, O., Blaschke, T., Gholamnia, K., Meena, S. R., Tiede, D., & Aryal, J. (2019). Evaluation of different machine learning methods and deep-learning convolutional neural networks for landslide detection. *Remote Sensing*, *11*(2), 196. https://doi.org/10.3390/rs11020196

Ghorbanzadeh, O., Gholamnia, K., & Ghamisi, P. (2022a). Landslide detection using deep learning and object-based image analysis. *Landslides*, *19*(4), 929–939. https://doi.org/10.1007/s10346-021-01843-x

Ghorbanzadeh, O., Gholamnia, K., & Ghamisi, P. (2022b). The application of ResU-net and OBIA for landslide detection from multi-temporal Sentinel-2 images. *Big Earth Data*, *7*(4), 961–985. https://doi.org/10.1080/20964471.2022.2031544

Ghosh, S., Carranza, E. J. M., van Westen, C. J., Jetten, V. G., & Bhattacharya, D. N. (2011). Selecting and weighting spatial predictors for empirical modeling of landslide susceptibility in the Darjeeling Himalayas (India). *Geomorphology*, *131*(1-2), 35–56. https://doi.org/10.1016/j.geomorph.2011.04.019

Ghosh, S., van Westen, C. J., Carranza, E. J. M., & Jetten, V. G. (2012). Integrating spatial, temporal, and magnitude probabilities for medium-scale landslide risk analysis in Darjeeling Himalayas, India. *Landslides, 9*(3), 371–384. https://doi.org/10.1007/s10346-011-0304-6

Ghosh, S., van Westen, C. J., Carranza, E. J. M., Jetten, V. G., Cardinali, M., Rossi, M., & Guzzetti, F. (2012). Generating event-based landslide maps in a data-scarce Himalayan environment for estimating temporal and magnitude probabilities. *Engineering Geology, 128*, 49–62. https://doi.org/10.1016/j.enggeo.2011.03.016

Gigović, L., Drobnjak, S., & Pamučar, D. (2019). The application of the hybrid GIS spatial multi-criteria decision analysis best–worst methodology for landslide susceptibility mapping. *ISPRS International Journal of Geo-Information*, *8*(2), 79. https://doi.org/10.3390/ijgi8020079

Glade, T. (1998). Establishing the frequency and magnitude of landslide-triggering rainstorm events in New Zealand. *Environmental Geology*, *35*, 160–174. https://doi.org/10.1007/s002540050302

Glade, T. (2003). Landslide occurrence as a response to land use change: A review of evidence from New Zealand. *CATENA*, *51*(3-4), 297–314. https://doi.org/10.1016/S0341-8162(02)00170-4

Glade, T., & Crozier, M. J. (2005). The nature of landslide hazard impact. In T. Glade, M. Anderson, & M. J. Crozier (Eds.), *Landslide hazard and risk* (pp. 41–74). John Wiley & Sons. https://doi.org/10.1002/9780470012659.ch2

Godfrey, A., Ciurean, R. L., van Westen, C. J., Kingma, N. C., & Glade, T. (2015). Assessing vulnerability of buildings to hydro-meteorological hazards using an expert based approach–An application in Nehoiu Valley, Romania. *International Journal of Disaster Risk Reduction*, *13*, 229–241. https://doi.org/10.1016/j.ijdrr.2015.06.001

Godt, J. W., Baum, R. L., Savage, W. Z., Salciarini, D., Schulz, W. H., & Harp, E. L. (2008). Transient deterministic shallow landslides modeling: Requirements for susceptibility and hazard assessments in a GIS framework. *Engineering Geology*, *102*(3–4), 214–226. https://doi.org/10.1016/j.enggeo.2008.03.019

Goetz, J. N., Brenning, A., Petschko, H., & Leopold, P. (2015). Evaluating machine learning and statistical prediction techniques for landslide susceptibility modeling. *Computers & Geosciences*, *81*, 1–11. https://doi.org/10.1016/j.cageo.2015.04.007

Gökceoglu, C., & Aksoy, H. (1996). Landslide susceptibility mapping of the slopes in the residual soils of the Mengen region (Turkey) by deterministic stability analyses and image processing techniques. *Engineering Geology*, *44*(1-4), 147–161. https://doi.org/10.1016/S0013-7952(97)81260-4

Goodchild, M. F. (2011). Scale in GIS: An overview. *Geomorphology*, *130*(1-2), 5–9. https://doi.org/10.1016/j.geomorph.2010.10.004

Gorsevski, P. V., Gessler, P. E., Foltz, R. B., & Elliot, W. J. (2006). Spatial prediction of landslide hazard using logistic regression and ROC analysis. *Transactions in GIS*, *10*(3), 395–415. https://doi.org/10.1111/j.1467-9671.2006.01004.x

Goto, E. A., Suarez, A. M., & Ye, H. (2022). Spatial analysis of social vulnerability in São Paulo city, Brazil. *Applied Geography*, *140*, 102653. https://doi.org/10.1016/j.apgeog.2022.102653

Greenway, D. R. (1987). Vegetation and slope stability. In M. G. Anderson & K. S. Richards (Eds.), *Slope stability: Geotechnical engineering and geomorphology* (pp. 187–230). John Wiley & Sons.

Guha, P., & Adak, K. (2014). Gender influence on entrepreneurship: A case study of Aizawl district of Mizoram. *Journal of Entrepreneurship and Management*, *3*(2), 9–13.

Guillard-Gonçalves, C., & Zêzere, J. L. (2018). Combining social vulnerability and physical vulnerability to analyse landslide risk at the municipal scale. *Geosciences, 8*(8), 294. https://doi.org/10.3390/geosciences8080294

Guillard-Gonçalves, C., Zêzere, J. L., Pereira, S., & Garcia, R. A. (2016). Assessment of physical vulnerability of buildings and analysis of landslide risk at the municipal scale: Application to the Loures municipality, Portugal. *Natural Hazards and Earth System Sciences*, *16*(2), 311–331. https://doi.org/10.5194/nhess-16-311-2016

Guo, Z., Zhang, L., & Li, Y. (2010). Increased dependence of humans on ecosystem services and biodiversity. *PloS ONE*, *5*(10), e13113. https://doi.org/10.1371/journal.pone.0013113

Gupta, R. P., & Joshi, B. C. (1990). Landslide hazard zoning using the GIS approach—a case study from the Ramganga catchment, Himalayas. *Engineering Geology*, *28*(1-2), 119–131. https://doi.org/10.1016/0013-7952(90)90037-2

Gupta, R. P., Saha, A. K., Arora, M. K., & Kumar, A. (1999). Landslide hazard zonation in a part of the Bhagirathi Valley, Garhwal Himalayas, using integrated remote sensing - GIS. *Himalayan Geology*, *20*(2), 71–85.

Guri, P. K., Champati Ray, P. K., & Patel, R. C. (2015). Spatial prediction of landslide susceptibility in parts of Garhwal Himalaya, India, using the weight of evidence modelling. *Environmental Monitoring and Assessment*, *187*(6), 324. https://doi.org/10.1007/s10661-015-4535-1

Gutiérrez, F., Sevil, J., & Migoń, P. (2023). Landslides in the Remolinos gypsum escarpment (NE Spain): Controls imposed by stratigraphy, fluvial erosion, and interstratal salt dissolution. *Landslides*, *20*(10), 2075–2093. https://doi.org/10.1007/s10346-023-02090-y

Guzzetti, F. (2005). *Landslide hazard and risk assessment* [Doctoral dissertation, Rheinische Friedrich-Wilhelms-Universität Bonn]. https://hdl.handle.net/20.500.11811/2644

Guzzetti, F., Cardinali, M., Reichenbach, P., & Carrara, A. (2000). Comparing landslide maps: A case study in the upper Tiber River basin, Central Italy. *Environmental Management*, *25*(3), 247–263. https://doi.org/10.1007/s002679910020

Guzzetti, F., Cardinali, M., Reichenbach, P., Cipolla, F., Sebastiani, C., Galli, M., & Salvati, P. (2004). Landslides triggered by the 23 November 2000 rainfall event in the Imperia Province, Western Liguria, Italy. *Engineering Geology*, *73*(3-4), 229–245. https://doi.org/10.1016/j.enggeo.2004.01.006

Guzzetti, F., Carrara, A., Cardinali, M., & Reichenbach, P. (1999). Landslide hazard evaluation: A review of current techniques and their application in a multi-scale study, Central Italy. *Geomorphology*, *31*(1-4), 181–216. https://doi.org/10.1016/S0169-555X(99)00078-1

Guzzetti, F., Galli, M., Reichenbach, P., Ardizzone, F., & Cardinali, M. (2006a). Landslide hazard assessment in the Collazzone area, Umbria, Central Italy. *Natural Hazards and Earth System Sciences*, *6*(1), 115–131. https://doi.org/10.5194/nhess-6-115-2006

Guzzetti, F., Malamud, B. D., Turcotte, D. L., & Reichenbach, P. (2002). Power-law correlations of landslide areas in central Italy. *Earth and Planetary Science Letters*, *195*(3-4), 169–183. https://doi.org/10.1016/S0012-821X(01)00589-1

Guzzetti, F., Mondini, A. C., Cardinali, M., Fiorucci, F., Santangelo, M., & Chang, K. T. (2012). Landslide inventory maps: New tools for an old problem. *Earth-Science Reviews*, *112*(1-2), 42–66. https://doi.org/10.1016/j.earscirev.2012.02.001

Guzzetti, F., Reichenbach, P., Ardizzone, F., Cardinali, M., & Galli, M. (2006b). Estimating the quality of landslide susceptibility models. *Geomorphology*, *81*(1-2), 166–184. https://doi.org/10.1016/j.geomorph.2006.04.007

Guzzetti, F., Reichenbach, P., Cardinali, M., Galli, M., & Ardizzone, F. (2005). Probabilistic landslide hazard assessment at the basin scale. *Geomorphology*, *72*(1-4), 272–299. https://doi.org/10.1016/j.geomorph.2005.06.002

Habumugisha, J. M., Chen, N., Rahman, M., Islam, M. M., Ahmad, H., Elbeltagi, A., Sharma, G., Liza, S. N., & Dewan, A. (2022). Landslide susceptibility mapping with deep learning algorithms. *Sustainability, 14*(3), 1734. https://doi.org/10.3390/su14031734

Hansen, A. (1984). Landslide hazard analysis. In D. Brunsden & D. B. Prior (Eds.), *Slope instability* (pp. 523–602). John Wiley and Sons.

Hansen, A., Franks, C. A. M., Kirk, P. A., Brimicombe, A. J., & Tung, F. (1995). Application of GIS to hazard assessment, with particular reference to landslides in Hong Kong. In A. Carrara & F. Guzzetti (Eds.), *Geographical information systems in assessing natural hazards* (pp. 299–334). Springer. https://doi.org/10.1007/978-94-015-8404-3_14

Haokip, L., Rinmuanpuii, P., Chakma, K., & Mallick, S. P. (2024). *Note on the preliminary assessment of landslides triggered due to Cyclone Remal in Aizawl, Serchhip and Saitual Districts, Mizoram*. Geological Survey of India, North Eastern Region.

Harp, E. L., & Jibson, R. W. (1996). Landslides triggered by the 1994 Northridge, California, earthquake. *Bulletin of the Seismological Society of America*, *86*(1B), S319–S332. https://doi.org/10.1785/BSSA08601BS319

Hart, A. (2024). Landslides. In G. Ciottone (Ed.), *Ciottone's Disaster Medicine* (3rd ed., pp. 640–643). Elsevier. https://doi.org/10.1016/B978-0-323-80932-0.00104-X

Haugen, E. D., & Kaynia, A. M. (2008). Vulnerability of structures impacted by debris flow. In Z. Chen, J.-M. Zhang, K. Ho, F.-Q. Wu, & Z.-K. Li (Eds.), *Landslides and engineered slopes: From the past to the future, Proceedings of the 10th international symposium on landslides and engineered slopes* (pp. 403–410). CRC Press. https://doi.org/10.1201/9780203885284-42

He, R., Zhang, W., Dou, J., Jiang, N., Xiao, H., & Zhou, J. (2024). Application of artificial intelligence in three aspects of landslide risk assessment: A comprehensive review. *Rock Mechanics Bulletin, 3*(4), 100144. https://doi.org/10.1016/j.rockmb.2024.100144

Hedding, D. W. (2020). Decoupling process from form in landscape evolution studies. *GSA Today*, *30*(2), 6. https://doi.org/10.1130/GSATG422C.1

Heim, A. (1882). Über bergstürze [About landslides]. *Naturforschende Gesellschafte Neujahrsblatt*, *84*, 31.

Heim, A. (1932). Bergstürz und Menschenleben [Landslides and human lives]. *Beiblatt zur Vierteljahrsschrift de Naturforschenden Gesellschaft in Zurich*, *77*, 1–217. (Reprinted by Bi-Tech Publishers).

Hervás, J., & Bobrowsky, P. (2009). Mapping: Inventories, susceptibility, hazard and risk. In K. Sassa & P. Canuti (Eds.), *Landslides–disaster risk reduction* (pp. 321–349). Springer. https://doi.org/10.1007/978-3-540-69970-5_19

Hewitt, K. (1997). *Regions of risk: A geographical introduction to disasters* (1st ed.). Routledge. https://doi.org/10.4324/9781315844206

Highland, L. (2004). *Landslide types and processes* (U.S. Geological Survey Fact Sheet 2004-3072). U.S. Geological Survey. http://pubs.er.usgs.gov/publication/fs20043072

Highland, L. M., & Bobrowsky, P. (2008). *The landslide handbook—A guide to understanding landslides* (Circular 1325). U.S. Geological Survey.

Hoehler, F. K. (2000). Bias and prevalence effects on kappa viewed in terms of sensitivity and specificity. *Journal of Clinical Epidemiology*, *53*(5), 499–503. https://doi.org/10.1016/S0895-4356(99)00174-2

Holub, M., & Fuchs, S. (2008). Benefits of local structural protection to mitigate torrent-related hazards. In C. A. Brebbia & E. Beriatos (Eds.), *Risk analysis VI: Simulation and hazard mitigation* (pp. 401–411). WIT Press.

Hong, H., Pradhan, B., Sameen, M. I., Kalantar, B., Zhu, A., & Chen, W. (2018). Improving the accuracy of landslide susceptibility model using a novel region-partitioning approach. *Landslides*, *15*, 753–772. https://doi.org/10.1007/s10346-017-0906-8

Horton, R. E. (1932). Drainage-basin characteristics. *Eos, Transactions American Geophysical Union*, *13*(1), 350–361. https://doi.org/10.1029/TR013i001p00350

Horton, R. E. (1945). Erosional development of streams and their drainage basins; hydrophysical approach to quantitative morphology. *Geological Society of America Bulletin*, *56*(3), 275–370. https://doi.org/10.1130/0016-7606(1945)56[275:EDOSAT]2.0.CO;2

Howe, E. (1909). *Landslides in the San Juan Mountains, Colorado, including a consideration of their causes and their classification* (Professional Paper 67). U.S. Geological Survey. https://doi.org/10.3133/pp67

Huabin, W., Gangjun, L., Weiya, X., & Gonghui, W. (2005). GIS-based landslide hazard assessment: An overview. *Progress in Physical Geography*, *29*(4), 548–567. https://doi.org/10.1191/0309133305pp462ra

Huang, J., Wu, X., Ling, S., Li, X., Wu, Y., Peng, L., & He, Z. (2022). A bibliometric and content analysis of research trends on GIS-based landslide susceptibility from 2001 to 2020. *Environmental Science and Pollution Research*, *29*(58), 86954–86993. https://doi.org/10.1007/s11356-022-23732-z

Huang, M. H., Schaeffer, C., Milillo, P., Randolph-Flagg, N. G., Smedley, A., Perissin, D., & Milillo, G. (2016). Seasonal slow-moving landslide and hazard in Aizawl, India revealed from InSAR. *AGU Fall Meeting Abstracts*, G21C-02.

Huang, Q., Wang, C., Meng, Y., Chen, J., & Yue, A. (2019). Landslide monitoring using change detection in multitemporal optical imagery. *IEEE Geoscience and Remote Sensing Letters*, *17*(2), 312–316. https://doi.org/10.1109/LGRS.2019.2918254

Hufschmidt, G. (2011). A comparative analysis of several vulnerability concepts. *Natural Hazards*, *58*, 621–643. https://doi.org/10.1007/s11069-011-9823-7

Hungr, O. (1997). Some methods of landslide hazard intensity mapping. In D. M. Cruden & R. Fell (Eds.), *Landslide risk assessment* (1st ed., pp. 215–226). Routledge. https://doi.org/10.1201/9780203749524-12

Hungr, O. (2016). A review of landslide hazard and risk assessment methodology. In S. Aversa, L. Cascini, L. Picarelli, & C. Scavia (Eds.), *Landslides and engineered slopes. Experience, theory and practice* (1st ed., pp. 3–27). CRC Press. https://doi.org/10.1201/9781315375007-1

Hungr, O., Leroueil, S., & Picarelli, L. (2014). The Varnes classification of landslide types, an update. *Landslides*, *11*(2), 167–194. https://doi.org/10.1007/s10346-013-0436-y

Hutchinson, J. N. (1968). Mass movement. In R. W. Fairbridge (Ed.), *Encyclopedia of geomorphology* (pp. 688–696). Springer. https://doi.org/10.1007/3-540-31060-6_238

Hutchinson, J. N. (1988). General report: Morphological and geotechnical parameters of landslides in relation to geology and hydrogeology. In C. Bonnard (Ed.), *Proceedings of the 5th International Symposium on Landslides* (Vol. 1, pp. 3–35). A. A. Balkema.

Hutchinson, J. N. (1992). Landslide hazard assessment. In D. H. Bell (Ed.), *Proceedings of the 6th International Symposium on Landslides* (pp. 1805–1841). A. A. Balkema.

IAEG (International Association of Engineering Geology). (1990). Suggested nomenclature for landslides. *Bulletin of the International Association of Engineering Geology*, *41*, 13–16. https://doi.org/10.1007/BF02590202

Ilia, I., & Tsangaratos, P. (2016). Applying weight of evidence method and sensitivity analysis to produce a landslide susceptibility map. *Landslides*, *13*, 379–397. https://doi.org/10.1007/s10346-015-0576-3

Ilinca, V., & Şandric, I. (2025). A review of UAV-based data applications for landslide mapping and monitoring. In I. Șandric, V. Ilinca, & Z. Chitu (Eds.), *Earth observation applications to landslide mapping, monitoring and modeling* (pp. 3–36). Elsevier. https://doi.org/10.1016/B978-0-12-823868-4.00003-9

IPCC (Intergovernmental Panel on Climate Change). (2014). *Climate change 2014: Impacts, adaptation, and vulnerability. Part A: Global and sectoral aspects. Contribution of Working Group II to the fifth assessment report of the Intergovernmental Panel on Climate Change*. Cambridge University Press.

Irigaray, C., Chacón, J., & Fernández, T. (1996). Comparative analysis of methods for landslide susceptibility mapping. In J. Chacón, C. Irigaray, & T. Fernández (Eds.), *Proceedings of the 8th International Conference and Field Trip on Landslides* (pp. 373–384). Balkema.

Irigaray, C., Del Castillo, T. F., Hamdouni, R. E., & Montero, J. C. (1999). Verification of landslide susceptibility mapping: A case study. *Earth Surface Processes and Landforms*, *24*(6), 537–544. https://doi.org/10.1002/(SICI)1096-9837(199906)24:6<537::AID-ESP965>3.0.CO;2-6

Irigaray, C., Fernández, T., El Hamdouni, R., & Chacón, J. (2007). Evaluation and validation of landslide-susceptibility maps obtained by a GIS matrix method: Examples from the Betic Cordillera (southern Spain). *Natural Hazards*, *41*, 61–79. https://doi.org/10.1007/s11069-006-9027-8

ISSMGE (International Society of Soil Mechanics and Ground Engineering). (2004). *Risk assessment – Glossary of terms*. TC32, Technical Committee on Risk Assessment and Management Glossary of Risk Assessment Terms – Version 1.

IUGS (International Union of Geological Sciences). (1997). Quantitative risk assessment for slopes and landslides - The state of the art. In D. M. Cruden & R. Fell (Eds.), *Landslide risk assessment* (1st ed., pp. 3–12). Routledge. https://doi.org/10.1201/9780203749524-1

Iverson, R. M. (2000). Landslide triggering by rain infiltration. *Water Resources Research*, *36*(7), 1897–1910. https://doi.org/10.1029/2000WR900090

Jaafari, A., Najafi, A., Pourghasemi, H. R., Rezaeian, J., & Sattarian, A. (2014). GIS-based frequency ratio and index of entropy models for landslide susceptibility assessment in the Caspian forest, northern Iran. *International Journal of Environmental Science and Technology*, *11*(4), 909–926. https://doi.org/10.1007/s13762-013-0464-0

Jaafari, A., Panahi, M., Pham, B. T., Shahabi, H., Bui, D. T., Rezaie, F., & Lee, S. (2019). Meta optimization of an adaptive neuro-fuzzy inference system with grey wolf optimizer and biogeography-based optimization algorithms for spatial prediction of landslide susceptibility. *CATENA*, *175*, 430–445. https://doi.org/10.1016/j.catena.2018.12.033

Jaboyedoff, M., Michoud, C., Derron, M. H., Voumard, J., Leibundgut, G., Sudmeier-Rieux, K., Nadim, F., & Leroi, E. (2018). Human-induced landslides: Toward the analysis of anthropogenic changes of the slope environment. In S. Aversa, L. Cascini, L. Picarelli, & C. Scavia (Eds.), *Landslides and engineered slopes: Experience, theory and practice* (pp. 217–232). CRC Press. https://doi.org/10.1201/9781315375007-12

Jade, S., & Sarkar, S. (1993). Statistical models for slope instability classification. *Engineering Geology*, *36*(1-2), 91–98. https://doi.org/10.1016/0013-7952(93)90021-4

Jaggi, G. S. (1986). A report on geoenvironmental appraisal of Aizawl Township. *Progress Report of Field Session 1985–86*. Geological Survey of India, North Eastern Region.

Jeong, S., Ko, J., & Kim, J. (2019). The effectiveness of a wireless sensor network system for landslide monitoring. *IEEE Access*, *8*, 8073–8086. https://doi.org/10.1109/ACCESS.2019.2960570

Ji, S., Yu, D., Shen, C., Li, W., & Xu, Q. (2020). Landslide detection from an open satellite imagery and digital elevation model dataset using attention boosted convolutional neural networks. *Landslides*, *17*, 1337–1352. https://doi.org/10.1007/s10346-020-01353-2

Jibson, R. W. (1996). Use of landslides for paleoseismic analysis. *Engineering Geology*, *43*(4), 291–323. https://doi.org/10.1016/S0013-7952(96)00039-7

Joseph, J. (2013). Measuring vulnerability to natural hazards: A macro framework. *Disasters*, *37*(2), 185–200. https://doi.org/10.1111/j.1467-7717.2012.01299.x

Joseph, V. R. (2022). Optimal ratio for data splitting. *Statistical Analysis and Data Mining: The ASA Data Science Journal*, *15*(4), 531–538. https://doi.org/10.1002/sam.11583

Kablan, M. K. A., Dongo, K., & Coulibaly, M. (2017). Assessment of social vulnerability to flood in urban Côte d'Ivoire using the MOVE framework. *Water, 9*(4), 292. https://doi.org/10.3390/w9040292

Kalaycıoğlu, M., Kalaycıoğlu, S., Çelik, K., Christie, R., & Filippi, M. E. (2023). An analysis of social vulnerability in a multi-hazard urban context for improving disaster risk reduction policies: The case of Sancaktepe, İstanbul. *International Journal of Disaster Risk Reduction*, *91*, 103679. https://doi.org/10.1016/j.ijdrr.2023.103679

Kamath, L. (2020). Refusing slum-centric mass housing: Indigenous urbanism and national housing programmes in Aizawl, India. *International Journal of Housing Policy*, *22*(4), 522–542. https://doi.org/10.1080/19491247.2020.1840905

Kang, H. S., & Kim, Y. T. (2016). The physical vulnerability of different types of building structure to debris flow events. *Natural Hazards*, *80*(3), 1475–1493. https://doi.org/10.1007/s11069-015-2032-z

Kanungo, D. P., Arora, M. K., Gupta, R. P., & Sarkar, S. (2008). Landslide risk assessment using concepts of danger pixels and fuzzy set theory in Darjeeling Himalayas. *Landslides, 5*(4), 407–416. https://doi.org/10.1007/s10346-008-0134-3

Kanungo, D. P., Arora, M. K., Sarkar, S., & Gupta, R. P. (2006). A comparative study of conventional, ANN black box, fuzzy and combined neural and fuzzy weighting procedures for landslide susceptibility zonation in Darjeeling Himalayas. *Engineering Geology*, *85*(3-4), 347–366. https://doi.org/10.1016/j.enggeo.2006.03.004

Kanungo, D. P., Arora, M. K., Sarkar, S., & Gupta, R. P. (2009). Landslide susceptibility zonation (LSZ) mapping–a review. *Journal of South Asia Disaster Studies*, *2*(1), 81–105.

Kappes, M. S., Papathoma-Köhle, M., & Keiler, M. (2012). Assessing physical vulnerability for multi-hazards using an indicator-based methodology. *Applied Geography*, *32*(2), 577–590. https://doi.org/10.1016/j.apgeog.2011.07.002

Kapuka, A., & Hlásny, T. (2020). Social vulnerability to natural hazards in Namibia: A district-based analysis. *Sustainability*, *12*(12), 4910. https://doi.org/10.3390/su12124910

Karantanellis, E., Marinos, V., Vassilakis, E., & Hölbling, D. (2021). Evaluation of machine learning algorithms for object-based mapping of landslide zones using UAV data. *Geosciences*, *11*(8), 305. https://doi.org/10.3390/geosciences11080305

Karsli, F., Atasoy, M., Yalcin, A., Reis, S., Demir, O., & Gokceoglu, C. (2009). Effects of land-use changes on landslides in a landslide-prone area (Ardesen, Rize, NE Turkey). *Environmental Monitoring and Assessment*, *156*, 241–255. https://doi.org/10.1007/s10661-008-0481-5

Kasai, M., Ikeda, M., Asahina, T., & Fujisawa, K. (2009). LiDAR-derived DEM evaluation of deep-seated landslides in a steep and rocky region of Japan. *Geomorphology*, *113*(1-2), 57–69. https://doi.org/10.1016/j.geomorph.2009.06.004

Kaur, H., Gupta, S., & Parkash, S. (2017). Comparative evaluation of various approaches for landslide hazard zoning: a critical review in Indian perspectives. *Spatial Information Research*, *25*, 389–398. https://doi.org/10.1007/s41324-017-0105-7

Kaur, H., Gupta, S., Parkash, S., & Thapa, R. (2023). Knowledge-driven method: A tool for landslide susceptibility zonation (LSZ). *Geology, Ecology, and Landscapes*, *7*(1), 1–15. https://doi.org/10.1080/24749508.2018.1558024

Kaur, H., Sarkar, R., Gupta, S., Parkash, S., Thapa, R., & Meena, S. R. (2022). The vulnerability of human population to landslide disaster: A case study of Sikkim Himalayas. In R. Sarkar, R. Shaw, & B. Pradhan (Eds.), *Impact of climate change, land use and land cover, and socio-economic dynamics on landslides* (pp. 319–333). Springer. https://doi.org/10.1007/978-981-16-7314-6_14

Kavzoglu, T., Colkesen, I., & Sahin, E. K. (2019). Machine learning techniques in landslide susceptibility mapping: A survey and a case study. In S. P. Pradhan, V. Vishal, & T. N. Singh (Eds.), *Landslides: Theory, practice and modelling* (pp. 283–301). Springer. https://doi.org/10.1007/978-3-319-77377-3_13

Kavzoglu, T., Sahin, E. K., & Colkesen, I. (2015). An assessment of multivariate and bivariate approaches in landslide susceptibility mapping: A case study of Duzkoy district. *Natural Hazards*, *76*, 471–496. https://doi.org/10.1007/s11069-014-1506-8

Keck, M., & Sakdapolrak, P. (2013). What is social resilience? Lessons learned and ways forward. *Erdkunde, 67*(1), 5–19. https://doi.org/10.3112/erdkunde.2013.01.02

Keefer, D. K. (1984). Landslides caused by earthquakes. *Geological Society of America Bulletin*, *95*(4), 406–421. https://doi.org/10.1130/0016-7606(1984)95<406:LCBE>2.0.CO;2

Keyport, R. N., Oommen, T., Martha, T. R., Sajinkumar, K. S., & Gierke, J. S. (2018). A comparative analysis of pixel-and object-based detection of landslides from very high-resolution images. *International Journal of Applied Earth Observation and Geoinformation*, *64*, 1–11. https://doi.org/10.1016/j.jag.2017.08.015

Khan, I., Bahuguna, H., & Kainthola, A. (2024). Regional landslide susceptibility zonation utilizing bivariate statistical techniques in the northwestern Himalayas, Jammu and Kashmir, India. *Journal of Earth System Science*, *133*(3), 157. https://doi.org/10.1007/s12040-024-02367-3

Khan, M. A., Mustaffa, Z., Harahap, I. S. H., Ibrahim, M. B., & Al-Atroush, M. E. (2022). Assessment of physical vulnerability and uncertainties for debris flow hazard: A review concerning climate change. *Land*, *11*(12), 2240. https://doi.org/10.3390/land11122240

Khan, S. (2012). Vulnerability assessments and their planning implications: A case study of the Hutt Valley, New Zealand. *Natural Hazards*, *64*(2), 1587–1607. https://doi.org/10.1007/s11069-012-0327-x

Khanna, K., Martha, T. R., Roy, P., & Kumar, K. V. (2021). Effect of time and space partitioning strategies of samples on regional landslide susceptibility modelling. *Landslides*, *18*, 2281–2294. https://doi.org/10.1007/s10346-021-01627-3

Khouz, A., Trindade, J., Oliveira, S. C., El Bchari, F., Bougadir, B., Garcia, R. A. C., & Jadoud, M. (2022). Landslide susceptibility assessment in the rocky coast subsystem of Essaouira, Morocco. *Natural Hazards and Earth System Sciences*, *22*(11), 3793–3814. https://doi.org/10.5194/nhess-22-3793-2022

Kienholz, H., Schneider, G., Bichsel, M., Grunder, M., & Mool, P. (1984). Mapping of mountain hazards and slope stability. *Mountain Research and Development*, *4*(3), 247–266. https://doi.org/10.2307/3673145

Kim, J., Lee, K., Jeong, S., & Kim, G. (2014). GIS-based prediction method of landslide susceptibility using a rainfall infiltration-groundwater flow model. *Engineering Geology*, *182*(A), 63–78. https://doi.org/10.1016/j.enggeo.2014.09.001

King, D. (2001). Uses and limitations of socioeconomic indicators of community vulnerability to natural hazards: Data and disasters in Northern Australia. *Natural Hazards*, *24*(2), 147–156. https://doi.org/10.1023/A:1011859507188

Kirschbaum, D., Stanley, T., & Zhou, Y. (2015). Spatial and temporal analysis of a global landslide catalog. *Geomorphology*, *249*, 4–15. https://doi.org/10.1016/j.geomorph.2015.03.016

Klose, M., Maurischat, P., & Damm, B. (2016). Landslide impacts in Germany: A historical and socioeconomic perspective. *Landslides*, *13*, 183–199. https://doi.org/10.1007/s10346-015-0643-9

Ko Ko, C., Flentje, P., & Chowdhury, R. (1999). Landslide risk assessment–Development of a hazard-consequence approach. In J. C. Jiang, Y. Norio, & T. Yamagami (Eds.), *Slope stability engineering* (1st ed., pp. 1309–1315). Routledge. https://doi.org/10.1201/9780203739600-120

Koirala, N. P., & Watkins, A. T. (1988). Bulk appraisal of slopes in Hong Kong. In C. Bonnard (Ed.), *Proceedings of the Fifth International Symposium on Landslides* (Vol. 2, pp. 1181–1186). A. A. Balkema.

Kok, M. T. J., & Jäger, J. (2013). Archetypical patterns of vulnerability to environmental change: An approach to bridging scales. Lessons learned from UNEP's fourth global environment outlook. In J. Birkmann (Ed.), *Measuring vulnerability to natural hazards: Towards disaster resilient societies* (2nd ed., pp. 148–164). United Nations University Press.

Krebs, P., Stocker, M., Pezzatti, G. B., & Conedera, M. (2015). An alternative approach to transverse and profile terrain curvature. *International Journal of Geographical Information Science*, *29*(4), 643–666. https://doi.org/10.1080/13658816.2014.995102

Krysik, J. L. (2018). Bivariate statistics and statistical inference. In J. L. Krysik (Ed.), *Research for effective social work practice* (4th ed., pp. 369–410). Routledge. https://doi.org/10.4324/9781315744384-12

Kudaibergenov, M., Nurakynov, S., Iskakov, B., Iskaliyeva, G., Maksum, Y., Orynbassarova, E., Akhmetov, B., & Sydyk, N. (2025). Application of artificial intelligence in landslide susceptibility assessment: Review of recent progress. *Remote Sensing*, *17*(1), 34. https://doi.org/10.3390/rs17010034

Kuhlicke, C. (2010). The dynamics of vulnerability: Some preliminary thoughts about the occurrence of 'radical surprises' and a case study on the 2002 flood (Germany). *Natural Hazards*, *55*(3), 671–688. https://doi.org/10.1007/s11069-010-9645-z

Kuhlicke, C., Scolobig, A., Tapsell, S., Steinführer, A., & De Marchi, B. (2011). Contextualizing social vulnerability: Findings from case studies across Europe. *Natural Hazards*, *58*(2), 789–810. https://doi.org/10.1007/s11069-011-9751-6

Kumar, R., & Anbalagan, R. (2015). Landslide susceptibility zonation in part of Tehri reservoir region using frequency ratio, fuzzy logic and GIS. *Journal of Earth System Science*, *124*, 431–448. https://doi.org/10.1007/s12040-015-0536-2

Kumar, S., & Gupta, V. (2021). Evaluation of spatial probability of landslides using bivariate and multivariate approaches in the Goriganga valley, Kumaun Himalaya, India. *Natural Hazards*, *109*(3), 2461–2488. https://doi.org/10.1007/s11069-021-04928-x

Kumar, S., & Verma, R. (2010). Geochemical analysis of Bhuban Formation of Surma Group in and around Aizawl and its significance. *Memoir of the Geological Society of India*, *75*, 193–207.

Kumar, S., Singh, T. N., & Sawmliana, C. (1997). On the instability problems in South Hlimen landslide, Mizoram. *Indian Journal of Engineering & Materials Sciences*, *4*(2), 78–80.

Lacroix, P., Zavala, B., Berthier, E., & Audin, L. (2013). Supervised method of landslide inventory using panchromatic SPOT5 images and application to the earthquake-triggered landslides of Pisco (Peru, 2007, Mw8.0). *Remote Sensing*, *5*(6), 2590–2616. https://doi.org/10.3390/rs5062590

Ladd, G. E. (1935). Landslides, subsidence and rockfalls. *Bulletin of American Railway Engineering Association*, *37*(377), 1–72.

Lalchhuanawma, H. C., & Khiangte, D. V. (2018). Urban governance in Aizawl: Challenges before urban local bodies towards development. *Mizoram University Journal of Humanities & Social Sciences*, *4*(1), 36–46.

Laldinpuia, Kumar, S., & Singh, T. N. (2011). Geotechnical studies of landslide at Ramhlun Vengthar, Aizawl, Mizoram. *Memoir of the Geological Society of India*, *77*, 251–258.

Laldinpuia, Kumar, S., & Singh, T. N. (2013). The 2013 rockslide disaster of Aizawl, Mizoram, India. *Science Vision*, *13*(2), 58–63.

Laldinpuia, Kumar, S., & Singh, T. N. (2014). 11th May, 2013 Laipuitlang Rockslide, Aizawl, Mizoram, North-East India. In K. Sassa, P. Canuti, & Y. Yin (Eds.), *Landslide science for a safer geoenvironment* (pp. 401–405). Springer. https://doi.org/10.1007/978-3-319-04996-0_61

Laldinpuia. (2019). Geological investigation and monitoring of Ramhlun Sports Complex landslide, Aizawl, India. *Science Vision*, *19*(3), 80–99. https://doi.org/10.33493/scivis.19.03.03

Laldintluanga, H., Lalbiakmawia, F., & Lalbiaknungi, R. (2016). Landslide hazard zonation along state highway between Aizawl city and Aibawk town, Mizoram, India using geospatial techniques. *International Journal of Engineering Sciences and Research Technology*, *5*(2), 342–355.

Lalhlimpuia, H., Zairemmawii, Kumar, S., & Laldinpuia. (2019). RMR and RHRS of Ngaizel road cutting section, Aizawl, Mizoram. *Senhri Journal of Multidisciplinary Studies*, *4*(2), 7–21.

Lallawmsanga, Lalthazuala, C., Lalhmingsangi, Lalhlimpuia, Kumar, S., & Laldinpuia. (2022). Assessment and analysis of geotechnical properties of Saron Veng landslide, Aizawl, Mizoram. In S. Mitra, K. Dasgupta, A. Dey, & R. Bedamatta (Eds.), *Disaster management and risk reduction: Multidisciplinary perspectives and approaches in the Indian context* (pp. 47–60). Springer. https://doi.org/10.1007/978-981-99-6395-9_3

Lallianpuii. (2017). Mizo urbanity, media infrastructure and the state. *The Newsletter*, *77*, 34. International Institute for Asian Studies.

Lallianthanga, R. K., & Laltanpuia, Z. D. (2008). Landslide hazard zonation mapping of Aizawl city using remote sensing and GIS techniques – A qualitative approach. *Bulletin of National Natural Resources Management System (B)*, *32*, 47–55.

Lallianthanga, R. K., & Laltanpuia, Z. D. (2014). Landslide hazard zonation mapping of Hnahthial Town, Mizoram, India using remote sensing & GIS. *International Journal of Engineering and Technical Research*, *2*(3), 56–63.

Lalremruati, R., & Ramaswamy, R. (2014). Street entrepreneurship among tribal women: Insights from Mizoram. *Small Enterprises Development and Management Extension Journal*, *41*(2), 27–42. https://doi.org/10.1177/0970846420140203

Laltanpuia, Z. D., Martha, T. R., & Rao, K. S. (2025). Integrating social and physical vulnerabilities to assess landslide risk in the Aizawl municipal area, Mizoram, India. *Journal of the Indian Society of Remote Sensing*, *53*(12), 4257–4279. https://doi.org/10.1007/s12524-025-02243-7

Laltanpuia, Z. D., Martha, T. R., Rao, K. S., & Khanna, K. (2024). Bivariate statistical models for landslide susceptibility mapping at local scale in the Aizawl municipal area, Mizoram, India. *Himalayan Geology*, *45*(1), 39–57.

Lanlan, J., Sarker, M. N. I., Ali, I., Firdaus, R. B. R., & Hossin, M. A. (2024). Vulnerability and resilience in the context of natural hazards: A critical conceptual analysis. *Environment, Development and Sustainability*, *26*(8), 19069–19092. https://doi.org/10.1007/s10668-023-03440-5

Lari, S., Frattini, P., & Crosta, G. B. (2014). A probabilistic approach for landslide hazard analysis. *Engineering Geology*, *182*(A), 3–14. https://doi.org/10.1016/j.enggeo.2014.07.015

Leal, M., Reis, E., Pereira, S., & Santos, P. P. (2021). Physical vulnerability assessment to flash floods using an indicator-based methodology based on building properties and flow parameters. *Journal of Flood Risk Management*, *14*(3), e12712. https://doi.org/10.1111/jfr3.12712

Lee, C. T., Huang, C. C., Lee, J. F., Pan, K. L., Lin, M. L., & Dong, J. J. (2008). Statistical approach to earthquake-induced landslide susceptibility. *Engineering Geology*, *100*(1-2), 43-58. https://doi.org/10.1016/j.enggeo.2008.03.004

Lee, D. H., Kim, Y. T., & Lee, S. R. (2020). Shallow landslide susceptibility models based on artificial neural networks considering the factor selection method and various non-linear activation functions. *Remote Sensing*, *12*(7), 1194. https://doi.org/10.3390/rs12071194

Lee, E. M. (2016). Landslide risk assessment: the challenge of communicating uncertainty to decision-makers. *Quarterly Journal of Engineering Geology and Hydrogeology, 49*(1), 21–35. https://doi.org/10.1144/qjegh2015-066

Lee, E. M., & Jones, D. K. (2014). *Landslide risk assessment* (2nd ed.). ICE Publishing. https://doi.org/10.1680/lra.66236

Lee, J. H., Park, H. J., & Jang, J. Y. (2017). Probabilistic analysis of shallow landslide susceptibility using physically based model and fuzzy point estimate method. In M. Mikoš, N. Casagli, Y. Yin, & K. Sassa (Eds.), *Advancing culture of living with landslides* (Vol. 4, pp. 221–227). Springer. https://doi.org/10.1007/978-3-319-53485-5_25

Lee, J. Y., & Van Zandt, S. (2019). Housing tenure and social vulnerability to disasters: A review of the evidence. *Journal of Planning Literature, 34*(2), 156–170. https://doi.org/10.1177/0885412218812080

Lee, S. (2019). Current and future status of GIS-based landslide susceptibility mapping: A literature review. *Korean Journal of Remote Sensing*, *35*(1), 179–193. https://doi.org/10.7780/kjrs.2019.35.1.12

Lee, S., & Min, K. (2001). Statistical analysis of landslide susceptibility at Yongin, Korea. *Environmental Geology*, *40*, 1095–1113. https://doi.org/10.1007/s002540100310

Lee, S., & Pradhan, B. (2007). Landslide hazard mapping at Selangor, Malaysia using frequency ratio and logistic regression models. *Landslides*, *4*(1), 33–41. https://doi.org/10.1007/s10346-006-0047-y

Lee, S., & Talib, J. A. (2005). Probabilistic landslide susceptibility and factor effect analysis. *Environmental Geology*, *47*, 982–990. https://doi.org/10.1007/s00254-005-1228-z

Lee, S., Ryu, J. H., Min, K., & Won, J. S. (2003). Landslide susceptibility analysis using GIS and artificial neural network. *Earth Surface Processes and Landforms*, *28*(12), 1361–1376. https://doi.org/10.1002/esp.593

Lee, Y.-J. (2014). Social vulnerability indicators as a sustainable planning tool. *Environmental Impact Assessment Review*, *44*, 31–42. https://doi.org/10.1016/j.eiar.2013.08.002

Lei, Y., Huang, J., Cui, Y., Jiang, S. H., Wu, S., & Ching, J. (2023). Time capsule for landslide risk assessment. *Georisk: Assessment and Management of Risk for Engineered Systems and Geohazards, 17*(4), 613–634. https://doi.org/10.1080/17499518.2023.2164899

Leone, F., Asté, J. P., & Leroi, E. (1996). Vulnerability assessment of elements exposed to mass-movements: Working toward a better risk perception. In K. Senneset (Ed.), *Landslides, glissements de terrain* (pp. 263–270). Balkema.

Leroi, E. (1996). Landslide hazard-risk maps at different scales: objectives, tools and developments. In K. Senneset (Ed.), *Proceedings of the 7th International Symposium on landslides* (vol. 1, pp. 35–51). A. A. Balkema.

Leroi, E., Bonnard, C., Fell, R., & McInnes, R. (2005). Risk assessment and management. In O. Hungr, R. Fell, R. Couture, & E. Eberhardt (Eds.), *Landslide risk management* (1st ed., pp. 169–208). CRC Press. https://doi.org/10.1201/9781439833711-9

Létal, A., Klimes, J., & Şandric, I. (2025). Building landslide inventory with LiDAR data and deep learning. In I. Șandric, V. Ilinca, & Z. Chitu (Eds.), *Earth observation applications to landslide mapping, monitoring and modeling* (pp. 297–311). Elsevier. https://doi.org/10.1016/B978-0-12-823868-4.00014-3

Li, G., Liu, D., Ruan, M., Zhang, Y., He, J., Guo, Z., Wang, H., & Cheng, M. (2025). Quantitative vulnerability assessment of buildings exposed to landslides under extreme rainfall scenarios. *Buildings, 15*(11), 1838. https://doi.org/10.3390/buildings15111838

Li, H., Mao, Z., Sun, J., Zhong, J., & Shi, S. (2023a). Landslide susceptibility mapping using weighted linear combination: A case of Gucheng Town in Ningxia, China. *Geotechnical and Geological Engineering*, *41*(2), 1247–1273. https://doi.org/10.1007/s10706-022-02333-0

Li, L., & Lan, H. (2023). Bivariate landslide susceptibility analysis: Clarification, optimization, open software, and preliminary comparison. *Remote Sensing*, *15*(5), 1418. https://doi.org/10.3390/rs15051418

Li, L., Lan, H., Guo, C., Zhang, Y., Li, Q., & Wu, Y. (2017). A modified frequency ratio method for landslide susceptibility assessment. *Landslides*, *14*, 727–741. https://doi.org/10.1007/s10346-016-0771-x

Li, L., Liu, J., Liu, H., Sun, B., Zhang, Z., Shi, Z., Ren, F., & Li, J. (2024). Effects of hillslope aspect on erosion rate of alpine meadows in the Three-River Headwater Region, China. *CATENA*, *239*, 107971. https://doi.org/10.1016/j.catena.2024.107971

Li, X., Cheng, J. L., & Yu, D. H. (2023b). A methodological framework of landslide quantitative risk assessment in areas with incomplete historical landslide information. *Journal of Mountain Science, 20*(9), 2665–2679. https://doi.org/10.1007/s11629-023-7950-8

Li, Y. (2025). The research on landslide detection in remote sensing images based on improved DeepLabv3+ method. *Scientific Reports*, *15*(1), 7957. https://doi.org/10.1038/s41598-025-92822-y

Li, Y., & Duan, W. (2024). Decoding vegetation's role in landslide susceptibility mapping: An integrated review of techniques and future directions. *Biogeotechnics*, *2*(1), 100056. https://doi.org/10.1016/j.bgtech.2023.100056

Li, Y., & Mo, P. (2019). A unified landslide classification system for loess slopes: A critical review. *Geomorphology*, *340*, 67–83. https://doi.org/10.1016/j.geomorph.2019.04.020

Li, Z., Nadim, F., Huang, H., Uzielli, M., & Lacasse, S. (2010). Quantitative vulnerability estimation for scenario-based landslide hazards. *Landslides*, *7*, 125–134. https://doi.org/10.1007/s10346-009-0190-3

Lima, P., Steger, S., Glade, T., & Murillo-García, F. G. (2022). Literature review and bibliometric analysis on data-driven assessment of landslide susceptibility. *Journal of Mountain Science*, *19*(6), 1670–1698. https://doi.org/10.1007/s11629-021-7254-9

Lin, M. L., & Tung, C. C. (2004). A GIS-based potential analysis of the landslides induced by the Chi-Chi earthquake. *Engineering Geology*, *71*(1-2), 63–77. https://doi.org/10.1016/S0013-7952(03)00126-1

Lissak, C. (2025). A review of the state-of-the-art use of satellite Earth observation data for landslide mapping and monitoring. In I. Șandric, V. Ilinca, & Z. Chitu (Eds.), *Earth observation applications to landslide mapping, monitoring and modeling* (pp. 37–67). Elsevier. https://doi.org/10.1016/B978-0-12-823868-4.00004-0

Liu, L. L., Zhang, Y. L., Xiao, T., & Yang, C. (2022). A frequency ratio–based sampling strategy for landslide susceptibility assessment. *Bulletin of Engineering Geology and the Environment*, *81*(9), 360. https://doi.org/10.1007/s10064-022-02836-3

Liu, N., Yang, Y., Li, N., Liang, S., Liu, H., & Li, C. (2024a). The stability issue of fractured rock mass slope under the influences of freeze–thaw cycle. *Scientific Reports*, *14*(1), 5674. https://doi.org/10.1038/s41598-024-56346-1

Liu, X., Shao, S., & Shao, S. (2024b). Landslide susceptibility zonation using the analytical hierarchy process (AHP) in the Great Xi'an Region, China. *Scientific Reports*, *14*(1), 2941. https://doi.org/10.1038/s41598-024-53630-y

Liu, Y., Huang, D., Peng, J., & Guo, Y. (2023). Analysis of the effect of rock layer structure on the toppling failure evolution of soft-hard interbedded anti-dip slopes. *Engineering Failure Analysis*, *145*, 107005. https://doi.org/10.1016/j.engfailanal.2022.107005

Lockner, D. A., & Beeler, N. M. (2002). Rock failure and earthquakes. In W. H. Lee, H. Kanamori, P. C. Jennings, & C. Kisslinger (Eds.), *International handbook of earthquake and engineering seismology* (Vol. 81, Part A, pp. 505–537). Elsevier. https://doi.org/10.1016/S0074-6142(02)80235-2

Lu, Z., Liu, G., Song, Z., Sun, K., Li, M., Chen, Y., Zhao, X., & Zhang, W. (2024). Advancements in technologies and methodologies of machine learning in landslide susceptibility research: Current trends and future directions. *Applied Sciences*, *14*(21), 9639. https://doi.org/10.3390/app14219639

Luo, H. Y., Zhang, L. L., & Zhang, L. M. (2019). Progressive failure of buildings under landslide impact. *Landslides, 16*(7), 1327–1340. https://doi.org/10.1007/s10346-019-01164-0

Luo, H. Y., Zhang, L. M., He, J., & Yin, K. S. (2022). Reliability-based formulation of building vulnerability to debris flow impacts. *Canadian Geotechnical Journal*, *59*(1), 40–54. https://doi.org/10.1139/cgj-2020-0120

Luo, H. Y., Zhang, L. M., Zhang, L. L., He, J., & Yin, K. S. (2023). Vulnerability of buildings to landslides: The state of the art and future needs. *Earth-Science Reviews*, *238*, 104329. https://doi.org/10.1016/j.earscirev.2023.104329

Ma, W., Dong, J., Wei, Z., Peng, L., Wu, Q., Wang, X., Dong, Y., & Wu, Y. (2023). Landslide susceptibility assessment using the certainty factor and deep neural network. *Frontiers in Earth Science*, *10*, 1091560. https://doi.org/10.3389/feart.2022.1091560

Maki Mateso, J. C., Bielders, C. L., Monsieurs, E., Depicker, A., Smets, B., Tambala, T., Bagalwa Mateso, L., & Dewitte, O. (2023). Characteristics and causes of natural and human-induced landslides in a tropical mountainous region: The rift flank west of Lake Kivu (Democratic Republic of the Congo). *Natural Hazards and Earth System Sciences*, *23*(2), 643–666. https://doi.org/10.5194/nhess-23-643-2023

Malamud, B. D., Turcotte, D. L., Guzzetti, F., & Reichenbach, P. (2004). Landslide inventories and their statistical properties. *Earth Surface Processes and Landforms*, *29*(6), 687–711. https://doi.org/10.1002/esp.1064

Mancini, F., Ceppi, C., & Ritrovato, G. (2010). GIS and statistical analysis for landslide susceptibility mapping in the Daunia area, Italy. *Natural Hazards and Earth System Sciences*, *10*(9), 1851–1864. https://doi.org/10.5194/nhess-10-1851-2010

Mandal, S. P., Chakrabarty, A., & Maity, P. (2018). Comparative evaluation of information value and frequency ratio in landslide susceptibility analysis along national highways of Sikkim Himalaya. *Spatial Information Research*, *26*, 127–141. https://doi.org/10.1007/s41324-017-0160-0

Mandal, S., & Mondal, S. (2019). *Geoinformatics and Modelling of Landslide Susceptibility and Risk: An RS & GIS-based Model Building Approach in the Eastern Himalaya*. Springer. https://doi.org/10.1007/978-3-030-10495-5

Mani, A., Kumari, M., & Badola, R. (2024). Landslide hazard zonation (LHZ) mapping of Doon Valley using multi-criteria analysis method based on remote sensing and GIS techniques. *Discover Geoscience*, *2*(1), Article 35. https://doi.org/10.1007/s44288-024-00044-y

Marjanović, M., Kovačević, M., Bajat, B., & Voženílek, V. (2011). Landslide susceptibility assessment using SVM machine learning algorithm. *Engineering Geology*, *123*(3), 225–234. https://doi.org/10.1016/j.enggeo.2011.09.006

Martha, T. R., & Kerle, N. (2010). Segment optimisation for object-based landslide detection. In E. A. Addink & F. M. B. van Coillie (Eds.), *GEOBIA 2010: Geographic object-based image analysis*. ISPRS Archives, XXXVIII-4/C7.

Martha, T. R., & Kerle, N. (2012). Creation of event-based landslide inventory from panchromatic images by object-oriented analysis. In R. Q. Feitosa (Ed.), *Proceedings of GEOBIA 2012: 4th International Conference on Geographic Object-Based Image Analysis* (pp. 53–57).

Martha, T. R., Kamala, P., Jose, J., Kumar, V. K., & Sankar, G. J. (2016a). Identification of new landslides from high resolution satellite data covering a large area using object-based change detection methods. *Journal of the Indian Society of Remote Sensing, 44*, 515–524. https://doi.org/10.1007/s12524-015-0532-7

Martha, T. R., Kerle, N., Jetten, V., van Westen, C. J., & Kumar, K. V. (2010a). Characterising spectral, spatial and morphometric properties of landslides for semi-automatic detection using object-oriented methods. *Geomorphology*, *116*(1-2), 24–36. https://doi.org/10.1016/j.geomorph.2009.10.004

Martha, T. R., Kerle, N., Jetten, V., van Westen, C. J., & Kumar, K. V. (2010b). Landslide volumetric analysis using Cartosat-1-derived DEMs. *IEEE Geoscience and Remote Sensing Letters*, *7*(3), 582–586. https://doi.org/10.1109/LGRS.2010.2041895

Martha, T. R., Kerle, N., Van Westen, C. J., Jetten, V., & Kumar, K. V. (2011). Segment optimization and data-driven thresholding for knowledge-based landslide detection by object-based image analysis. *IEEE Transactions on Geoscience and Remote Sensing*, *49*(12), 4928–4943. https://doi.org/10.1109/TGRS.2011.2151866

Martha, T. R., Kerle, N., Van Westen, C. J., Jetten, V., & Kumar, K. V. (2012). Object-oriented analysis of multi-temporal panchromatic images for creation of historical landslide inventories. *ISPRS Journal of Photogrammetry and Remote Sensing*, *67*, 105–119. https://doi.org/10.1016/j.isprsjprs.2011.11.004

Martha, T. R., Reddy, P. S., Bhatt, C. M., Raj, K. B. G., Nalini, J., Padmanabha, E. A., Narender, B., Kumar, K. V., Muralikrishnan, S., Rao, G. S., Diwakar, P. G., & Dadhwal, V. K. (2016b). Debris volume estimation and monitoring of Phuktal river landslide-dammed lake in the Zanskar Himalayas, India using Cartosat-2 images. *Landslides*, *14*, 373–383. https://doi.org/10.1007/s10346-016-0749-8

Martha, T. R., Roy, P., Jain, N., Khanna, K., Mrinalni, K., Kumar, K. V., & Rao, P. V. N. (2021). Geospatial landslide inventory of India—An insight into occurrence and exposure on a national scale. *Landslides*, *18*(6), 2125–2141. https://doi.org/10.1007/s10346-021-01645-1

Martha, T. R., van Westen, C. J., Kerle, N., Jetten, V., & Kumar, K. V. (2013). Landslide hazard and risk assessment using semi-automatically created landslide inventories. *Geomorphology*, *184*, 139–150. https://doi.org/10.1016/j.geomorph.2012.12.001

Martinsen, O. (1994). Mass movements. In A. Maltman (Ed.), *The geological deformation of sediments* (pp. 127–165). Springer. https://doi.org/10.1007/978-94-011-0731-0_5

Mathew, J., Jha, V. K., & Rawat, G. S. (2007). Weights of evidence modelling for landslide hazard zonation mapping in part of Bhagirathi valley, Uttarakhand. *Current Science*, *92*(5), 628–638. https://www.jstor.org/stable/24097851

Mazumder, D., Das, R., Das, S., & Singh, T. N. (2025). Understanding the landslide trigger mechanism in gently dipping shale beds: A case study from Aizawl, Mizoram, India. *Journal of Earth System Science, 134*(3), 184. https://doi.org/10.1007/s12040-025-02647-6

Mazzorana, B., Comiti, F., Scherer, C., & Fuchs, S. (2012). Developing consistent scenarios to assess flood hazards in mountain streams. *Journal of Environmental Management*, *94*(1), 112–124. https://doi.org/10.1016/j.jenvman.2011.06.030

Mazzorana, B., Hübl, J., & Fuchs, S. (2009). Improving risk assessment by defining consistent and reliable system scenarios. *Natural Hazards and Earth System Sciences*, *9*(1), 145–159. https://doi.org/10.5194/nhess-9-145-2009

McCall, A. G. (1980). *The Lushai Hills district cover*. The Tribal Research Institute, Government of Mizoram.

McGuire, L. A., Rengers, F. K., Kean, J. W., Coe, J. A., Mirus, B. B., Baum, R. L., & Godt, J. W. (2016). Elucidating the role of vegetation in the initiation of rainfall-induced shallow landslides: Insights from an extreme rainfall event in the Colorado Front Range. *Geophysical Research Letters*, *43*(17), 9084–9092. https://doi.org/10.1002/2016GL070741

McKean, J., & Roering, J. (2004). Objective landslide detection and surface morphology mapping using high-resolution airborne laser altimetry. *Geomorphology*, *57*(3-4), 331–351. https://doi.org/10.1016/S0169-555X(03)00164-8

McLaughlin, S., McKenna, J., & Cooper, J. A. G. (2002). Socio-economic data in coastal vulnerability indices: Constraints and opportunities. *Journal of Coastal Research*, *36*, 487–497. https://doi.org/10.2112/1551-5036-36.sp1.487

Meena, S. R., & Nachappa, T. G. (2019). Impact of spatial resolution of digital elevation model on landslide susceptibility mapping: A case study in Kullu Valley, Himalayas. *Geosciences*, *9*(8), 360. https://doi.org/10.3390/geosciences9080360

Meena, S. R., Soares, L. P., Grohmann, C. H., van Westen, C., Bhuyan, K., Singh, R. P., Floris, M., & Catani, F. (2022). Landslide detection in the Himalayas using machine learning algorithms and U-Net. *Landslides*, *19*(5), 1209–1229. https://doi.org/10.1007/s10346-022-01861-3

Meisina, C., & Scarabelli, S. (2007). A comparative analysis of terrain stability models for predicting shallow landslides in colluvial soils. *Geomorphology*, *87*(3), 207–223. https://doi.org/10.1016/j.geomorph.2006.03.039

Merghadi, A., Yunus, A. P., Dou, J., Whiteley, J., ThaiPham, B., Bui, D. T., Avtar, R., & Abderrahmane, B. (2020). Machine learning methods for landslide susceptibility studies: A comparative overview of algorithm performance. *Earth-Science Reviews*, *207*, 103225. https://doi.org/10.1016/j.earscirev.2020.103225

Metternicht, G., Hurni, L., & Gogu, R. (2005). Remote sensing of landslides: An analysis of the potential contribution to geo-spatial systems for hazard assessment in mountainous environments. *Remote Sensing of Environment*, *98*(2-3), 284–303. https://doi.org/10.1016/j.rse.2005.08.004

Michael-Leiba, M., Baynes, F., Scott, G., & Granger, K. (2002). Quantitative landslide risk assessment of Cairns. *Australian Geomechanics*, *37*(3), 1–13. https://search.informit.org/doi/10.3316/informit.810826097829201

Michael-Leiba, M., Baynes, F., Scott, G., & Granger, K. (2003). Regional landslide risk to the Cairns community. *Natural Hazards, 30*(2), 233–249. https://doi.org/10.1023/A:1026122518661

Mihalić Arbanas, S., Bernat Gazibara, S., Krkač, M., Sinčić, M., Lukačić, H., Jagodnik, P., & Arbanas, Ž. (2023). Landslide detection and spatial prediction: Application of data and information from landslide maps. In I. Alcántara-Ayala, Ž. Arbanas, D. Huntley, K. Konagai, M. Mikoš, K. Sassa, S. Sassa, H. Tang, & B. Tiwari (Eds.), *Progress in landslide research and technology* (Vol. 1, Part 2, pp. 195–212). Springer. https://doi.org/10.1007/978-3-031-18471-0_16

Mirdda, H. A., Bera, S., & Chatterjee, R. (2022). Vulnerability assessment of mountainous households to landslides: A multidimensional study in the rural Himalayas. *International Journal of Disaster Risk Reduction*, *71*, 102809. https://doi.org/10.1016/j.ijdrr.2022.102809

MIRSAC (Mizoram Remote Sensing Application Centre). (2011). *Atlas of micro-level landslide hazard zonation mapping of Aizawl city and selected towns of Mizoram*. Mizoram Remote Sensing Application Centre, Science & Technology, Government of Mizoram.

MIRSAC (Mizoram Remote Sensing Application Centre). (2019). *Hazard Risk and Vulnerability Analysis of eight district headquarters of Mizoram: Aizawl city*. Mizoram Remote Sensing Application Centre, Science & Technology, Government of Mizoram.

Moirangcha, L. H., Jana, P., Imtikumzuk, Chakraborty, D., Chowdhuri, S. N., Dharmwal, G. S., & Kesiezie, N. (2014). Seismic and landslide hazard assessment of Aizawl town, Mizoram. *Report of Field Session 2012–13 & 2013–14*. Geological Survey of India, North Eastern Region.

Mollard, J. D., & Janes, J. R. (1984). *Air photo interpretation and the Canadian landscape*. Energy, Mines and Resources Canada.

Mondini, A. C., Guzzetti, F., & Melillo, M. (2023). Deep learning forecast of rainfall-induced shallow landslides. *Nature Communications*, *14*(1), 2466. https://doi.org/10.1038/s41467-023-38135-y

Mondini, A. C., Guzzetti, F., Chang, K. T., Monserrat, O., Martha, T. R., & Manconi, A. (2021). Landslide failures detection and mapping using synthetic aperture radar: Past, present and future. *Earth-Science Reviews*, *216*, 103574. https://doi.org/10.1016/j.earscirev.2021.103574

Montgomery, D. R., & Dietrich, W. E. (1994). A physically based model for the topographic control on shallow landsliding. *Water Resources Research*, *30*(4), 1153–1171. https://doi.org/10.1029/93WR02979

Moore, I. D., Grayson, R. B., & Ladson, A. R. (1991). Digital terrain modelling: A review of hydrological, geomorphological, and biological applications. *Hydrological Processes*, *5*(1), 3–30. https://doi.org/10.1002/hyp.3360050103

MoRTH (Ministry of Road Transport and Highways). (2011). Description of National Highways. *The Gazette of India: Extraordinary, Part II—Section 3(ii)*. Ministry of Road Transport and Highways, Govt. of India.

Mostyn, G., & Sullivan, T. (2002). Quantitative Risk Assessment of the Thredbo Landslide. *Australian Geomechanics*, *37*(2), 169–181. https://search.informit.org/doi/10.3316/informit.810527970289070

Mousavi, S. Z., Kavian, A., Soleimani, K., Mousavi, S. R., & Shirzadi, A. (2011). GIS-based spatial prediction of landslide susceptibility using logistic regression model. *Geomatics, Natural Hazards and Risk*, *2*(1), 33–50. https://doi.org/10.1080/19475705.2010.532975

Müller, J. (1979). Josef Stini: Contributions to engineering geology and slope movement investigations. In B. Voight (Ed.), *Developments in geotechnical engineering* (Vol. 14, Part B, pp. 95–110). Elsevier. https://doi.org/10.1016/B978-0-444-41508-0.500 09-0

Murillo-García, F. G., Alcántara-Ayala, I., Ardizzone, F., Cardinali, M., Fiourucci, F., & Guzzetti, F. (2015). Satellite stereoscopic pair images of very high resolution: A step forward for the development of landslide inventories. *Landslides*, *12*(2), 277–291. https://doi.org/10.1007/s10346-014-0473-1

Murillo-García, F. G., Rossi, M., Ardizzone, F., Fiorucci, F., & Alcántara-Ayala, I. (2017). Hazard and population vulnerability analysis: A step towards landslide risk assessment. *Journal of Mountain Science, 14*(7), 1241–1261. https://doi.org/10.1007/s11629-016-4179-9

Muthu, R. P. (2005). *A preliminary geotechnical report on Aizawl City Vehicular Tunnel Project Aizawl District, Mizoram* (Progress Report of Field Session 2003–04). Geological Survey of India, North Eastern Region.

Nadim, F. (2005). Administrative report: TC32–Engineering practice of risk assessment and management. In *Proceedings of the 16th International Conference on Soil Mechanics and Geotechnical Engineering* (pp. 3513–3516). IOS Press. https://doi.org/10.3233/978-1-61499-656-9-3513

Nath, R. R., Sharma, M. L., & Tyagi, A. (2020). Review of the current practice on inclusion of seismicity in landslide susceptibility zonation: A case study for Garhwal Himalaya. *Himalayan Geology, 41*(2), 222–233.

Nemčok, A., Pašek, J., & Rybář, J. (1972). Classification of landslides and other mass movements. *Rock Mechanics*, *4*, 71–78. https://doi.org/10.1007/BF01239137

Neuhäuser, B., & Terhorst, B. (2007). Landslide susceptibility assessment using "weights-of-evidence" applied to a study area at the Jurassic escarpment (SW-Germany). *Geomorphology*, *86*(1-2), 12–24. https://doi.org/10.1016/j.geomorph.2006.08.002

Neuhäuser, B., Damm, B., & Terhorst, B. (2012). GIS-based assessment of landslide susceptibility on the base of the weights-of-evidence model. *Landslides*, *9*, 511–528. https://doi.org/10.1007/s10346-011-0305-5

Neuland, H. (1976). A prediction model of landslips. *CATENA*, *3*(2), 215–230. https://doi.org/10.1016/0341-8162(76)90011-4

Ng, C. W. W., Yang, B., Liu, Z. Q., Kwan, J. S. H., & Chen, L. (2021). Spatiotemporal modelling of rainfall-induced landslides using machine learning. *Landslides*, *18*(7), 2499–2514. https://doi.org/10.1007/s10346-021-01662-0

Ngo, E. B. (2012). Elderly people and disaster. In B. Wisner, J. C. Gaillard, & I. Kelman (Eds.), *Handbook of hazards and disaster risk reduction* (pp. 447–458). Routledge. https://doi.org/10.4324/9780203844236-48

Nguyen, C. V., Horne, R., Fien, J., & Cheong, F. (2017). Assessment of social vulnerability to climate change at the local scale: Development and application of a Social Vulnerability Index. *Climatic Change*, *143*(3), 355–370. https://doi.org/10.1007/s10584-017-2012-2

Nguyen, V. V., Pham, B. T., Vu, B. T., Prakash, I., Jha, S., Shahabi, H., Shirzadi, A., Ba, D. N., Kumar, R., Chatterjee, J. M., & Bui, D. T. (2019). Hybrid machine learning approaches for landslide susceptibility modeling. *Forests*, *10*(2), 157. https://doi.org/10.3390/f10020157

Nohani, E., Moharrami, M., Sharafi, S., Khosravi, K., Pradhan, B., Pham, B. T., Lee, S., & Melesse, A. M. (2019). Landslide susceptibility mapping using different GIS-based bivariate models. *Water*, *11*(7), 1402. https://doi.org/10.3390/w11071402

Nor Diana, M. I., Muhamad, N., Taha, M. R., Osman, A., & Alam, M. M. (2021). Social vulnerability assessment for landslide hazards in Malaysia: A systematic review study. *Land*, *10*(3), 315. https://doi.org/10.3390/land10030315

Novellino, A., Pennington, C., Leeming, K., Taylor, S., Alvarez, I. G., McAllister, E., Arnhardt, C., & Winson, A. (2024). Mapping landslides from space: A review. *Landslides*, *21*(5), 1041–1052. https://doi.org/10.1007/s10346-024-02215-x

NRSC (National Remote Sensing Centre). (2023). *Landslide Atlas of India*. Indian Space Research Organisation (ISRO), Department of Space, Government of India.

O'Brien, K., Leichenko, R., Kelkar, U., Venema, H., Aandahl, G., Tompkins, H., Javed, A., Bhadwal, S., Barg, S., Nygaard, L., & West, J. (2004). Mapping vulnerability to multiple stressors: Climate change and globalization in India. *Global Environmental Change*, *14*(4), 303–313. https://doi.org/10.1016/j.gloenvcha.2004.01.001

O'Keefe, P., Westgate, K., & Wisner, B. (1976). Taking the naturalness out of natural disasters. *Nature*, *260*, 566–567. https://doi.org/10.1038/260566a0

Oh, H.-J., & Lee, S. (2017). Shallow landslide susceptibility modeling using the data mining models artificial neural network and boosted tree. *Applied Sciences*, *7*(10), 1000. https://doi.org/10.3390/app7101000

Ohlmacher, G. C., & Davis, J. C. (2003). Using multiple logistic regression and GIS technology to predict landslide hazard in northeast Kansas, USA. *Engineering Geology*, *69*(3-4), 331–343. https://doi.org/10.1016/S0013-7952(03)00069-3

Osawa, H., Matsushi, Y., Matsuura, S., Okamoto, T., Shibasaki, T., & Hirashima, H. (2018). Seasonal transition of hydrological processes in a slow-moving landslide in a snowy region. *Hydrological Processes*, *32*(17), 2695–2707. https://doi.org/10.1002/hyp.13212

Pachauri, A. K., & Pant, M. (1992). Landslide hazard mapping based on geological attributes. *Engineering Geology*, *32*(1-2), 81–100. https://doi.org/10.1016/0013-7952(92)90020-Y

Pack, R. T., Tarboton, D. G., & Goodwin, C. N. (1998). The SINMAP approach to terrain stability mapping. In D. Moore & O. Hungr (Eds.), *Proceedings of the 8th Congress of the International Association of Engineering Geology* (Vol. 2, pp. 1157–1166). A. A. Balkema.

Pal, S. C., Das, B., & Malik, S. (2019). Potential landslide vulnerability zonation using integrated analytic hierarchy process and GIS technique of Upper Rangit Catchment Area, West Sikkim, India. *Journal of the Indian Society of Remote Sensing*, *47*, 1643–1655. https://doi.org/10.1007/s12524-019-01009-2

Pandey, V. K., Sharma, K. K., Pourghasemi, H. R., & Bandooni, S. K. (2019). Sedimentological characteristics and application of machine learning techniques for landslide susceptibility modelling along the highway corridor Nahan to Rajgarh (Himachal Pradesh), India. *CATENA*, *182*, 104150. https://doi.org/10.1016/j.catena.2019.104150

Pant, S., & Tabrez, S. (2024). Exploring the impact of climate change factors on landslide in the Himalayan state of Mizoram. In H. Sajjad, M. A. Siddiqui, A. Rahman, L. Siddiqui, H. R. Naqvi, & A. Shakeel (Eds.), *Landslide risk assessment and mitigation in India* (pp. 187–200). Springer. https://doi.org/10.1007/978-981-97-5485-4_13

Papathoma-Köhle, M. (2016). Vulnerability curves vs. vulnerability indicators: Application of an indicator-based methodology for debris-flow hazards. *Natural Hazards and Earth System Sciences*, *16*(8), 1771–1790. https://doi.org/10.5194/nhess-16-1771-2016

Papathoma-Köhle, M., Gems, B., Sturm, M., & Fuchs, S. (2017). Matrices, curves and indicators: A review of approaches to assess physical vulnerability to debris flows. *Earth-Science Reviews*, *171*, 272–288. https://doi.org/10.1016/j.earscirev.2017.06.007

Papathoma-Köhle, M., Kappes, M., Keiler, M., & Glade, T. (2011). Physical vulnerability assessment for alpine hazards: State of the art and future needs. *Natural Hazards*, *58*, 645–680. https://doi.org/10.1007/s11069-010-9632-4

Papathoma-Köhle, M., Neuhäuser, B., Ratzinger, K., Wenzel, H., & Dominey-Howes, D. (2007). Elements at risk as a framework for assessing the vulnerability of communities to landslides. *Natural Hazards and Earth System Sciences*, *7*(6), 765–779. https://doi.org/10.5194/nhess-7-765-2007

Papathoma-Köhle, M., Schlögl, M., & Fuchs, S. (2019). Vulnerability indicators for natural hazards: An innovative selection and weighting approach. *Scientific Reports*, *9*(1), 15026. https://doi.org/10.1038/s41598-019-50257-2

Papathoma-Köhle, M., Totschnig, R., Keiler, M., & Glade, T. (2012). A new vulnerability function for debris flow: The importance of physical vulnerability assessment in alpine areas. In G. Koboltschnig, J. Hübl, & J. Braun (Eds.), *Proceedings of the 12th Congress INTERPRAEVENT 2012* (pp. 1033–1043). International Research Society INTERPRAEVENT.

Papathoma-Köhle, M., Zischg, A., Fuchs, S., Glade, T., & Keiler, M. (2015). Loss estimation for landslides in mountain areas–An integrated toolbox for vulnerability assessment and damage documentation. *Environmental Modelling & Software*, *63*, 156–169. https://doi.org/10.1016/j.envsoft.2014.10.003

Pardee, J. W. (2012). Living through displacement: Housing insecurity among low-income evacuees. In L. Weber & L. Peek (Eds.), *Displaced: Life in the Katrina diaspora* (pp. 63–78). University of Texas Press. https://doi.org/10.7560/735774-008

Pardeshi, S. D., Autade, S. E., & Pardeshi, S. S. (2013). Landslide hazard assessment: Recent trends and techniques. *SpringerPlus*, *2*, 523. https://doi.org/10.1186/2193-1801-2-523

Parisi, F., & Sabella, G. (2017). Flow-type landslide fragility of reinforced concrete framed buildings. *Engineering Structures*, *131*, 28–43. https://doi.org/10.1016/j.engstruct.2016.10.013

Parkash, S. (2013). Earthquake related landslides in the Indian Himalaya: Experiences from the past and implications for the future. In C. Margottini, P. Canuti, & K. Sassa (Eds.), *Landslide science and practice* (pp. 327–334). Springer. https://doi.org/10.1007/978-3-642-31427-8_42

Peek, L. (2008). Children and disasters: Understanding vulnerability, developing capacities, and promoting resilience—An introduction. *Children, Youth and Environments, 18*(1), 1–29. https://doi.org/10.1353/cye.2008.0052

Pelling, M. (2013). Review of global risk index projects: Conclusions for sub-national and local approaches. In J. Birkmann (Ed.), *Measuring vulnerability to natural hazards: Towards disaster resilient societies* (2nd ed., pp. 167–196). United Nations University Press.

Pengapenga, C., & Mzuza, M. K. (2023). Application of Pressure and Release Model to assess flood impact in Mitondo Area, Chikwawa District, Malawi. *Novel Perspectives of Geography, Environment and Earth Sciences*, *8*, 145–155. https://doi.org/10.9734/bpi/npgees/v8/10379F

Pereira, S., Garcia, R. A., Zêzere, J. L., Oliveira, S. C., & Silva, M. (2017). Landslide quantitative risk analysis of buildings at the municipal scale based on a rainfall triggering scenario. *Geomatics, Natural Hazards and Risk, 8*(2), 624–648. https://doi.org/10.1080/19475705.2016.1250116

Pereira, S., Santos, P. P., Zêzere, J. L., Tavares, A. O., Garcia, R. A. C., & Oliveira, S. C. (2020). A landslide risk index for municipal land use planning in Portugal. *Science of The Total Environment, 735*, 139463. https://doi.org/10.1016/j.scitotenv.2020.139463

Pereira, S., Zêzere, J. L., & Bateira, C. (2012). Technical note: Assessing predictive capacity and conditional independence of landslide predisposing factors for shallow landslide susceptibility models. *Natural Hazards and Earth System Sciences*, *12*(4), 979–988. https://doi.org/10.5194/nhess-12-979-2012

Perera, E. N. C., Jayawardana, D. T., Ranagalage, M., Dissanayake, D. M. S. L. B., & Wijenayaka, H. M. D. S. (2020). Introduce a framework for landslide risk assessment using geospatial analysis: a case study from Kegalle District, Sri Lanka. *Modeling Earth Systems and Environment, 6*(4), 2415–2431. https://doi.org/10.1007/s40808-020-00811-z

Peres, D. J., & Cancelliere, A. (2014). Derivation and evaluation of landslide-triggering thresholds by a Monte Carlo approach. *Hydrology and Earth System Sciences*, *18*(12), 4913–4931. https://doi.org/10.5194/hess-18-4913-2014

Petley, D. (2012a). Global patterns of loss of life from landslides. *Geology*, *40*(10), 927–930. https://doi.org/10.1130/G33217.1

Petley, D. (2012b). Remote sensing techniques and landslides. In J. J. Clague & D. Stead (Eds.), *Landslides: Types, mechanisms and modeling* (pp. 159–171). Cambridge University Press. https://doi.org/10.1017/CBO9780511740367.015

Petschko, H., Brenning, A., Bell, R., Goetz, J., & Glade, T. (2014). Assessing the quality of landslide susceptibility maps–case study Lower Austria. *Natural Hazards and Earth System Sciences*, *14*(1), 95–118. https://doi.org/10.5194/nhess-14-95-2014

Pham, B. T., Bui, D. T, Pourghasemi, H. R., Indra, P., & Dholakia, M. B. (2017). Landslide susceptibility assessment in the Uttarakhand area (India) using GIS: A comparison study of prediction capability of naïve bayes, multilayer perceptron neural networks, and functional trees methods. *Theoretical and Applied Climatology*, *128*, 255–273. https://doi.org/10.1007/s00704-015-1702-9

Phinzi, K., & Szabó, S. (2024). Predictive machine learning for gully susceptibility modeling with geo-environmental covariates: Main drivers, model performance, and computational efficiency. *Natural Hazards*, *120*(8), 7211–7244. https://doi.org/10.1007/s11069-024-06481-9

Pipatpongsa, T., Fang, K., Leelasukseree, C., & Chaiwan, A. (2022). Stability analysis of laterally confined slope lying on inclined bedding plane. *Landslides*, *19*(8), 1861–1879. https://doi.org/10.1007/s10346-022-01873-z

Posner, A. J., & Georgakakos, K. P. (2015). Normalized landslide index method for susceptibility map development in El Salvador. *Natural Hazards*, *79*, 1825–1845. https://doi.org/10.1007/s11069-015-1930-4

Pourghasemi, H. R., Mohammady, M., & Pradhan, B. (2012a). Landslide susceptibility mapping using index of entropy and conditional probability models in GIS: Safarood Basin, Iran. *CATENA*, *97*, 71–84. https://doi.org/10.1016/j.catena.2012.05.005

Pourghasemi, H. R., Pradhan, B., & Gokceoglu, C. (2012b). Application of fuzzy logic and analytical hierarchy process (AHP) to landslide susceptibility mapping at Haraz watershed, Iran. *Natural Hazards*, *63*(2), 965–996. https://doi.org/10.1007/s11069-012-0217-2

Pourghasemi, H. R., Yansari, Z. T., Panagos, P., & Pradhan, B. (2018). Analysis and evaluation of landslide susceptibility: A review on articles published during 2005–2016 (periods of 2005–2012 and 2013–2016). *Arabian Journal of Geosciences*, *11*, 193. https://doi.org/10.1007/s12517-018-3531-5

Pradhan, A. M. S., & Kim, Y. T. (2014). Relative effect method of landslide susceptibility zonation in weathered granite soil: A case study in Deokjeok-ri Creek, South Korea. *Natural Hazards*, *72*, 1189–1217. https://doi.org/10.1007/s11069-014-1065-z

Pradhan, B. (2010). Landslide susceptibility mapping of a catchment area using frequency ratio, fuzzy logic and multivariate logistic regression approaches. *Journal of the Indian Society of Remote Sensing*, *38*, 301–320. https://doi.org/10.1007/s12524-010-0020-z

Pradhan, B. (2013). A comparative study on the predictive ability of the decision tree, support vector machine and neuro-fuzzy models in landslide susceptibility mapping using GIS. *Computers & Geosciences*, *51*, 350–365. https://doi.org/10.1016/j.cageo.2012.08.023

Pradhan, B., & Lee, S. (2010). Delineation of landslide hazard areas on Penang Island, Malaysia, by using frequency ratio, logistic regression, and artificial neural network models. *Environmental Earth Sciences*, *60*, 1037–1054. https://doi.org/10.1007/s12665-009-0245-8

Pradhan, B., Dikshit, A., Lee, S., & Kim, H. (2023). An explainable AI (XAI) model for landslide susceptibility modeling. *Applied Soft Computing*, *142*, 110324. https://doi.org/10.1016/j.asoc.2023.110324

Pradhan, B., Oh, H. J., & Buchroithner, M. (2010). Weights-of-evidence model applied to landslide susceptibility mapping in a tropical hilly area. *Geomatics, Natural Hazards and Risk*, *1*(3), 199–223. https://doi.org/10.1080/19475705.2010.498151

Prasad, L. M. (1983). *Report on the geological investigations of landslides in Aizawl Town, Mizoram* (Report of Field Session 1982–83). Geological Survey of India, North Eastern Region.

Pugliese Viloria, A. d. J., Folini, A., Carrion, D., & Brovelli, M. A. (2024). Hazard susceptibility mapping with machine and deep learning: A literature review. *Remote Sensing*, *16*(18), 3374. https://doi.org/10.3390/rs16183374

Puissant, A., Van Den Eeckhaut, M., Malet, J. P., & Maquaire, O. (2014). Landslide consequence analysis: a region-scale indicator-based methodology. *Landslides, 11*(5), 843–858. https://doi.org/10.1007/s10346-013-0429-x

Qiu, H., Xu, Y., Tang, B., Su, L., Li, Y., Yang, D., & Ullah, M. (2024). Interpretable landslide susceptibility evaluation based on model optimization. *Land*, *13*(5), 639. https://doi.org/10.3390/land13050639

Quan Luna, B., Blahut, J., van Westen, C. J., Sterlacchini, S., van Asch, T. W. J., & Akbas, S. O. (2011). The application of numerical debris flow modelling for the generation of physical vulnerability curves. *Natural Hazards and Earth System Sciences*, *11*(7), 2047–2060. https://doi.org/10.5194/nhess-11-2047-2011

Rakshit, R., & Bezbaruah, D. (2016). Morphotectonic aspects in and around Aizawl, Mizoram of NE India. *South East Asian Journal of Sedimentary Basin Research*, *2-3-4*(1), 28–36.

Rakshit, R., Lalhmingsangi, Bezbaruah, D., & Bharali, B. (2017). Morphotectonic and sedimentological aspects in describing the relationship with ancient failure surfaces in southern part of Aizawl anticline, Mizoram, India. *Science Vision*, *17*(4), 204–216. https://doi.org/10.33493/scivis.17.04.04

Ram, P., & Gupta, V. (2022). Landslide hazard, vulnerability, and risk assessment (HVRA), Mussoorie township, lesser himalaya, India. *Environment, Development and Sustainability, 24*(1), 473–501. https://doi.org/10.1007/s10668-021-01449-2

Ram, P., Gupta, V., Devi, M., & Vishwakarma, N. (2020). Landslide susceptibility mapping using bivariate statistical method for the hilly township of Mussoorie and its surrounding areas, Uttarakhand Himalaya. *Journal of Earth System Science*, *129*, 167. https://doi.org/10.1007/s12040-020-01428-7

Ramesh, V., & Anbazhagan, S. (2015). Landslide susceptibility mapping along Kolli hills Ghat road section (India) using frequency ratio, relative effect and fuzzy logic models. *Environmental Earth Sciences*, *73*, 8009–8021. https://doi.org/10.1007/s12665-014-3954-6

Rao, C. U. B., & Verma, R. (2017). Micro-zonation of landslide hazards between Aizawl city and Lengpui Airport, Mizoram, India, using geo-informatics. *International Journal of Basic & Applied Sciences*, *17*(5), 7–19.

Rautela, P., & Lakhera, R. C. (2000). Landslide risk analysis between Giri and Tons rivers in Himachal Himalaya (India). *International Journal of Applied Earth Observation and Geoinformation*, *2*(3-4), 153–160. https://doi.org/10.1016/S0303-2434(00)85009-6

Rawat, J. S., & Joshi, R. C. (2012). Remote-sensing and GIS-based landslide-susceptibility zonation using the landslide index method in Igo River Basin, Eastern Himalaya, India. *International Journal of Remote Sensing*, *33*(12), 3751–3767. https://doi.org/10.1080/01431161.2011.633121

Regmi, A. D., & Agrawal, N. (2022). A simple method for landslide risk assessment in the Rivière Aux Vases basin, Quebec, Canada. *Progress in Disaster Science, 16*, 100247. https://doi.org/10.1016/j.pdisas.2022.100247

Regmi, A. D., Yoshida, K., Nagata, H., Pradhan, A. M. S., Pradhan, B., & Pourghasemi, H. R. (2013). The relationship between geology and rock weathering on the rock instability along Mugling–Narayanghat road corridor, Central Nepal Himalaya. *Natural Hazards*, *66*, 501–532. https://doi.org/10.1007/s11069-012-0497-6

Reichenbach, P., Galli, M., Cardinali, M., Guzzetti, F., & Ardizzone, F. (2005). Geomorphological mapping to assess landslide risk: Concepts, methods and applications in the Umbria region of Central Italy. In T. Glade, M. G. Anderson, & M. J. Crozier (Eds.), *Landslide hazard and risk* (pp. 429–468). John Wiley & Sons Ltd. https://doi.org/10.1002/9780470012659.ch15

Reichenbach, P., Rossi, M., Malamud, B. D., Mihir, M., & Guzzetti, F. (2018). A review of statistically-based landslide susceptibility models. *Earth-Science Reviews*, *180*, 60–91. https://doi.org/10.1016/j.earscirev.2018.03.001

Remondo, J., González, A., De Terán, J. R. D., Cendrero, A., Fabbri, A., & Chung, C-J. F. (2003b). Validation of landslide susceptibility maps; examples and applications from a case study in Northern Spain. *Natural Hazards*, *30*, 437–449. https://doi.org/10.1023/B:NHAZ.0000007201.80743.fc

Remondo, J., González-Díez, A., De Terán, J. R. D., & Cendrero, A. (2003a). Landslide susceptibility models utilising spatial data analysis techniques. A case study from the lower Deba Valley, Guipúzcoa (Spain). *Natural Hazards*, *30*, 267–279. https://doi.org/10.1023/B:NHAZ.0000007202.12543.3a

Renaud, F. G., Sudmeier-Rieux, K., & Estrella, M. (2013). The relevance of ecosystems for disaster risk reduction. In F. G. Renaud, K. Sudmeier-Rieux, & M. Estrella (Eds.), *The role of ecosystems in disaster risk reduction* (pp. 3–25). United Nations University Press.

Reubens, B., Poesen, J., Danjon, F., Geudens, G., & Muys, B. (2007). The role of fine and coarse roots in shallow slope stability and soil erosion control with a focus on root system architecture: A review. *Trees*, *21*(4), 385–402. https://doi.org/10.1007/s00468-007-0132-4

Reynolds, C. E., Steedman, J. C., & Threlfall, A. J. (2007). *Reinforced concrete designer's handbook* (11th ed.). CRC Press. https://doi.org/10.4324/9780203087756

Rheinberger, C. M., Romang, H. E., & Bründl, M. (2013). Proportional loss functions for debris flow events. *Natural Hazards and Earth System Sciences*, *13*(8), 2147–2156. https://doi.org/10.5194/nhess-13-2147-2013

Riaz, M. T., Basharat, M., Brunetti, M. T., & Riaz, M. T. (2023). Semi-quantitative landslide risk assessment of district Muzaffarabad, northwestern Himalayas, Pakistan. *Stochastic Environmental Research and Risk Assessment, 37*(9), 3551–3570. https://doi.org/10.1007/s00477-023-02462-9

Rib, H. T., & Liang, T. (1978). Recognition and identification. In R. L. Schuster & R. J. Krizek (Eds.), *Landslide: Analysis and control* (Transportation Research Board Special Report 176, pp. 34–80). National Academy of Sciences.

Rodgers, J., & Tobin, T. (2014). Building resilience to earthquakes and landslides in Aizawl, India. *The Leading Edge*, *33*(12), 1364–1370. https://doi.org/10.1190/tle33121364.1

Rohmingthangi, G., Kypacharili, F. C., Mukherjee, A. B., & Mipun, B. S. (2022). Landslide risk dynamics modeling using AHP-TOPSIS model, computational intelligence methods, and geospatial analytics: A case study of Aizawl City, Mizoram—India. In S. C. Satapathy, P. Peer, J. Tang, V. Bhateja, & A. Ghosh (Eds.), *Intelligent data engineering and analytics. Smart innovation, systems and technologies* (Vol. 266, pp. 397–410). Springer. https://doi.org/10.1007/978-981-16-6624-7_40

Rossi, G., Catani, F., Leoni, L., Segoni, S., & Tofani, V. (2013). HIRESSS: A physically based slope stability simulator for HPC applications. *Natural Hazards and Earth System Sciences*, *13*(1), 151–166. https://doi.org/10.5194/nhess-13-151-2013

Rossi, M., Guzzetti, F., Reichenbach, P., Mondini, A. C., & Peruccacci, S. (2010). Optimal landslide susceptibility zonation based on multiple forecasts. *Geomorphology*, *114*(3), 129–142. https://doi.org/10.1016/j.geomorph.2009.06.020

Rouse Jr., J. W., Haas, R. H., Deering, D. W., Schell, J. A., & Harlan, J. C. (1974). *Monitoring the vernal advancement and retrogradation (green wave effect) of natural vegetation*. NASA Report No. E75-10354.

Roy, J., Saha, S., Arabameri, A., Blaschke, T., & Bui, D. T. (2019). A novel ensemble approach for landslide susceptibility mapping (LSM) in Darjeeling and Kalimpong districts, West Bengal, India. *Remote Sensing*, *11*(23), 2866. https://doi.org/10.3390/rs11232866

Roy, P., Ghosal, K., & Paul, P. K. (2022). Landslide susceptibility mapping of Kalimpong in Eastern Himalayan Region using a Rprop ANN approach. *Journal of Earth System Science, 131*(2), 130. https://doi.org/10.1007/s12040-022-01877-2

Rufat, S. (2024). Conceptual models of vulnerability or vulnerabilities. In S. Rufat & P. Metzger (Eds.), *Vulnerability, territory, population: From critique to public policy* (pp. 25–42). Wiley-ISTE. https://doi.org/10.1002/9781394299249.ch2

Rufat, S., Tate, E., Burton, C. G., & Maroof, A. S. (2015). Social vulnerability to floods: Review of case studies and implications for measurement. *International Journal of Disaster Risk Reduction*, *14*(4), 470–486. https://doi.org/10.1016/j.ijdrr.2015.09.013

Rufat, S., Tate, E., Emrich, C. T., & Antolini, F. (2019). How valid are social vulnerability models? *Annals of the American Association of Geographers*, *109*(4), 1131–1153. https://doi.org/10.1080/24694452.2018.1535887

Ruggieri, S., Cardellicchio, A., Leggieri, V., & Uva, G. (2021). Machine-learning based vulnerability analysis of existing buildings. *Automation in Construction*, *132*, 103936. https://doi.org/10.1016/j.autcon.2021.103936

Rygel, L., O’sullivan, D., & Yarnal, B. (2006). A method for constructing a social vulnerability index: An application to hurricane storm surges in a developed country. *Mitigation and Adaptation Strategies for Global Change*, *11*(3), 741–764.

Sadath, A. C., & Acharya, R. H. (2017). Assessing the extent and intensity of energy poverty using multidimensional energy poverty index: Empirical evidence from households in India. *Energy Policy, 102*, 540–550. https://doi.org/10.1016/j.enpol.2016.12.056

Saha, A. K., Gupta, R. P., Sarkar, I., Arora, M. K., & Csaplovics, E. (2005). An approach for GIS-based statistical landslide susceptibility zonation—with a case study in the Himalayas. *Landslides*, *2*, 61–69. https://doi.org/10.1007/s10346-004-0039-8

Saha, S., Roy, J., Hembram, T. K., Pradhan, B., Dikshit, A., Abdul Maulud, K. N., & Alamri, A. M. (2021). Comparison between deep learning and tree-based machine learning approaches for landslide susceptibility mapping. *Water*, *13*(19), 2664. https://doi.org/10.3390/w13192664

Sahin, E. K., Colkesen, I., & Kavzoglu, T. (2020). A comparative assessment of canonical correlation forest, random forest, rotation forest and logistic regression methods for landslide susceptibility mapping. *Geocarto International*, *35*(4), 341–363. https://doi.org/10.1080/10106049.2018.1516248

Saitluanga, B. L. (2014). Spatial pattern of urban livability in Himalayan Region: A case of Aizawl City, India. *Social Indicators Research*, *117*(2), 541–559. https://doi.org/10.1007/s11205-013-0362-3

Saitluanga, B. L. (2017a). *Himalayan quality of life — A study of Aizawl City*. Springer International Publishing. https://doi.org/10.1007/978-3-319-53780-1

Saitluanga, B. L. (2017b). Vertical differentiation in urban space: A case of Aizawl city. *Singapore Journal of Tropical Geography*, *38*(2), 216–228. https://doi.org/10.1111/sjtg.12194

Saitluanga, B. L. (2018). *Towards a sustainable smart city: The case of Aizawl* (ORF Special Report No. 73). Observer Research Foundation.

Saitluanga, B. L., & Pachuau, R. (2015). Spatio-temporal analysis of population growth in Aizawl City. *Geographic*, *10*, 40–50.

Sajinkumar, K. S., Anbazhagan, S., Pradeepkumar, A. P., & Rani, V. R. (2011). Weathering and landslide occurrences in parts of Western Ghats, Kerala. *Journal of the Geological Society of India*, *78*, 249–257. https://doi.org/10.1007/s12594-011-0089-1

Salvati, P., Balducci, V., Bianchi, C., Guzzetti, F., & Tonelli, G. (2009). A WebGIS for the dissemination of information on historical landslides and floods in Umbria, Italy. *Geoinformatica*, *13*, 305–322. https://doi.org/10.1007/s10707-008-0072-1

Sandric, I., Chitu, Z., Ilinca, V., & Irimia, R. (2024). Using high-resolution UAV imagery and artificial intelligence to detect and map landslide cracks automatically. *Landslides*, *21*(10), 2535–2543. https://doi.org/10.1007/s10346-024-02295-9

Sangeeta, & Maheshwari, B. K. (2022). Landslide susceptibility, social vulnerability, and risk assessment in Kumaun Himalaya, Uttarakhand, India. *Arabian Journal of Geosciences*, *15*(20), 1600. https://doi.org/10.1007/s12517-022-10869-x

Sangeeta, Maheshwari, B. K., & Kanungo, D. P. (2020). GIS-based pre-and post-earthquake landslide susceptibility zonation with reference to 1999 Chamoli earthquake. *Journal of Earth System Science*, *129*, 55. https://doi.org/10.1007/s12040-019-1319-y

Sangi, L., Ralte, Z., Roluahpuia, B., Dinpuia, L., Lalnunmawia, J., Tlau, L., Sailo, S., Lawmkima, H., Vanthangliana, V., Lalremruatfela, C., & Tluangkima, M. (2025). Preliminary investigation on Cyclone Remal-induced landslides in Aizawl, Mizoram, Northeast India, on the 28th of May 2024. *Landslides*, *22*, 1563–1575. https://doi.org/10.1007/s10346-025-02477-z

Santacana, N., Baeza, B., Corominas, J., De Paz, A., & Marturiá, J. (2003). A GIS-based multivariate statistical analysis for shallow landslide susceptibility mapping in La Pobla de Lillet area (Eastern Pyrenees, Spain). *Natural Hazards, 30*, 281–295. https://doi.org/10.1023/B:NHAZ.0000007169.28860.80

Santos, P. P., Zêzere, J. L., Pereira, S., Rocha, J., & Tavares, A. O. (2022). A novel approach to measuring spatiotemporal changes in social vulnerability at the local level in Portugal. *International Journal of Disaster Risk Science*, *13*(6), 842–861. https://doi.org/10.1007/s13753-022-00455-w

Sardana, S., Verma, A. K., Singh, A., & Laldinpuia. (2019b). Comparative analysis of rockmass characterization techniques for the stability prediction of road cut slopes along NH-44A, Mizoram, India. *Bulletin of Engineering Geology and the Environment, 78*(8), 5977–5989. https://doi.org/10.1007/s10064-019-01493-3

Sardana, S., Verma, A. K., Verma, R., & Singh, T. N. (2019a). Rock slope stability along road cut of Kulikawn to Saikhamakawn of Aizawl, Mizoram, India. *Natural Hazards, 99*(2), 753–767. https://doi.org/10.1007/s11069-019-03772-4

Sarkar, S. (2018). Landslide risk assessment in parts of the Darjeeling Himalayas, India. In P. Samui, D. Kim, & C. Ghosh (Eds.), *Integrating disaster science and management: Global case studies in mitigation and recovery* (pp. 99–108). Elsevier. https://doi.org/10.1016/B978-0-12-812056-9.00007-5

Sarkar, S., Kanungo, D. P., & Mehrotra, G. S. (1995). Landslide hazard zonation: A case study in Garhwal Himalaya, India. *Mountain Research and Development, 15*(4), 301–309. https://doi.org/10.2307/3673806

Sarkar, S., Roy, A. K., & Martha, T. R. (2013). Landslide susceptibility assessment using information value method in parts of the Darjeeling Himalayas. *Journal of the Geological Society of India*, *82*, 351–362. https://doi.org/10.1007/s12594-013-0162-z

Savarenskii, P. F. (1937). *Inzhenernaya geologiya [Engineering Geology]*. ONTI NKTP SSSR.

Sawaiyan, S. C., & Moirangcha, L. H. (2007). *Report on urban geological studies of Aizawl Town, Mizoram* (Report of Field Session 2004–05). Geological Survey of India, North Eastern Region.

Scaioni, M., Longoni, L., Melillo, V., & Papini, M. (2014). Remote sensing for landslide investigations: An overview of recent achievements and perspectives. *Remote Sensing, 6*(10), 9600–9652. https://doi.org/10.3390/rs6109600

Schaeffer, C., Huang, M. H., Smedley, A., Sitar, N., & Dreger, D. S. (2014). Landslide hazard in Aizawl, India revealed from field and geodetic observations and hillslope stability analysis. *AGU Fall Meeting Abstracts*, NH43A-3795.

Schmidtlein, M. C., Deutsch, R. C., Piegorsch, W. W., & Cutter, S. L. (2008). A sensitivity analysis of the Social Vulnerability Index. *Risk Analysis*, *28*(4), 1099–1114. https://doi.org/10.1111/j.1539-6924.2008.01072.x

Schmidtlein, M. C., Shafer, J. M., Berry, M., & Cutter, S. L. (2011). Modeled earthquake losses and social vulnerability in Charleston, South Carolina. *Applied Geography*, *31*(1), 269–281. https://doi.org/10.1016/j.apgeog.2010.06.001

Schneiderbauer, S., & Ehrlich, D. (2004). *Risk, hazard and people's vulnerability to natural hazards: A review of definitions, concepts and data* (EUR 21410 EN). European Commission Joint Research Centre.

Schneiderbauer, S., Calliari, E., Eidsvig, U., & Hagenlocher, M. (2017). The most recent view of vulnerability. In K. Poljanšek, M. Marin Ferrer, T. De Groeve, & I. Clark (Eds.), *Science for disaster risk management 2017: Knowing better and losing less* (pp. 70–84). Publications Office of the European Union. https://doi.org/10.2788/842809

Scolobig, A., Broto, V. C., & Zabala, A. (2008). Integrating multiple perspectives in social multicriteria evaluation of flood-mitigation alternatives: The case of Malborghetto-Valbruna. *Environment and Planning C: Government and Policy*, *26*(6), 1143–1161. https://doi.org/10.1068/c0765s

Segoni, S., Ajin, R. S., Nocentini, N., & Fanti, R. (2024). Insights gained from the review of landslide susceptibility assessment studies in Italy. *Remote Sensing*, *16*(23), 4491. https://doi.org/10.3390/rs16234491

Selamat, S. N., Abd Majid, N., & Mohd Taib, A. (2023). A comparative assessment of sampling ratios using artificial neural network (ANN) for landslide predictive model in Langat River Basin, Selangor, Malaysia. *Sustainability*, *15*(1), 861. https://doi.org/10.3390/su15010861

Shadman Roodposhti, M., Aryal, J., Shahabi, H., & Safarrad, T. (2016). Fuzzy Shannon entropy: A hybrid GIS-based landslide susceptibility mapping method. *Entropy*, *18*(10), 343. https://doi.org/10.3390/e18100343

Shanmugam, G., & Wang, Y. (2015). The landslide problem. *Journal of Palaeogeography*, *4*(2), 109–166. https://doi.org/10.3724/SP.J.1261.2015.00071

Shano, L., Raghuvanshi, T. K., & Meten, M. (2020). Landslide susceptibility evaluation and hazard zonation techniques–a review. *Geoenvironmental Disasters*, *7*, 18. https://doi.org/10.1186/s40677-020-00152-0

Shano, L., Raghuvanshi, T. K., & Meten, M. (2022). Fuzzy set theory and pixel-based landslide risk assessment: the case of Shafe and Baso catchments, Gamo highland, Ethiopia. *Earth Science Informatics, 15*(2), 993–1006. https://doi.org/10.1007/s12145-022-00774-y

Sharma, S., & Mahajan, A. K. (2018). Comparative evaluation of GIS-based landslide susceptibility mapping using statistical and heuristic approach for Dharamshala region of Kangra Valley, India. *Geoenvironmental Disasters*, *5*, 4. https://doi.org/10.1186/s40677-018-0097-1

Sharpe, C. F. S. (1938). *Landslides and related phenomena: A study of mass-movements of soil and rock*. Columbia University Press.

Shen, P., Zhang, L. M., Chen, H. X., & Gao, L. (2017). Role of vegetation restoration in mitigating hillslope erosion and debris flows. *Engineering Geology*, *216*, 122–133. https://doi.org/10.1016/j.enggeo.2016.11.019

Shi, F., Li, L., Wu, X., Wang, Y., & Niu, R. (2024). Building vulnerability to landslides: Broad-scale assessment in Xinxing County, China. *Sensors*, *24*(13), 4366. https://doi.org/10.3390/s24134366

Shirzadi, A., Solaimani, K., Roshan, M. H., Kavian, A., Chapi, K., Shahabi, H., Keesstra, S., Ahmad, B. B., & Bui, D. T. (2019). Uncertainties of prediction accuracy in shallow landslide modeling: Sample size and raster resolution. *CATENA*, *178*, 172–188. https://doi.org/10.1016/j.catena.2019.03.017

Shroder, Jr., J. F., Cvercková, L., & Mulhern, K. L. (2005). Slope-failure analysis and classification: Review of a century of effort. *Physical Geography*, *26*(3), 216–247. https://doi.org/10.2747/0272-3646.26.3.216

Silva, M., & Pereira, S. (2014). Assessment of physical vulnerability and potential losses of buildings due to shallow slides. *Natural Hazards*, *72*, 1029–1050. https://doi.org/10.1007/s11069-014-1052-4

Sim, K. B., Lee, M. L., & Wong, S. Y. (2022). A review of landslide acceptable risk and tolerable risk. *Geoenvironmental Disasters, 9*(1), 3. https://doi.org/10.1186/s40677-022-00205-6

Singh, A. K. (2010). Bioengineering techniques of slope stabilization and landslide mitigation. *Disaster Prevention and Management*, *19*(3), 384–397. https://doi.org/10.1108/09653561011052547

Singh, A., Kanungo, D. P., & Pal, S. (2018). A modified approach for semi-quantitative estimation of physical vulnerability of buildings exposed to different landslide intensity scenarios. *Georisk: Assessment and Management of Risk for Engineered Systems and Geohazards*, *13*(1), 66–81. https://doi.org/10.1080/17499518.2018.1501076

Singh, A., Kanungo, D. P., & Pal, S. (2019). Physical vulnerability assessment of buildings exposed to landslides in India. *Natural Hazards*, *96*, 753–790. https://doi.org/10.1007/s11069-018-03568-y

Singh, A., Pal, S., & Kanungo, D. P. (2021). An integrated approach for landslide susceptibility–vulnerability–risk assessment of building infrastructures in hilly regions of India. *Environment, Development and Sustainability*, *23*, 5058–5095. https://doi.org/10.1007/s10668-020-00804-z

Singh, A., Pal, S., Kanungo, D. P., & Pareek, N. (2017a). An overview of recent developments in landslide vulnerability assessment-presentation of a new conceptual framework. In M. Mikos, B. Tiwari, Y. Yin, & K. Sassa (Eds.), *Advancing culture of living with landslides* (pp. 795–802). Springer. https://doi.org/10.1007/978-3-319-53498-5_91

Singh, P. K., Ratan, D., Singh, K. K., & Singh, T. N. (2016). Landslide in fractured and stratified rocks - A case from Aizawl, Mizoram, India. *Proceedings of the conference on Recent Advances in Rock Engineering (RARE 2016)*, (pp. 375–380). https://doi.org/10.2991/rare-16.2016.59

Singh, P. K., Singh, K. K., & Singh, T. N. (2017b). Slope failure in stratified rocks: A case from NE Himalaya, India. *Landslides, 14*(4), 1319–1331. https://doi.org/10.1007/s10346-016-0785-4

Skempton, A. W. (1953). Soil mechanics in relation to geology. *Proceedings of the Yorkshire Geological Society*, *29*(1), 33–62. https://doi.org/10.1144/pygs.29.1.33

Soeters, R., & van Westen, C. J. (1996). Slope instability recognition, analysis and zonation. In A. K. Turner & R. L. Schuster (Eds.), *Landslides: Investigation and mitigation* (Transportation Research Board Special Report 247, pp. 129–177). National Academy of Sciences.

Spencer, G., & Thompson, J. (2024). Children and young people's perspectives on disasters–mental health, agency and vulnerability: A scoping review. *International Journal of Disaster Risk Reduction, 108*, 104495. https://doi.org/10.1016/j.ijdrr.2024.104495

Spielman, S. E., Tuccillo, J., Folch, D. C., Schweikert, A., Davies, R., Wood, N., & Tate, E. (2020). Evaluating social vulnerability indicators: Criteria and their application to the Social Vulnerability Index. *Natural Hazards*, *100*(1), 417–436. https://doi.org/10.1007/s11069-019-03820-z

Srivastava, M. S., Bhatia, S. K., Sarkar, S., & Sinha, R. G. (1993). *A report on landslide investigations following heavy rains of June 1993, Aizawl Town, Mizoram* (Report of Field Session 1992–93). Geological Survey of India, North Eastern Region.

SRSC (State Remote Sensing Application Centre). (2006). *Natural resources mapping of Mizoram using Remote Sensing & GIS: Aizawl District (A project report)*. Science, Technology & Environment, Planning Department, Government of Mizoram.

Stallings, R. A. (2006). Causality and "natural" disasters. *Contemporary Sociology*, *35*(3), 223–227. https://doi.org/10.1177/009430610603500305

Stanley, T. A., Soobitsky, R. B., Amatya, P. M., & Kirschbaum, D. B. (2024). Landslide hazard is projected to increase across High Mountain Asia. *Earth's Future*, *12*(10), e2023EF004325. https://doi.org/10.1029/2023EF004325

Stead, D., & Wolter, A. (2015). A critical review of rock slope failure mechanisms: The importance of structural geology. *Journal of Structural Geology*, *74*, 1–23. https://doi.org/10.1016/j.jsg.2015.02.002

Steger, S., Brenning, A., Bell, R., Petschko, H., & Glade, T. (2016). Exploring discrepancies between quantitative validation results and the geomorphic plausibility of statistical landslide susceptibility maps. *Geomorphology*, *262*, 8–23. https://doi.org/10.1016/j.geomorph.2016.03.015

Steger, S., Mair, V., Kofler, C., Pittore, M., Zebisch, M., & Schneiderbauer, S. (2021). Correlation does not imply geomorphic causation in data-driven landslide susceptibility modelling–Benefits of exploring landslide data collection effects. *Science of The Total Environment*, *776*, 145935. https://doi.org/10.1016/j.scitotenv.2021.145935

Steger, S., Schmaltz, E., & Glade, T. (2020). The (f)utility to account for pre-failure topography in data-driven landslide susceptibility modelling. *Geomorphology*, *354*, 107041. https://doi.org/10.1016/j.geomorph.2020.107041

Stehman, S. V. (1997). Selecting and interpreting measures of thematic classification accuracy. *Remote Sensing of Environment*, *62*(1), 77–89. https://doi.org/10.1016/S0034-4257(97)00083-7

Steinberg, T. (2000). *Acts of God: The unnatural history of natural disaster in America*. Oxford University Press.

Sterlacchini, S., Akbas, S. O., Blahut, J., Mavrouli, O. C., Garcia, C., Luna, B. Q., & Corominas, J. (2014). Methods for the characterization of the vulnerability of elements at risk. In T. van Asch, J. Corominas, S. Greiving, J.-P. Malet, & S. Sterlacchini (Eds.), *Mountain risks: From prediction to management and governance* (pp. 233–273). Springer. https://doi.org/10.1007/978-94-007-6769-0_8

Sterlacchini, S., Ballabio, C., Blahut, J., Masetti, M., & Sorichetta, A. (2011). Spatial agreement of predicted patterns in landslide susceptibility maps. *Geomorphology*, *125*(1), 51–61. https://doi.org/10.1016/j.geomorph.2010.09.004

Sterlacchini, S., Frigerio, S., Giacomelli, P., & Brambilla, M. (2007). Landslide risk analysis: a multi-disciplinary methodological approach. *Natural Hazards and Earth System Sciences, 7*(6), 657–675. https://doi.org/10.5194/nhess-7-657-2007

Stiny, J. (1910). *Die Muren [Debris Flows]*. Verlag der Wagner'schen Universitäts-buchhandlung.

Stock, A., Davidson, R. A., Kendra, J., Martins, V. N., Ewing, B., Nozick, L. K., Starbird, K., & Leon-Corwin, M. (2023). Household impacts of interruption to electric power and water services. *Natural Hazards, 115*(3), 2279–2306. https://doi.org/10.1007/s11069-022-05638-8

Sujatha, E. R., & Sridhar, V. (2021). Landslide susceptibility analysis: A logistic regression model case study in Coonoor, India. *Hydrology*, *8*(1), 41. https://doi.org/10.3390/hydrology8010041

Sujatha, E. R., & Sudharsan, J. S. (2024). Landslide susceptibility mapping methods—a review. In G. K. Panda, R. Shaw, S. C. Pal, U. Chatterjee, & A. Saha (Eds.), *Landslide: Susceptibility, risk assessment and sustainability* (pp. 87–102). Springer. https://doi.org/10.1007/978-3-031-56591-5_4

Sun, D., Ding, Y., Wen, H., Zhang, F., Zhang, J., Gu, Q., & Zhang, J. (2024). SHAP-PDP hybrid interpretation of decision-making mechanism of machine learning-based landslide susceptibility mapping: A case study at Wushan District, China. *The Egyptian Journal of Remote Sensing and Space Sciences*, *27*(3), 508–523. https://doi.org/10.1016/j.ejrs.2024.06.005

Sun, X., Zeng, P., Li, T., Zhang, T., Feng, X., & Jimenez, R. (2021). Run-out distance exceedance probability evaluation and hazard zoning of an individual landslide. *Landslides*, *18*, 1295–1308. https://doi.org/10.1007/s10346-020-01545-w

Susman, P., O'Keefe, P., & Wisner, B. (1984). Global disasters, a radical interpretation. In K. Hewitt (Ed.), *Interpretations of calamity: From the viewpoint of human ecology* (1st ed., pp. 263–283). Routledge. https://doi.org/10.4324/9780429329579-14

Swamy, M. M. (1992). *A report on the geotechnical study of S. Hlimen landslide of August 9, 1992, Aizawl, Mizoram* (Report for the Field Season 1991-92). Geological Survey of India, North Eastern Region.

Sweta, K., Goswami, A., Nath, R. R., & Bahuguna, I. M. (2022). Performance assessment for three statistical models of landslide susceptibility zonation mapping: A case study for Dharamshala Region, Himachal Pradesh, India. *Journal of Earth System Science*, *131*(3), 143. https://doi.org/10.1007/s12040-022-01881-6

Swets, J. A. (1988). Measuring the accuracy of diagnostic systems. *Science*, *240*(4857), 1285–1293. https://doi.org/10.1126/science.3287615

Tang, D., Jiang, Z., Yuan, T., & Li, Y. (2020). Stability analysis of soil slope subjected to perched water condition. *KSCE Journal of Civil Engineering*, *24*(9), 2581–2590. https://doi.org/10.1007/s12205-020-1728-0

Tapsell, S., McCarthy, S., Faulkner, H., & Alexander, M. (2010). *Social vulnerability to natural hazards* (CapHaz-Net WP4 Report). Flood Hazard Research Centre, Middlesex University.

Tarbotton, C., Dall'Osso, F., Dominey-Howes, D., & Goff, J. (2015). The use of empirical vulnerability functions to assess the response of buildings to tsunami impact: Comparative review and summary of best practice. *Earth-Science Reviews*, *142*, 120–134. https://doi.org/10.1016/j.earscirev.2015.01.002

Tasnuva, A., Hossain, M. R., Salam, R., Islam, A. R. M. T., Patwary, M. M., & Ibrahim, S. M. (2021). Employing social vulnerability index to assess household social vulnerability of natural hazards: An evidence from southwest coastal Bangladesh. *Environment, Development and Sustainability*, *23*(7), 10223–10245. https://doi.org/10.1007/s10668-020-01054-9

Tate, E. (2012). Social vulnerability indices: A comparative assessment using uncertainty and sensitivity analysis. *Natural Hazards*, *63*(2), 325–347. https://doi.org/10.1007/s11069-012-0152-2

Tate, E. (2013). Uncertainty analysis for a social vulnerability index. *Annals of the Association of American Geographers*, *103*(3), 526–543. https://doi.org/10.1080/00045608.2012.700616

Tate, E., Cutter, S. L., & Berry, M. (2010). Integrated multihazard mapping. *Environment and Planning B: Planning and Design*, *37*(4), 646–663. https://doi.org/10.1068/b35157

Tavakkoli Piralilou, S., Shahabi, H., Jarihani, B., Ghorbanzadeh, O., Blaschke, T., Gholamnia, K., Meena, S. R., & Aryal, J. (2019). Landslide detection using multi-scale image segmentation and different machine learning models in the Higher Himalayas. *Remote Sensing*, *11*(21), 2575. https://doi.org/10.3390/rs11212575

Teke, A., & Kavzoglu, T. (2024a). Towards artificially intelligent landslide susceptibility mapping: A critical review and open questions. In G. K. Panda, R. Shaw, S. C. Pal, U. Chatterjee, & A. Saha (Eds.), *Landslide: Susceptibility, risk assessment and sustainability* (pp. 153–182). Springer. https://doi.org/10.1007/978-3-031-56591-5_6

Teke, A., & Kavzoglu, T. (2024b). Exploring the decision-making process of ensemble learning algorithms in landslide susceptibility mapping: Insights from local and global eXplainable AI analyses. *Advances in Space Research*, *74*(8), 3765–3785. https://doi.org/10.1016/j.asr.2024.06.082

Terhorst, B., & Kreja, R. (2009). Slope stability modelling with SINMAP in a settlement area of the Swabian Alb. *Landslides*, *6*, 309–319. https://doi.org/10.1007/s10346-009-0167-2

Terlien, M. T. J. (1998). The determination of statistical and deterministic hydrological landslide-triggering thresholds. *Environmental Geology*, *35*, 124–130. https://doi.org/10.1007/s002540050299

Terlien, M. T. J., van Westen, C. J., & van Asch, T. W. J. (1995). Deterministic modelling in GIS-based landslide hazard assessment. In A. Carrara & F. Guzzetti (Eds.), *Geographical information systems in assessing natural hazards* (pp. 57–77). Springer. https://doi.org/10.1007/978-94-015-8404-3_4

Terzaghi, K. (1950). Mechanism of landslides. In S. Paige (Ed.), *Application of geology to engineering practice (Berkey Volume)* (pp. 83–124). Geological Society of America. https://doi.org/10.1130/Berkey.1950.83

Thanhlira, R. (1983). *Aw! Zawlkhawpui*. D. M. Press.

Thywissen, K. (2006). *Components of risk – A comparative glossary* (Publication Series No. 2/2006). United Nations University Institute for Environment and Human Security.

Tierney, K. (2006). Social inequality, hazards, and disasters. In R. J. Daniels, D. F. Kettl, & H. Kunreuther (Eds.), *On risk and disaster: Lessons from Hurricane Katrina* (pp. 109–128). University of Pennsylvania Press. https://doi.org/10.9783/9780812205473.109

Tierney, K. (2022). Social vulnerability and resilience to environmental hazards. In T. K. McGee & E. C. Penning-Rowsell (Eds.), *Routledge handbook of environmental hazards and society* (pp. 171–184). Routledge. https://doi.org/10.4324/9780367854584-16

Timmerman, P. (1981). *Vulnerability, resilience and the collapse of society: A review of models and possible climatic applications*. Institute for Environmental Studies, University of Toronto.

Tiwari, R. P., & Kumar, S. (1996). Geology of the area around Bawngkawn, Aizawl District, Mizoram, India. *Miscellaneous Publication, 3*, 1–10. The Geological & Research Centre.

Tiwari, R. P., & Kumar, S. (1997). South Hlimen landslide in Mizoram — A pointer. *ENVIS Bulletin – Himalayan Ecology and Development*, *5*(2), 12–13.

Tiwari, R. P., Sharma, B. L., & Singh, B. (1996). Geotechnical appraisal of Bawngkawn landslide, Aizawl, Mizoram. In *Proceedings of the International Conference on Disaster and Mitigation* (pp. A4125–A4131).

Török, I. (2018). Qualitative assessment of social vulnerability to flood hazards in Romania. *Sustainability*, *10*(10), 3780. https://doi.org/10.3390/su10103780

Totschnig, R., & Fuchs, S. (2013). Mountain torrents: Quantifying vulnerability and assessing uncertainties. *Engineering Geology*, *155*, 31–44. https://doi.org/10.1016/j.enggeo.2012.12.019

Totschnig, R., Sedlacek, W., & Fuchs, S. (2011). A quantitative vulnerability function for fluvial sediment transport. *Natural Hazards*, *58*, 681–703. https://doi.org/10.1007/s11069-010-9623-5

Turcotte, D. L., Malamud, B. D., Guzzetti, F., & Reichenbach, P. (2002). Self-organization, the cascade model, and natural hazards. *Proceedings of the National Academy of Sciences*, *99*(1), 2530–2537. https://doi.org/10.1073/pnas.012582199

Turner, A. K. (2018). Social and environmental impacts of landslides. *Innovative Infrastructure Solutions, 3*(1), 70. https://doi.org/10.1007/s41062-018-0175-y

Turner, A. K., & Schuster, R. L. (Eds.). (1996). *Landslides: Investigation and mitigation* (Transportation Research Board Special Report 247). National Academy of Sciences.

Turner, B. L., Kasperson, R. E., Matson, P. A., McCarthy, J. J., Corell, R. W., Christensen, L., Eckley, N., Kasperson, J. X., Luers, A., Martello, M. L., Polsky, C., Pulsipher, A., & Schiller, A. (2003). A framework for vulnerability analysis in sustainability science. *Proceedings of the National Academy of Sciences*, *100*(14), 8074–8079. https://doi.org/10.1073/pnas.1231335100

Tyagi, A., Tiwari, R. K., & James, N. (2022). A review on spatial, temporal and magnitude prediction of landslide hazard. *Journal of Asian Earth Sciences: X*, *7*, 100099. https://doi.org/10.1016/j.jaesx.2022.100099

UNDRO (Office of the United Nations Disaster Relief Co-ordinator). (1984). *Disaster prevention and mitigation: A compendium of current knowledge. Preparedness aspects* (Vol. 11). UN Publications.

UNDRR (United Nations Office for Disaster Risk Reduction). (2020). *Hazard Definition and Classification Review: Technical Report*. https://doi.org/10.24948/2020.03

UNISDR (United Nations International Strategy for Disaster Reduction). (2009). *Terminology on disaster risk reduction*. UN Publications.

UNISDR (United Nations International Strategy for Disaster Reduction). (2004). *Living with risk: A global review of disaster reduction initiatives*. UN Publications.

USDA. (1994). *Keys to soil taxonomy* (6th ed.). Natural Resource Conservation Service, U.S. Department of Agriculture.

Uzielli, M., Catani, F., Tofani, V., & Casagli, N. (2015a). Risk analysis for the Ancona landslide—I: Characterization of landslide kinematics. *Landslides*, *12*, 69–82. https://doi.org/10.1007/s10346-014-0474-0

Uzielli, M., Catani, F., Tofani, V., & Casagli, N. (2015b). Risk analysis for the Ancona landslide—II: Estimation of risk to buildings. *Landslides*, *12*, 83–100. https://doi.org/10.1007/s10346-014-0477-x

Vakhshoori, V., & Zare, M. (2016). Landslide susceptibility mapping by comparing weight of evidence, fuzzy logic, and frequency ratio methods. *Geomatics, Natural Hazards and Risk*, *7*(5), 1731–1752. https://doi.org/10.1080/19475705.2016.1144655

Vakhshoori, V., & Zare, M. (2018). Is the ROC curve a reliable tool to compare the validity of landslide susceptibility maps? *Geomatics, Natural Hazards and Risk*, *9*(1), 249–266. https://doi.org/10.1080/19475705.2018.1424043

Van Dao, D., Jaafari, A., Bayat, M., Mafi-Gholami, D., Qi, C., Moayedi, H., Phong, T. V., Ly, H.-B., Le, T-T., Trinh, P.T., Luu, C., Quoc, N. K., Thanh, B. N., & Pham, B. T. (2020). A spatially explicit deep learning neural network model for the prediction of landslide susceptibility. *CATENA*, *188*, 104451. https://doi.org/10.1016/j.catena.2019.104451

van Den Eeckhaut, M., & Hervás, J. (2012). State of the art of national landslide databases in Europe and their potential for assessing landslide susceptibility, hazard and risk. *Geomorphology, 139-140*, 545–558. https://doi.org/10.1016/j.geomorph.2011.12.006

van Den Eeckhaut, M., Kerle, N., Poesen, J., & Hervás, J. (2012). Object-oriented identification of forested landslides with derivatives of single pulse LiDAR data. *Geomorphology*, *173-174*, 30–42. https://doi.org/10.1016/j.geomorph.2012.05.024

van Den Eeckhaut, M., Muys, B., Van Loy, K., Poesen, J., & Beeckman, H. (2009a). Evidence for repeated re-activation of old landslides under forest. *Earth Surface Processes and Landforms*, *34*(3), 352–365. https://doi.org/10.1002/esp.1727

van Den Eeckhaut, M., Poesen, J., Verstraeten, G., Vanacker, V., Nyssen, J., Moeyersons, J., van Beek, L. P. H., & Vandekerckhove, L. (2007). Use of LiDAR-derived images for mapping old landslides under forest. *Earth Surface Processes and Landforms*, *32*(5), 754–769. https://doi.org/10.1002/esp.1417

van Den Eeckhaut, M., Reichenbach, P., Guzzetti, F., Rossi, M., & Poesen, J. (2009b). Combined landslide inventory and susceptibility assessment based on different mapping units: An example from the Flemish Ardennes, Belgium. *Natural Hazards and Earth System Sciences*, *9*(2), 507–521. https://doi.org/10.5194/nhess-9-507-2009

van Westen, C. J. (1993). *Application of geographic information systems to landslide hazard zonation* (Doctoral Dissertation), ITC Publication No. 15. International Institute for Aerospace and Earth Resources Survey. https://research.utwente.nl/files/313533007/vanwesten.pdf

van Westen, C. J. (2004). Geo-information tools for landslide risk assessment: an overview of recent developments. In W. Lacerda, M. Ehrlich, S. A. B. Fontoura, & A. S. F. Sayao (Eds.), *Landslides: evaluation and stabilization* (vol. 1, pp. 39–56). CRC Press. https://doi.org/10.1201/b16816-12

van Westen, C. J., & Terlien, M. T. J. (1996). An approach towards deterministic landslide hazard analysis in GIS. A case study from Manizales (Colombia). *Earth Surface Processes and Landforms*, *21*(9), 853–868. https://doi.org/10.1002/(SICI)1096-9837(199609)21:9<853::AID-ESP676>3.0.CO;2-C

van Westen, C. J., Alkema, D., Damen, M. C. J., Kerle, N., & Kingma. N. C. (2011). *Multi-Hazard Risk Assessment: Distance Education Course, Guide Book*. United Nations University – ITC School on Disaster Geo- information Management.

van Westen, C. J., Castellanos, E., & Kuriakose, S. L. (2008). Spatial data for landslide susceptibility, hazard, and vulnerability assessment: An overview. *Engineering Geology*, *102*(3-4), 112–131. https://doi.org/10.1016/j.enggeo.2008.03.010

van Westen, C. J., Jaiswal, P., Ghosh, S., Martha, T. R., & Kuriakose, S. L. (2012). Landslide inventory, hazard and risk assessment in India. In B. Pradhan & M. Buchroithner (Eds.), *Terrigenous mass movements* (pp. 239–282). Springer. https://doi.org/10.1007/978-3-642-25495-6_9

van Westen, C. J., Rengers, N., & Soeters, R. (2003). Use of geomorphological information in indirect landslide susceptibility assessment. *Natural Hazards*, *30*, 399–419. https://doi.org/10.1023/B:NHAZ.0000007097.42735.9e

van Westen, C. J., Rengers, N., Terlien, M. T. J., & Soeters, R. (1997). Prediction of the occurrence of slope instability phenomenal through GIS-based hazard zonation. *Geologische Rundschau*, *86*(2), 404–414. https://doi.org/10.1007/s005310050149 van Westen, C. J., van Asch, T. W. J., & Soeters, R. (2006). Landslide hazard and risk zonation—Why is it still so difficult? *Bulletin of Engineering Geology and the Environment*, *65*, 167–184. https://doi.org/10.1007/s10064-005-0023-0

Varnes, D. J. (1958). Landslide types and processes. In E. B. Eckel (Ed.), *Landslides and engineering practice* (Highway Research Board Special Report 29, pp. 20–47). National Academy of Sciences.

Varnes, D. J. (1978). Slope movement types and processes. In R. L. Schuster & R. J. Krizek (Eds.), *Landslides: Analysis and control* (Transportation Research Board Special Report 176, pp. 11–33). National Academy of Sciences.

Varnes, D. J. (1984). *Landslide hazard zonation: A review of principles and practice*. UNESCO.

Vasudevan, N., & Ramanathan, K. (2016). Geological factors contributing to landslides: case studies of a few landslides in different regions of India. *IOP Conference Series: Earth and Environmental Science*, *30*, Article 012011. https://doi.org/10.1088/1755-1315/30/1/012011

Vatsa, K. S. (2004). Risk, vulnerability, and asset-based approach to disaster risk management. *International Journal of Sociology and Social Policy*, *24*(10/11), 1–48. https://doi.org/10.1108/01443330410791055

Vázquez-González, C., Ávila-Foucat, V. S., Ortiz-Lozano, L., Moreno-Casasola, P., & Granados-Barba, A. (2021). Analytical framework for assessing the social-ecological system trajectory considering the resilience-vulnerability dynamic interaction in the context of disasters. *International Journal of Disaster Risk Reduction, 59*, 102232. https://doi.org/10.1016/j.ijdrr.2021.102232

Verma, R. (2014a). Landslide hazard in Mizoram: Case study of Laipuitlang landslide, Aizawl. *International Journal of Science and Research, 3*(6), 2262–2266.

Verma, R. (2014b). Ngaizel landslide, Aizawl, Mizoram, India: A case of wedge failure. *Asian Academic Research Journal of Multidisciplinary, 1*(22), 422–429.

Verma, R. (2019). Case study of College Veng road section landslide, Aizawl, Mizoram, India. *Senhri Journal of Multidisciplinary Studies, 4*(2), 1–6.

Verma, R., & Blick, J. (2018). Landslide hazard estimation in Thakthing Veng road section, Aizawl, Mizoram. *International Journal of Civil Engineering and Technology*, *9*(4), 298–307.

Verma, R., Rao, C. U. B., Blick, J., Gaopatwe, M., & Malsawmtluanga. (2021). Failure mechanism of Rangvamual landslide, Aizawl, Mizoram, India. *Disaster Advances, 14*(3), 1–9.

Verstappen, H. T. (1983). *Applied geomorphology: Geomorphological surveys for environmental development*. Elsevier.

Vinoth, M., Prasad, P. S., Mathur, S., & Kumar, K. (2022). Investigation and design of remedial measures for landslide in Hunthar Veng, Mizoram—A case study. In C. N. V. S. Reddy, K. Muthukkumaran, & R. Vaidya (Eds.), *Stability of slopes and underground excavations: Proceedings of Indian Geotechnical Conference 2020* (Vol. 3, pp. 79–90). Springer. https://doi.org/10.1007/978-981-16-5601-9_8

von Szombathely, M., Hanf, F. S., Bareis, J., Meier, L., Oßenbrügge, J., & Pohl, T. (2023). An index-based approach to assess social vulnerability for Hamburg, Germany. *International Journal of Disaster Risk Science*, *14*(5), 782–794. https://doi.org/10.1007/s13753-023-00517-7

Wang, H. B., Wu, S. R., Shi, J. S., & Li, B. (2013b). Qualitative hazard and risk assessment of landslides: a practical framework for a case study in China. *Natural Hazards, 69*(3), 1281–1294. https://doi.org/10.1007/s11069-011-0008-1

Wang, H. F., Lin, Z. Y., Xiao, Y., Lu, H. T., Zhang, W., Zhan, Y. J., & Yan, Y. (2019a). Ecological risk assessment of landslide disasters based on potential loss of ecosystem services. *The Journal of Applied Ecology, 30*(10), 3553–3562. https://doi.org/10.13287/j.1001-9332.201910.019

Wang, H., & Mao, J. (2025). Physical vulnerability of masonry building to the slow-moving landslide: Insight from numerical simulation. *Frontiers in Earth Science*, *13*, 1591525. https://doi.org/10.3389/feart.2025.1591525

Wang, H., Zhang, L., Luo, H., He, J., & Cheung, R. W. M. (2021). AI-powered landslide susceptibility assessment in Hong Kong. *Engineering Geology*, *288*, 106103. https://doi.org/10.1016/j.enggeo.2021.106103

Wang, L. J., Sawada, K., & Moriguchi, S. (2013a). Landslide susceptibility analysis with logistic regression model based on FCM sampling strategy. *Computers & Geosciences*, *57*, 81–92. https://doi.org/10.1016/j.cageo.2013.04.006

Wang, N., Zhang, H., Dahal, A., Cheng, W., Zhao, M., & Lombardo, L. (2024). On the use of explainable AI for susceptibility modeling: Examining the spatial pattern of SHAP values. *Geoscience Frontiers*, *15*(4), 101800. https://doi.org/10.1016/j.gsf.2024.101800

Wang, Q., & Li, W. (2017). A GIS-based comparative evaluation of analytical hierarchy process and frequency ratio models for landslide susceptibility mapping. *Physical Geography*, *38*(4), 318–337. https://doi.org/10.1080/02723646.2017.1294522

Wang, Q., Guo, Y., Li, W., He, J., & Wu, Z. (2019b). Predictive modeling of landslide hazards in Wen County, northwestern China based on information value, weights-of-evidence, and certainty factor. *Geomatics, Natural Hazards and Risk*, *10*(1), 820–835. https://doi.org/10.1080/19475705.2018.1549111

Wang, Q., Li, W., Chen, W., & Bai, H. (2015). GIS-based assessment of landslide susceptibility using certainty factor and index of entropy models for the Qianyang County of Baoji city, China. *Journal of Earth System Science*, *124*(7), 1399–1415. https://doi.org/10.1007/s12040-015-0624-3

Wang, Y., Fang, Z., Wang, M., Peng, L., & Hong, H. (2020). Comparative study of landslide susceptibility mapping with different recurrent neural networks. *Computers & Geosciences*, *138*, 104445. https://doi.org/10.1016/j.cageo.2020.104445

Wasowski, J., & Bovenga, F. (2014). Investigating landslides and unstable slopes with satellite Multi Temporal Interferometry: Current issues and future perspectives. *Engineering Geology*, *174*, 103–138. https://doi.org/10.1016/j.enggeo.2014.03.003

Weichselgartner, J. (2001). Disaster mitigation: The concept of vulnerability revisited. *Disaster Prevention and Management*, *10*(2), 85–95. https://doi.org/10.1108/09653560110388609

Welle, T., Birkmann, J., Krause, D., Suarez, D. C., Setiadi, N. J., & Wolfertz, J. (2013). The World Risk Index: A concept for the assessment of risk and vulnerability at global/national scales. In J. Birkmann (Ed.), *Measuring vulnerability to natural hazards: Towards disaster resilient societies* (2nd ed., pp. 219–250). United Nations University Press.

Welsh-Huggins, S. J., Rodgers, J. E., Holmes, W. T., & Liel, A. B. (2017). *Seismic vulnerability of reinforced concrete hillside buildings in Northeast India* [Paper presentation]. 16th World Conference on Earthquake Engineering, Santiago, Chile. https://www.iitk.ac.in/nicee/wcee/article/WCEE2017-2998.pdf

Wieczorek, G. F. (1984). Preparing a detailed landslide-inventory map for hazard evaluation and reduction. *Bulletin of the Association of Engineering Geologists*, *21*(3), 337–342. https://doi.org/10.2113/gseegeosci.xxi.3.337

Wieczorek, G. F., & Snyder, J. B. (2009). Monitoring slope movements. In R. Young & L. Norby (Eds.), *Geological monitoring* (pp. 245–271). Geological Society of America. https://doi.org/10.1130/2009.monitoring(11)

Wise, M. P., Moore, G. D., & VanDine, D. F. (2004). Definitions of terms and framework for landslide risk management. In M. P. Wise, G. D. Moore, & D. F. VanDine (Eds.), *Landslide risk case studies in forest development planning and operations* (pp. 5–12). Ministry of Forests, British Columbia.

Wisner, B., & Luce, H. R. (1993). Disaster vulnerability: Scale, power and daily life. *GeoJournal*, *30*, 127–140. https://doi.org/10.1007/BF00808129

Wisner, B., Blaikie, P., Cannon, T., & Davis, I. (2004). *At Risk: Natural Hazards, People's Vulnerability and Disasters* (2nd ed.). Routledge. https://doi.org/10.4324/9780203714775

WP/WLI (Working Party on World Landslide Inventory). (1990). A suggested method for reporting a landslide. *Bulletin of the International Association of Engineering Geology*, *41*, 5–12. https://doi.org/10.1007/BF02590201

WP/WLI (Working Party on World Landslide Inventory). (1991). A suggested method for a landslide summary. *Bulletin of the International Association of Engineering Geology*, *43*, 101–110. https://doi.org/10.1007/BF02590177

WP/WLI (Working Party on World Landslide Inventory). (1993). A suggested method for describing the activity of a landslide. *Bulletin of the International Association of Engineering Geology*, *47*, 53–57. https://doi.org/10.1007/BF02639593

WP/WLI (Working Party on World Landslide Inventory). (1995). A suggested method for describing the rate of movement of a landslide. *Bulletin of the International Association of Engineering Geology*, *52*, 75–78. https://doi.org/10.1007/BF02639593

Wright, R. H., Campbell, R. H., & Nilsen, T. H. (1974). Preparation and use of isopleth maps of landslide deposits. *Geology*, *2*(10), 483–485. https://doi.org/10.1130/0091-7613(1974)2<483:PAUOIM>2.0.CO;2

Wu, S.-Y., Yarnal, B., & Fisher, A. (2002). Vulnerability of coastal communities to sea-level rise: A case study of Cape May County, New Jersey, USA. *Climate Research*, *22*(3), 255–270. https://doi.org/10.3354/cr022255

Wu, W., & Sidle, R. (1995). A distributed slope stability model for steep forested basins. *Water Resources Research*, *31*(8), 2097–2110. https://doi.org/10.1029/95WR01136

Wu, Y., Li, W., Wang, Q., Liu, Q., Yang, D., Xing, M., Pei, Y., & Yan, S. (2016). Landslide susceptibility assessment using frequency ratio, statistical index and certainty factor models for the Gangu County, China. *Arabian Journal of Geosciences*, *9*, 1–16. https://doi.org/10.1007/s12517-015-2112-0

Xia, S., Xia, Y., Yu, H., Liu, Q., Luo, Y., Wang, G., & Chen, Z. (2019). Transferring ensemble representations using deep convolutional neural networks for small-scale image classification. *IEEE Access*, *7*, 168175–168186. https://doi.org/10.1109/ACCESS.2019.2912908

Xian, Y., Wei, X., Zhou, H., Chen, N., Liu, Y., Liu, F., & Sun, H. (2022). Snowmelt-triggered reactivation of a loess landslide in Yili, Xinjiang, China: Mode and mechanism. *Landslides*, *19*(8), 1843–1860. https://doi.org/10.1007/s10346-022-01879-7

Xiao, Y., Tang, X., Li, Y., Huang, H., & An, B. W. (2022). Social vulnerability assessment of landslide disaster based on improved TOPSIS method: Case study of eleven small towns in China. *Ecological Indicators*, *143*, 109316. https://doi.org/10.1016/j.ecolind.2022.109316

Xu, Q., Zhao, B., Dai, K., Dong, X., Li, W., Zhu, X., Yang, Y., Xiao, X., Wang, X., Huang, J., Lu, H., Deng, B., & Ge, D. (2023). Remote sensing for landslide investigations: A progress report from China. *Engineering Geology*, *321*, 107156. https://doi.org/10.1016/j.enggeo.2023.107156

Yang, S. R. (2017). Assessment of rainfall-induced landslide susceptibility using GIS-based slope unit approach. *Journal of Performance of Constructed Facilities*, *31*(4), 04017026. https://doi.org/10.1061/(ASCE)CF.1943-5509.0000997

Yarnal, B. (2007). Vulnerability and all that jazz: Addressing vulnerability in New Orleans after Hurricane Katrina. *Technology in Society*, *29*(2), 249–255. https://doi.org/10.1016/j.techsoc.2007.01.011

Ye, C., Wu, H., Oguchi, T., Tang, Y., Pei, X., & Wu, Y. (2025). Physically based and data-driven models for landslide susceptibility assessment: Principles, applications, and challenges. *Remote Sensing*, *17*(13), 2280. https://doi.org/10.3390/rs17132280

Yilmaz, I. (2009). Landslide susceptibility mapping using frequency ratio, logistic regression, artificial neural networks and their comparison: A case study from Kat landslides (Tokat—Turkey). *Computers & Geosciences*, *35*(6), 1125–1138. https://doi.org/10.1016/j.cageo.2008.08.007

Yin, K. L., & Yan, T. Z. (1988). Statistical prediction model for slope instability of metamorphosed rocks. In C. Bonnard (Ed.), *Proceedings of the Fifth International Symposium on Landslides* (Vol. 2, pp. 1269–1272). A. A. Balkema.

Yoon, D. K. (2012). Assessment of social vulnerability to natural disasters: A comparative study. *Natural Hazards*, *63*(2), 823–843. https://doi.org/10.1007/s11069-012-0189-2

Yordanov, V., & Brovelli, M. A. (2021). Application of various strategies and methodologies for landslide susceptibility maps on a basin scale: The case study of Val Tartano, Italy. *Applied Geomatics*, *13*(3), 287–309. https://doi.org/10.1007/s12518-020-00344-1

Youssef, A. M., & Pourghasemi, H. R. (2021). Landslide susceptibility mapping using machine learning algorithms and comparison of their performance at Abha Basin, Asir Region, Saudi Arabia. *Geoscience Frontiers*, *12*(2), 639–655. https://doi.org/10.1016/j.gsf.2020.05.010

Yu, X., Xia, Y., Zhou, J., & Jiang, W. (2023). Landslide susceptibility mapping based on multitemporal remote sensing image change detection and multiexponential band math. *Sustainability*, *15*(3), 2226. https://doi.org/10.3390/su15032226

Yuan, X., Liu, C., Nie, R., Yang, Z., Li, W., Dai, X., Cheng, J., Zhang, J., Ma, L., Fu, X., Tang, M., Xu, Y., & Lu, H. (2022). A comparative analysis of certainty factor-based machine learning methods for collapse and landslide susceptibility mapping in Wenchuan County, China. *Remote Sensing*, *14*(14), 3259. https://doi.org/10.3390/rs14143259

Zaruba, Q., & Mencl, V. (1969). *Landslides and their control*. Elsevier.

Zawla, K. (1989). *Mizo pi pute leh an thlahte chanchin* (5th ed.). Gosen Press.

Zêzere, J. L., Pereira, S., Melo, R., Oliveira, S. C., & Garcia, R. A. C. (2017). Mapping landslide susceptibility using data-driven methods. *Science of The Total Environment*, *589*, 250–267. https://doi.org/10.1016/j.scitotenv.2017.02.188

Zêzere, J. L., Reis, E., Garcia, R., Oliveira, S., Rodrigues, M. L., Vieira, G., & Ferreira, A. B. (2004). Integration of spatial and temporal data for the definition of different landslide hazard scenarios in the area north of Lisbon (Portugal). *Natural Hazards and Earth System Sciences*, *4*(1), 133–146. https://doi.org/10.5194/nhess-4-133-2004

Zhang, G., Cai, Y., Zheng, Z., Zhen, J., Liu, Y., & Huang, K. (2016a). Integration of the statistical index method and the analytic hierarchy process technique for the assessment of landslide susceptibility in Huizhou, China. *CATENA*, *142*, 233–244. https://doi.org/10.1016/j.catena.2016.03.028

Zhang, H., Zhao, Y., & Pedersen, J. (2020). Capital assets framework for analysing household vulnerability during disaster. *Disasters, 44*(4), 687–707. https://doi.org/10.1111/disa.12393

Zhang, J., Guo, Z. X., Wang, D., & Qian, H. (2016b). The quantitative estimation of the vulnerability of brick and concrete wall impacted by an experimental boulder. *Natural Hazards and Earth System Sciences*, *16*(2), 299–309. https://doi.org/10.5194/nhess-16-299-2016

Zhang, L. L., Zhang, J., Zhang, L. M., & Tang, W. H. (2011). Stability analysis of rainfall-induced slope failure: A review. *Geotechnical Engineering*, *164*(5), 299–316. https://doi.org/10.1680/geng.2011.164.5.299

Zhang, Y. (2008). Pan-sharpening for improved information extraction. In Z. Li, J. Chen, & E. Baltsavias (Eds.), *Advances in photogrammetry*, *remote sensing and spatial information sciences* (pp. 203–222). CRC Press. https://doi.org/10.1201/9780203888445-21

Zhao, B., Dai, Q., Han, D., Dai, H., Mao, J., & Zhuo, L. (2019). Probabilistic thresholds for landslides warning by integrating soil moisture conditions with rainfall thresholds. *Journal of Hydrology*, *574*, 276–287. https://doi.org/10.1016/j.jhydrol.2019.04.062

Zhao, Z., Liu, Z. Y., & Xu, C. (2021). Slope unit-based landslide susceptibility mapping using certainty factor, support vector machine, random forest, CF-SVM and CF-RF models. *Frontiers in Earth Science*, *9*, 589630. https://doi.org/10.3389/feart.2021.589630

Zhou, C., Yin, K., Cao, Y., Ahmed, B., & Fu, X. (2018). A novel method for landslide displacement prediction by integrating advanced computational intelligence algorithms. *Scientific Reports*, *8*(1), 7287. https://doi.org/10.1038/s41598-018-25567-6

Zhou, X., Wen, H., Li, Z., Zhang, H., & Zhang, W. (2022). An interpretable model for the susceptibility of rainfall-induced shallow landslides based on SHAP and XGBoost. *Geocarto International*, *37*(26), 13419–13450. https://doi.org/10.1080/10106049.2022.2076928

Zhou, Y., Li, N., Wu, W., Wu, J., & Shi, P. (2014). Local spatial and temporal factors influencing population and societal vulnerability to natural disasters. *Risk Analysis*, *34*(4), 614–639. https://doi.org/10.1111/risa.12193

Zuo, P., Zhao, W., Yan, W., Jin, J., Yan, C., Wu, B., Shao, X., Wang, W., Zhou, Z., & Wang, J. (2025). Landslide susceptibility mapping using an LSTM model with feature-selecting for the Yangtze River basin in China. *Water*, *17*(2), 167. https://doi.org/10.3390/w17020167

BRIEF BIO-DATA OF THE CANDIDATE

Personal Details:

Name	: Z.D. LALTANPUIA
Father's Name	: Z.D. ZOTLUANGA
Address	: Mission Vengthlang, Aizawl, Mizoram.
Religion	: Christianity
Marital Status	: Married
Educational Qualification	: M.Sc. (Geology); CSIR-UGC NET (2010)

Education:

Jan 1991 – Mar 1994	: Christian High School, Serkawn, Lunglei
Jul 1994 – Apr 1996	: Lunglei Govt. College, Lunglei
Jul 1996 – Apr 1999	: Pachhunga University College, Aizawl
Jul 1999 – May 2001	: University of Mysore, Manasagangothri, Mysore

Experience:

June 2004 – Sep 2006	Project Scientist State Remote Sensing Centre (SRSC), Science, Technology & Environment Wing, Planning Department, Govt. of Mizoram.
Oct 2006 – Aug 2018	Scientific Officer/Scientist Mizoram Remote Sensing Application Centre (MIRSAC), Directorate of Science & Technology, Planning Department, Govt. of Mizoram.
Sep 2018 – Till date	Senior Scientist Mizoram Remote Sensing Application Centre (MIRSAC), Directorate of Science & Technology, Planning Department, Govt. of Mizoram.
Aug 2018 – Till date	Ph.D. Research Scholar Department of Geology, Mizoram University, Aizawl.

Activities:

1. Attended a 12-week training Programme on "*Remote Sensing Technology & its Applications*" from 28th June to 17th September, 2004 at National Remote Sensing Agency, Hyderabad, A.P.
2. Attended "*Workshop on regional Strategy for Management of Natural Disasters – Earthquake Hazard Management & Mitigation*" on 7th – 8th June, 2010 at North East Institute of Science & Technology (NEIST), Jorhat, Assam.
3. Attended training course on "*Seismic Hazard Assessment using Probabilistic Technique*" at Wadia Institute of Himalayan Geology, Dehra Dun on 16th August – 2nd September, 2011.
4. Attended training course on "*Space Enabled Geoinformation for Disaster Management*" conducted by Disaster Management Support Programme of DOS/ISRO during 31st October – 4th November, 2011 at National Remote Sensing Centre (NRSC), Hyderabad, A.P.
5. Co-ordinator in the Mizoram Science Congress 2018, during 4th – 5th October, 2018.
6. Presented a paper in the 3-days National Workshop on "*Landslide Hazard in Southern Mizoram*" during 24th – 26th October, 2019 at Lunglei Govt. College, Lunglei.
7. Presented a paper in the National Symposium on "*Innovations in Geospatial Technology for Sustainable Development with special emphasis on North Eastern Region*" jointly organised by Indian Society of Geomatics and Indian Society of Remote Sensing during 20th – 22nd November, 2019 at North Eastern Space Application Centre, Shillong.
8. Presented a paper in the International Seminar on "*Recent Advances in Science and Technology*" organized by North East Academy of Science and Technology (NEAST), during 16th - 18th November, 2020.
9. Presented a paper in the State Level Seminar on "*2020 Earthquakes in Mizoram*" organized by Directorate of Science & Technology, Govt. of Mizoram, on 15th January, 2021.
10. Speaker/Resource Person in the "*Natural Hazards and Disaster Mitigation of Mizoram*" Workshop organized by the Department of Geography and Resource Management, Mizoram University and Rajiv Gandhi National Institute of Youth Development, Govt. of India, during 8th – 10th March, 2021.
11. Speaker/Resource Person in the Webinar Workshop on "*Rapid Visual Screening of Buildings for Earthquake Safety*" during 17th – 18th March, 2021 conducted by National Institute of Disaster Management, Ministry of Home Affairs, Govt. of India, New Delhi.

12. Attended training course on "*Training on Concepts of LiDAR Technology and Applications in Geosciences*" on 24th September, 2021 conducted by Geological Survey of India Training Institute, Hyderabad.
13. Attended training course on "*Remote Sensing and Geospatial Technology for Landslide Mitigation and Management in North Eastern Region*" conducted by National Institute of Technology (NIT), Aizawl and Indian Institute of Technology (IIT), Tirupati on 24th – 28th July, 2022 at National Institute of Technology (NIT), Aizawl.
14. Attended National Symposium on "*Geospatial Technology: Journey from Data to Intelligence*" jointly organised by GeoSmart India, Indian Society of Remote Sensing, and Indian Society of Geomatics during 15th – 17th November, 2022 at HICC, Hyderabad.
15. Attended training course on "*Applications of Remote Sensing and GIS in Disaster Management*" conducted by Geological Survey of India (GSI) Training Institute, Hyderabad, during 21st – 28th February, 2023.
16. Attended training course on "*Applications of Space Technology in Geosciences, Engineering and Disaster Management*" conducted by Geological Survey of India (GSI) Training Institute, Hyderabad, on 31st March, 2023.
17. Attended Brainstorming Meet on "*Geodynamic and Geohazard Applications using InSAR: New opportunities with NISAR*" during 11th – 12th October, 2023 at National Remote Sensing Centre (NRSC), Hyderabad, Telengana.
18. Attended Workshop on "*Space Technology in Disaster Risk Management*" organized by National Institute of Disaster Management (NIDM), Ministry of Home Affairs (MHA) and National Remote Sensing Centre (NRSC), Indian Space Research Organization (ISRO) during 4th – 5th December, 2023 at NIDM, New Delhi.
19. Attended Workshop on "*Space Technology in Disaster Risk Management*" jointly organized by National Institute of Disaster Management (NIDM), Ministry of Home Affairs (MHA), National Remote Sensing Centre (NRSC), Indian Space Research Organization (ISRO), and North Eastern Space Applications Centre (NESAC) during 27th – 28th May, 2024 at NESAC, Shillong.
20. Attended training course on "*Advanced Multicriteria Decision Making (MCDM) Techniques*" conducted by Department of Geography & Resource Management, Mizoram University, Aizawl during 24th January – 22nd March, 2025.

Major Projects:

1. Natural Resources Mapping of Mizoram
2. Landslide Hazard Zonation Mapping of Aizawl city & Lunglei town

3. Disaster Management System of Mizoram
4. Groundwater Prospects and Quality Mapping of Mizoram
5. Hazard Risk and Vulnerability Assessment (HRVA) of Aizawl District
6. Hazard Risk and Vulnerability Assessment (HRVA) of Aizawl city and Seven District Headquarters of Mizoram
7. Satellite Integrated Landslide Assessment & Alert System (SILAAS)

Publications from Ph.D Research:

1. Laltanpuia, Z. D., Martha, T. R., Rao, K. S., & Khanna, K. (2024). Bivariate statistical models for Landslide susceptibility mapping at local scale in the Aizawl municipal area, Mizoram, India. *Himalayan Geology, 45*(1), 39-57.
2. Laltanpuia, Z. D., Martha, T. R., & Rao, K. S. (2025). Integrating Social and Physical Vulnerabilities to Assess Landslide Risk in the Aizawl Municipal Area, Mizoram, India. *Journal of the Indian Society of Remote Sensing, 53*(12), 4257–4279. https://doi.org/10.1007/s12524-025-02243-7

Other Publications:

1. Lallianthanga, R. K. & Laltanpuia, Z. D. (2008). Landslide Hazard Zonation of Aizawl town using Remote Sensing and GIS Techniques—A qualitative approach. *Bulletin of National Natural Resources Management System, 32*, 47–55.
2. Lallianthanga, R. K. & Laltanpuia, Z. D. (2013). Landslide Hazard Zonation of Lunglei town, Mizoram, India using high resolution satellite data. *International Journal of Advanced Remote Sensing & GIS, 2*(1), 148–159.
3. Lallianthanga, R. K., Laltanpuia, Z. D. & Sailo, R. L. (2013). Landslide hazard zonation of Lawngtlai town, Mizoram, India using high resolution satellite data. *International Journal of Engineering and Science, 3*(6), 36–46.
4. Lallianthanga, R. K. & Laltanpuia, Z. D. (2014). Landslide Hazard Zonation Mapping of Hnahthial town, Mizoram, India using Remote Sensing and GIS. *International Journal of Engineering and Technical Research, 2*(3), 56–63.
5. Chenkual, L., Laltanpuia, Z. D., & Lalbiakmawia, F. (2016). Landslide Hazard Zonation (LHZ) of Lawngtlai District, Mizoram, India using Remote Sensing and GIS. *International Journal of Innovative Research in Science, Engineering and Technology, 5*(7), 13455–13460.
6. Chenkual, L., Lalbiakmawia, F., & Laltanpuia, Z.D. (2016). Landslide Hazard Zonation (LHZ) of Saiha District, Mizoram, India using Remote Sensing and GIS. *International Journal of Engineering Science and Computing, 6*(7), 8724–8728.

PARTICULARS OF THE CANDIDATE

Name of Candidate: Z.D. LALTANPUIA

Degree: Doctor of Philosophy

Department: Department of Geology, Mizoram University

Title of Thesis: Landslide Hazard, Vulnerability and Risk Assessment of Aizawl Municipal Area, Mizoram, India Using Geospatial Techniques

Date of Admission: 28th July, 2018

Approval of Research Proposal:

1. **DRC** : 8th March, 2019
2. **BOS** : 5th April, 2019
3. **School Board :** 26th April, 2019

MZU Registration No. 1807373

Ph.D. Registration No. & Date: MZU/Ph.D/1277 of 03.08.2018

Extension (if any): 2 years, vide No. 16-2/MZU(Acad)/24/14-15, Dt. 3rd July, 2024

(Dr J. MALSAWMA)

Head
Department of Geology and
Centre for Petroleum Exploration (CPEX)
Mizoram University

HIMALAYAN GEOLOGY

(An International Journal of Geosciences)

Vol. 45, No. 1, 2024

WADIA INSTITUTE OF HIMALAYAN GEOLOGY
Dehradun 248001, India

HIMALAYAN GEOLOGY

Vol. 45, No. 1, 2024

CONTENTS

	Pages
RAYMOND A. DURAISWAMI, AKSHAY A. KELKAR, TAHIRA N. SHAIKH, NITIN R. KARMALKAR, MALLIKA K. JONNALAGADDA, ARISTLE MONTEIRO, HEMANT PEDNEKAR, DEEPAK KUMAR SAHU : Compositional diversity in spinels from the Nidar ophiolite peridotites, Ladakh, India: A record of complex petrogenetic evolution	1-25
GURVINDER SINGH, MAHESH THAKUR, JAVED N. MALIK : Holocene shortening along the Himalayan Frontal Thrust in the Nahan Salient, Western Himalaya, India	26-38
Z.D. LALTANPUIA, TAPAS R. MARTHA, K. SRINIVASA RAO, KIRTI KHANNA : Bivariate statistical models for Landslide susceptibility mapping at local scale in the Aizawl municipal area, Mizoram, India	39-57
POOJA RAJPUT, A.K. MAHAJAN : Risk scenario of Himachal Pradesh considering the 1905 Kangra earthquake by using Deterministic approach	58-74
SHASHI KANT RAI, RAKESH SAHU, SUNIL DHAR, NAVEEN TRIPATHI, ARUN KUMAR : Rapid expansion of proglacial lake and deglaciation of host glacier in Kishtwar Himalaya, Jammu and Kashmir, India, from 1993 to 2020	75-88
SUMAN KONAR, BAPPA MUKHERJEE, KALACHAND SAIN : Machine learning assisted gas hydrate saturation proxy: A case study from KG basin, India	89-107
BHAVUK SHARMA, ATUL ADITYA PANDEY, SURESH KUMAR : Assessment of groundwater quality of the area in and around Kharagpur Hills, Munger-Jamui, Bihar	108-122
PARAMJEET SINGH, SHAILENDRA KUMAR CHAUDHARY, MANISHA SANDHU, RAVINDRA PRATAP SINGH, AMIT SAGWAL : Mio-Pliocene tectonic activity along the Main Boundary Thrust and exhumation of the Amritpur Granite Body, Kumaun region, northwestern Himalaya	123-137
SUBHRA MULLICK, SUBHAJIT SINHA : Evidence of fluvial to marine transition in the Siwalik rocks of the Itanagar area, Arunachal Pradesh, India: Implication for the regional paleogeography	138-154

Published by Wadia Institute of Himalayan Geology, 33 General Mahadeo Singh Road, Dehradun 248001, India

ISSN 0971-8966

Himalayan Geology, Vol. 45 (1), 2024, pp. 39-57, Printed in India

Bivariate statistical models for Landslide susceptibility mapping at local scale in the Aizawl municipal area, Mizoram, India

Z.D. LALTANPUIA[1,3], TAPAS R. MARTHA[2*], K. SRINIVASA RAO[3], KIRTI KHANNA[2]
[1]*Mizoram Remote Sensing Application Centre (MIRSAC), Aizawl, Mizoram, India*
[2]*National Remote Sensing Centre (NRSC), ISRO, Hyderabad, Telangana, India*
[3]*Department of Geology, Mizoram University, Aizawl, Mizoram, India*
**Email (Corresponding author): tapas_martha@nrsc.gov.in*

Abstract: Landslide is the most frequent and prevalent form of natural hazards experienced by the state of Mizoram in India. Due to climatic extremes and anthropogenic disturbances, landslide susceptibility maps need periodic updation to meet present day requirements. In this study, landslide susceptibility mapping of Aizawl Municipal Area has been attempted using three bivariate statistical models, namely, Information Value (IV), Frequency Ratio (FR) and Weight of Evidence (WofE) models. Based on field survey, historical records and from Google Earth image interpretation, a total of 381 landslides have been mapped within the study area which were split into two parts i.e., 70% of the landslides were used for model calibration while the remaining 30% were used for validation. Twelve landslide conditioning parameters including Slope, Aspect, Elevation, Lithology, Drainage Density, Lineament Density, Normalized Difference Vegetation Index (NDVI), Land Use/Land Cover (LULC), Plan Curvature, Profile Curvature, Stream Power Index (SPI) and Topographical Wetness Index (TWI) were prepared from a 10m resolution DEM of Cartosat-1 data, Sentinel-2 data and Google Earth image. Landslide susceptibility maps were prepared showing three susceptible classes ranging from low to high susceptibility. The resulting maps have been validated using the area under the receiver operating characteristic curve which showed success rate for IV, FR and WofE models as 83.8%, 83.7% and 83.9% respectively. Similarly, the prediction rate for the three models are found to be 83.7%, 83.5% and 83.7%. The landslide susceptibility map was compared with the previous map prepared by GSI. Results show many new areas are now under higher hazard category in the Aizawl municipal area.

Keywords: Aizawl Municipal, Bivariate Statistical Model, Landslide Susceptibility, ROC

INTRODUCTION

Landslides are the movements of masses of rock, earth or debris down a slope under the effect of gravity (Cruden & Varnes 1996). They constitute one of the most widespread and damaging natural hazards in mountainous regions. Landslides occur because of the favourable topographic conditions (e.g. steep slope), which is further exasperated by extreme rainfall, earthquakes and human activities (Sarkar *et al.* 2013). Landslide research has drawn global attention owing to the increasing consciousness of its impact on the socio-economic aspect, and the growing pressure of urbanization on the mountain environment (Aleotti & Chowdhury 1999). Landslides cause misery to public which results in loss of life, damage to property, disruption of communication networks and hamper developmental works thus causing economic burden on the society. It has been recorded that worldwide total deaths and damages caused by landslide alone during a span of 10 years (2010-2020) amounts to 9,486 and more than 3.6 billion dollars (US) respectively (OFDA/CRED 2020).

India is a vast country with varied topographic as well as climatic conditions. About 12.6% of land area across the country is prone to landslide hazard (Kaur *et al.* 2017; Sharma 2020). In India, landslide activity is mostly observed in the Himalayan region, the Western Ghats and the Nilgiri ranges (Martha *et al.* 2021). In 2019, the National Disaster Management Authority (NDMA) estimated that the annual losses from landslides in India were approximately in the range of INR 150–200 crores (Das *et al.* 2022). In the Indian Himalayan alone, landslide causes about 200 annual deaths, which adds up to 30% of such losses occurred on a global scale (Naithani 1999). These figures are likely to increase in the present day considering the climatic change scenarios and the fast pace of population growth in these regions. The landslides in the Himalayan region account for nearly 15% of the rainfall-induced landslides occurring worldwide (Dikshit *et al.* 2020). This shows that the Himalayan region is one of the most severe landslide hot-spot areas in the world.

Landslide studies in Mizoram and Aizawl city have been taken up by several workers in order to find out the causative factors for slope instability, and to provide suitable mitigation measures. Most of these studies were concentrated on individual landslide or site-specific, and synoptic studies in the form of hazard or susceptibility mapping are, however rare. Few studies in the form of hazard or susceptibility mapping on large scale are available. For example, Lallianthanga & Laltanpuia (2008) have carried out landslide hazard zonation mapping for entire Aizawl city. Moirangcha *et al.* (2014) undertook earthquake and landslide hazard assessment within Aizawl Master Plan area. Barman *et al.* (2019) have taken up delineation of potential landslide prone zones in the northwestern part of Aizawl city. These studies have confirmed that the inherent nature of the terrain and anthropogeny are the major factors of slope instability in Aizawl city.

To minimize the damages caused by landslides, and to formulate strategic land use planning, researchers around the world prepare landslide hazard and/or susceptibility zonation maps. They depict the areas where slope failures are likely to occur. This spatial zoning of landslides is utilized for the hazard and risk assessment studies (Cardinali *et al.* 2006; van Westen *et al.* 2008). By definition, landslide susceptibility is the spatial probability or the likelihood of landslide occurrence in an area based on the local environmental and geological conditions (Brabb 1984; Guzzetti *et al.* 2006). The

Journal of the Indian Society of Remote Sensing
https://doi.org/10.1007/s12524-025-02243-7

RESEARCH ARTICLE

Integrating Social and Physical Vulnerabilities to Assess Landslide Risk in the Aizawl Municipal Area, Mizoram, India

Z. D. Laltanpuia[1,3] · **Tapas R. Martha**[2] · **K. Srinivasa Rao**[3]

Received: 18 February 2025 / Accepted: 21 May 2025

Abstract

Landslide risk assessment is a key component of disaster risk reduction for habitations in growing hilly towns located in the Himalaya. This study presents the assessment of landslide risk in the Aizawl municipal area, the capital city of Mizoram state in India, by integrating social and physical vulnerabilities with the landslide susceptibility map. Social vulnerability was assessed using a framework considering the sensitivity and lack of resilience of the resident populations using Census 2011 data. A matrix-based approach was used to evaluate the physical vulnerability of the buildings and roads based on their construction materials and exposure to landslide hazards. Both the social and physical vulnerabilities were summed to generate the combined vulnerability. Finally, the landslide risk map was generated for the built structures of the study area. Results revealed that the female population emerged as the most significant contributor to the social vulnerability. Reinforced Cement Concrete (RCC) building and metalled road were more resilient while Assam-Type (AT) building and unmetalled road were more vulnerable in terms of the physical vulnerability. The result also showed that the peripheral areas have higher combined vulnerability than the central parts of the municipal area. The risk assessment confirmed that landslide risk is not entirely determined by hazard intensity, but is significantly influenced by the vulnerability of exposed elements. The study provided an important baseline evaluation for landslide risk assessment in data-scarce areas, and also served as valuable information for policy-makers and urban planners to formulate risk reduction measures in Aizawl and similar contexts worldwide.

Keywords Aizawl municipality · Landslide risk assessment · Physical vulnerability · Social vulnerability

Introduction

Landslides constitute one of the most damaging natural hazards in mountainous environments (Petley et al., 2007; Wu et al., 2023), and affect society at varying spatial and temporal scales (Glade & Crozier, 2005). The assessment of landslide hazard, vulnerability and risk constituted one of the most important measures to minimize the impact of landslide disaster (Fu et al., 2020; Liu & Miao, 2018). This comprehensive approach integrates the assessment of the physical, environmental, economic and social factors that contribute to the susceptibility of areas and communities to landslide hazards. By understanding these factors, effective strategies can be formulated to reduce the risks and mitigate the consequences of landslides (Galve et al., 2015; Lacasse & Nadim, 2009).

It is well known that vulnerability assessment is one of the key components in the process of evaluating landslide risk. Vulnerability is a concept that is widely used across various disciplines. Therefore, its definition can vary depending on the context and discipline in which it is applied. These divergent views on the definitions of vulnerability can be broadly categorized into two: i) from the perspective of natural science, and ii) from the social science perspective (Ciurean et al., 2013; Fuchs et al., 2012; Sterlacchini et al.,

✉ Tapas R. Martha
tapas_martha@nrsc.gov.in

Z. D. Laltanpuia
tanpuiazadeng@gmail.com

K. Srinivasa Rao
raomzu@gmail.com

[1] Mizoram Remote Sensing Application Centre (MIRSAC), Aizawl, Mizoram, India

[2] National Remote Sensing Centre (NRSC), ISRO, Hyderabad, Telangana, India

[3] Department of Geology, Mizoram University, Aizawl, Mizoram, India

Published online: 04 July 2025

ABSTRACT

LANDSLIDE HAZARD, VULNERABILITY AND RISK ASSESSMENT OF AIZAWL MUNICIPAL AREA, MIZORAM, INDIA USING GEOSPATIAL TECHNIQUES

An Abstract Submitted in Partial Fulfilment of the Requirements for the Degree of Doctor of Philosophy

Z. D. LALTANPUIA

MZU Registration: 1807373

Ph. D. Registration: MZU/Ph.D/1277 of 03.08.2018

DEPARTMENT OF GEOLOGY

SCHOOL OF EARTH SCIENCES & NATURAL RESOURCES MANAGEMENT

MIZORAM UNIVERSITY

NOVEMBER, 2025

LANDSLIDE HAZARD, VULNERABILITY AND RISK ASSESSMENT OF AIZAWL MUNICIPAL AREA, MIZORAM, INDIA USING GEOSPATIAL TECHNIQUES

By

Z. D. LALTANPUIA

Department of Geology

Prof. K. SRINIVASA RAO

Supervisor

Department of Geology, Mizoram University, Aizawl, Mizoram

Dr TAPAS R. MARTHA

Co-Supervisor

Geosciences Group, National Remote Sensing Centre (NRSC)

Indian Space Research Organisation (ISRO), Hyderabad, Telengana

Submitted

In partial fulfilment of the requirement of the Degree of

Doctor of Philosophy in Geology of Mizoram University, Aizawl

ABSTRACT

Landslides are recognized globally as highly destructive natural hazards, constituting approximately 9% of worldwide natural disasters during the 1990s, and are estimated to claim the lives of roughly 1000 people annually. Owing to climatic change scenarios and rapid population growth in the hilly regions, these figures are likely to increase further. Mizoram, situated in the Northeast Indian Himalayas, is considered as one of the most landslide-prone regions in the country, having topped the list in recording the highest number of landslide incidences during 1998 to 2021. Aizawl city, in particular, has experienced decades of rapid and uncontrolled urbanization which results in haphazard construction activities along the steep and unstable slopes. This adds to the increased landslide vulnerability and risk to the infrastructures and the local residents.

A number of landslide studies in the form of hazard/susceptibility zonation, geotechnical, and site-specific investigations were taken up within Aizawl city. However, detailed studies on the physical, socio-economic and demographic aspects of vulnerability and the subsequent risk assessment remain scarce and limited. Consequently, the main objective of this research was to assess the landslide risk in the study area which was derived from the combined analyses of landslide hazard/susceptibility and both the physical and socioeconomic vulnerabilities. To achieve this aim, the study focused on mapping the landslide-prone areas, assessing the physical and social aspects of vulnerability, and evaluating the degree of landslide risk within the Aizawl municipal area.

The present study holds considerable significance as its findings contribute to enhancing disaster management practices within Mizoram by providing spatial insights into landslide susceptibility, vulnerability, and risk. The findings are expected to provide better-informed policy-making, strategic urban planning, and the implementation of targeted mitigation measures within the study area. Furthermore, the evaluation of both the physical and socio-economic vulnerabilities offer important perspectives that have been overlooked in conventional landslide studies. It also provides a broader understanding of landslide vulnerability and risk on the built infrastructures. The methodo-

logy employed in this research presents a replicable framework for other landslide-prone areas facing similar geographic and socio-economic challenges.

The landslide susceptibility assessment of the study area was carried out using quantitative bivariate statistical models, viz., Information Value (IV), Frequency Ratio (FR), and Weight of Evidence (WofE) models. The methodology involved developing a landslide inventory consisting of 381 rainfall-induced shallow landslides, collected from historical records, field surveys, and interpretation of satellite imagery. These were randomly segregated into 70% (267 landslides) for training, and 30% (114 landslides) for validation. Twelve landslide conditioning factors were generated from remote sensing data and fieldwork, which includes Aspect, Elevation, Drainage density, Land use/land cover (LULC), Lineament density, Lithology, Normalized Difference Vegetation Index (NDVI), Plan and Profile Curvatures, Slope angle, Stream Power Index (SPI), and Topographical Wetness Index (TWI).

The bivariate models calculated a Landslide Susceptibility Index (LSI) by assigning weights based on the relative density of landslide pixels within each factor class, from which the landslide susceptibility maps were generated. The reliability and predictive performance of the resulting maps were assessed and validated using the Receiver Operating Characteristic (ROC) curve and the Area Under the Curve (AUC) analyses.

The results demonstrated that all three models performed satisfactorily in generating reliable landslide susceptibility maps. The Weight of Evidence (WofE) model showed marginally higher performance, achieving a success rate of 83.93% and a prediction rate of 83.79%. The IV and FR models followed closely, with success rates of 83.85% and 83.72%, and prediction rates of 83.71% and 83.58%, respectively. The spatial distribution analysis revealed that the moderate susceptibility zone occupied the maximum area across all three models.

Analysis of the spatial correlation between the conditioning factors and landslide occurrences revealed important factors of slope instability. Strong spatial associations were observed in the barren land and scrubland classes of the LULC, shale, and steep slopes, particularly those ranging from 25–45 degrees. Higher values of both the SPI and TWI factors also showed positive association, which suggested a significant hydrological influence on instability. Conversely, areas characterized by dense vegetation (high NDVI values) showed a negative spatial association, which confirmed the role of vegetation in providing stability and natural anchorage to slope materials.

The assessment of social vulnerability utilized socio-economic and demographic data from the 2011 Census of India, supplemented by data on the elderly population from the *Mizo Upa Pawl* (MUP) organization. The methodology employed a framework which considered sensitivity and lack of resilience variables. A total of ten indicators, five each for sensitivity and lack of resilience were selected based on data availability and relevance of the study area. All the indicators were standardized and then averaged to generate the social vulnerability index.

The analysis revealed that the highest level of social vulnerability was mostly confined in the peripheral areas. This was characterized by higher concentrations of low-income households, non-workers, and those residing in rented accommodations, along with higher dependency ratios. The core and central part of the study area was mainly dominated by the low and moderate vulnerability. Further analysis showed that female population emerged as the most influencing factor to the overall social vulnerability of the study area. While low income and lack of electricity were found to be the least contributing indicators, they indicated the existence of economically fragile urban poor segments which require targeted support.

The physical vulnerability assessment focused on buildings and road networks, derived from manual digitization of Google Earth image and validated through fieldwork. The buildings were categorized into Reinforced Cement Concrete (RCC), Semi-RCC, and Assam-Type (AT) based on the construction materials, while the roads were classified as metalled, bridges, and unmetalled roads. Numerical weights ranging from 1 to 3 were assigned to both the building and road classes based on their respective inherent structural resilience. A GIS-based intersectional analysis between the weighted infrastructures and landslide hazard map using a matrix-based approach was employed to derive the physical vulnerability index.

The findings indicated that the RCC structures and the metalled road have the highest resilience, and contributed predominantly to the low vulnerability class. Conversely, traditional AT buildings and unmetalled roads were characterized as intrinsically fragile which fell mostly into the moderate or high vulnerability classes. The Semi-RCC buildings and bridges were distributed across all the vulnerability classes. The study revealed the importance of construction materials and structural integrity in determining the physical vulnerability of buildings and roads to landslide hazard. It was also observed that the RCC structures account for more than 50% of the building stock which is suggestive of an increasing trend towards increased resilience in the built environment in the municipal area.

The social and physical vulnerabilities were integrated through direct summation of their respective class values to produce the combined vulnerability index. It was found that the overall vulnerability is determined by the interaction of both the physical and social vulnerabilities. The results revealed that the peripheral areas were characterized by higher combined vulnerability levels than the central areas. “This pattern matches with the common urban development trends in which the new and less-planned developments occur at the peripheral areas, while the central part is more developed and well-established in terms of infrastructures and services”.

The landslide risk index was generated by combining the landslide hazard map and the combined vulnerability map. The risk assessment considered only the physical infrastructures, and does not include population due to data limitations. Majority of the RCC buildings and metalled roads fell in the low risk class, while the AT buildings and unmetalled road predominantly fell in the high risk class. The Semi-RCC and bridges, on the other hand, exhibited a more evenly distributed risk pattern across the high, the moderate, and the low risk classes.

The findings revealed that landslide risk is not only influenced by the intensity of the hazard, but is remarkably determined by the vulnerability of exposed elements. This shows that integration of both hazard and vulnerability dimension in the risk assessment is necessary to avoid under- or over-estimation of the actual risk, particularly in rapidly urbanizing areas with heterogeneous social and physical vulnerabilities. The results also highlighted the urgent need for comprehensive landslide risk reduction strategies in the Aizawl municipal area.

Based on these findings, the study provides strategic recommendations for future risk management, including prioritizing interventions in high-risk zones, upgrading drainage networks, and enacting targeted social development initiatives, especially in the high social vulnerability areas. Recommendations for future research emphasize the need for systematic landslide inventory mapping to capture comprehensive spatio-temporal details, incorporating dynamic triggering factors like rainfall variability, and updating vulnerability data (both social and physical) to include more indicators like building age, maintenance status, and economic quantification of losses. Continual updating of susceptibility/hazard maps is also recommended to reflect the dynamic nature of urbanization and climate change impacts. This research provides a foundational resource intended to guide policymakers, planners, and disaster management authorities toward developing a resilient and sustainable future for the Aizawl municipal area.